INVESTIGATING THE TCA CYCLE DURING HEMATOPOIESIS: A TEMPORAL AND SPATIAL CHARACTERIZATION IN THE *DROSOPHILA* LYMPH GLAND

A THESIS TO BE SUBMITTED TO

THE UNIVERSITY OF TRANS-DISCIPLINARY HEALTH SCIENCES AND TECHNOLOGY

FOR THE AWARD OF THE DEGREE OF
DOCTOR OF PHILOSOPHY

BY

AJAY KUMAR

UNDER THE GUIDANCE OF

DR. TINA MUKHERJEE

INSTITUTE FOR STEM CELL SCIENCE AND REGENERATIVE MEDICINE, BENGALURU

November 2025

THE UNIVERSITY OF TRANS-DISCIPLINARY HEALTH SCIENCES AND TECHNOLOGY

Private University Established in Karnataka by ACT 35 of 2013

BENGALURU – 560064

DECLARATION BY THE CANDIDATE

I declare that this thesis entitled **"Investigating the TCA cycle during hematopoiesis: a temporal and spatial characterization in the *Drosophila* lymph gland**" submitted for the award of Doctor of Philosophy to THE UNIVERSITY OF TRANS-DISCIPLINARY HEALTH SCIENCES AND TECHNOLOGY, Bengaluru, is my original work, conducted under the supervision of my guide, **Dr. Tina Mukherjee**. I also wish to inform that no part of the research has been submitted for a degree or examination at any university. References, assistance, and material obtained from other sources have been duly acknowledged.

I hereby confirm the originality of the work and that there is no plagiarism in any part of the dissertation.

Place: **Bengaluru**

Date: **27th November 2025**

Name of candidate: **Ajay Kumar**

Reg. No.: **20219021473**

(November 2019)

Signature of the Candidate

THE UNIVERSITY OF TRANS-DISCIPLINARY HEALTH SCIENCES AND TECHNOLOGY

Private University Established in Karnataka by ACT 35 of 2013

BENGALURU – 560064

CERTIFICATE

This is to certify that the work incorporated in this thesis **"Investigating the TCA cycle during hematopoiesis: a temporal and spatial characterization in the *Drosophila* lymph gland**" submitted by **Ajay Kumar** was carried out under my supervision. No part of this thesis has been submitted for a degree or examination at any university. References, assistance, and material obtained from other sources have been duly acknowledged. I hereby confirm the originality of the work and that there is no plagiarism in any part of the dissertation.

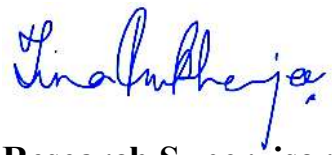

Research Supervisor

Dr. Tina Mukherjee
Associate Investigator
Institute for Stem Cell Science and Regenerative Medicine
Bengaluru, 560065

Date: 27th November 2025

ACKNOWLEDGEMENTS

I will always be deeply indebted to the host of individuals who have made innumerable contributions towards completing my thesis. It is my great pleasure and privilege to express the sense of gratitude and respect to Tina for her meticulous supervision right from the inception to the completion of this work. Her expert guidance helped me to overcome seemingly insurmountable problems. I consider *myself* fortunate for having had the chance to work under her guidance. Apart from being a mentor, I would also like to appreciate her role as a senior/friend who was always approachable and cared enough to have a spirited discussion about my project. I have learnt a lot from her which has shaped up my scientific thinking.

inStem and BLiSc Campus is undoubtedly one of the best places to pursue research. I thank the present and past Directors, Maneesha, Apurva, Jitu and Shashi for maintaining a conducive and pleasant working environment. I would also like to express my sincere thanks to the faculty members at inStem and NCBS for providing valuable and insightful suggestions. I would also like to thank my thesis committee members Gaiti and Arvind for the critical inputs they offered during the meetings.

Dr. S. K. Singh at FHT, IARI, New Delhi to provide me with the initial exposure to research during my B.Sc., even though there was no dissertation in my curriculum he still accepted me to his lab and gave me full independence to work alone, Dr. M. K. Arunasree Lab at UOH, Hyderabad for my Master's dissertation and Dr. Dipak Dutta Lab at IMTech, Chandigarh, where I worked as Project Assistant. These people laid the foundations for my PhD journey, for which I will always be grateful.

I'm extremely thankful to the present and past MAD lab members for being so helpful throughout and for all the suggestions regarding the projects. Time spent on campus and especially in the lab would not have been so exciting without all the wonderful people around. It was a wonderful experience learning, talking, discussing, arguing and interacting with lively people around me and it is not possible to acknowledge everything they have done for me in the past 6 years. I would also like to thank all the present and the past members of the labs at inStem and NCBS who have shared reagents, graciously allowed me to use their equipment, slots, etc. whenever required. My stay at inStem would not have been the same without the

various support staff at inStem including Instrumentation, IT, CIFF, fly facility, purchase, canteen staff and administration. A special thanks to the staff at the kitchen who made fly media day-in-day-out. Special thanks too, to Raju, Sunitha, Valsala and Mayur who kept paperwork in order.

My stay on BLiSc campus would not have been smooth without the sports complex, which is one of the amazing in terms of available sports options as well as maintenance by the dedicated staff. Apart from my work at lab, sports facility is the place where I have spent most of my time and made numerous wonderful friends, Ravi, Asha, Abhi, Prashanth, Bhushan, Prashanta, Manjunath, Ranjith, Praveen, Baba, Kumar, Ashwin, Jigme, karthik and many many more, these are the people who kept me sane during this journey.

Thanks to UGC-JRF and DBT/Wellcome Trust India Alliance for funding me. I also thank DBT for funding my ISDB conference visit. A huge thanks to Ravi Kumar at TDU for helping with the PhD registration and further processes.

Most importantly, my parents, my siblings and my wife deserve the best. Without their love, support and belief, I may not have reached this milestone in life. I will always be grateful to my parents for believing in me and letting me follow my own path, even though I had to mostly stay away from them.

(Ajay Kumar)

TABLE OF CONTENTS

DECLARATION BY THE CANDIDATE……ii

CERTIFICATE…….....iii

ACKNOWLEDGEMENTS……....iv

LIST OF FIGURES……....ix

LIST OF TABLES……..xi

ABBREVIATIONS…….....xii

SYNOPSIS……..xv

LIST OF PUBLICATIONS FROM PH.D. STUDIES…….xvii

LIST OF PH.D. WORK PRESENTATION IN CONFERENCES……xvii

1. Introduction……1

1.1 Haematopoiesis in Drosophila melanogaster…….....1

1.2 Lymph gland: Drosophila hematopoietic organ…….....1

1.3 Different zones of Lymph Gland……...2

1.3.1 Posterior Signalling Centre (PSC)……..3

1.3.2 Medullary Zone (MZ)…….3

1.3.3 Intermediary Zone (IZ)……...4

1.3.4 Cortical zone (CZ)……..5

1.4 Blood cell types…….....5

1.4.1 Plasmatocytes…….6

1.4.2 Crystal Cells……...6

1.4.3 Lamellocytes……..7

1.5 Mitochondria and TCA cycle……7

1.6 Acetyl-CoA……9

1.7 TCA cycle metabolites and their functions:…….10

1.7.1 Citrate……10

1.7.2 cis-Aconitate…….11

1.7.3 Itaconate……11

1.7.4 Isocitrate……11

1.7.5 α-ketoglutarate……..12

1.7.6 Glutamine and Glutamate……13

1.7.7 Succinyl-CoA……15

1.7.8 Succinate……...15

1.7.9 Fumarate……15

1.7.10 Malate and Oxaloacetate……16
1.8 Regulation of TCA cycle……16
1.9 Variations of TCA cycle: When TCA cycle is not much of a cycle……18
2. Aims and Objective……..20
2.1 Understand the role of TCA cycle in the maintenance and differentiation of blood progenitors…20
2.2 Investigate the contribution of TCA cycle in the regulation of lymph gland size……20
2.3 Investigate the cyclic nature of TCA cycle……21
3. TCA cycle balancing maintenance and differentiation of blood progenitors in lymph gland..21
3.1 TCA cycle controls progenitor maintenance in MZ……..…..21
3.2 TCA cycle regulate fate specification in CZ……..…..29
3.3 TCA cycle regulation in IZ of lymph gland……33
3.4 TCA enzymes transcript distribution in the LG……..….38
4. TCA cycle metabolites regulating progenitor proliferation and thereby controlling growth of lymph gland……..42
4.1 Source of citrate during LG development……..…..42
4.2 TCA cycle disconnect between iso-citrate and α-KG……..…44
4.3 Temporal analysis of LG growth……..…48
4.4 Importance of citrate for the development of lymph gland…….57
4.5 Importance of succinate for the development of lymph gland……61
5. Gene expression profile in TCA cycle mutants……65
6. Material and methods……..78
6.1 Drosophila husbandry, stocks and genetics……..78
6.2 Immunostaining and immunohistochemistry……78
6.3 Imaging and quantification of lymph gland phenotypes……...79
6.3.1 Lymph gland and Zone area analysis……..79
6.3.2 Crystals cells, and Caspase 3+ cells analysis……..80
6.3.3 Total, Dome+, and Dome- nuclei analysis……..80
6.3.4 Mitotic index for Dome+ and Dome- population……...80
6.4 SABER FISH……80
6.5 Metabolite supplementation……..97
6.6 RNA sequencing……...97
6.7 Software and Statistical analyses……..98
7. Discussion……..99
7.1 Temporal and spatial regulation of TCA cycle…….99
7.2 TCA cycle metabolites as regulators or signalling molecules……..99
7.3 Building up of TCA cycle……...100
8. References……...102

LIST OF FIGURES

Figure 1: Schematic to represent haematopoiesis in Drosophila……...2
Figure 2: Schematic to represent TCA cycle and shunting of its intermediates between mitochondria and cytosol……9
Figure 3: TCA cycle metabolites involved in chromatin modifications and DNA methylation……...10
Figure 4: Various Immunological functions performed by TCA cycle intermediates……....11
Figure 5: TCA cycle metabolites involved in HIF-α stabilization……..14
Figure 6: Glutamine metabolism within the cell……15
Figure 7: Regulation of TCA cycle via PDH complex……...18
Figure 8: Temporal and spatial growth of lymph gland and the GAL4 driver's expression in the respective zones of lymph gland……..22
Figure 9: TCA cycle in medullary zone is important for maintenance of blood progenitors in lymph gland of Drosophila larva……..23
Figure 10: Loss of TCA cycle in MZ favors plasmatocytes fate……24
Figure 11: Loss of TCA cycle in MZ negatively affect the crystal cell population……....25
Figure 12: TCA cycle in core progenitors (Tep4+; MZ) is important for maintenance of blood progenitors in lymph gland of Drosophila larva……...26
Figure 13: Blocking TCA cycle in core progenitors increases plasmatocytes (P1+) population in LG……..27
Figure 14: Blocking TCA cycle in core progenitors impact crystal cell (PPO+) population in LG……..28
Figure 15: α-Kdh regulates the proliferative capacity of cortical zone in LG……30
Figure 16: Loss of TCA cycle in CZ increases plasmatocyte fate in LG……31
Figure 17: Loss of certain steps of TCA cycle in CZ leads to reduction in crystal cell population in LG……32
Figure 18: Loss of TCA cycle in IZ favours plasmatocyte fate in LG……34
Figure 19: Loss of TCA cycle in IZ impacts crystal cell fate in LG……....35
Figure 20: Summary of TCA cycle regulation in different zones.....36
Figure 21: Schematic representation of SABER FISH technique……...38
Figure 22: Positive control LG images of SABER FISH to verify the technique……39
Figure 23a: Temporal distribution of TCA cycle enzymes transcripts, involved in LG growth, using SABER FISH……..40
Figure 23b: Temporal distribution of TCA cycle enzymes transcript, using SABER FISH……....41
Figure 24: Pdha derived Acetyl CoA does not fuel the TCA cycle in the early growth of LG in Drosophila larva……43
Figure 25: Pyruvate carboxylase (Pcb) catalysed Oxaloacetate (OA) fuels the TCA cycle in the early growth of LG in Drosophila larva……...45
Figure 26: Gdh fuels the TCA cycle via α-Kdh to regulated progenitor homeostasis and growth of LG in early development of Drosophila larva……47
Figure 27: Temporal analysis of CS^{RNAi}, $mAcon1^{RNAi}$, $\alpha\text{-}Kdh^{RNAi}$ and *GdhRNAi*……50
Figure 28: Quantification for temporal analysis for CS^{RNAi}, $mAcon1^{RNAi}$, $\alpha\text{-}Kdh^{RNAi}$, and Gdh^{RNAi}……..51
Figure 29: Temporal analysis to get the mitotic index for CS^{RNAi}, $mAcon1^{RNAi}$, $\alpha\text{-}Kdh^{RNAi}$ and *GdhRNAi*……..53
Figure 30: Temporal analysis for differentiation profile in CS^{RNAi}, $mAcon1^{RNAi}$, $\alpha\text{-}Kdh^{RNAi}$ and Gdh^{RNAi}……....54
Figure 31: Developmental profile of Sdh^{RNAi} and Mdh^{RNAi} in LG of Drosophila larva……56

Figure 32a: Citrate is necessary for the early development of LG in Drosophila larva……..58
Figure 32b: Citrate is necessary for the early development of LG in Drosophila larva……...60
Figure 33: Citrate and succinate food supplementation from the hatching itself to rescue the LG growth……62
Figure 34: Quantification for temporal analysis for *CS^{RNAi}*, *mAcon1^{RNAi}*, *α-Kdh^{RNAi}* and *Gdh^{RNAi}*……63
Figure 35: The making of TCA cycle from early growth of LG to the maintaninance of progenitors……64
Figure 36: PCA of the mapped reads for both batches together (*DW, Control; DS, Sdha^{RNAi}; DK, α-Kdh^{RNAi}; DA, mAcon1^{RNAi}; DM, Mdh^{RNAi}; DP, Pdha^{RNAi}*)……..67
Figure 37: Heatmap of 6 samples, showing top 50 genes with most variance (*DW, Control; DS, Sdha^{RNAi}; DK, α-Kdh^{RNAi}*; I and II are replicates)……68
Figure 38: Heatmap of 12 samples, showing top 50 genes with most variance *(DW, Control; DA, mAcon1^{RNAi}; DM, Mdh^{RNAi}; DP, Pdha^{RNAi}* ; Ia, IIa and IIIa are replicate**s)……...**69
Figure 39: Volcano plot showing top DEGs for DK vs DW……70
Figure 40: Volcano plot showing top DEGs for DS vs DW……71
Figure 41: Volcano plot showing top DEGs for DP vs DW……72
Figure 42: Volcano plot showing top DEGs for DM vs DW……73
Figure 43: Volcano plot showing top DEGs for DA vs DW……74
Figure 44: GO terms analysis of (A-B) *α-Kdh^{RNAi}* and (C-D) *Sdha^{RNAi}* (both upregulated and downregulated) (*DS, Sdha^{RNAi}; DK, α-Kdh^{RNAi}*)…….....75
Figure 45: GO terms analysis of (A-B) *mAcon1^{RNAi}* and (C-D) *Mdh^{RNAi}* (both upregulated and downregulated) (*DA, mAcon1^{RNAi}; DM, Mdh^{RNAi}*)……..…76
Figure 46: GO terms analysis of (A-B) *Pdha^{RNAi}* (both upregulated and downregulated) (*DP, Pdha^{RNAi}*), (C-D) Venn diagram representing overlap between all the mutants (Upregulated and downregulated)…….……...77

LIST OF TABLES

Table 1: RNA sequencing read statistics for the Batch-1 (DW, Control; DS, SdhaRNAi; DK, α-KdhRNAi)……65
Table 2: RNA sequencing read statistics for the Batch-2 (*DW, Control; DA, mAcon1^{RNAi}; DM, Mdh^{RNAi}; DP, Pdha^{RNAi}*)……66
Table 3: RNA sequencing read statistics between Batch-1 and Batch-2 controls (DW_I, Control Batch 1, DW_Ia, control Batch-2)……..66
Table 4: Fly lines used in the study and their source……78
Table 5: Antibodies used in the study and their sources……..79
Table 6: Primers for *Hml*……..82
Table 7: Primers for *Dome*……83
Table 8: Primers for *Kdh*……..84
Table 9: Primers for *Sdha*……86
Table 10: Primers for *Pdha*……..87
Table 11: Primers for *Gdh*……88
Table 12: Primers for *Skap*……89
Table 13: Primers for *CS*……90
Table 14: Primers for *mAcon1*……91
Table 15: Primers for *Idh*……93
Table 16: Primers for *Mdh2*……94
Table 17: Primers for *Pcb*……95
Table 18: List of Hairpins used ……96
Table 19: List of Imagers used ……97

ABBREVIATIONS

Dilps	*Drosophila* insulin like peptides
Dpp	decapentaplegic
Srp	Serpent
OA	oxaloacetate
mt-	mitochondria
α-KG	α-Keto Glutarate
ACLY/ATPCL	ATP citrate lyase
ETC	electron transport chain
TCA cycle	Tricarboxylic acid cycle
CS	citrate synthase
mAcon1	mt-Aconitase
Idh	Isocitrate dehydrogenase
α-Kdh	α-Keto Glutrate dehydrogenase
Skap	Succinate-CoA ligase
Sdha	Succinate dehydrogenase subunit a
Fum	*Fum*arase
*Mdh*2	Malate dehydrogenase 2
VDRC	Vienna *Drosophila* Resource Center
BDSC	Bloomington *Drosophila* Stock Center
PBS	Phosphate buffer saline
PBST	Phosphate buffer saline and Triton-X 100
PBSTw	Phosphate buffer saline and Tween-20
P1	Nimrod C1
Pxn	Peroxidasin
PPO	Prophenol oxidase
pH3	phosphorylated Histone 3
mys	myospheroid (β-integrin)
msn	misshapen
vkg	viking
Lz	lozenge
Ush	U-shaped (Friend of GATA member)

Crq	croquemort
Gcm	glial cell missing
SPARC	secreted protein acidic cysteine-rich
AGM	aorta–gonad–mesonephros
Hml	hemolectin
Tep4	thioester-containing protein 4
CHIZ	combined hematopoietic intermediate zone
CZ	Cortical Zone
IZ	Intermediary Zone
MZ	Medullary Zone
PSC	Posterior Signalling Centre
Gdh	Glutamate dehydrogenase
LG	Lymph Gland
Pdha	Pyruvate dehydrogenase Subunit-a
Pcb	Pyruvate decarboxylase
NGS	Normal Goat Serum
PCA	Principal Component Analysis
IRG1	immune-responsive gene 1
BMS*CS*	Bone Marrow derived Stem Cells
PPARγ	Peroxisome proliferator-activated receptor gamma
NO	Nitric oxide
PGE2	Prostaglandin E2
HATs	Histone Acetyl Transferases
PTMs	Post Translational Modifications
IFNγ	interferon-γ
L1	attila
Arj	Asrij
ECM	extra cellular matrix
Dop2R	Dopamine-2 like receptor
DW	*dome*MESOGAL4, UAS-GFP X Control (w1118)
DM	*dome*MESOGAL4, UAS-GFP X $Mdh2^{RNAi}$
DA	*dome*MESOGAL4, UAS-GFP X *mAcon1RNAi*
DK	*dome*MESOGAL4, UAS-GFP X α-Kdh^{RNAi}

DS	*dome*MESOGAL4, UAS-GFP X $Sdha^{RNAi}$
DP	*dome*MESOGAL4, UAS-GFP X $Pdha^{RNAi}$
Wg	wingless
CF	citrate food
SF	succinate food
AEL	after egg laying
SABER FISH	Signal Amplification By Exchange Reaction Fluorescence *In-Situ* Hybridization
ROS	reactive oxygen species
PD*P1*	pyruvate dehydrogenase phosphatases
PDK	Pyruvate dehydrogenase kinase
OXPHOS	Oxidative phosphorylation
CIC	citrate carrier
DMF	dimethyl Fumarate
MS	multiple sclerosis
KDMs	Lysine demethylases
GPCR	G-protein coupled receptor
SUCNR1	Succinate receptor-1
LPS	lipopolysaccharides
IL1-β	Interleukin 1-β
GOT-2	Glutamic oxaloacetic transaminase 2
NEAAs	Non-essential amino acids
GLS	glutaminase
GPT2	Glutamic-pyruvic transaminase 2
HIF1	Hypoxia inducible factor 1
VHL	von Hippel-Lindau tumor-suppressor factor
OGDD	2-oxoglutarate-dependent dioxygenases
KEA*P1*	Kelch-like ECH-associated protein 1
NRF2/NFE2C2	nuclear factor erythroid 2-related factor 2
ATF3	cyclic AMP-dependent transcription factor
DMI	Dimethyl Itaconate
AD	Alzheimer’s Disease
MCI	mild cognitive impairment

SYNOPSIS

Chapter 1: Introduction

Haematopoiesis in *Drosophila melanogaster*

Haematopoiesis, the process of blood cell development, is a fundamental biological phenomenon conserved across metazoans. *Drosophila melanogaster*, a model organism, has contributed significantly to our understanding of haematopoiesis due to its genetic tractability and developmental simplicity. Despite differences in complexity between *Drosophila* and vertebrates, the fundamental principles and genetic pathways regulating blood cell development are remarkably conserved, making *Drosophila* an ideal system for studying haematopoiesis. In *Drosophila*, haematopoiesis occurs in two waves; first one is called Embryonic or primitive Haematopoiesis occurs during embryonic stage 5 from the head mesoderm, which is marked by the expression of mammalian GATA homologue Serpent (Srp) (1–3). The second wave or definitive haematopoiesis, initiates from lateral mesoderm derived from the anterior trunk segment during mid-embryogenesis give rise to a small population of cells which homes around the dorsal vessel/heart and will subsequently develop into a hematopoietic organ called Lymph gland (4, 5). The lymphoid lineage in *Drosophila* is found to be absent whereas the hemocytes present are comparative to the mammalian myeloid (6–9). Prohemocytes are multipotent progenitors which give rise to three mature blood cell populations, functionally important for all stages of life, namely plasmatocytes, crystal cells and lamellocytes (10–13)**.**

TCA cycle and its variations

Mitochondria is regarded as an organelle of extreme importance to the cell as it is considered as the powerhouse of the cell, as it is the main site for ATP production in the oxidative respiration. But mitochondria have much more to its credit than this; the usual notion is that mitochondria execute its activity under the nuclear command, however it is now established that its rather bidirectional regulation. For complex and high energy functions (e.g. differentiation, stress adaptation, etc.) cells have to take mitochondrial fitness into account. Also mitochondria can influence nuclear genes to regulate different cellular functions (14)**.** Cellular respiration is a food web of biochemical reactions that fuels the growth and survival of the cell which in turn supports the organism, through three major outputs; energy (ATP),

reducing equivalents (glutathione, NADH, FAD, etc.), and macromolecular precursors (Amino acids, nucleotides, simple sugars). Conventionally TCA cycle begins with the condensation of oxaloacetate (OA; 4-carbon) with acetyl CoA (2-carbon) to generate citrate (6-carbon). Subsequent reactions oxidize citrate to generate two CO_2 molecules, one GTP, four reducing equivalents (three NADH and one $FADH_2$) and finally regenerate the OAA. (15, 16). But there are versions of TCA cycle reported across the literature in different cell states, e.g. conversion of pyruvate to mt-OA and glutaminolysis (glutamine to α-KG, through glutamate) in the events of citrate being exported to cytosol; glutamine dependent reductive carboxylation, here the cycle runs backward from glutamine derived α-KG to produce citrate, due to non-functional ETC (17–19). Citrate-malate shuttle is being utilised by cancer cells, Immune cells as well as ES*CS* to send the citrate out in the cytosol, where it is broken down with the help of ATP Citrate Lyase (ACL) into OAA and acetyl CoA, followed by cytosolic-OA reduced to malate and transported back to the mitochondria. Another scenario where non-canonical TCA cycle can come into play is when oxygen cannot be accessed as terminal electron acceptor, due to ETC inhibition, *SDH* complex reduces Fumarate to succinate and Fumarate acts as the electron acceptor to adapt the cell in oxygen limiting conditions (20–22).

Similar to above mentioned scenarios our work also highlights an interesting non-canonical version of TCA cycle which takes place in the *Drosophila* larval lymph gland development where only a few steps are found to be necessary, in comparison to the progenitor maintenance, where almost all the steps (*CS* to *Sdh*) are found to be important. Our work also brings out the importance of citrate in the early development of lymph gland by regulating progenitor and non-progenitor proliferation and keeping a check on the differentiation.

The current study titled **'metabolic regulation of blood progenitor homeostasis by TCA cycle for *Drosophila* larval development'** is divided into six chapters. The first chapter highlights and reviews the literature on *Drosophila* haematopoiesis and TCA cycle and its variants, as well as discusses open questions. The second chapter describes the objectives of the study highlighting the role of TCA cycle in the development of lymph gland as well as maintenance of progenitor population in lymph gland. The third chapter deals with material and methods of the thesis, *Drosophila* geneti*CS*, immunohistochemistry, confocal imaging and metabolite supplementation to achieve the objectives of the thesis. Chapter four discusses the findings of the thesis and is divided into four main parts. Chapter four (Part 1) of the thesis, highlights the importance of TCA cycle for the maintenance and development of blood progenitors in lymph gland. Chapter four (Part 2) deals with the disconnect between aconitase

and *α-Kdh*in the early development of lymph gland. Chapter four (Part 3) traces the developmental defect of lymph gland growth by temporal analysis in different mutants (*CS*, *mAcon1* and *α-Kdh*). Chapter four (Part 4) establishes Citrate in progenitor compartment is necessary early in the development for the growth of lymph gland. The Fifth chapter highlights future directions and our contribution to current understanding of similar mechanisms during blood-progenitor development in both invertebrates and vertebrates.

Chapter 2: Objectives

This thesis work describes **"metabolic regulation of blood progenitor homeostasis by TCA cycle for *Drosophila* larval development",** highlights that the TCA cycle controls the development, maintenance and differentiation of progenitors in lymph gland. For the development part, we have identified that only a few steps (OA to Succinyl CoA) not the whole TCA cycle regulates the lymph gland development. Whereas the whole cycle, except for *Fum* and *Mdh*, contribute for the maintenance of progenitor population. Which propose the idea that a variant of TCA cycle with a few steps comes up first during the development, which later on completes as a full cycle regulating the maintenance and differentiation of blood cells.

The specific objectives of this thesis are described below:

1. To understand the importance of TCA cycle in the development, maintenance, heterogeneity and differentiation of blood progenitors
2. To understand the metabolic aspect of LG size defect through temporal analysis in progenitor population

Chapter 3: Materials and Methods

Various *Drosophila* stocks used in this study were obtained from Vienna *Drosophila* Resource Centre (VDRC), Bloomington *Drosophila* Stock centre (BDSC) or were requested from the different research groups. All fly stocks were reared on corn meal agar medium with yeast supplementation at 25°C incubator unless specified. The crosses involving RNAi lines were maintained at 29ºC to maximize the efficacy of the Gal4/UAS RNAi system. Controls refers to either w1118 (control) or Gal4 drivers crossed with w1118. For staining blood cell progenitors, 3rd instar larval lymph glands were dissected out in 1X PBS and fixed in 4% formaldehyde solution, for 15 min. Post-fixation the tissues were permeabilized by 3 washes of 15 min each in 0.3% PBST (0.3% Triton-X in 1X PBS). Tissues were then blocked in 5%

NGS (Normal Goat Serum), followed by overnight primary antibody treatment. Next day tissues were washed (as earlier) and incubated in secondary antibodies for 2-3 hours, followed by washing (as earlier) and mounting in mounting media. Immunohistochemistry on lymph gland was performed with the following primary antibodies: mouse α-*P1* (1:30, I. Ando), rabbit α-*Pxn* (1:1000, J. Shim), mouse α-Myo (1:100, DSHB), rabbit α-*PPO* (1:200, H. M. Müller), and α-DHE (1:1000, Life technologies), rabbit α-pH3 (1:100; *CS*T 3642S), rabbit α-Caspase 3 (1:200; *CS*T 9661S). All the secondary antibodies were used at 1:500 dilutions, those are FITC, Cy3 and Cy5 (Jackson Immuno Research Laboratories) and Alexa Fluor 488, 546, 647 (Invitrogen). Nuclei were visualized using DAPI/Hoechst-33342 (Sigma B2261). Samples were mounted in mounting media (Vectashield, Vector Laboratories). Immuno-stained images of lymph glands were acquired using Olympus FV3000 confocal microscopy on 40X oil-immersion objective. Image was scanned with a frame size of 800 X 800 with 0.5/1/2um thickness for Z-stack, depending upon the experiment. All images were quantified using ImageJ software (NIH, USA). For that roughly, middle two confocal Z-stacks were merged and area was selected according to the respective staining and measured with the help of freehand selection tool of ImageJ software, followed by using the "measure tool" under "analysis tool" to get the area values. This was done for respective zones, where *Tep4* or *Dome* area represents the progenitor zone, *Dome*/*Pxn* area represent differentiating or intermediary zone, *Pxn*/*P1* and Hml/*P1* area represent differentiated zone. The areas were represented in percent values with respect to the total area of the respective lobe. Controls were analysed in parallel to the tests every time. A minimum of 10-15 animals were analysed each time and the experiment was repeated at least three times. The quantifications represent the mean (% area) of the independent experimental sets. Crystal cell population, as well as Caspase 3+ cells were analysed by counting total number of cells across the Z-stacks by merging all the stacks of lymph gland. These cell counts are represented as the total number of cells per lymph gland lobe. To count the total nuclei, we used the ImageJ software (NIH, USA). All the stacks of the lymph gland were merged with the help of "Z stack tool" and the primary lobe was outlined by the freehand selection tool, followed by "clear outside tool" under "edit option" to remove the other tissues (e.g. ring gland, secondary, tertiary lobes, dorsal vessel etc.). The nuclei of the remaining primary lobe were then threshold using "threshold tool" under "Image-adjust option" to obtain 8-bit image in single channel. The image obtained is then subjected to "watershed tool" under "Process-Binary option" followed by "particle analysis" with particle size 3-infinity and circularity of 0.04-1.00. This gave the total number of particles (nuclei) which were marked by Hoechst dye, in blue channel. Similarly, for *Dome*+ nuclei only green

channel was subjected to this mentioned processing and for the *Dome*- nuclei *Dome*$^{+}$ nuclei were subtracted from total nuclei for the respective lobes. Total pH3^{+} cells were counted by merging all the Z-stack together to give total number of pH3^{+} cells in the entire lobe. For assessing pH3^{+} population in *Dome*$^{+}$ zone, *dome*GFP channel was overlaid onto pH3 channel and for the *Dome*$^{-}$ pH3^{+} cells *Dome*$^{+}$ pH3^{+} cells were reduced from total pH3+ cells. Supplemented food was prepared by adding metabolites (1% citrate and 3% succinate; weight/volume) to the regular fly food. Eggs or larvae of respective stages were transferred to the supplemented food according to the experimental requirements for lymph gland analysis. In early feeding only the larvae were transferred back to the regular food after rearing on supplemented food for further development. Controls for the respective experiments were always treated similarly. All statistical analyses were performed using GraphPad Prism 10 software and Microsoft Excel 2010. The medians were analysed using Mann-Whitney test, two-tailed and means were analysed with unpaired t-test, two-tailed. For all the experiments batch effects were plotted.

Chapter 4: Results and Conclusions

4.1 TCA cycle is necessary for the maintenance and development of blood progenitors in lymph gland

To investigate the influence of this metabolic cycling in the maintenance of progenitor homeostasis and development of lymph gland, we utilized the binary system approach (UAS-GAL4). We systematically knock down each step of the TCA cycle with the help of four different GAL4s, which were temporally segregated but at the same time overlapping to certain extent. The GAL4s used in the study are *Tep4-GAL4,UASmcherry* (Core or subset of progenitors*), domeMESO-GAL4,UAS-GFP* (MZ), *ChIZ-GAL4* (IZ), *and Hml-GAL4,UAS-2X EGFP* (CZ) in the order of their temporal expression.

By perturbing the enzymes of TCA cycle individually in the progenitor compartment at wandering 3rd instar larval stage, with *domeMESO-GAL4,UAS-GFP* drivers we observed two very different phenotypes arising independent of each other. One of the phenotypes was found to be related to maintenance of the progenitor pool and regulation of differentiation. Here we found that for the progenitor maintenance, the TCA cycle was found to be functioning together for almost its entire length except for *Fum* and *Mdh* steps, which did not show any progenitor loss or increase in differentiation profile. The loss of progenitor population was observed by

loss of GFP positive area expressed by *domeMESO-GAL4,UAS-GFP* compared to respective controls. For *domeMESO-GAL4,UAS-GFP* driver the reduction in the progenitor population is either compensated by increase in the double positive (*Dome*$^{+}$ *Pxn*$^{+}$) population or the *Pxn*$^{+}$ only population, we also observed around 15% increase in the plasmatocyte population marked by *P1*. The crystal cells, marked by *PPO* were found to be significantly decreased in the *CS, mAcon1, α-Kdh, Skap* and *Sdha* whereas there was a significant increase in the crystal cells in the *Idh* step while no change was observed in the *Fum and Mdh2* steps. Lamellocytes were not observed by manipulating any step of the TCA cycle.

We also tried to understand the influence of the subset of early progenitors on the lymph gland with the help of *Tep4-GAL4,UASmcherry*. Upon knocking down individual steps of the TCA cycle in these progenitor subset, the loss of progenitor was observed in all the steps at wandering 3rd instar larval lymph gland. This loss of progenitor population was found to be compensated by *Tep4- Pxn-* population, which is speculated to be *Dome*$^{+}$ only population, as no significant changes were noted in the *Pxn+* population. No significant change was observed in the plasmatocyte population (*P1*$^{+}$)**,** whereas crystal cells, marked by *PPO* were found to be significantly decreased in the *CS, mAcon1, α-Kdh, Skap* and *Sdha* whereas there was a significant increase in the crystal cells in the *Idh* step while no change was observed in the *Fum and Mdh2* steps.

Also to understand whether this regulation on progenitor maintenance is autonomous or non-autonomous, we also perform the knock down of TCA in the differentiating population with the help of *ChIZ-GAL4* (IZ), and *Hml-GAL4,UAS-2X EGFP* (CZ) drivers marking respective zones. *ChIZ-GAL4* marks the IZ which is an overlapping population of MZ and CZ (*Dome*$^{+}$ Hml^{+}). Manipulating the TCA cycle in this compartment does not lead to any increase in the differentiating population area (*Pxn*$^{+}$) which indirectly highlights that there is no feedback from this population to the progenitor maintenance involving TCA cycle. In case of CZ marked by *Hml-GAL4,UAS-2X EGFP,* we did not observed any change in the either of the differentiating population (Hml^{+} area or *Pxn*$^{+}$ area), this further strengthens the results from *ChIZ-GAL4* and highlights the fact that the progenitor homeostasis is the autonomous function of the progenitor compartment through TCA cycle.

The other phenotype observed due to the knockdown of TCA cycle genes in the progenitor compartment was a growth defect of the lymph gland. With *domeMESO-GAL4,UAS-GFP* driver we observed the lymph gland growth defect at *CS, mAcon1, and α-Kdh*steps

whereas with *Tep4-GAL4,UASmcherry* driver the growth defect was observed at *mAcon1 and α-Kdh*only highlighting two important aspects; firstly *CS* is not necessary in the *Tep4* compartment of the growth and second is that TCA does not run as a cycle early in development at least for the growth of lymph gland as the *Idh* step which connects *mAcon1* with *α-Kdh*does not show growth defect in any of the progenitor compartments. Similar results were seen in the IZ where growth defects were observed in *mAcon1, Idh and α-Kdh,* suggesting the coming together of the whole cycle whereas in CZ growth defect were observed in *CS, mAcon1, and α-Kdh* steps.

4.2 What fuels *A-Kdh*for early development of lymph gland in progenitors

The next question we asked was if not *CS* and *mAcon1,* what fuels the *α-Kdh*enzyme? From the available literature we got to know that the *Gdh* can also work reversibly and convert the glutamate into alpha-keto Glutrate. We first tested *Gdh* for the progenitor loss, differentiation profile and growth defect at 3rd install larval stage as was done for all other steps. We found that *GdhRNAi* recapitulated all the phenotypes of the *α-Kdh*knockdown from decrease in progenitor population, increase in double positive ($Dome^{+}Pxn^{+}$) population, increase in *P1* population, decrease in PPO^{+} crystal cells to growth defect. This convinced us to believe that *A-Kdh*was fueled by *Gdh* in the early development of LG. We further did the temporal analysis of the *Gdh* and found that similar to the *α-Kdh*, the growth defect was observed in *Gdh* at 48h itself, both $Dome^{+}$ and $Dome^{-}$ compartments were equally compromised similar to *α-Kdh* and also the mitotic activity (pH3) was also equally compromised in both the compartments. These results further validate the connection between *α-Kdh*and *Gdh*.

4.3 Temporal analysis of lymph gland development in *CS, mAcon* and *α-Kdh*knockdowns

The growth defect phenotype was common amongst all three CS^{RNAi}, *mAcon1RNAi* and $\alpha\text{-}Kdh^{RNAi}$ mutants, at wandering 3rd instar larval stage. It could be due to two different scenarios: a) due to cell death (apoptosis) and b) due to non-proliferation (cell cycle arrest). We first explored the apoptosis possibility; where we stained the wandering 3rd instar larval lymph gland with Cleaved-Caspase 3 antibody to mark apoptotic nuclei in all the mutant backgrounds with growth phenotype. We used Hml^{Δ}*-Gal4, UAS-GFP; UAS-Hid* as a positive control for Hid being activator of apoptosis, Caspase 3 puncta were observed around the nuclei. Whereas the mutants in study did not show any considerable change in comparison to the positive control, which negated apoptosis as a reason for size defect.

To understand the lymph gland growth defect due to knockdown of certain steps of TCA cycle we tracked the development of lymph gland temporally at 48h, 72h, 96h and 120h respectively. For this study we utilized the progenitor specific *domeMESO-GAL4,UAS-GFP*. Upon temporal analysis we found both CS^{RNAi} and $mAcon1^{RNAi}$ had shown growth defect at 96h whereas α-Kdh^{RNAi} had shown growth defect at the 48h time point itself; growth defect was analysed by counting the total number of nuclei per LG lobe in the mutants compared to the respective controls. When we further analysed the $Dome^{+}$ vs $Dome^{-}$ population in the respective lobes, we observed that the $Dome^{+}$ population was found to be reduced in both CS^{RNAi} and $mAcon1^{RNAi}$ at the 72h itself highlighting the fact that the growth defect arising at the 96h is the result of reduction in the $Dome^{+}$ (Progenitor) population. Growth defect was not observed at the 72h itself due to the compensatory effect of *Dome-* (non-progenitor) population, but this population also could not compensate for long and therefore growth defect was observed at the 96h. Whereas in α-Kdh^{RNAi} the defect was equally noticed in both $Dome^{+}$ as well as *Dome-* compartments from the 48h itself.

To understand why the proliferative capacity of the $Dome^{+}$ (progenitors) cells is compromised we checked the differentiation profile of the LG temporally with the help of differentiation markers *Pxn* and *P1*. To our surprise in both CS^{RNAi} and *mAcon1RNAi* mutants we observed precocious differentiation, as we saw *Pxn* and to certain extent *P1* positive cells at 48h itself, whereas the same wasn't observed for the α-Kdh^{RNAi} mutant. This was an important finding as here the cells were found to be dividing to differentiate rather than dividing to proliferate and this could be the major reason for *CS* and *mAcon1* enzyme knockdown to end up in small LG. These results also highlight another important aspect that *α-Kdh*enzyme doesn't function in sync with the *CS* and *mAcon1* even though all of them had the same end phenotype (growth defect). Also knockdown of *Idh*, which is a connection between these enzymes, in TCA cycle, do not show any growth defect, this further supports the fact that *α-Kdh* is functioning independent of both *CS* and *mAcon1* at least early in development for the growth of LG.

4.4 Citrate in progenitor compartment is necessary early in the development for the growth of lymph gland

Since loss of *CS* and *mAcon1* led to the growth defects we next tried to rescue the phenotype by supplementing the affected/ lost metabolite. We started with the supplementation of the product of *CS* (Citrate). With the help of available literature and screening we standardize the concentration of citrate to be 1% weight/volume. We transferred the embryos to 1% CF and

allowed them to grow and dissected the LG at 3rd instar larval stage (120h). To our surprise the *CS* mutant LG further reduced and even control LG reared on 1% CF, compared to their own replicates on NF (Normal fly food), had shown the growth defect, since the larvae were reared completely on the supplemented food, the defect might be due to excess of citrate, which can also act as a stress signal. We then divided the larval growth trajectory into two parts based on the timing of onset of differentiation i.e., pre-differentiation and post-differentiation phase separated at 60h AEL time point. We next transferred the 2nd instar larvae at 60h AEL onto the 1%CF and allowed it to develop and at wandering 3rd instar (120h) dissected the LG for the analysis. Here also we could not rescue the growth defect. Finally, we transferred the embryos to the 1% CF and at 60h AEL (Pre-differentiation phase), they were again transferred back to the NF for further development and again at 120h of development the LG were dissected out and this time we saw growth defects being rescued. We also confirmed the rescue of the progenitor homeostasis with the help of *Pxn* and *P1* in 1% CF supplementation till 60h AEL. These results highlight the importance of citrate in early development of lymph gland.

Chapter 5: Discussion

With the provided data we have shown that early in development TCA cycle does not behave cyclic rather act as discrete set of steps regulating growth non-autonomously (*CS* and *mAcon1*) as well as autonomously (*α-Kdh* and *Gdh*). Here *CS* and *mAcon1* non autonomously promote progenitor proliferation by inhibiting the differentiation as well as checking the proliferation of non-progenitor population. This indirectly helps the *α-Kdh* and *Gdh* to promote progenitor proliferation autonomously. We have established the requirement of the citrate in the early development (upto 60h) of the lymph gland with the help of 1% citrate supplementation in the food. Later around the 60h AEL it was found that *Idh* bridges the gap between *mAcon1* and *α-Kdh*, which also coincides with the time developmentally where the differentiation kicks in, and with our results too, we found that TCA becomes important for the maintenance of the blood progenitors by keeping a check on differentiation.

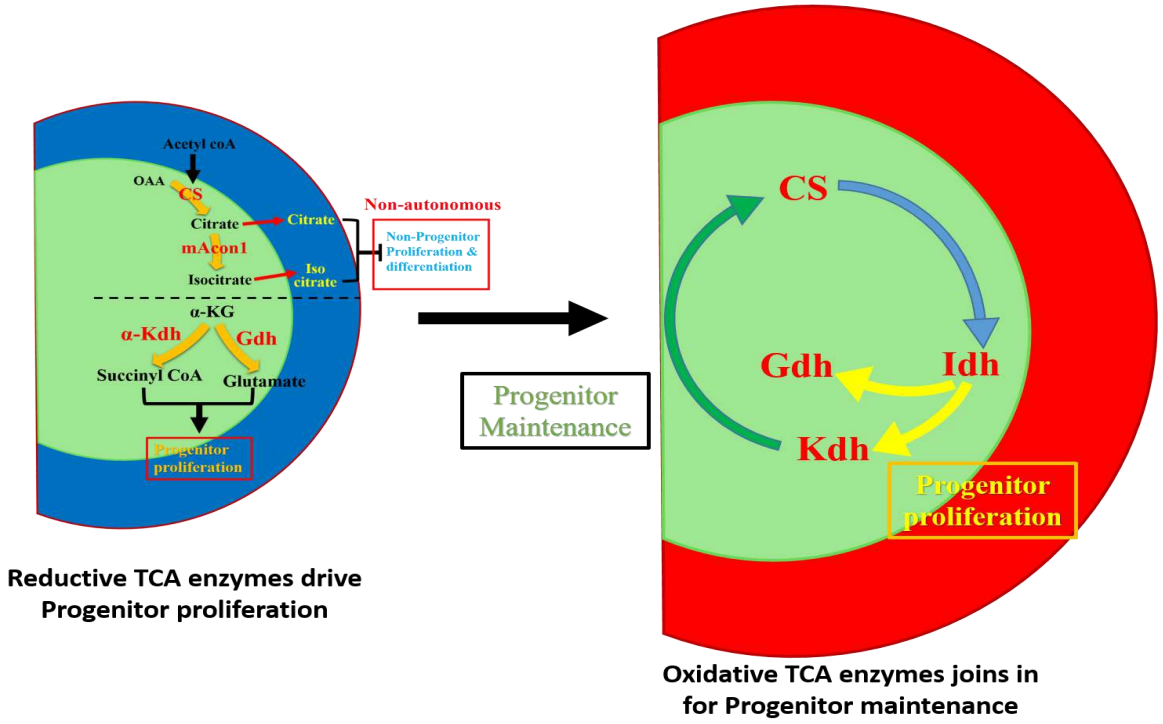

Figure 1. **Group of discrete steps regulating lymph gland growth to the cyclic TCA for the maintenance of blood progenitors.** The model describes the importance of TCA cycle enzymes regulating growth and progenitor maintenance in lymph gland. All enzymes that promotes growth are shown in red, whereas their metabolites are shown in black. The first picture shows the transition from discrete steps important for growth in early development (till 60h AEL) to cyclic TCA important for progenitor maintenance post 60h AEL in the second picture. The green zone in the lymph gland cartoon represent the progenitor zone (MZ), blue zone represents the differentiating population (IZ) and the red zone represent the differentiated zone (CZ).

REFERNCES OF SYNOPSIS

1. T. Lebestky, T. Chang, V. Hartenstein, U. Banerjee, Specification of *Drosophila* hematopoietic lineage by conserved transcription factors. *Science* **288**, 146–149 (2000).

2. K. P. Rehorn, H. Thelen, A. M. Michelson, R. Reuter, A molecular aspect of hematopoiesis and endoderm development common to vertebrates and *Drosophila*. *Dev. Camb. Engl.* **122**, 4023–4031 (1996).

3. U. Tepass, L. I. Fessler, A. Aziz, V. Hartenstein, Embryonic origin of hemocytes and their relationship to cell death in *Drosophila*. *Dev. Camb. Engl.* **120**, 1829–1837 (1994).

4. A. Holz, B. Bossinger, T. Strasser, W. Janning, R. Klapper, The two origins of hemocytes in *Drosophila*. *Dev. Camb. Engl.* **130**, 4955–4962 (2003).

5. A. Rugendorff, A. Younossi-Hartenstein, V. Hartenstein, Embryonic origin and differentiation of the *Drosophila* heart. *Rouxs Arch. Dev. Biol.* **203**, 266–280 (1994).

6. S. Akira, K. Takeda, T. Kaisho, Toll-like receptors: critical proteins linking innate and acquired immunity. *Nat. Immunol.* **2**, 675–680 (2001).

7. S. Cherry, N. Silverman, Host-pathogen interactions in *drosophila*: new tricks from an old friend. *Nat. Immunol.* **7**, 911–917 (2006).

8. D. Hultmark, Insect immunology. Ancient relationships. *Nature* **367**, 116–117 (1994).

9. A. Kleino, N. Silverman, The *Drosophila* IMD pathway in the activation of the humoral immune response. *Dev. Comp. Immunol.* **42**, 25–35 (2014).

10. C. J. Evans, U. Banerjee, Transcriptional regulation of hematopoiesis in *Drosophila*. *Blood Cells. Mol. Dis.* **30**, 223–228 (2003).

11. V. Hartenstein, Blood cells and blood cell development in the animal kingdom. *Annu. Rev. Cell Dev. Biol.* **22**, 677–712 (2006).

12. R. Lanot, D. Zachary, F. Holder, M. Meister, Postembryonic hematopoiesis in *Drosophila*. *Dev. Biol.* **230**, 243–257 (2001).

13. B. Lemaitre, E. Nicolas, L. Michaut, J. M. Reichhart, J. A. Hoffmann, The dorsoventral regulatory gene cassette spätzle/Toll/cactus controls the potent antifungal response in *Drosophila* adults. *Cell* **86**, 973–983 (1996).

14. N. S. Chandel, Evolution of Mitochondria as Signaling Organelles. *Cell Metab.* **22**, 204–206 (2015).

15. H. A. Krebs, L. V. Eggleston, The oxidation of pyruvate in pigeon breast muscle. *Biochem. J.* **34**, 442–459 (1940).

16. D. G. Ryan, L. A. J. O'Neill, Krebs Cycle Reborn in Macrophage Immunometabolism. *Annu. Rev. Immunol.* **38**, 289–313 (2020).

17. C. Lussey-Lepoutre, *et al.*, Loss of succinate dehydrogenase activity results in dependency on pyruvate carboxylation for cellular anabolism. *Nat. Commun.* **6**, 8784 (2015).

18. C. M. Metallo, *et al.*, Reductive glutamine metabolism by *IDH*1 mediates lipogenesis under hypoxia. *Nature* **481**, 380–384 (2011).

19. A. R. Mullen, *et al.*, Reductive carboxylation supports growth in tumour cells with defective mitochondria. *Nature* **481**, 385–388 (2011).

20. C. M. Bisbach, *et al.*, Succinate Can Shuttle Reducing Power from the Hypoxic Retina to the O2-Rich Pigment Epithelium. *Cell Rep.* **31**, 107606 (2020).

21. E. T. Chouchani, *et al.*, Ischaemic accumulation of succinate controls reperfusion injury through mitochondrial ROS. *Nature* **515**, 431–435 (2014).

22. J. B. Spinelli, *et al.*, Fumarate is a terminal electron acceptor in the mammalian electron transport chain. *Science* **374**, 1227–1237 (2021).

LIST OF PUBLICATIONS DURING PhD

1. Kapoor A, Tomar A*, Mukherjee T. (2023). Pumping up the blood progenitors by Piezo. Proc Natl Acad Sci U S A. 2023 Jun 6;120(23): e2306004120. doi: 10.1073/pnas.2306004120. (*Co- First author)
2. Goyal, M., Tomar, A., Madhwal, S., & Mukherjee, T. (2022). Blood progenitor redox homeostasis through olfaction-derived systemic GABA in hematopoietic growth control in *Drosophila*. Development (Cambridge, England), 149(8), dev199550. https://doi.org/10.1242/dev.199550
3. Preethi P, Tomar, A., Madhwal, S., & Mukherjee, T. (2020). Immune Control of Animal Growth in Homeostasis and Nutritional Stress in *Drosophila*. Frontiers in Immunology. https://doi.org/10.3389/fimmu.2020.01528

LIST OF Ph.D. WORK PRESENTATION IN CONFERENCES

1. Poster presented at International Society for Stem Cell Research (ISSCR 2024), Hamburg, Germany (10-13 July 2024)
2. Poster presented at 19th International Congress of Developmental Biology by ISDB, Algarve Congress Centre, Herdade dos Salgados, Guia, Portugal (16-20 Oct 2022)
3. Poster presented at International Society for Stem Cell Research (ISSCR 2022), San Francisco (Virtual) (15-18 June 2022)
4. Poster presented at Indian *Drosophila* Research meeting (InDRC), by Indian Institute of Science Education and Research (IISER), Kolkata (Virtual). (13-17 Dec 2021)

1. Introduction

1.1 Haematopoiesis in *Drosophila melanogaster*

Haematopoiesis, the process of blood cell development, is a fundamental biological phenomenon conserved across metazoans. *Drosophila melanogaster*, a model organism, has contributed significantly to our understanding of haematopoiesis due to its genetic tractability and developmental simplicity. Despite differences in complexity between *Drosophila* and vertebrates, the fundamental principles and genetic pathways regulating blood cell development are remarkably conserved, making *Drosophila* an ideal system for studying haematopoiesis. In *Drosophila*, haematopoiesis occurs in two waves; the first, called embryonic or primitive haematopoiesis occurs during embryonic stage 5 from the head mesoderm, which is marked by the expression of mammalian GATA homologue Serpent (Srp) (Figure 1A) (1–3). The second wave or definitive haematopoiesis, initiates from the lateral mesoderm derived from the anterior trunk segment during mid-embryogenesis give rise to a small population of cells which homes around the dorsal vessel/heart and will subsequently develop into a hematopoietic organ called lymph gland (Figure 1B-C) (4, 5). The lymphoid lineage in *Drosophila* is absent whereas the hemocytes present are comparable to the mammalian myeloid lineage (6, 8, 9). Hemocytes in *Drosophila* majorly play two significant roles: 1) developmentally they identify and remove dead cells and debris, and also secrete and remodel extracellular matrix (ECM) components critical to morphogenesis; 2) immunity, where hemocytes in crosstalk with fat body (major source of antimicrobial peptides (AMPs), clears out the pathogens (23–28).

1.2 Lymph gland: *Drosophila* hematopoietic organ

During the definitive wave of haematopoiesis, cardiac mesoderm gives rise to both dorsal vessel as well as a cluster of cells around the dorsal vessel, which later on constitute lymph gland (5). These hemangioblast cells, arising from cardiac mesoderm, proliferate asymmetrically to produce one daughter cell which belongs to the dorsal vessel and the other to the lymph gland (29), this process is analogous to the vertebral aorta–gonad–mesonephros (AGM) mesenchyme (30). Unlike primitive haematopoiesis, lymph gland hemocytes do not differentiate in the embryo; rather, they proliferate extensively during the early larval development, giving rise to 3-4 bilobed structures, namely primary, secondary, tertiary and quaternary lobes (31) (Figure1B-C). Differentiation in the lymph gland is observed around the

late 2nd instar larva in the primary lobe with the expression of Lozenge (*Lz*), a crystal cell marker (1).

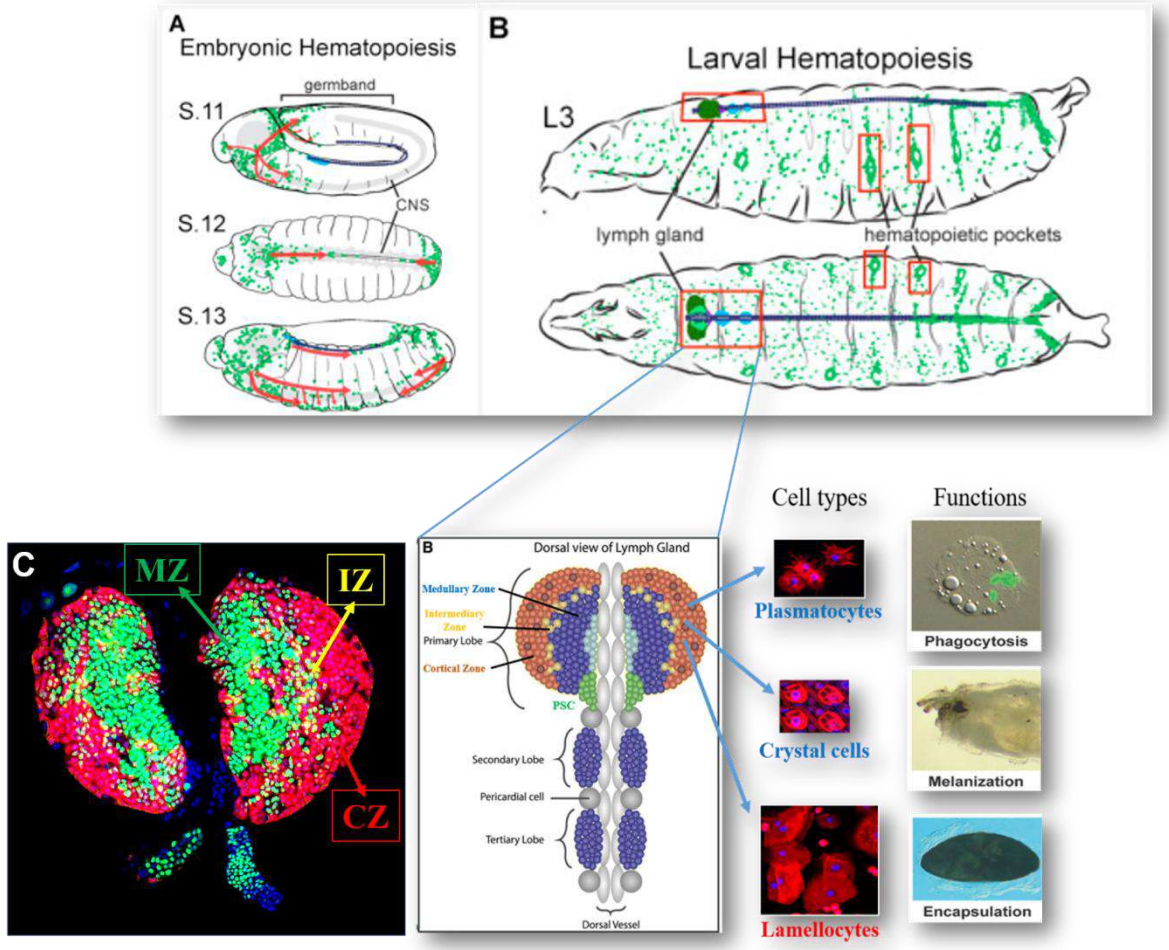

Figure 1: Schematic to represent haematopoiesis in *Drosophila*.

(A) pictorial representation of embryonic haematopoiesis in *Drosophila*. **(B)** Representation of larval haematopoiesis i.e., circulating pool and lymph gland, also zonal representation of lymph gland with all three blood cell types and their general immune function. (C) confocal image of LG highlighting zonation MZ (*Dome*$^{+}$; green), IZ (*Dome*$^{+}$ Hml^{+}; yellow) and CZ (Hml^{+}; red). This figure is a modified version from three different authors (32–34)

1.3 Different zones of Lymph Gland

On the basis of developmental markers, the anterior-most primary lobes of the lymph gland can further be divided into several zones, each zone harbours cells with distinct identities in terms of their maturation and functionality. These zones are medullary zone (MZ), intermediary zone (IZ), cortical zone (CZ) and posterior signalling centre (PSC) (Figure 1C). This subdivision of the primary lobe highlights spatial and temporal regulation during larval development.

1.3.1 Posterior Signalling Centre (PSC)

It is the first zone to be demarcated as a separate cluster in the embryo, which also develops into 30-40 cells by 3rd instar larval stage and reside at the posterior end of the primary lobe (Figure1B). These PSC cells do not contribute to the blood cell population; rather, they serve as a niche to regulate the maintenance or differentiation of blood progenitor cells in the lymph gland (35–44). Antennapedia (*Antp*), hedgehog (*Hh*), and collier, are the identification markers for PSC cells (36, 41, 45). Antp overexpression leads to an increase in PSC cells, which indirectly increases progenitor maintenance and suppresses progenitor proliferation (1, 36, 41). *Dpp* and *Wg* pathways work antagonistically to each other to maintain the size of PSC, where *Dpp* acts as an inhibitor of PSC proliferation, whereas *Wg* supports the PSC proliferation (43, 46). PSC growth and proliferation are also regulated by the insulin pathway, *Drosophila* Insulin like peptides (*dilps*) are expressed in glia, neurons and fat body, but not in lymph gland (35, 44, 47, 48), highlighting the systemic regulation of PSC.

1.3.2 Medullary Zone (MZ)

The MZ consists of the blood progenitor cells, which are dependent on a plethora of signals originating from three different sources: autonomous/autocrine signals from the MZ itself, secreted/paracrine signals from different zones of LG and systemic signals as a result of internal and external sensing (37, 38, 49–51). These progenitor cells can be specifically marked by the expression of Serpent (Srp), Odd, thioester-containing protein 4 (*Tep4*), *dome*less (*Dome*), *Wg/wnt*, E-cad, and ROS (52, 53). During 1st and early 2nd instar larval stage, most non-PSC cells of LG are *Dome*$^{+}$, except for a few pre-progenitors. These *Dome+* cells are found to be extensively proliferative until mid to late 2nd instar stage, after which the proliferation slows down as differentiation is first observed in the LG and IZ and CZ becomes prominently different from MZ (38, 50). The MZ cells are tightly arranged and maintain their progenitor state due to their expression of adhesion molecule E-cadherin (E-cad), as loss of E-cad expression in MZ induces cell differentiation (38, 54, 55). Loss of *Wg* signalling results in the E-cad dependent progenitor differentiation, leading to an increase in the IZ cells (expressing both MZ and CZ markers), whereas overexpression of *Wg* results in progenitor expansion and almost loss of entire CZ (46). Loss of *hh* signalling in the PSC does not alter PSC growth, however it results in significant differentiation in LG (41, 56). Ca^{2+} signalling via GABA-BR (metabotropic type GABA receptor), through PSC is important for early LG development, as

loss of this leads to size defects. On the other hand, MZ autonomous Ca^{2+} signalling is required for the maintenance of progenitor state (57).

The JAK/STAT pathway, through its receptor *Dome*, is also known to regulate MZ progenitors, via binding to cytokines Unpaired 1–3 (Upd1–3) (38, 40, 58, 59). At the same time U-shaped *(Ush)*, another target of JAK/STAT promotes E-cad and *Ptc* expression to impede differentiation (Gao et al. 2009, 2013). *Ush* expression subsequently goes down as the cells mature and transit towards CZ. Asrij (Arj), *Drosophila* homolog of Ociad1 (Ovarian carcinoma immune-reactive antigen domain-containing 1), an endosomal trafficking protein, also prevents differentiation in the MZ (60, 61). Loss of *Arj* results in loss of MZ and PSC cells, increase in plasmatocytes and crystal cells and reduction in E-cad levels in MZ. Also loss of *Arj* leads to over-proliferation as well as increase in crystal cell numbers in the posterior lobes of LG (60, 61). Physiologically generated ROS function as an important signalling molecule, observed in a gradient with higher levels in MZ that gradually decrease into differentiated cells in CZ (53). Artificial depletion of ROS levels from the MZ arrest their differentiation/maturation and increase in ROS levels results in hyper-differentiation (53). Another small molecule Dopamine (synthesised and secreted by both progenitors and PSC cells) is shown to regulate LG growth kinetic by regulating the cell cycle transition in progenitors i.e. synthesis and internalisation of dopamine (i-dopamine) for S/G2 transition and Dop2R receptor based signalling (e-dopamine) for G2/M transition (62).

1.3.3 Intermediary Zone (IZ)

Around mid to late 2^{nd} instar larval LG begins expression of Hemolectin (*Hml*) and Peroxidasin (*Pxn*) almost at the same time but independently, alongside their expression of *Dome* (progenitor marker), at the edge of the LG. These cells are called intermediary progenitors as they continue to express their progenitor markers and do not express terminal differentiation markers for any of the three mature blood cell types. The majority of these IZ cells are found to be both Hml and *Pxn* positive but a few express only *Hml* or *Pxn*. To study/mark these intermediary progenitors Spratford and coworkers at Banerjee lab designed CHIZ GAL4 (combined hematopoietic intermediate zone-GAL4), a split GAL4 construct marking *domeless* (*domeMESO-GFP*) and Hemolectin (Hml^{Δ}*-DsRed*) overlapping population (63).

1.3.4 Cortical zone (CZ)

The outer/peripheral part of the LG which harbours differentiated hemocytes is called CZ. This zone is identified by specific markers like *Hml*, Lozenge (*Lz*) and Prophenoloxidase (*PPO*) (crystal cell markers), *Pxn* and *NimC1* (*P1*) (Plasmatocytes) in homeostasis and attila (*L1*) and misshapen (*msn*) (lamellocytes) in infection or other stress conditions (24, 64–70). The majority of the cortical zone comprises plasmatocytes, making up about 95-97% of LG. Contrary to E-cad expression in MZ, the CZ is loosely bound cells which express high levels of the collagen-binding protein SPARC (secreted protein acidic cysteine-rich) (52). Similarly, in mature embryonic hemocytes for proper deposition of collagen, SPARC expression is very important, during basal lamina formation (71). Viking (*Vkg*) and α1 (Cg25C), Collagen IV subunits are also found throughout the LG, although transcriptional reporters for α1 are detected in the CZ only, indicative of the role of mature hemocytes in secretion and thereby distribution of Collagen IV in entire LG (35, 38, 72, 73). Adenosine deaminase growth factor A (*Adgf-A*) based signalling from CZ is also important to regulate the progenitor proliferation (by reducing extracellular adenosine levels) and differentiation (by counterbalancing *hh*-signalling) (42). This equilibrium signal is activated when PSC derived *Pvf1* (*PDGF*- and *VEGF*-related factor 1) ligands are sensed by *Pvr* (*PDGF*- and *VEGF*-receptor related) in CZ (42).

1.4 Blood cell types

Prohemocytes are multipotent progenitors that give rise to three mature blood cell populations, functionally important for all stages of life, namely plasmatocytes, crystal cells and lamellocytes (10–13) (Figure 1C). Plasmatocytes due to their ability to clear microorganisms, cell debris, and secrete AMPs, ECM proteins to maintain internal homeostasis and tackle foreign invasion (74–79). Crystal cells are functionally similar to mammalian platelets as they help in wound healing as wells as in the melanization response via ROS production to neutralize the pathogen (79–81). Lamellocytes are not part of the homeostatic repertoire of hemocytes. They are stress-induced cells, mainly observed during wasp infestation, injury or tissue damage. Their primary role is to encapsulate wasp eggs and restrict them from accessing larval hemolymph nutrient. (12, 81–84).

1.4.1 Plasmatocytes

These are 8-10 μm, round cells, which have higher volume of cytoplasm than their precursors, constitute around 95-97% of total hemocytes and express Glial-cells-missing (*Gcm*) as their differentiation signature (1, 12, 81, 85). Their primary role is phagocytosis therefore their cytoplasm contains an excess of lysosomes and endoplasmic reticulum (3, 12, 79, 81, 86). Plasmatocytes identify the apoptotic cells through their scavenger receptor croquemort *(crq),* which belong to the CD36 class of receptors; a mammalian Ortholog is the CED-1 homolog Draper, isoforms of the immunoglobulin-superfamily receptor Dscam, and the α-PS3 (encoded by *scab*)/Integrin βν heterodimer (25, 87–89). In addition to phagocytosis, plasmatocytes are also found to secrete and remodel ECM proteins, (e.g. Peroxidasin (*Pxn*), *Dcg1* and Viking (*Vkg*), Laminin (24, 70) and secrete antimicrobial peptides (AMPs) (e.g. Cecropin A1, Drosomycin, and Diptericin, aiding the fat body in humoral immunity) (90–92). The most important function of plasmatocytes apart from response to infection is to remove cell debris during pupal development generated during metamorphosis (12, 93)

1.4.2 Crystal Cells

Crystal cells differ from plasmatocytes due to their somewhat larger size (10-12 μm), non-phagocytic nature, fewer ribosomes and absence of cytoplasmic processes (81). The name crystal cell comes from the paracrystalline inclusions present in them, which are part of the melanization cascade. A simple way to identify or visualize the crystal cells is by heating the larvae, due to which the melanization cascade is activated (12, 94). Pro-phenol oxidase (*PPO*) is the zymogen form which can be activated by *Hayan* and *Sp7* (95, 96). Upon activation Phenoloxidase (PO) converts phenols to quinones, which subsequently polymerize into melanin. Three different genes are present in *Drosophila*, out of which *PPO1* and *PPO2* are expressed in crystal cells, primarily involved in melanization, whereas *PPO3* is expressed in lamellocytes (52, 97, 98).

Although crystal cells are reported in the embryonic stage itself, their function is unknown. However their function is well annotated in the larval stage, where crystal cells help in wound healing through melanization or neutralizing bacterial through ROS generation (95, 97, 98). Throughout the life cycle of *Drosophila* crystal cells constitute only 3-5% of total hemocytes in homeostasis (12, 77). *Srp*, *Lz*, and U-shaped (Friend of GATA homolog) works together to specify as well as limit the number of crystal cells in an organism.

1.4.3 Lamellocytes

Lamellocytes are large (15–40 μm across), flat, non-phagocytic and adherent cells with irregular margins and relatively small nucleus (12, 81). Although they are not typically found in healthy animal, they are induced during stress conditions e.g. wasp parasitization, injury or tissue damage. Their primary function is to encapsulate and neutralize objects too large for plasmatocytes to engulf (80, 84). Lamellocytes are identified by the presence of proteins like *Atilla*, β-PS integrin (encoded by *myospheroid*, *mys*), α-PS4 integrin, *misshapen (msn), Puckered, PPO3, and L6 or L2* antigens (52, 77, 82, 99, 100) reviewed in (64, 66, 75, 98).

Although *mys* is considered a lamellocytes marker, it is also expressed in prohemocytes and in plasmatocytes. Furthermore *mys* is not essential for lamellocytes maturation, rather it is important for encapsulation of wasp eggs and melanotic tumor formation, via Rac1 (Rho-GTPase) activation of Focal adhesion kinase(52, 101–103).

1.5 Mitochondria and TCA cycle

Mitochondria are regarded as an organelle of extreme importance to the cell as they are considered as the powerhouse of the cell, as it is the main site for ATP production in the oxidative respiration. But mitochondria have much more to its credit than this; the usual notion is that mitochondria execute its activity under the nuclear command, however it is now established that it is rather bidirectionally regulated. For complex and high energy functions (eg. differentiation, stress adaptation, etc.) cells have to take mitochondrial fitness into account. Also mitochondria can influence nuclear genes to regulate different cellular functions (104). Typically, there are four well-known mechanisms by which mitochondrial influence the cell: these are cytochrome c to induce cell death, mitochondrial fission and fusion via AMPK activation, ROS production for transcription factor activation, and mt-DNA release for immune response activation (105–108). But recent studies have highlighted a fifth mechanism where TCA cycle intermediates, which were earlier considered as by-products, play a critical role in cell fate and functional regulation via chromatin modifications, DNA methylation, and PTM's of various proteins. Cellular respiration is a food web of biochemical reactions that fuels the growth and survival of the cell which in turn supports the organism, through three major outputs; energy (ATP), reducing equivalents (glutathione, NADH, FAD, etc.), and macromolecular precursors (Amino acids, nucleotides, simple sugars).

TCA cycle, also known as citric acid cycle (due to citrate being the first product) or Kreb's cycle (named after the scientist) is a set of chemical reactions, utilised by aerobic organisms, where the product of one reaction becomes a reactant for next, to generate chemical energy from carbohydrates, fatty acids and proteins. The TCA cycle operates in the mt-matrix, surrounded anteriorby double mt-membranes, which separates energy production from consumption

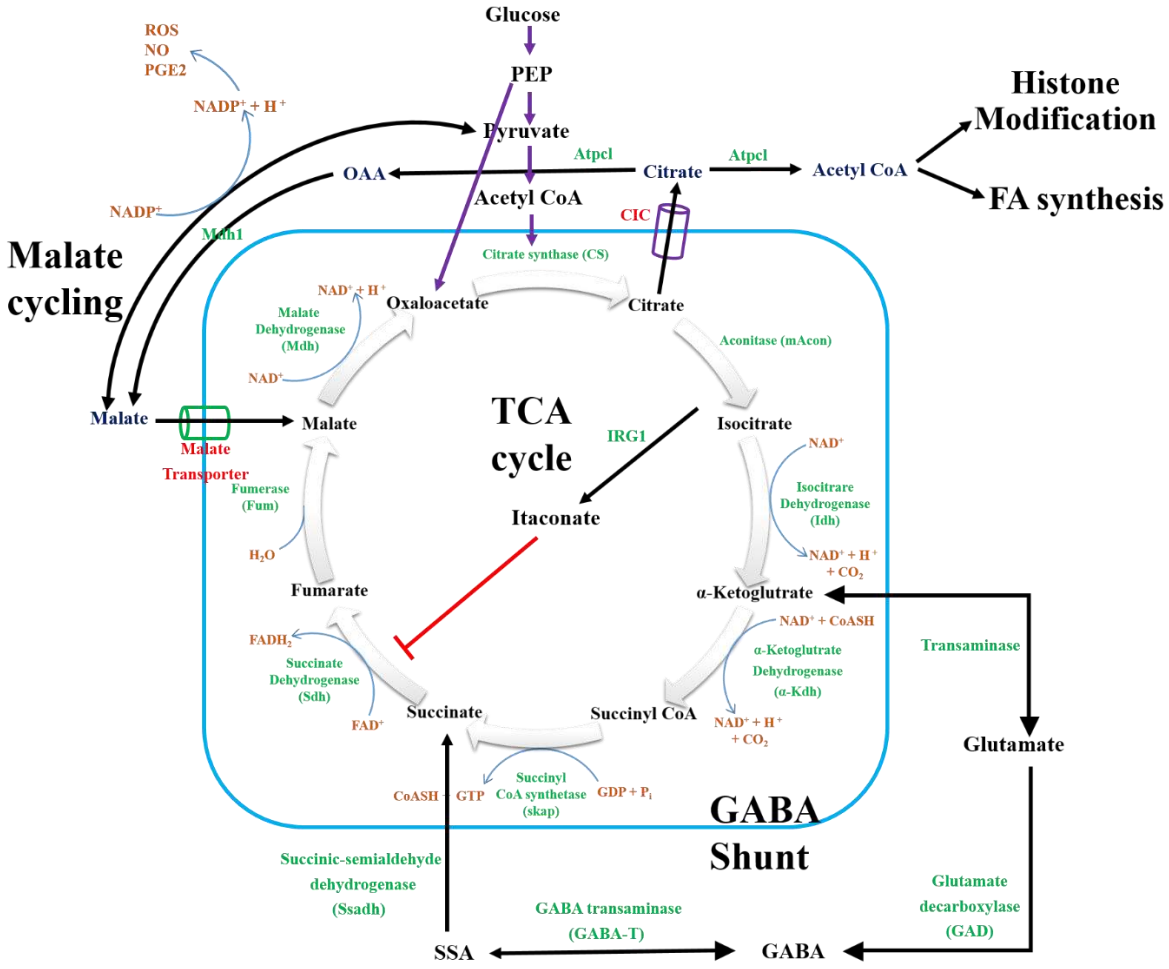

Figure 2: Schematic to represent TCA cycle and shunting of its intermediates between mitochondria and cytosol.

and also retains TCA intermediates inside the mitochondria. These intermediates can be transported out with the help of various shuttle systems operating between the mitochondria and cytosol, depending on cellular demand.

TCA cycle is an amphibolic pathway as it participates in both catabolism and anabolism processes (Figure 2). mt-citrate is transported to cytosol through the citrate carrier (CIC), where it is broken down into Acetyl-CoA and oxaloacetate (OA) for lipid and nucleotide synthesis,

this is called cataplerosis. Whenever TCA cycle intermediates are shuttled away from the mitochondria, the cycle is replenished through various anaplerotic strategies e.g. pyruvate decarboxylase converts pyruvate into OA and glutaminolysis to replenish α-KG via glutamine and glutamate. In case of dysfunctional ETC, glutamine-dependent reductive carboxylation helps in TCA intermediates maintenance (19).

1.6 Acetyl-CoA

Acetyl-CoA is a two-carbon thioester compound that is crucial for the functioning of the TCA cycle. It can be generated by different sources in different compartments of the cell e.g. in mitochondria, it can be generated from the pyruvate oxidation, fatty acid oxidation, or degradation of amino acids such as leucine, isoleucine and tryptophan. It can also act as precursor and metabolic intermediate in several reactions, such as synthesis of fatty acid, sterols and certain amino acids like glutamate, proline and arginine. The most notable function of Acetyl-CoA is its ability to donate acetyl groups for histone acetylation, one of the major post-translational modifications (PTMs) (109, 110) (Figure 3, 4). Acetylation of Histones is catalysed by Histone acetyltransferases (HATs), which are regulated by the levels of Acetyl-CoA produced through different sources such as glycolysis, fatty acid oxidation and cell proliferation (111). Cancer cells exploit this mechanism to promote their proliferation by upregulating enzymes like ATP citrate lyase (ACLY) (Hatzivassiliou, G. et al. 2005). Similarly, normal T-cells increase their cytosolic Acetyl-CoA levels to enhance their interferon-γ (IFNγ) production through histone acetylation (112).

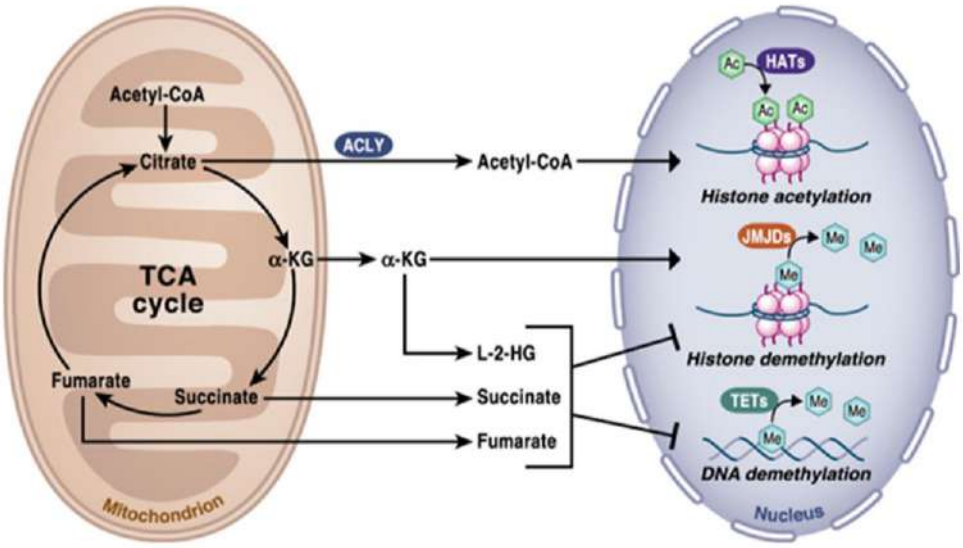

Figure 3: TCA cycle metabolites involved in chromatin modifications and DNA methylation (113).

Histone acetylation is also necessary for the activation of macrophage and dendritic cells (D*CS*). This is achieved by truncated TCA cycle leading to citrate accumulation. Consequently, lipopolysaccharide (LPS) induced macrophages upregulate their ACLY expression, leading to an increase in cytosolic Acetyl-CoA levels (114).

1.7 TCA cycle metabolites and their functions:

1.7.1 Citrate

The condensation of oxaloacetate (OA) and Acetyl-CoA produces citrate, catalysed by citrate synthase (*CS*) enzyme. mt-Citrate accumulation can inhibit PDH and succinate dehydrogenase (*SDH*) (115, 116). The citrate transporter SLC25A1 has been shown to be upregulated in pro-inflammatory macrophages in NF-kB or STAT-dependent manner, facilitating tehtransport of citrate into cytosol, where it is converted into Acetyl-CoA via ACLY (114, 116–119) (Figure 4). The export and breakdown of mt-citrate have also been linked to the production of nitric

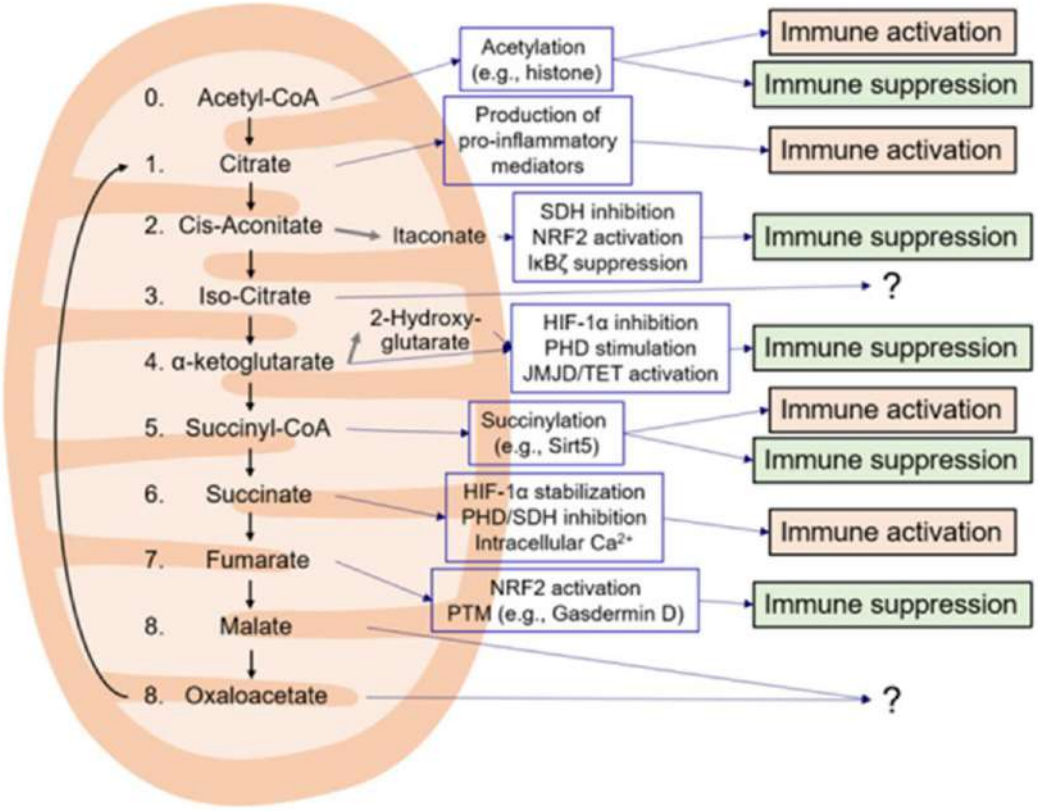

Figure 4: Various Immunological functions performed by TCA cycle intermediates (121).

oxide (NO), ROS and prostaglandin E2 (PGE2), other important proinflammatory mediators of macrophages (114, 116–118). Citrate is also shown to exert protective and anti-apoptotic

effects on bone marrow stromal cells (BMS*CS*) under oxidative stress, by regulating Peroxisome proliferator-activated receptor gamma (PPARγ), a nuclear receptor protein which acts as a transcription factor (120).

1.7.2 *cis*-Aconitate

cis-Aconitate is formed by the reversible conversion of citrate to isocitrate, catalyzed by aconitase (also known as aconitate hydratase). Mitochondrial aconitase belongs to an iron-sulfur [4Fe- 4S]-containing dehydratase family. It is very susceptible to oxidative damage such that exposure to ROS or free radicals results in the release of iron from iron-sulfur [4Fe- 4S] cluster thereby rendering aconitase non-functional. Dysfunctional aconitase activity has been linked to neurodegenerative disorders (122). Mitochondrial aconitase is also important in peripheral lymphocytes, where reduced aconitase activity has been observed in Alzheimer's disease (AD) and mild cognitive impairment (MCI) (123). Cis-aconitate is also a precursor of itaconate.

1.7.3 Itaconate

It is formed by the decarboxylation of cis-aconitate, catalysed by immune-responsive gene 1 (IRG1) or cis-aconitate decarboxylase. In LPS-induced macrophage, itaconate is upregulated and exerts strong immunosuppressive effect. Since itaconate is impermeable to cell membrane, its derivatives like dimethyl itaconate (DMI) and 4-octylitaconate are commonly used in intracellular studies. These studies identified itaconate as a suppressor of succinate dehydrogenase (*SDH*), connecting the TCA cycle and electron transport chain (ETC), thereby modulating the immunity and viral replication (124–127) (Figure 4). Also through alkylation of Kelch-like ECH-associated protein 1 (KEA*P1*) protein, itaconate activates nuclear factor erythroid 2-related factor 2 (NRF2 or NFE2L2) pathway, and activates the cyclic AMP-dependent transcription factor (ATF3) by regulating the translation of IκBζ (128–130) (Figure 4). Itaconate is known to possess anti-bactericidal activity through its ability to inhibit isocitrate lyase, a critical enzyme of glyoxylate shunt. Pathogens majorly utilise glyoxylate shunt under glucose deficit conditions.

1.7.4 Isocitrate

Isocitrate is formed by the isomerization of citrate, also catalyzed by aconitase. Pro-inflammatory macrophages increase their isocitrate to α-ketoglutarate ratio by downregulating isocitrate dehydrogenase (*IDH*). Pro- inflammatory dendritic cells (D*CS*) and macrophages

also exhibit increased glycolytic flux and truncated TCA cycle, in which glucose derived pyruvate enters the TCA cycle but cannot continue beyond citrate/isocitrate. (116, 131, 132). Under homeostatic conditions, *IDH*1 (cytosolic isoform) is not expressed in cells activated by pro-inflammatory stimuli, but under glucose limiting conditions mRNA expression of *IDH*1 is increased in pro- inflammatory macrophages (116, 133, 134).

1.7.5 α-ketoglutarate

α-Ketoglutarate (α-KG) or 2-oxoglutarate is formed by oxidative decarboxylation of isocitrate, and the reaction is catalysed by *IDH*. It can also be generated by a reversible reaction catalysed by glutamate dehydrogenase (*GDH*) which involves the deamination of glutamate and glutamine (135–137). α-KG is an essential co-substrate for a family of phylogenetically conserved enzymes 2-oxoglutarate-dependent dioxygenases (2-OGDD). This family catalyses hydroxylation of various substrates e.g. nucleic acid, proteins, lipids and metabolic intermediates generating succinate and CO_2. 2-OGDD functioning is regulated by various intracellular metabolites e.g. α-KG to succinate ratio, Ascorbic acid, Fe^{2+} (cofactor) and O_2 (co-substrate) promotes enzyme activity, whereas Fumarate, 2-Hydroxyglutarate (2-HG) acts as inhibitors. Anti-inflammatory (IL-4 induced) macrophages are found to be accumulating α-KG, whereas the same is inhibitory for pro-inflammatory (IL-1β expressing) macrophages, but low α-KG levels activates M1 macrophages to enhance endotoxin tolerance (16, 138, 139). Another critical function of 2-OGDD, together with Prolyl-hydroxylases (PHD1–3), is the regulation of Hypoxia inducible factor (HIF-1) to ascertain O_2 homeostasis. PHDs, under normoxia, hydroxylate the proline residue on HIF-1α (sima), marking it for poly-ubiquitination via the von Hippel-Lindau tumor suppressor (VHL) protein and subsequently leading to its degradation (Figure 4 and 5).

Whereas under hypoxia, or pseudohypoxia (low levels of α-KG or Fe^{2+}, high levels of succinate, Fumarate, L-2-HG and mitochondrial ROS), PHDs activity is compromised, resulting in HIF-1α or HIF-2α accumulation and their subsequent translocation to the nucleus, where they regulate gene expression associated with metabolism, angiogenesis, erythropoiesis and immunity (140–143). α-KG can be transported from the mitochondrial matrix to the cytoplasm via α-KG/malate antiporter (in inner mt-membrane) and through the voltage-dependent anion channel (VDAC) (in outer mt-membrane) (135, 144). α-KG also serve as a substrate for chromatin modifying enzymes like Jumonji C domain containing lysine

demethylases (KDM2-7) and DNA methylation enzymes, including the ten-eleven translocation hydroxylases (TET1-3) (Figure 4).

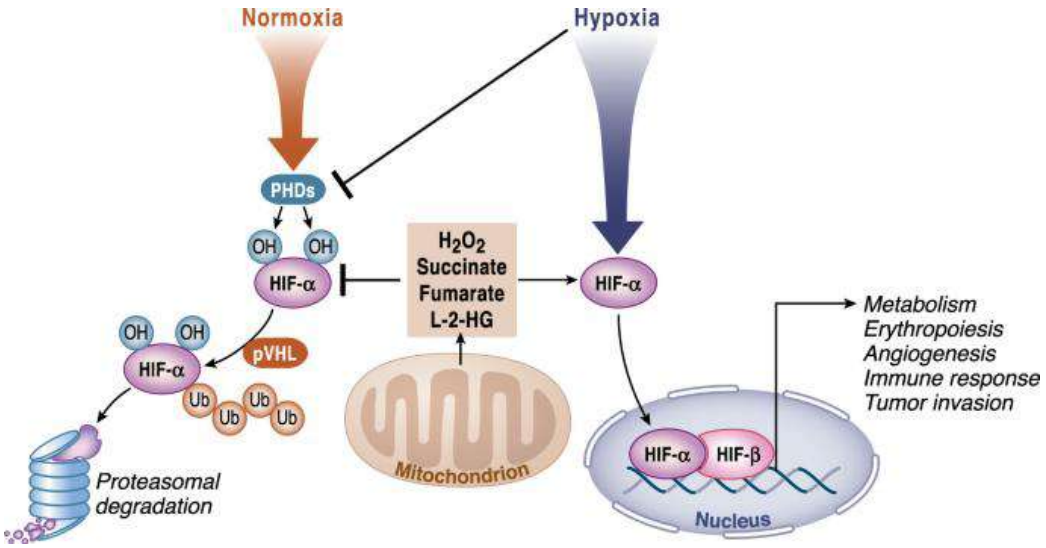

Figure 5: TCA cycle metabolites involved in HIF-α stabilization. (113)

1.7.6 Glutamine and Glutamate

Glucose and glutamine are versatile substrates that can compensate for each other to maintain TCA cycle function. Glutamine enters the cells through glutamine transporters presents in the plasma membrane, such as SLC1A5, SLC38A1, and SLC38A2 and can be utilised in the synthesis of hexosamine, nucleotides, and asparagine in the cytoplasm (145) (Figure 6). From the cytoplasm to the mitochondria, glutamine is transported through SLC1A5 variant transporter in mt-membrane, where it is converted into glutamate by Glutaminase (GLS) enzyme and releases ammonium ions (146–149). mt-glutamate can be converted into is α-KG by *GDH*1 or other mt-aminotransferases including glutamic-pyruvic transaminase 2 (GPT2) and glutamic-oxaloacetic transaminase 2 (GOT2) (Figure 6). Glutamine/glutamate derived α-KG can also be converted into isocitrate/citrate via carboxylation, which can subsequently be broken down into OAA and Acetyl-CoA. This route is preferred in brown adipocytes to produce fatty acids (150). mt-glutamate can also be transported to the cytosol via SLC25A18 and SLC25A22 transporters, where it contributes to glutathione synthesis and production of non-essential amino acids (NEAAs) (alanine, proline, aspartate, asparagine, and arginine) as well as an exchange factor for importing extracellular cysteine via SLC7A11 (151) (Figure 6).

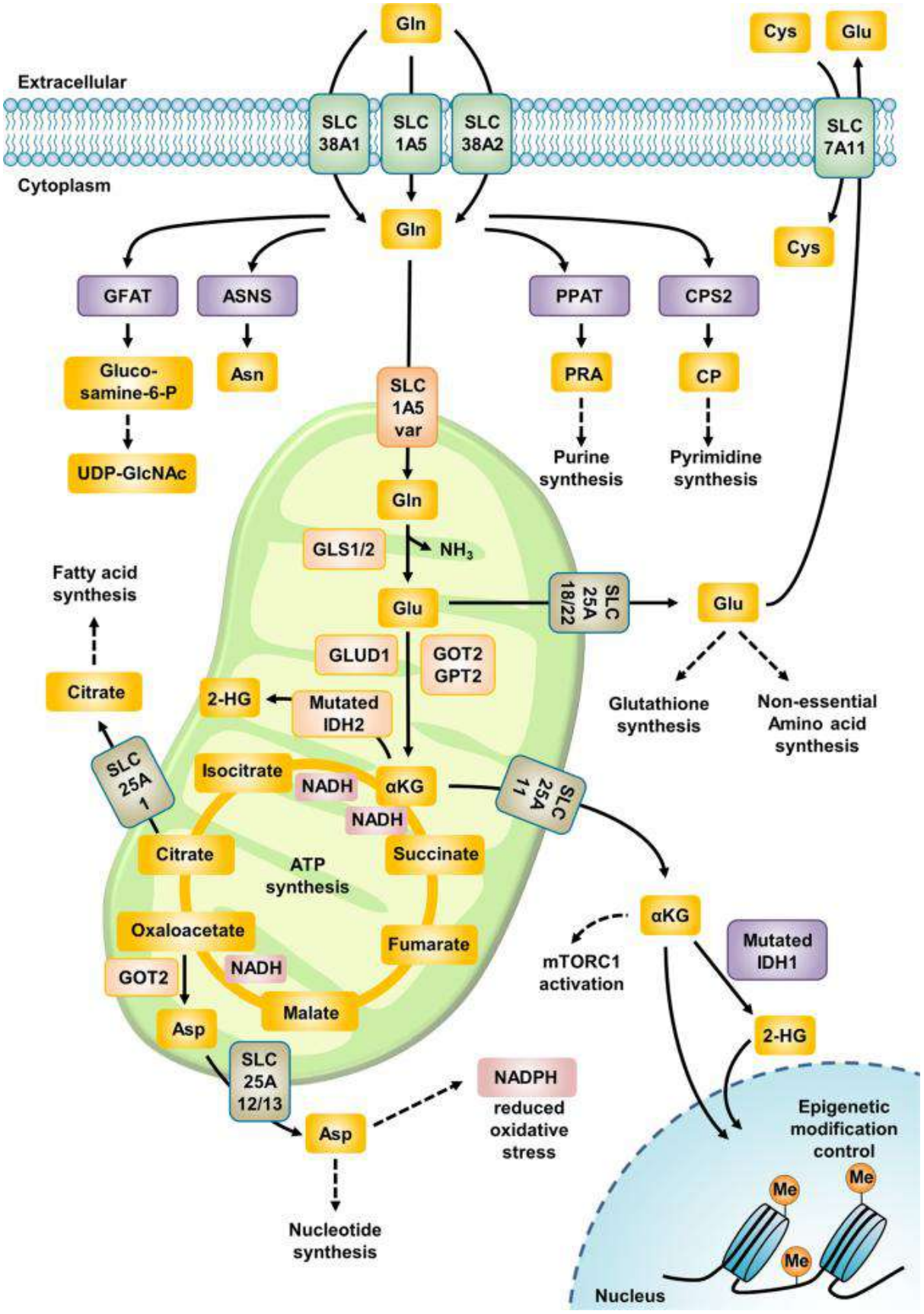

Figure 6: Glutamine metabolism within the cell (149)

1.7.7 Succinyl-CoA

Decarboxylation of α-KG by α-ketoglutarate dehydrogenase (*α-Kdh*), a rate limiting enzyme in TCA cycle flux, produces succinyl-CoA (152, 153). *α-Kdh* functions as a redox sensor; it is inhibited by mt-ROS, whereas mitochondrial acidification caused by elevated cytosolic calcium levels promotes *α-Kdh*activity (152, 154–156). High levels of Succinyl-CoA can result in succinylation of lysine in various proteins e.g. in macrophages, LPS-induced succinylation of lysine 311 of pyruvate kinase M2 (PKM2), inhibits its activity and rather induces IL-1β secretion (138, 157–162) (Figure 4). Inflammatory effect of succinylation is case dependent and leads to a variety of immune responses as certain succinylated proteins in M1 macrophages are found to be immunosuppressive (120, 138, 160) (Figure 4).

1.7.8 Succinate

In the TCA cycle, succinate is formed by succinyl-CoA synthetase through hydrolytic catalysis of CoA. Alternatively, gamma-aminobutyric acid (GABA)-shunt pathway, a bypass to TCA cycle, where glutamine is used to generate glutamate, GABA, succinic semialdehyde, and finally into succinate (160, 163). LPS-induced macrophages elevate their succinate levels for Hypoxia inducible factor-1α (HIF-1α) stabilization and complex-II mediated oxidation of succinate is necessary for transcriptional activation of Interleukin-1β (IL-1β) (160, 164) (Figure 4 and 5). LPS induction based succinate oxidation for ubiquinone accumulation and increased mitochondrial membrane potential increases the ROS production through Complex-I dependent Reverse electron transfer (RET). ROS production via succinate driven RET is also observed in ischemia reperfusion injury in heart and brain (21, 165). Gram negative bacteria like E. coli or S. enterica induced macrophages are shown to elevate complex-II activity at the expense of Complex-I highlighting succinate dehydrogenase (*SDH*) pro-inflammatory support (166). Besides its intracellular functions, succinate can also act as signalling molecule through succinate receptor 1 (SUCNR1), a G-protein coupled receptor (GPCR) member. Dendritic cells and macrophages, through paracrine and autocrine modes, get functionally activated through the SUCNR1 receptor (167). Furthermore, succinate can also cause the accumulation of HIF-1α in the presence of oxygen by inhibiting pyruvate dehydrogenase (PDH), another mechanism exploited by cancer cells, called pseudohypoxia (168) (Figure 4 and 5).

1.7.9 Fumarate

Fumarate is produced by dehydrogenation of Succinate through *SDH* enzyme. Activation of macrophages and monocytes due to pro-inflammatory cues like LPS, IFN-γ leads to

accumulation of Fumarate in modified TCA cycle through the aspartate-arginosuccinate shunt (126, 132, 169–172). Fumarate also regulates protein succinylation by regulating chromatin modification e.g. Fumarate accumulation via anaplerosis of glutamine due to proinflammatory signals is necessary for acquired immunity (173). Fumarate derivatives like dimethyl Fumarate (DMF) can regulate T-cell function and is currently in use for autoimmune diseases like multiple sclerosis (MS), and psoriasis (174). Fumarate accumulation leads to product dependent inhibition of DNA demethylases and lysine demethylases (KDMs) (173, 175–178) (Figure 5).

1.7.10 Malate and Oxaloacetate

L-Malate is formed by the hydration of Fumarate catalysed by Fumarate hydratase (FH), which is subsequently oxidised to form oxaloacetate (OA) by the action of mitochondrial malate dehydrogenase (mt-*MDH*/*MDH*2) as a part of TCA cycle. Whereas cytosolic *MDH* (c-*MDH*/*MDH*1) converts OA into malate and with the help of malate-aspartate shuttle it can be pumped into the mitochondria. Under normal conditions, OA and NADH are continuously utilised by citrate synthase (*CS*) and ETC respectively, therefore, mt-*MDH* always works in the direction of OA formation (179–181). It is also known that increase in mitochondrial NADH levels due to preferential use of fatty acid oxidation inhibits PDH activity, for the conversion of pyruvate to acetyl-CoA (182–185). In these scenarios (e.g. starvation or untreated diabetes) pyruvate is diverted to synthesise OA and shifts the *MDH* equilibrium from OA to malate synthesis (186–190). Malate, depending on cellular demand, can also be transported between mitochondria and cytosol with the help of several carriers, these are 1) SLC25A11 : also known as α-KG carrier as it exchanges α-KG for malate, 2) SLC25A10 : dicarboxylate carrier, it exports mt-malate in exchange of inorganic phosphate, 3) SLC25A1 : citrate carrier (CIC), exchange c-malate for mt-citrate/isocitrate (144, 191–193). Although malate and OA is not much shown to be linked to immunity, but in LPS-induced macrophages malate accumulation is reported and OA is found to act as a strong inhibitor of *SDH* to limit succinate oxidation post ischemia (160, 194, 195).

1.8 Regulation of TCA cycle

Since, TCA cycle functions as a crucial biosynthetic hub as well as cellular energy regulator in tandem with OXPHOS, the system has developed multiple nodes (rate limiting steps) for the

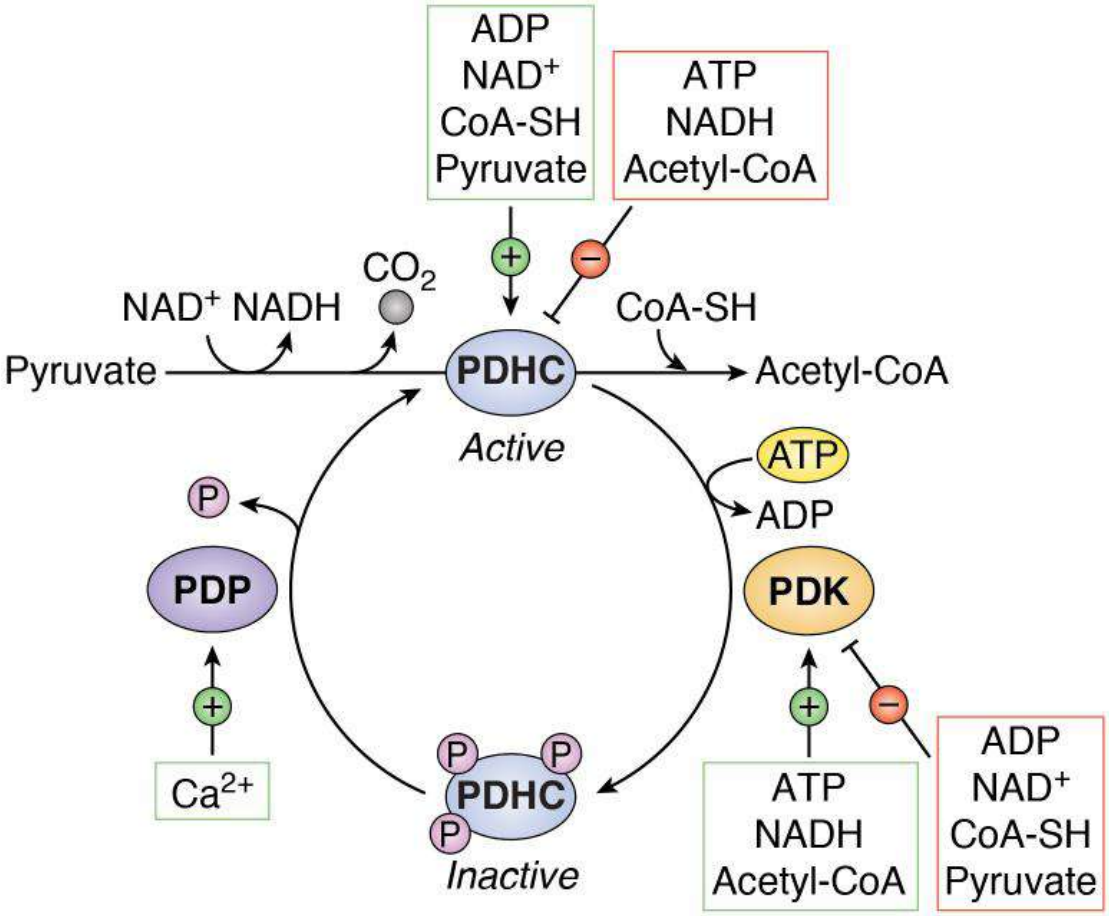

Figure 7: Regulation of TCA cycle via PDH complex.

TCA cycle regulation. There are multiple ways in which TCA cycle is being regulated e.g. allosteric regulation and covalent modification of TCA enzymes, and ion-mediated regulation. TCA cycle's metabolic flux is tightly regulated by both positive as well as negative allosteric regulation. *CS*, *IDH* and *α-KDH* are rate limiting nodes of TCA cycle, which are allosterically inhibited by high NADH levels, through a feedback from ETC due to overloading of NADH onto complex I and complex II and thereby prevent the generation of ROS (104, 113, 196) (Figure 7). High ATP/ADP ratio is also an allosteric inhibitor of *IDH*, resulting in slowing down of the cycle upon surplus energy availability (197) (Figure 7). Succinyl-CoA inhibits α-*α-KDH* in substrate dependent manner whereas inhibits *CS* allosterically (113, 198). PDH enzyme complex is activated by pyruvate and inhibited by Acetyl-CoA in substrate and product dependent manner, also PDH is negatively regulated by high NADH levels. PDH is also negatively regulated through covalent modification, by phosphorylation of three serine

residues on pyruvate dehydrogenase E1 alpha subunit, catalysed by pyruvate dehydrogenase kinases (PDKs; PDK1–4) (199). This inhibitory phosphorylation can be reversed by pyruvate dehydrogenase phosphatases (PDPs; PD*P1* and PDP2). Higher concentration of NAD^+, ADP, and pyruvate activates PDH, on the contrary higher NADH, ATP, and high Acetyl-CoA levels activates PDKs (200) (Figure 7).

Calcium (Ca^{2+}) is a well-established intracellular messenger in numerous biological processes. mt-Ca^{2+} uptake majorly occurs through mt-calcium uniporter, present in the inner mt-membrane, which is regulated by membrane potential generated by ETC activity (201) (Figure 7). mt-Ca^{2+} directly influences *IDH* and *α-Kdh*by physically interacting with the enzymes and thereby decreasing their K_M for isocitrate and α-KG respectively (202). mt-Ca^{2+} levels can also activate PDH via PD*P1* mediated dephosphorylation (202, 203). Both cytosolic and mt-Aconitase contain iron-sulfur (4Fe–4S) clusters, which makes aconitase activity sensitive to cellular iron levels (204). Also due to the 4Fe–4S cluster, aconitase is susceptible to ROS mediated inactivation (204).

1.9 Variations of TCA cycle: When TCA cycle is not much of a cycle.

Conventionally TCA cycle begins with the condensation of OAA (4-carbon) with acetyl CoA (2-carbon) to generate citrate (6-carbon). Subsequent reactions oxidize citrate to generate two CO2 molecules, one GTP, four reducing equivalents (three NADH and one FADH2) and finally regenerate the OA (15, 16). But there are versions of TCA cycle reported across the literature in different cell states, e.g. conversion of pyruvate to mt-OA and glutaminolysis (glutamine to α-KG, through glutamate) in the events of citrate being exported to cytosol; glutamine dependent reductive carboxylation, here the cycle runs backward from glutamine derived α-KG to produce citrate, due to non-functional ETC (17–19). Citrate-malate shuttle is being utilised by cancer cells, Immune cells as well as ES*CS* to send the citrate out in the cytosol, where it is broken down with the help of ATP Citrate Lyase (ACLY) into OAA and acetyl CoA, followed by cytosolic-OAA reduced to malate and transported back to the mitochondria. Here the citrate-malate shuttle acts as an electron shuttle as well as supporting continuous regeneration of citrate to maintain TCA intermediates homeostasis too (205–209). Another scenario where non-canonical TCA cycle can come into play is when oxygen cannot be accessed as terminal electron acceptor, due to ETC inhibition, *SDH* complex reduces Fumarate to succinate and Fumarate acts as the electron acceptor to adapt the cell in oxygen limiting conditions (20–22).

Competing to above mentioned scenarios our work highlights coming together or building up of TCA cycle which takes place in the *Drosophila* larval lymph gland development where only a few steps are found to be necessary, in comparison to the progenitor maintenance, where almost all the steps (*CS* to *SDH*) are found to be important. Our work also brings out the importance of citrate in the early development of lymph gland by regulating progenitor and non-progenitor proliferation and keeping a check on the differentiation.

2. AIMS AND OBJECTIVE

2.1 Understand the role of TCA cycle in the maintenance and differentiation of blood progenitors.

To understand the role of the TCA cycle in maintenance and differentiation, we performed genetic knockdown of all the successive steps/enzymes of the TCA cycle. We also temporally and spatially manipulated the TCA cycle in different zones of the lymph gland using various available GAL4 drivers, which mark distinct but overlapping cell populations arising during lymph gland development. The results for this section were analysed at the wandering 3rd instar larval stage, even though the manipulations began at the embryonic stage. The findings from this section highlight differential regulation of TCA cycle in different compartments/zones of the lymph gland.

2.2 Investigate the contribution of TCA cycle in the regulation of lymph gland size.

In this section, we explored the results from the previous section in greater depth to understand the involvement of few enzymes of TCA cycle. These enzymes predominantly regulate progenitor proliferation, along with inhibition of precocious differentiation of progenitors and the premature proliferation of non-progenitors, thereby ensuring the desired initial lymph gland growth during early development. This was followed by the rescue of lymph gland growth, as well as precocious differentiation, through the supplementation of desired metabolite at the appropriate developmental stage.

2.3 To investigate the cyclic nature of TCA cycle.

In this section, we explored the making of TCA cycle, from the initial steps necessary for progenitor proliferation to whole cycle coming together for the progenitor maintenance, with the help of results from the previous two sections as well as RNA sequencing performed with different TCA cycle mutants.

3. TCA cycle balance maintenance and differentiation of blood progenitors in lymph gland.

3.1 TCA cycle controls progenitor maintenance in MZ

To investigate the influence of this metabolic cycling in the maintenance of progenitor homeostasis and development of lymph gland, we utilized the binary system approach (UAS-GAL4). We systematically depleted each step of the TCA cycle with the help of four different GAL4s, which were temporally and spatially segregated but at the same time overlapping to a certain extent. The GAL4s used in the study are *Tep4-GAL4,UASmcherry* (Core or subset of

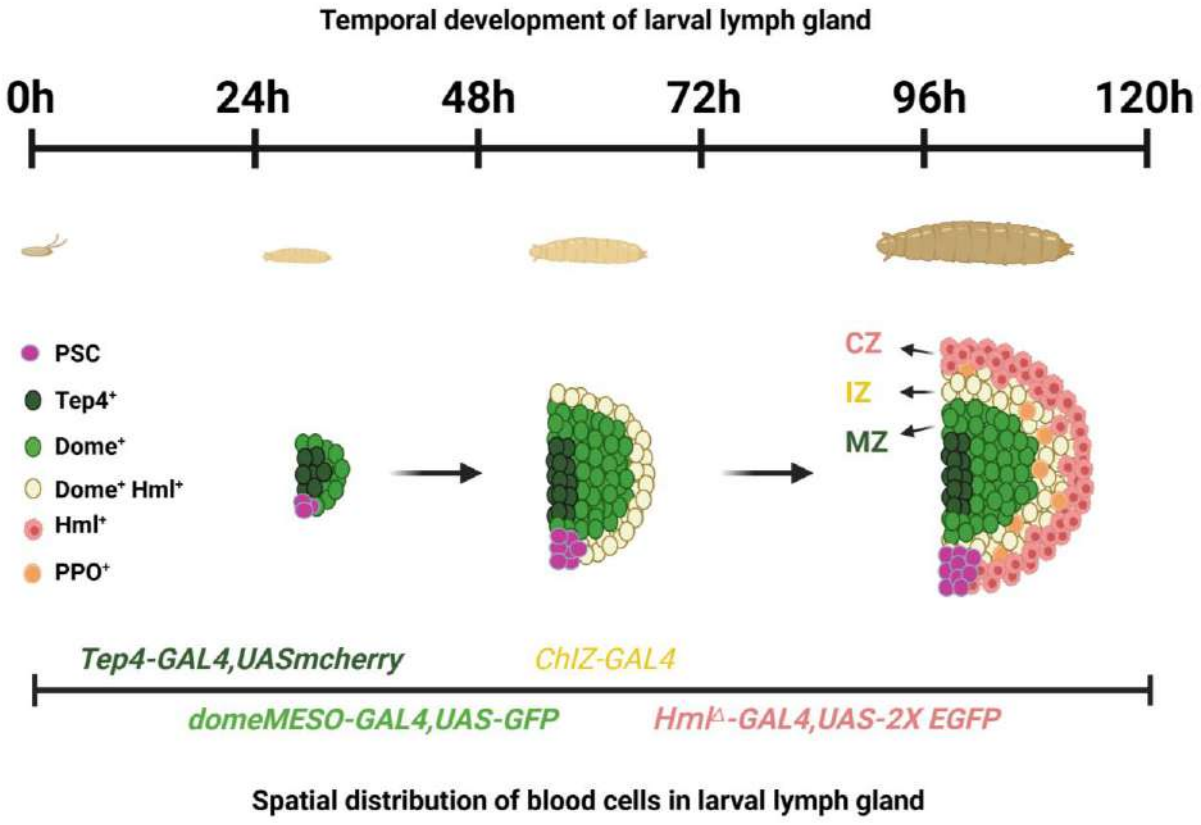

Figure 8: Temporal and spatial growth of lymph gland and the GAL4 driver's expression in the respective zones of lymph gland.

progenitors), *domeMESO-GAL4,UAS-GFP* (MZ), *ChIZ-GAL4* (IZ), and *Hml$^{\Delta}$-GAL4,UAS-2X EGFP* (CZ) in the order of their temporal expression (Figure 8). For the knockdown of TCA cycle genes, multiple *UAS-RNAi* lines were used for each step, wherever available, from which the line showing best phenotype was selected, or previously established and published lines were used. By perturbing the enzymes of TCA cycle individually in the progenitor compartment at wandering 3rd instar larval stage, with *domeMESO-GAL4,UAS-GFP* (pan

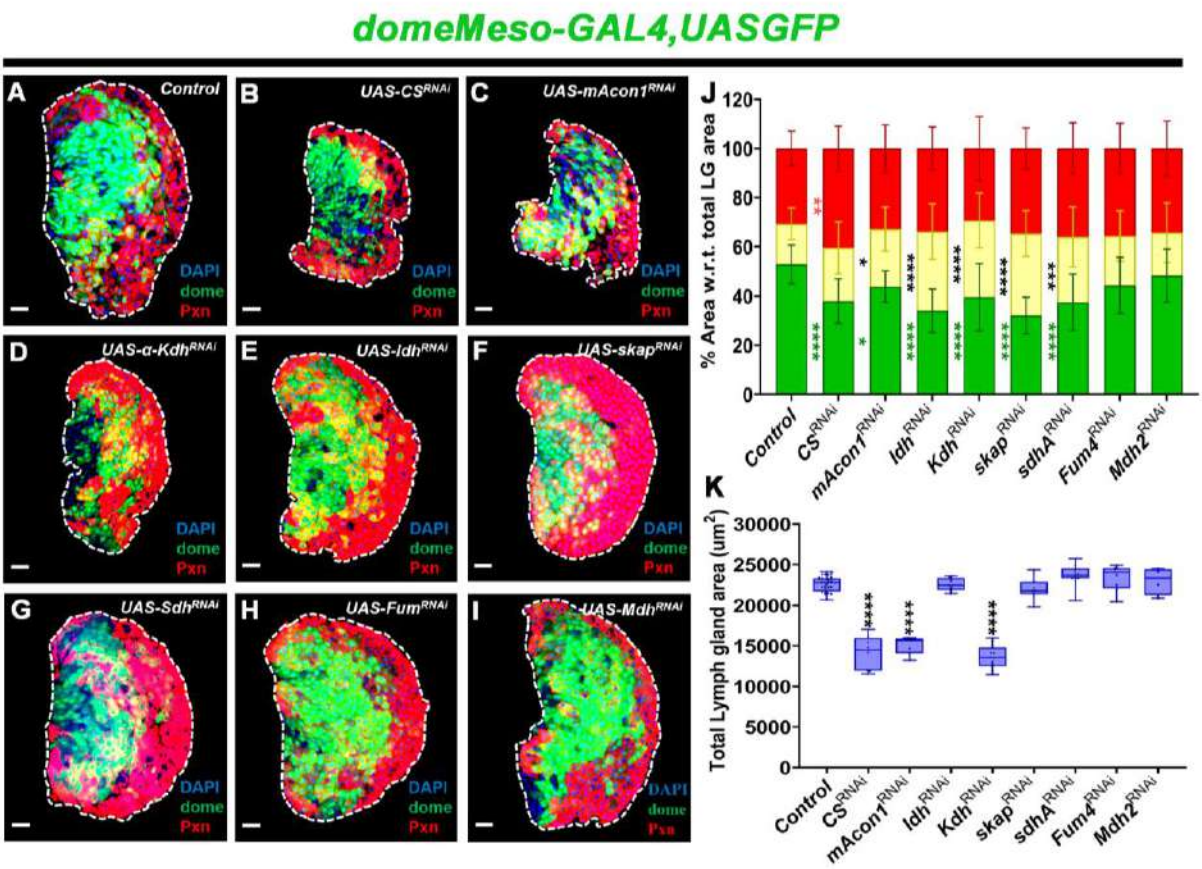

Figure 9: TCA cycle in medullary zone is important for maintenance of blood progenitors in lymph gland of *Drosophila* larva.

(A) *Control (domeMeso-Gal4,UAS-GFP/+)* lymph gland showing general distribution of progenitors (green) and differentiating (yellow and red) population at 3rd instar larval stage, **(B)** expressing *CS^{RNAi} (domeMeso-Gal4,UAS-GFP;UAS-CS^{RNAi})*, ***(C)*** *mAcon1^{RNAi} (domeMeso-Gal4,UAS-GFP;UAS-mAcon1^{RNAi})* and ***(D)*** *α-Kdh^{RNAi} (domeMeso-Gal4,UAS-GFP;UAS-α-Kdh^{RNAi})* showing smaller LG size as compared to ***(A)*** control, ***(E)*** *Idh^{RNAi} (domeMeso-Gal4,UAS-GFP;UAS-Idh^{RNAi})*, ***(F)*** *Skap^{RNAi} (domeMeso-Gal4,UAS-GFP;UAS-Skap^{RNAi})*, and (**G**) *Sdh^{RNAi} (domeMeso-Gal4,UAS-GFP;UAS-Sdh^{RNAi})*, **(B-G)** lymph glands showing reduction in progenitor (green) cells and concomitant increase in differentiating population (yellow or red), compare to **(A)** *control*. ***(H)*** *Fum^{RNAi} (domeMeso-Gal4,UAS-GFP;UAS-Fum^{RNAi})*,and **(I)** *Mdh^{RNAi} (domeMeso-Gal4,UAS-GFP;UAS-Mdh^{RNAi})*, both of these genotypes do not show any size or maintenance defect as compared to **(A)** control. ***(J)*** Quantification is relative % area with respect to total lymph gland area for maintenance and differentiation profile, *domeMeso>GFP/+ (*control, *n=85)*, *domeMeso>GFP/CS^{RNAi}* (n=21, green: p<0.0001; yellow: p=0.7833; red: p=0.0077), *domeMeso>GFP/mAcon1^{RNAi}* (n=23, green: p=0.0209; yellow: p<0.0001; red: p>0.9999), *domeMeso>GFP/α-Kdh^{RNAi}* (n=41, green: p<0.0001; yellow: p=1197; red: p>0.9999), *domeMeso>GFP/Idh^{RNAi}* (n=75, green: p<0.0001; yellow: p<0.0001; red: p=0.9927), *domeMeso>GFP/Skap^{RNAi}* (n=51, green: p<0.0001; yellow: p<0.0001; red: p=0.5696), *domeMeso>GFP/Sdh*^{RNAi} (n=82, green: p<0.0001; yellow: p=0.0004; red: p=0.1149), *domeMeso>GFP/Fum^{RNAi}* (n=42, green: p=0.1160; yellow: p=0.4135; red: p=0.2021), *domeMeso>GFP/Mdh^{RNAi}* (n=32, green: p=0.8834; yellow: p=0.2064; red: p=0.5932), **(K)** Quantification in terms of total lymph gland area, *dome*Meso>GFP/+ (control, n=106), *domeMeso>GFP/CS^{RNAi}* (n=82, p<0.0001), *domeMeso>GFP/mAcon1^{RNAi}* (n=56, p<0.0001), *domeMeso>GFP/α-Kdh^{RNAi}* (n=96, p<0.0001), *domeMeso>GFP/Idh^{RNAi}* (n=85, p>0.9999), *domeMeso>GFP/Skap^{RNAi}* (n=66, p=0.9073), *domeMeso>GFP/Sdh^{RNAi}* (n=111, p=0.1446), *domeMeso>GFP/Fum^{RNAi}* (n=76, p=0.6249), *domeMeso>GFP/Mdh^{RNAi}* (n=58, p=0.9974). Data is presented as median plots (*p<0.05; **p<0.01; ***p<0.001; ****p<0.0001), ordinary one-way ANNOVA. Scale bar: 20μm. 'n'=lymph gland lobes. DAPI marks DNA, Progenitors (*Dome^{+}*; Green), Differentiating population (*Pxn^{+}*; Red), Double positive (*Dome^{+} Pxn^{+}*; Yellow). Comparisons for significance are with control values.

progenitor) drivers we observed two very different phenotypes arising independent of each other. One of the phenotypes was found to be related to maintenance of the progenitor pool and regulation of differentiation and the other was growth defect in the LG (Figure 9 A-J). For the progenitor maintenance, the TCA cycle was found to be functioning together for almost its entire length except for *Fum* and *Mdh* steps, which did not show any progenitor loss or increase in differentiation profile (Figure 9: A-I, J). The loss of progenitor population was observed by loss of GFP positive area expressed by *domeMESO-GAL4,UAS-GFP* compared to respective controls. For the differentiation profile, we resorted to immunostaining to mark the differentiating populations (*Pxn, P1, PPO* and *Mys*) alongside the internal GFP tagged with *dome*. This allowed us to identify the status of Plasmatocytes (*Pxn, P1*), Crystal cells (*PPO*) and Lamellocytes (*Mys*), were used for all three blood cell types of *Drosophila*. In the case of *domeMESO-GAL4,UAS-GFP* driver, the reduction in the progenitor population was either compensated by an increase in the double positive ($Dome^+$ Pxn^+) population or the Pxn^+ only population (Figure 9: A-I, J). We also observed around 15% increase in the plasmatocyte population, marked by *P1* (Figure 10: A-J). The crystal cells, marked by *PPO* were found to be significantly decreased in the *CS, mAcon1, α-Kdh, Skap* and *Sdha* knockdowns, whereas a significant increase was detected in the *Idh* knockdown. No change was observed in the *Fum* and *Mdh2* knockdowns (Figure 11: A1-J1). Lamellocytes were not observed upon manipulating any step of the TCA cycle.

To understand whether the TCA cycle mediated progenitor maintenance and differentiation regulation is specific to the *Dome* population, we also manipulated TCA cycle activity in a subset of early progenitors, which consists of two populations: $Tep4^+$ only and $Tep4^+$ $Dome^+$ progenitors. For this, we used *Tep4-GAL4,UASmcherry*, which marks progenitors with an mcherry fluorescent tag (shown in the figure as green) and this served as our readout for progenitor specific phenotype. Upon knockdown of individual steps of the TCA cycle in this progenitor subset, a loss of progenitors (Green) was observed in all steps at the wandering 3rd instar larval lymph gland (Figure 12: A, C-K). This loss of progenitors was compensated by $Tep4^-$ Pxn^- (Blue) cells, speculated to represent $Dome^+$ only population, or by Pxn^+ (Red) cells (Figure 12: A, C-K). A significant increase in the plasmatocyte population ($P1^+$; Magenta) was also observed in *CS, mAcon1, Skap, Sdha* and *Mdh* knockdowns (Figure 13: A-J). Crystal cells, marked by *PPO*, were significantly increased in *CS and Idh* knockdowns but reduced in

mAcon1 and α-Kdh knockdowns, while no change was observed in *Sdh, Fum* and *Mdh2* knockdowns (Figure 14: A-J). Lamellocytes were not detected under homeostatic knockdowns.

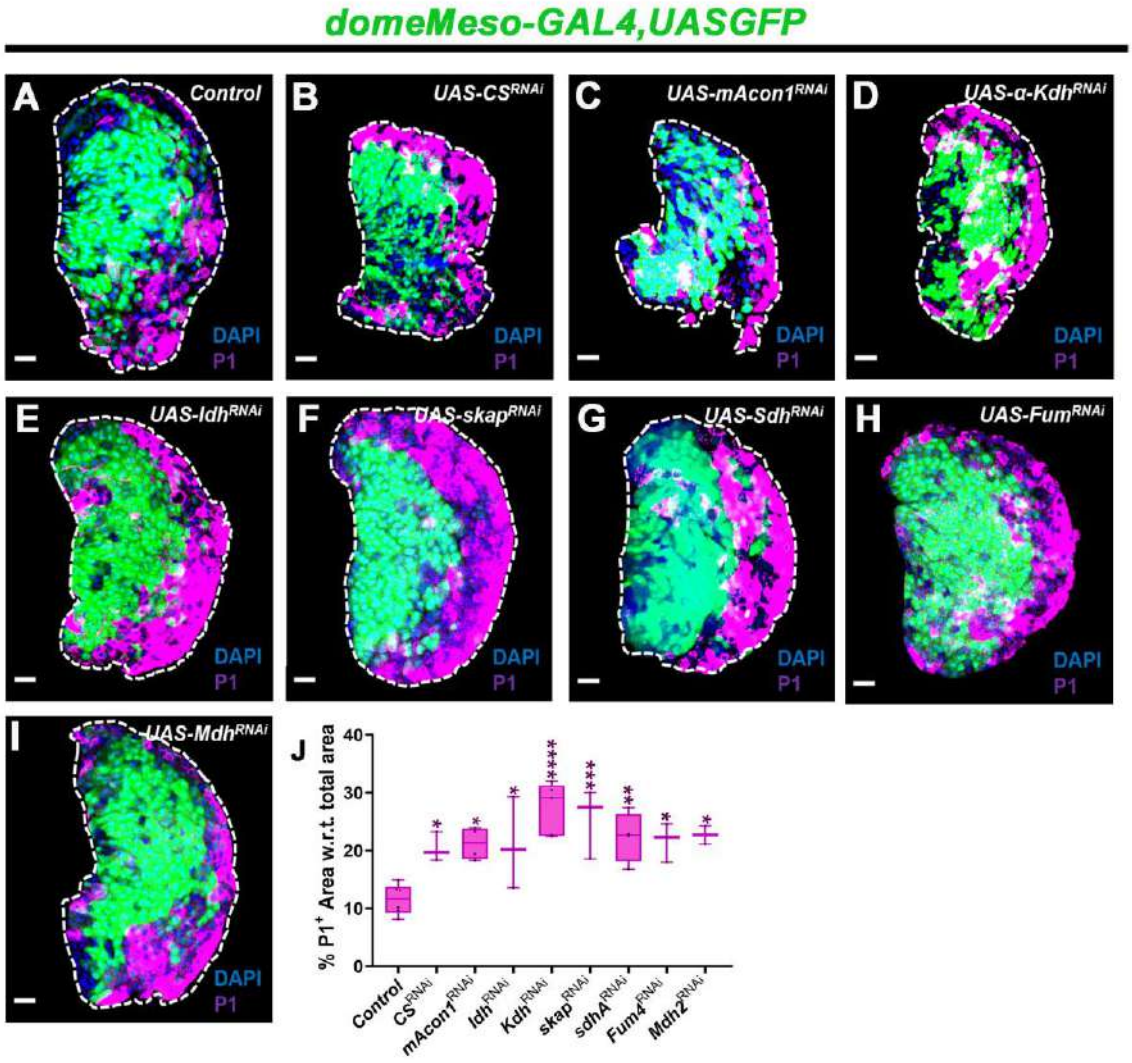

Figure 10: Loss of TCA cycle in MZ favors plasmatocytes fate.

(A) *Control* (*domeMeso-Gal4,UAS-GFP/+*) lymph gland showing general distribution of progenitors (green) and differentiated plasmatocytes (*P1*$^{+}$; magenta) population at 3rd instar larval stage, **(B)** expressing *CS*^{RNAi} (*domeMeso-Gal4,UAS-GFP;UAS-CS*^{RNAi}), **(C)** *mAcon1*^{RNAi} (*domeMeso-Gal4,UAS-GFP;UAS-mAcon1*^{RNAi}), **(D)** *α-Kdh*^{RNAi} (*domeMeso-Gal4,UAS-GFP;UAS-α-Kdh*^{RNAi}), **(E)** *Idh*^{RNAi} (*domeMeso-Gal4,UAS-GFP;UAS-Idh*^{RNAi}), **(F)** *Skap*^{RNAi} (*domeMeso-Gal4,UAS-GFP;UAS-Skap*^{RNAi}), **(G)** *Sdh*^{RNAi} (*domeMeso-Gal4,UAS-GFP;UAS-Sdh*^{RNAi}), **(H)** *Fum*^{RNAi} (*domeMeso-Gal4,UAS-GFP;UAS-Fum*^{RNAi}),and **(I)** *Mdh*^{RNAi} (*domeMeso-Gal4,UAS-GFP;UAS-Mdh*^{RNAi}), **(B-I)** lymph glands shows increase in differentiated population (plasmatocytes; magenta), compare to **(A)** *control*. **(J)** Quantification is relative % area with respect to total lymph gland area for maintenance and differentiation profile, *domeMeso>GFP/+* (*control*, n=54), *domeMeso>GFP/CS*^{RNAi} (n=25 p<0.0448), *domeMeso>GFP/mAcon1*^{RNAi} (n=30, p<0.0119), *domeMeso>GFP/A-Kdh*^{RNAi} (n=41, p<0.0001), *domeMeso>GFP/Idh*^{RNAi} (n=33, p>0.02888), *domeMeso>GFP/Skap*^{RNAi} (n=35, p=0.0008), *domeMeso>GFP/Sdh*^{RNAi} (n=33, p=0.0043), *domeMeso>GFP/Fum*^{RNAi} (n=33, p=0.0178), *domeMeso>GFP/Mdh*^{RNAi} (n=25, p=0.0254). Data is presented as median plots (*p<0.05; **p<0.01; ***p<0.001; ****p<0.0001), ordinary one-way ANOVA. Scale bar: 20µm. 'n'=lymph gland lobes. DAPI marks DNA, Progenitors (*Dome*$^{+}$; Green), Differentiated population (magenta). Comparisons for significance are with control values.

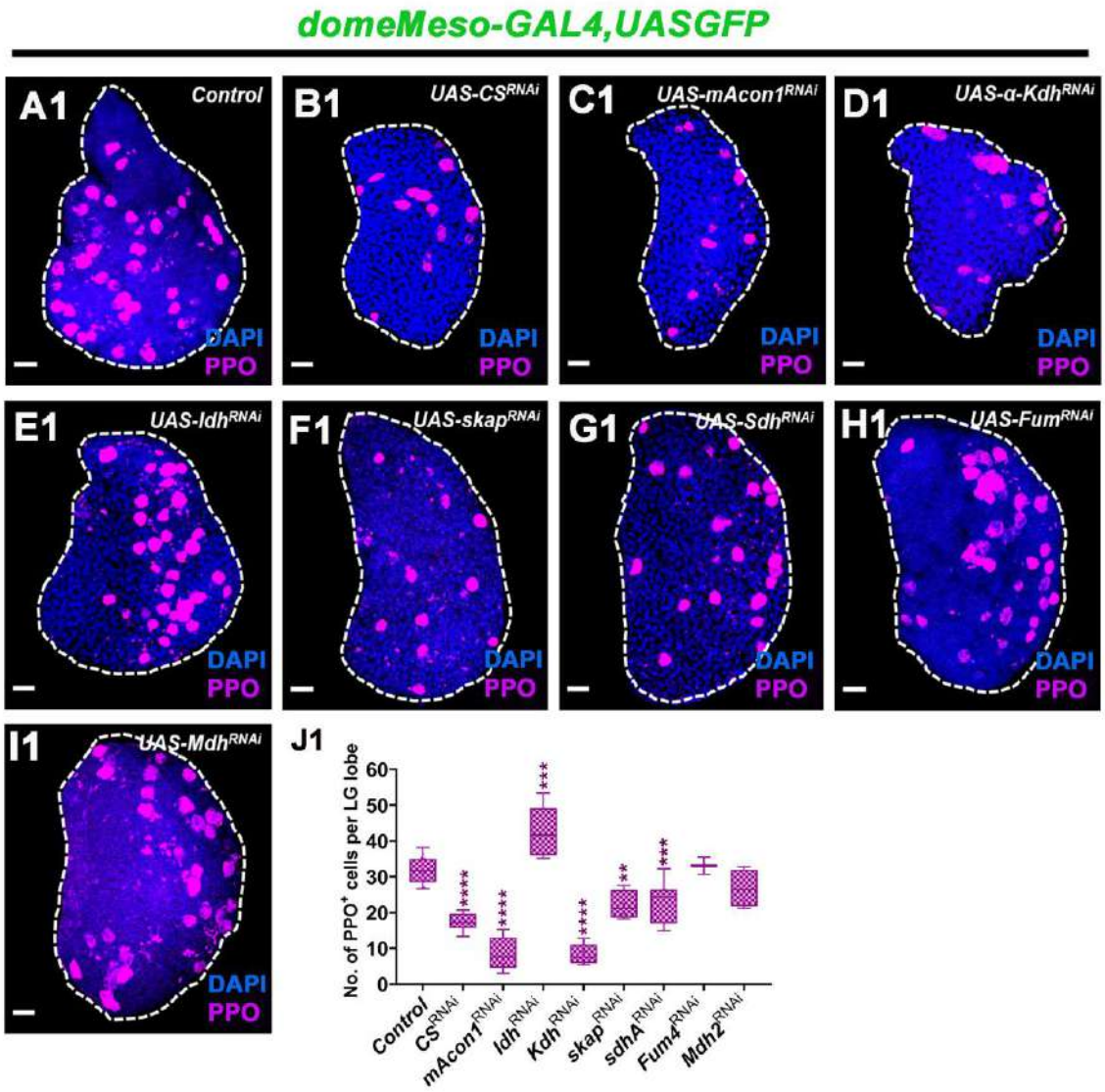

Figure 11: Loss of TCA cycle in MZ negatively affect the crystal cell population.

(A1) *Control (domeMeso-Gal4,UAS-GFP/+)* lymph gland showing general distribution of mature crystal cells (*PPO*$^{+}$; magenta) population at 3rd instar larval stage, **(B1)** expressing *CS*^{RNAi} (*domeMeso-Gal4,UAS-GFP;UAS-CS*^{RNAi}), **(C1)** *mAcon1*^{RNAi} *(domeMeso-Gal4,UAS-GFP;UAS-mAcon1*^{RNAi}), **(D1)** *α-Kdh*^{RNAi} (*domeMeso-Gal4,UAS-GFP;UAS-α-Kdh*^{RNAi}), (**E1)** *Idh*^{RNAi} (*domeMeso-Gal4,UAS-GFP;UAS-Idh*^{RNAi}), (**F1)** *Skap*^{RNAi} *(domeMeso-Gal4,UAS-GFP;UAS-Skap*^{RNAi}), (**G1)** *Sdh*^{RNAi} (*domeMeso-Gal4,UAS-GFP;UAS-Sdh*^{RNAi}), **(H1)** *Fum*^{RNAi} (*domeMeso-Gal4,UAS-GFP;UAS-Fum*^{RNAi}),and **(I1)** *Mdh*^{RNAi} (*domeMeso-Gal4,UAS-GFP;UAS-Mdh*^{RNAi}), **(B1-D1 and F1-G1)** lymph glands shows decrease in crystal cells, whereas **(E1)** shows increase in crystal cell population (*PPO*$^{+}$; magenta), compare to **(A1)** control. **(J1)** Quantification is total number of crystal cells (*PPO+*) cells in entire LG lobe, *domeMeso>GFP/+ (control*, n=96), *domeMeso>GFP/CS*^{RNAi} (n=62, p<0.0001), *domeMeso>GFP/mAcon1*^{RNAi} (n=71, p<0.0001), *domeMeso>GFP/A-Kdh*^{RNAi} (n=69, p<0.0001), *domeMeso>GFP/Idh*^{RNAi} (n=66, p=0.0002), *domeMeso>GFP/Skap*^{RNAi} (n=34, p=0.0024), *domeMeso>GFP/Sdh*^{RNAi} (n=87, p=0.0005), *domeMeso>GFP/Fum*^{RNAi} (n=28, p=0.9999), *domeMeso>GFP/Mdh*^{RNAi} (n=46, p=0.2964). Data is presented as median plots (*p<0.05; **p<0.01; ***p<0.001; ****p<0.0001), ordinary one-way ANOVA. Scale bar: 20µm. 'n'=lymph gland lobes. DAPI marks DNA, Progenitors (*Dome*$^{+}$; Green), Differentiated population (magenta). Comparisons for significance are with control values.

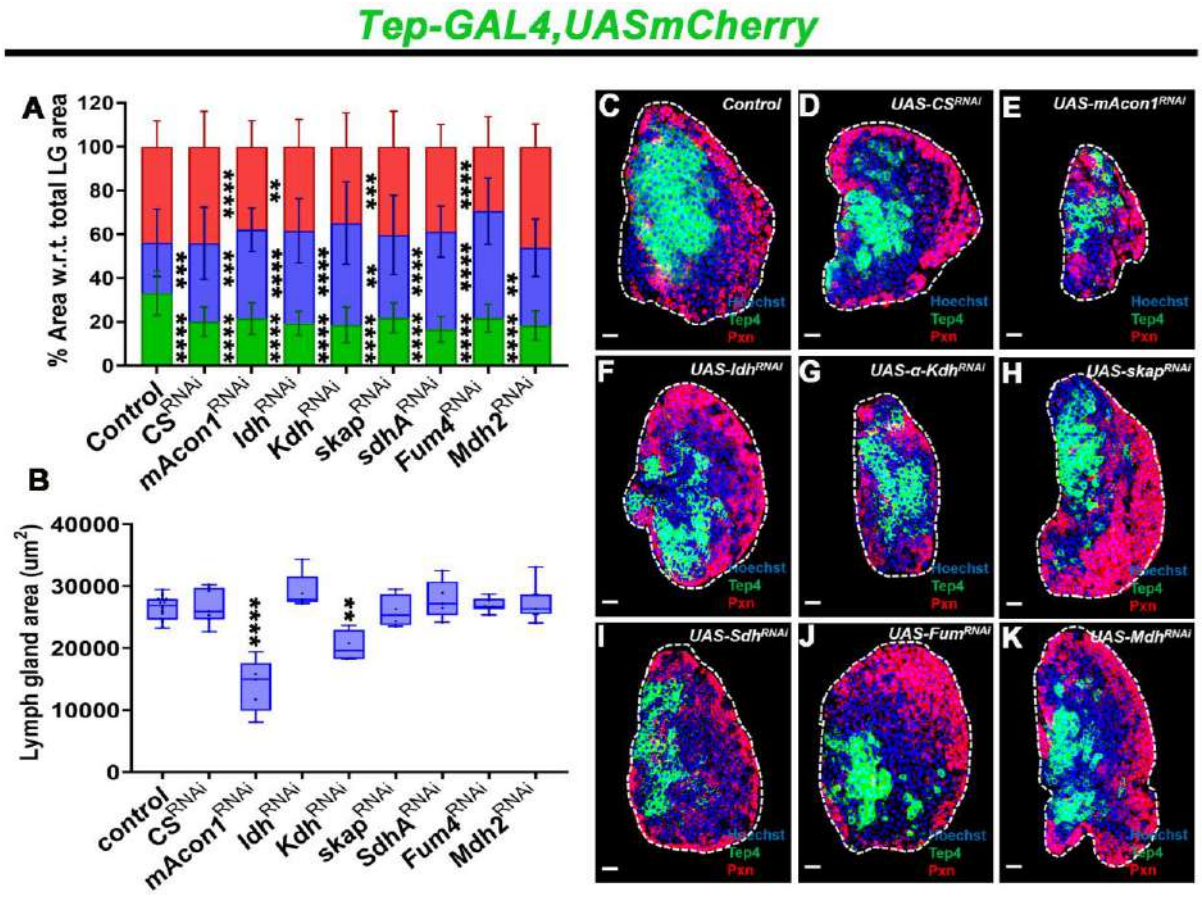

Figure 12: TCA cycle in core progenitors (*Tep4*$^{+}$; MZ) is important for maintenance of blood progenitors in lymph gland of *Drosophila* larva.

(A) graph representing quantification of progenitor (*Tep4*$^{+}$; green), differentiating (blue and red) population. **(B)** graph representing the size in terms of total area of lymph gland. **(C)** *Control* (*Tep4-GAL4,UASmcherry /+*) lymph gland showing general distribution of progenitors (*Tep4+*; green) and differentiating (blue and red) population at 3rd instar larval stage, **(D)** expressing *CS*^{RNAi} *(Tep4-GAL4,UASmcherry/UAS-CS*^{RNAi}), **(E)** *mAcon1*^{RNAi} (*Tep4-GAL4,UASmcherry/UAS-mAcon1*^{RNAi}), **(F)** *Idh*^{RNAi} (*domeMeso-Gal4,UAS-GFP/UAS-Idh*^{RNAi}), **(G)** *α-Kdh*^{RNAi} (*Tep4-GAL4,UASmcherr/UAS-α-Kdh*^{RNAi}), **(H)** *Skap*^{RNAi} (*domeMeso-Gal4,UAS-GFP/UAS-Skap*^{RNAi}), **(I)** *Sdh*^{RNAi} (*Tep4-GAL4,UASmcherr/UAS-Sdh*^{RNAi}), **(J)** *Fum*^{RNAi} (*Tep4-GAL4,UASmcherry/UAS-Fum*^{RNAi}),and **(K)** *Mdh*^{RNAi} (*Tep4-GAL4,UASmcherry/UAS-Mdh*^{RNAi}), **(D-K)** lymph glands showing reduction in progenitor (green) cells and concomitant increase in differentiating population (blue or red), compare to **(C)** control. **(E, G)** both lymph glands show smaller size as compared to **(C)** control. **(A)** Quantification is relative % area with respect to total lymph gland area for maintenance and differentiation profile, *Tep4-GAL4,UASmcherry /+ (control*, n=51), *Tep4-GAL4,UASmcherry/CS*^{RNAi} (n=36, green: p<0.0001; blue: p=0.0010; red: p=0.9999), *Tep4-GAL4,UASmcherry/mAcon1*^{RNAi} (n=17, green: p<0.0001; blue: p=0.0004; red: p<0.0001), *domeMeso>GFP/Idh*^{RNAi} (n=26, green: p<0.0001; blue: p<0.0001; red: p=0.0058), *Tep4-GAL4,UASmcherry/α-Kdh*^{RNAi} (n=15, green: p<0.0001; blue: p<0.0001; red: p=0.0675), *Tep4-GAL4,UASmcherry/Skap*^{RNAi} (n=22, green: p<0.0001; blue: p=0.0012; red: p=0.0010), *Tep4*-GAL4,UASmcherry /*Sdh*^{RNAi} (n=17, green: p<0.0001; blue: p<0.0001; red: p=0.2962), *Tep4-GAL4,UASmcherry /Fum*^{RNAi} (n=25, green: p<0.0001; blue: p<0.0001; red: p<0.0001), *domeMeso>GFP/Mdh*^{RNAi} (n=28, green: p<0.0001; blue: p=0.0040; red: p=0.6686), **(B)** Quantification in terms of total lymph gland area, *Tep4-GAL4,UASmcherry /+* (control, n=94), *Tep4-GAL4,UASmcherry /CS*^{RNAi} (n=83, p>0.9999), *Tep4-GAL4,UASmcherry/mAcon1RNAi* (n=43, p<0.0001), *Tep4-GAL4,UASmcherry/Idh*^{RNAi} (n=51, p=0.4150), *Tep4-GAL4,UASmcherry/α-Kdh*^{RNAi} (n=34, p=0.0024), *Tep4-GAL4,UASmcherry/Skap*^{RNAi} (n=28, p>0.9999), *Tep4-GAL4,UASmcherry/Sdh*^{RNAi} (n=48, p=0.9497), *Tep4-GAL4,UASmcherry/Fum*^{RNAi} (n=55, p>0.9999), *Tep4-GAL4,UASmcherry/Mdh*^{RNAi} (n=80, p=0.9912). Data is presented as median plots (*p<0.05; **p<0.01; ***p<0.001; ****p<0.0001), ordinary one-way ANOVA. Scale bar: 20µm. 'n'=lymph gland lobes. DAPI marks DNA, Progenitors (*Tep4*$^{+}$; Green), Differentiating population (*Pxn*$^{+}$; Red). Comparisons for significance are with control values.

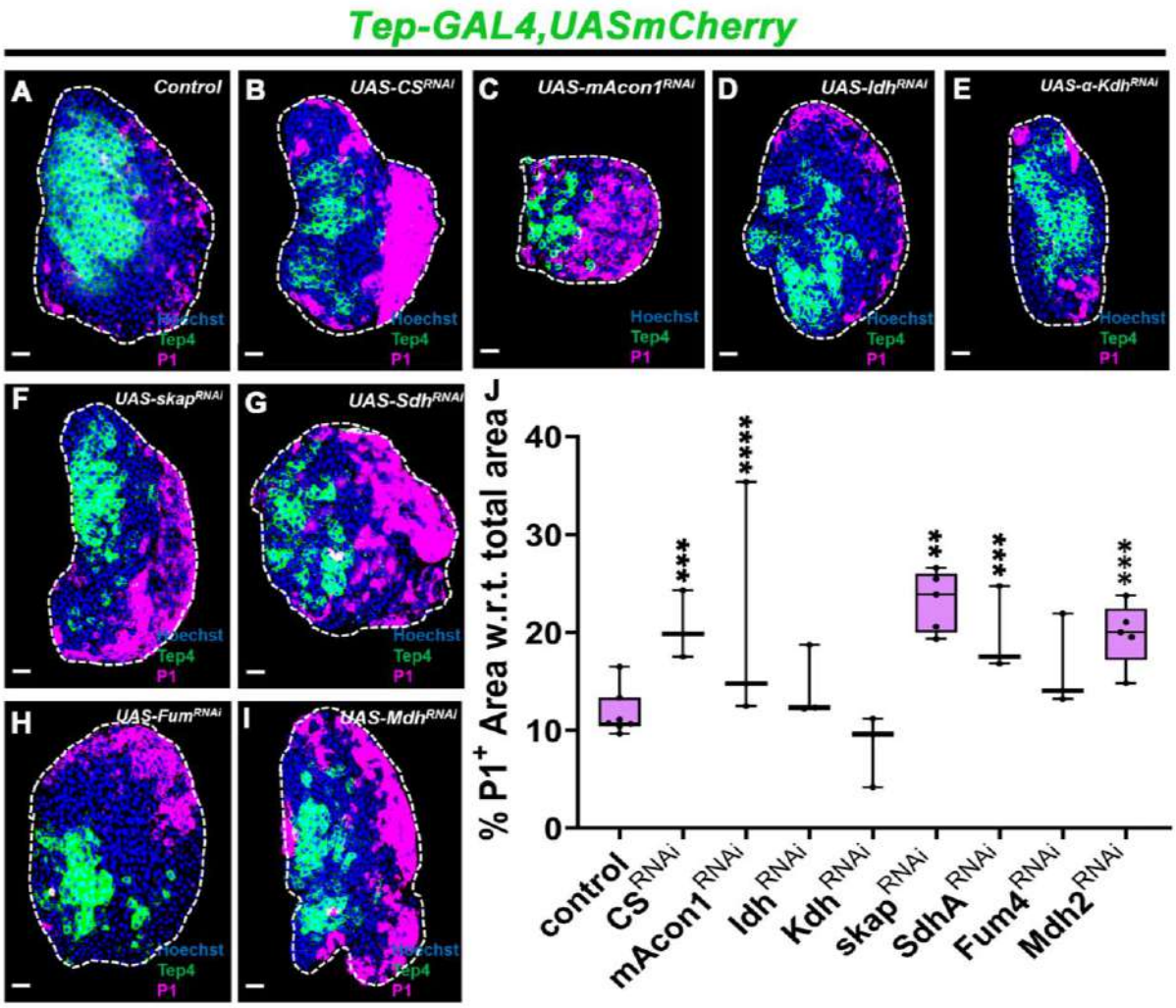

Figure 13: Blocking TCA cycle in core progenitors increases plasmatocytes (*P1*$^{+}$) population in LG.

(A) *Control* (*Tep4-GAL4,UASmcherry/+*) lymph gland showing general distribution of mature plasmatocytes (*P1*$^{+}$; magenta) population at 3rd instar larval stage, **(B)** expressing *CS*^{RNAi} (*Tep4-GAL4,UASmcherry;UAS-CS*^{RNAi}), **(C)** *mAcon1*^{RNAi} (*Tep4-GAL4,UASmcherry;UAS-mAcon1*^{RNAi}), **(D)** *α-Kdh*^{RNAi} (*Tep4-GAL4,UASmcherry;UAS-α-Kdh*^{RNAi}), **(E)** *Idh*^{RNAi} (*Tep4-GAL4,UASmcherry;UAS-Idh*^{RNAi}), **(F)** *Skap*^{RNAi} (*Tep4-GAL4,UASmcherry;UAS-Skap*^{RNAi}), **(G)** *Sdh*^{RNAi} (*Tep4-GAL4,UASmcherry;UAS-Sdh*^{RNAi}), **(H)** *Fum*^{RNAi} (*Tep4-GAL4,UASmcherry;UAS-Fum*^{RNAi}),and **(I)** *Mdh*^{RNAi} (*Tep4-GAL4,UASmcherry;UAS-Mdh*^{RNAi}), **(B-C and F-G, I)** lymph glands shows increase in plasmatocytes, compare to **(A)** *control*. **(J)** Quantification is relative % area with respect to total lymph gland area for plasmatocyte (magenta), *Tep4-GAL4,UASmcherry /+* (*control*, n=51), *Tep4-GAL4,UASmcherry/CS*^{RNAi} (n=41, p=0.0008), *Tep4-GAL4,UASmcherry/mAcon1*^{RNAi} (n=19, p<0.0001), *Tep4-GAL4,UASmcherry/A-Kdh*^{RNAi} (n=26, p=0.2850), *Tep4-GAL4,UASmcherry/Idh*^{RNAi} (n=26, p=0.3535), *Tep4-GAL4,UASmcherry/Skap*^{RNAi} (n=22, p=0.0054), *Tep4-GAL4,UASmcherry/Sdh*^{RNAi} (n=39, p=0.0004), *Tep4-GAL4,UASmcherry/Fum*^{RNAi} (n=31, p=0.4882), *Tep4-GAL4,UASmcherry/Mdh*^{RNAi} (n=67, p=0.0008). Data is presented as median plots (*p<0.05; **p<0.01; ***p<0.001; ****p<0.0001), ordinary one-way ANOVA. Scale bar: 20µm. 'n'=lymph gland lobes. DAPI marks DNA, Progenitors (*Dome*$^{+}$; Green), Differentiated plasmatocyte population (magenta). Comparisons for significance are with control values.

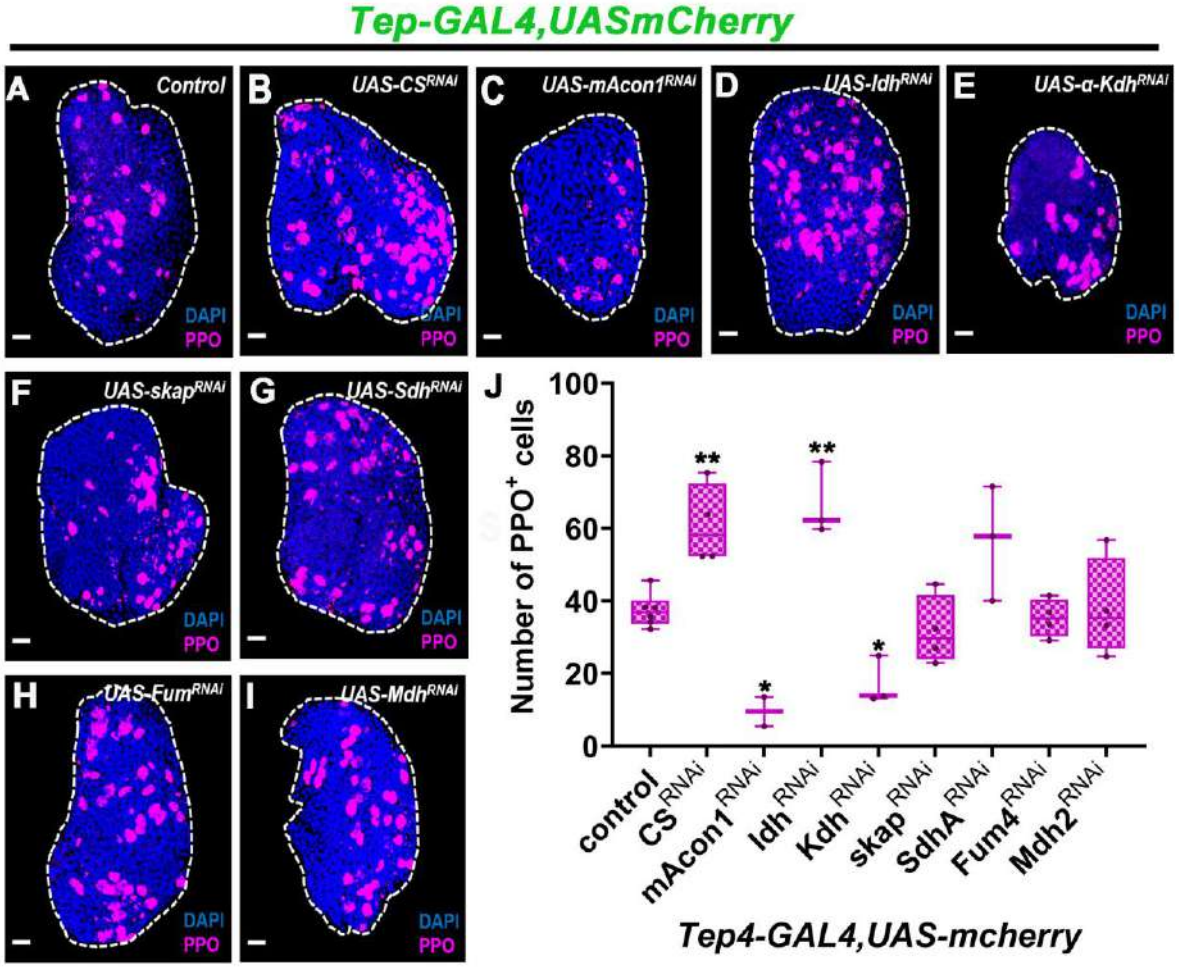

Figure 14: Blocking TCA cycle in core progenitors impact crystal cell (*PPO*$^{+}$) population in LG.

(A)*Control* (*Tep4-GAL4,UASmcherry/+*) lymph gland showing general distribution of mature crystal cells (*PPO*$^{+}$; magenta) population at 3rd instar larval stage, **(B)** expressing *CS*^{RNAi} (*Tep4-GAL4,UASmcherry;UAS-CS*^{RNAi}), **(C)** *mAcon1*^{RNAi} (*Tep4-GAL4,UASmcherry;UAS-mAcon1*^{RNAi}), **(D)** *α-KdhRNAi* (*Tep4-GAL4,UASmcherry;UAS-α-Kdh*^{RNAi}), **(E)** *Idh*^{RNAi} (*Tep4-GAL4,UASmcherry;UAS-Idh*^{RNAi}), **(F)** *Skap*^{RNAi} (*Tep4-GAL4,UASmcherry;UAS-Skap*^{RNAi}), **(G)** *Sdh*^{RNAi} (*Tep4-GAL4,UASmcherry;UAS-Sdh*^{RNAi}), **(H)** *Fum*^{RNAi} (*Tep4-GAL4,UASmcherry;UAS-Fum*^{RNAi}),and **(I)** *Mdh*^{RNAi} (*Tep4-GAL4,UASmcherry;UAS-Mdh*^{RNAi}), **(B and D)** lymph glands shows increase in crystal cells, whereas (**C** and **E)** shows decrease in crystal cell population (*PPO*$^{+}$; magenta), compare to **(A)** *control*. **(J)** Quantification is total number of crystal cells (*PPO*+) cells in entire LG lobe, *Tep4-GAL4,UASmcherry /+* (*control*, n=74), *Tep4-GAL4,UASmcherry/CS*^{RNAi} (n=49, p=0.0060), *Tep4-GAL4,UASmcherry/mAcon1*^{RNAi} (n=18, p=0.0108), *Tep4-GAL4,UASmcherry/A-Kdh*^{RNAi} (n=30, p=0.0437), *Tep4-GAL4,UASmcherry/Idh*^{RNAi} (n=60, p=0.0016), *Tep4-GAL4,UASmcherry/Skap*^{RNAi} (n=47, p=0.9433), *Tep4-GAL4,UASmcherry/Sdh*^{RNAi} (n=56, p=0.0611), *Tep4-GAL4,UASmcherry/Fum*^{RNAi} (n=43, p>0.9999), *Tep4-GAL4,UASmcherry/Mdh*^{RNAi} (n=76, p>0.9999). Data is presented as median plots (*p<0.05; **p<0.01; ***p<0.001; ****p<0.0001), ordinary one-way ANOVA. Scale bar: 20μm. 'n'=lymph gland lobes. DAPI marks DNA, crystal cells (magenta). Comparisons for significance are with control values.

These phenotypes were largely similar to those seen with *Dome* (Pan progenitor) phenotypes, with some exceptions. This suggests that most phenotypes arise from the *Tep4*$^{+}$ *Dome*$^{+}$ progenitor population, whereas exceptions may reflect contributions of individual *Tep4*$^{+}$ or *Dome*$^{+}$ subsets. For example, progenitor loss and differentiation phenotype in *Fum*^{RNAi} and *Mdh*^{RNAi}, and the increase in crystal cells in *CS*^{RNAi} (contrary to the *Dome* specific decrease in crystal cells under *CS*^{RNAi}), likely originate from *Tep4*$^{+}$ cells. Conversely, the loss of crystal cells in *Skap*^{RNAi} and *Sdha*^{RNAi} appears to derive from *Dome*+ progenitors. However, due to the lack of appropriate reagents, this hypothesis could not be tested further.

3.2 TCA cycle regulate fate specification in CZ

To determine whether the regulation of progenitor maintenance is cell-autonomous or non-autonomous, we knockdown TCA cycle enzymes in the differentiating population using *Hml*$^{\Delta}$*-GAL4,UAS-2X EGFP* (CZ) driver. Knockdown of TCA cycle genes in CZ cells did not produce changes in the Hml^{+} population, except in the *α-Kdh* ^{RNAi} background, where a reduction of Hml^{+} (green) cells was observed. This reduction indirectly suggests as expansion of progenitors (blue) (Figure 15: D, J). We next examined blood cell specific markers; for plasmatocytes, *Pxn*$^{+}$ (red) population was found to be reduced in *mAcon1*^{RNAi}, *α-Kdh*^{RNAi} and *Fum*^{RNAi}, and this reduction was compensated by an increase in *P1+* (magenta), a terminal differentiation marker for plasmatocytes, in all cases. These results indicate that specific steps of the TCA cycle regulate plasmatocyte differentiation in CZ (Figure 16: C-E, H, J). For crystal cells (magenta), reductions were observed only in *CS*^{RNAi}, *mAcon1*^{RNAi} and *α-Kdh*^{RNAi}, with no change in other knockdowns (Figure 17: B-D, J).

Another phenotype observed following TCA cycle knockdowns in the LG was growth defect. Surprisingly, regulation of this phenotype differed across zones. In the pan-progenitor compartment (*Dome*$^{+}$; MZ), using *domeMESO-GAL4,UAS-GFP* driver, growth defect was seen upon *CS*, *mAcon1*, and *α-Kdh* knockdowns (Figure 9: B; D-G). In contrast, in the subset of progenitors marked by *Tep4-GAL4,UASmcherry* driver, growth defects were observed only with *mAcon1* and *α-Kdh* knockdowns (Figure 12: B; E, G). This differential regulation of LG size in core (*Tep4*$^{+}$) vs total (*Dome*$^{+}$) progenitor highlights two important aspects of growth regulation: firstly, *CS* is dispensable in *Tep4*$^{+}$ only cells during early development of the LG, and second, the TCA does not operate as a complete cycle early in early development, at least with respet to lymph gland growth, since *Idh* knockdown which biochemically connects *mAcon1*did not produce growth defect in either progenitor compartment.

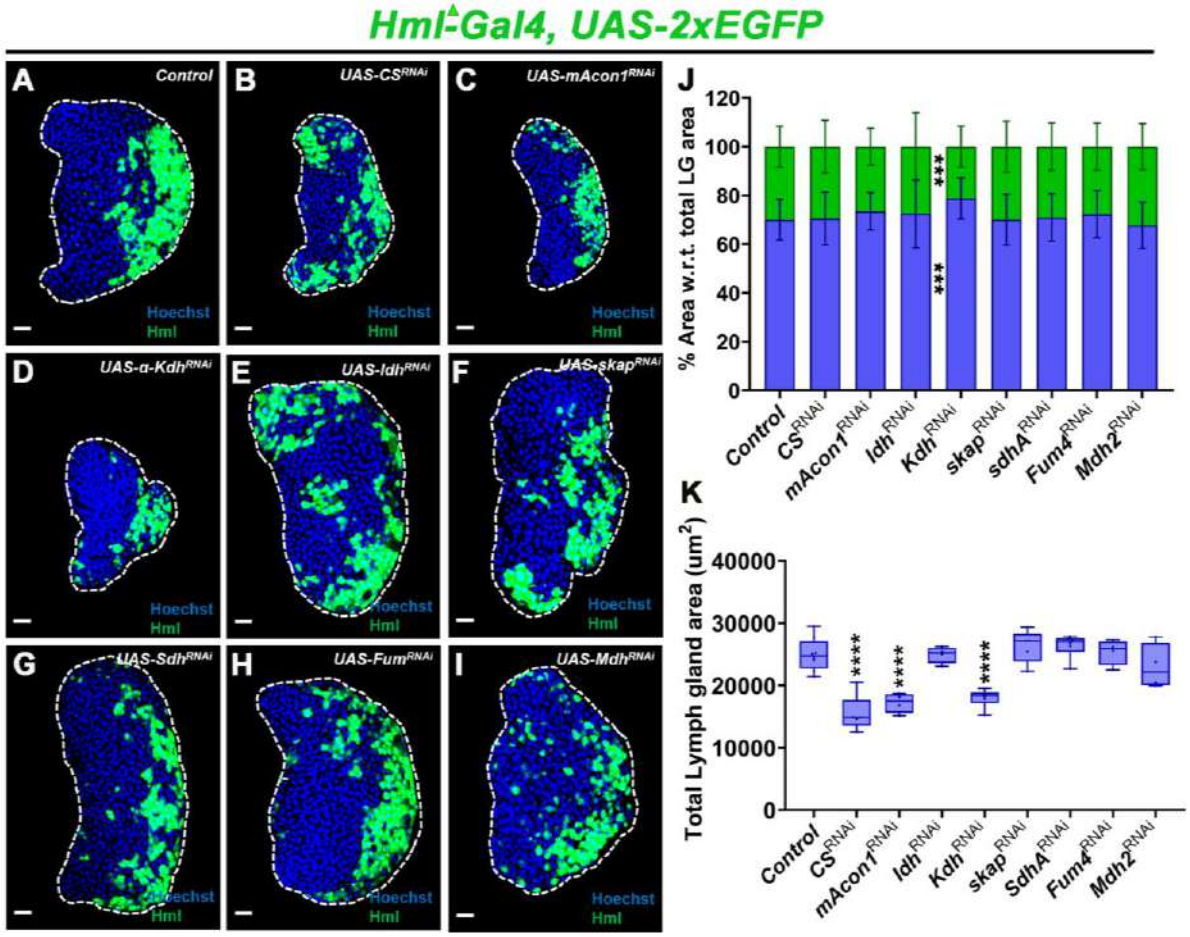

Figure 15: *α-Kdh* regulates the proliferative capacity of cortical zone in LG.

(A) *Control* (*Hml$^{\Delta}$-GAL4,UAS-2X EGFP/+*) lymph gland showing general distribution of mature plasmatocytes (*P1^{+}*; magenta) population at 3rd instar larval stage, **(B)** expressing *CS^{RNAi}* (*Hml$^{\Delta}$-GAL4,UAS-2X EGFP;UAS-CS^{RNAi}*), **(C)** *mAcon1^{RNAi}* (*Hml$^{\Delta}$-GAL4,UAS-2X EGFP;UAS-mAcon1^{RNAi}*), **(D)** *α-Kdh^{RNAi}* (*Hml$^{\Delta}$-GAL4,UAS-2X EGFP;UAS-α-Kdh^{RNAi}*), (**E**) *Idh^{RNAi}* (*Hml$^{\Delta}$-GAL4,UAS-2X EGFP;UAS-Idh^{RNAi}*), (**F**) *Skap^{RNAi}* (*Hml$^{\Delta}$-GAL4,UAS-2X EGFP;UAS-Skap^{RNAi}*), (**G**) *Sdh^{RNAi}* (*Hml$^{\Delta}$-GAL4,UAS-2X EGFP;UAS-Sdh^{RNAi}*), **(H)** *Fum^{RNAi}* (*Hml$^{\Delta}$-GAL4,UAS-2X EGFP;UAS-Fum^{RNAi}*),and **(I)** *Mdh^{RNAi}* (*Hml$^{\Delta}$-GAL4,UAS-2X EGFP;UAS-Mdh^{RNAi}*), **(B-C and F-G, I)** lymph glands shows increase in plasmatocytes, compare to **(A)** *control*. **(J)** Quantification is relative % area with respect to total lymph gland area for maintenance and differentiation profile, *Hml$^{\Delta}$-GAL4,UAS-2X EGFP /+* (*control*, n=60), *Hml$^{\Delta}$-GAL4,UAS-2X EGFP /CS^{RNAi}* (n=60, blue: p>0.9999; green: p>0.9999), *Hml$^{\Delta}$-GAL4,UAS-2X EGFP/mAcon1^{RNAi}* (n=48, blue: p=0.3800; green: p=0.3800), *Hml$^{\Delta}$-GAL4,UAS-2X EGFP/α-Kdh^{RNAi}* (n=34, blue: p=0.0004; green: p=0.0004), *Hml$^{\Delta}$-GAL4,UAS-2X EGFP /Idh^{RNAi}* (n=39, blue: p=0.8091; green: p=0.8091), *Hml$^{\Delta}$-GAL4,UAS-2X EGFP/Skap^{RNAi}* (n=38, blue: p>0.9999; green: p>0.9999), *Hml$^{\Delta}$-GAL4,UAS-2X EGFP/Sdh^{RNAi}* (n=51, blue: p=0.9994; green: p=0.9994), *Hml$^{\Delta}$-GAL4,UAS-2X EGFP/Fum^{RNAi}* (n=45, blue: p=0.8338; green: p=0.8338), *Hml$^{\Delta}$-GAL4,UAS-2X EGFP/Mdh^{RNAi}* (n=47, blue: p=0.7882; green: p=0.7882), Quantification is relative % area with respect to total lymph gland area for Hml+ (green) cells, *Hml$^{\Delta}$-GAL4,UAS-2X EGFP/+* (*control*, n=47), *Hml$^{\Delta}$-GAL4,UAS-2X EGFP/CS^{RNAi}* (n=61, p<0.0001), *Hml$^{\Delta}$-GAL4,UAS-2X EGFP /mAcon1^{RNAi}* (n=47, p<0.0001), *Hml$^{\Delta}$-GAL4,UAS-2X EGFP/α-Kdh^{RNAi}* (n=33, p<0.0001), *Hml$^{\Delta}$-GAL4,UAS-2X EGFP /Idh^{RNAi}* (n=40, p>0.9999), *Hml$^{\Delta}$-GAL4,UAS-2X EGFP /Skap^{RNAi}* (n=38, p=0.9197), *Hml$^{\Delta}$-GAL4,UAS-2X EGFP /Sdh^{RNAi}* (n=48, p=0.8555), *Hml$^{\Delta}$-GAL4,UAS-2X EGFP /Fum^{RNAi}* (n=54, p>0.9999), *Hml$^{\Delta}$-GAL4,UAS-2X EGFP /Mdh^{RNAi}* (n=47, p=0.7138). Data is presented as median plots (*p<0.05; **p<0.01; ***p<0.001; ****p<0.0001), ordinary one-way ANOVA. Scale bar: 20µm. 'n'=lymph gland lobes. DAPI marks DNA, Progenitors (blue), Differentiating population (green). Comparisons for significance are with control values.

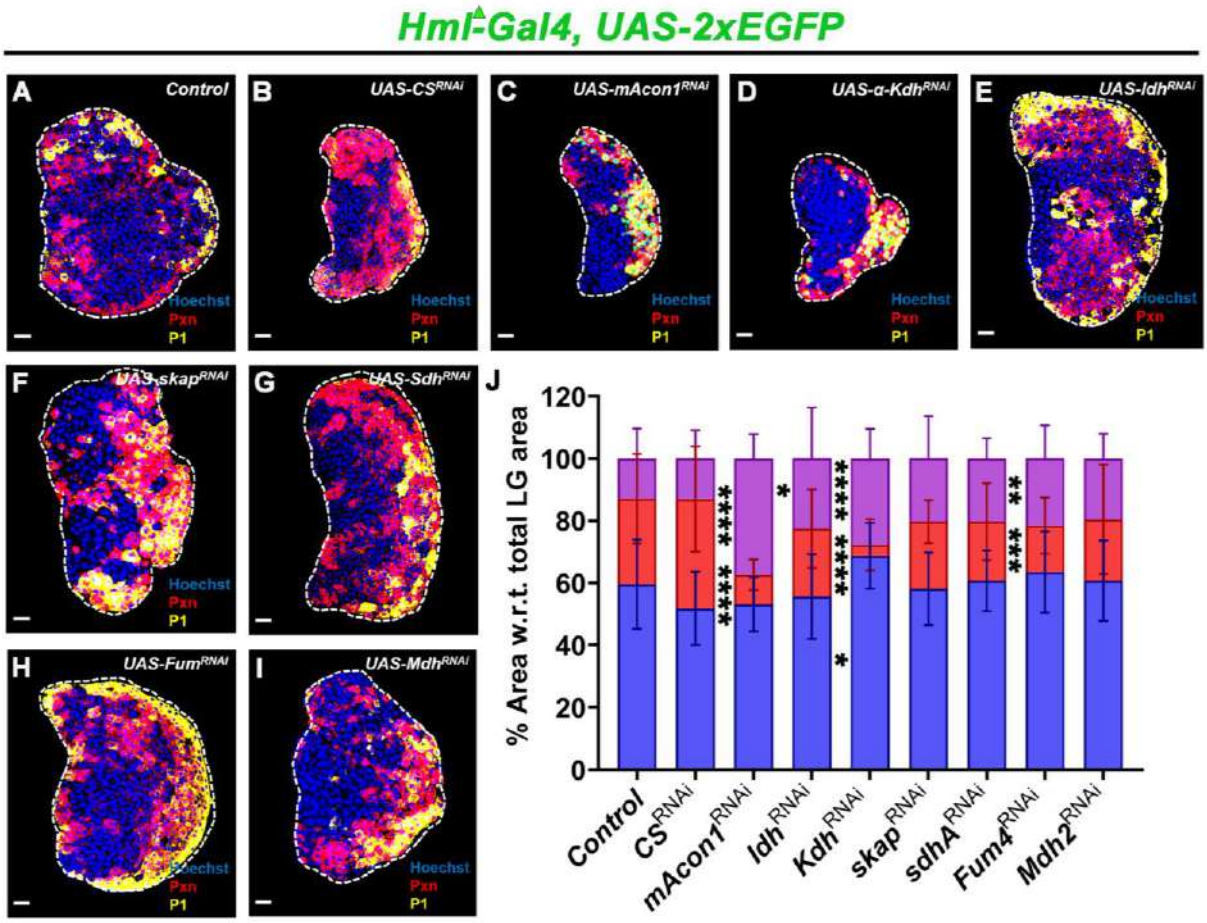

Figure 16: Loss of TCA cycle in CZ increases plasmatocyte fate in LG.

(A) *Control* (*Hml$^{\Delta}$-GAL4,UAS-2X EGFP/+*) lymph gland showing general distribution of mature plasmatocytes (*Pxn^{+}*; red and *P1^{+}*; magenta) population at 3rd instar larval stage, **(B)** expressing *CS^{RNAi}* (*Hml$^{\Delta}$-GAL4,UAS-2X EGFP;UAS-CS^{RNAi}*), **(C)** *mAcon1^{RNAi}* (*Hml$^{\Delta}$-GAL4,UAS-2X EGFP;UAS-mAcon1^{RNAi}*), **(D)** *α-Kdh^{RNAi}* (*Hml$^{\Delta}$-GAL4,UAS-2X EGFP;UAS-α-Kdh^{RNAi}*), **(E)** *Idh^{RNAi}* (*Hml$^{\Delta}$-GAL4,UAS-2X EGFP;UAS-Idh^{RNAi}*), **(F)** *Skap^{RNAi}* (*Hml$^{\Delta}$-GAL4,UAS-2X EGFP;UAS-Skap^{RNAi}*), **(G)** *Sdh^{RNAi}* (*Hml$^{\Delta}$-GAL4,UAS-2X EGFP;UAS-Sdh^{RNAi}*), **(H)** *Fum^{RNAi}* (*Hml$^{\Delta}$-GAL4,UAS-2X EGFP;UAS-Fum^{RNAi}*),and **(I)** *Mdh^{RNAi}* (*Hml$^{\Delta}$-GAL4,UAS-2X EGFP;UAS-Mdh^{RNAi}*), **(C, E and H)** lymph glands shows decrease in early plasmatocytes marker (*Pxn*+; red), this decrease is due to expansion of mature plasmatocytes (*P1^{+}*; magenta), and no effect on progenitors (blue) was observed except for *α-Kdh^{RNAi}* compare to **(A)** *control*. **(J)** Quantification is relative % area with respect to total lymph gland area for *Pxn^{+}* (red) and *P1^{+}* (magenta) cells, *Hml$^{\Delta}$-GAL4,UAS-2X EGFP/+* (*control*, n=38), *Hml$^{\Delta}$-GAL4,UAS-2X EGFP/CS^{RNAi}* (n=21, blue, p=0.1406; red, p=0.1666; magenta, p>0.9999), *Hml$^{\Delta}$-GAL4,UAS-2X EGFP /mAcon1RNAi* (n=14, blue, p=0.4891; red, p<0.0001; magenta, p<0.0001), *Hml$^{\Delta}$-GAL4,UAS-2X EGFP/α-Kdh^{RNAi}* (n=23, blue, p=0.0433; red, p<0.0001; magenta, p<0.0001), *Hml$^{\Delta}$-GAL4,UAS-2X EGFP /Idh^{RNAi}* (n=17, blue, p=0.8805; red, p=0.5812; magenta, p=0.0116), *Hml$^{\Delta}$-GAL4,UAS-2X EGFP /Skap^{RNAi}* (n=12, blue, p=0.9999; red, p=0.6820; magenta, p=0.1956), *Hml$^{\Delta}$-GAL4,UAS-2X EGFP /Sdh^{RNAi}* (n=13, blue, p>0.9999; red, p=0.2257; magenta, p=0.1683), *Hml$^{\Delta}$-GAL4,UAS-2X EGFP /Fum^{RNAi}* (n=29, blue, p=0.7853; red, p=0.0006; magenta, p=0.0061), *Hml$^{\Delta}$-GAL4,UAS-2X EGFP /Mdh^{RNAi}* (n=20, blue, p>0.9999; red, p=0.1763; magenta, p=0.1388). Data is presented as median plots (*p<0.05; **p<0.01; ***p<0.001; ****p<0.0001), ordinary one-way ANOVA. Scale bar: 20µm. 'n'=lymph gland lobes. DAPI marks DNA, Progenitors (blue), Differentiating population (*Pxn^{+}*; red and *P1^{+}*; magenta). Comparisons for significance are with control values.

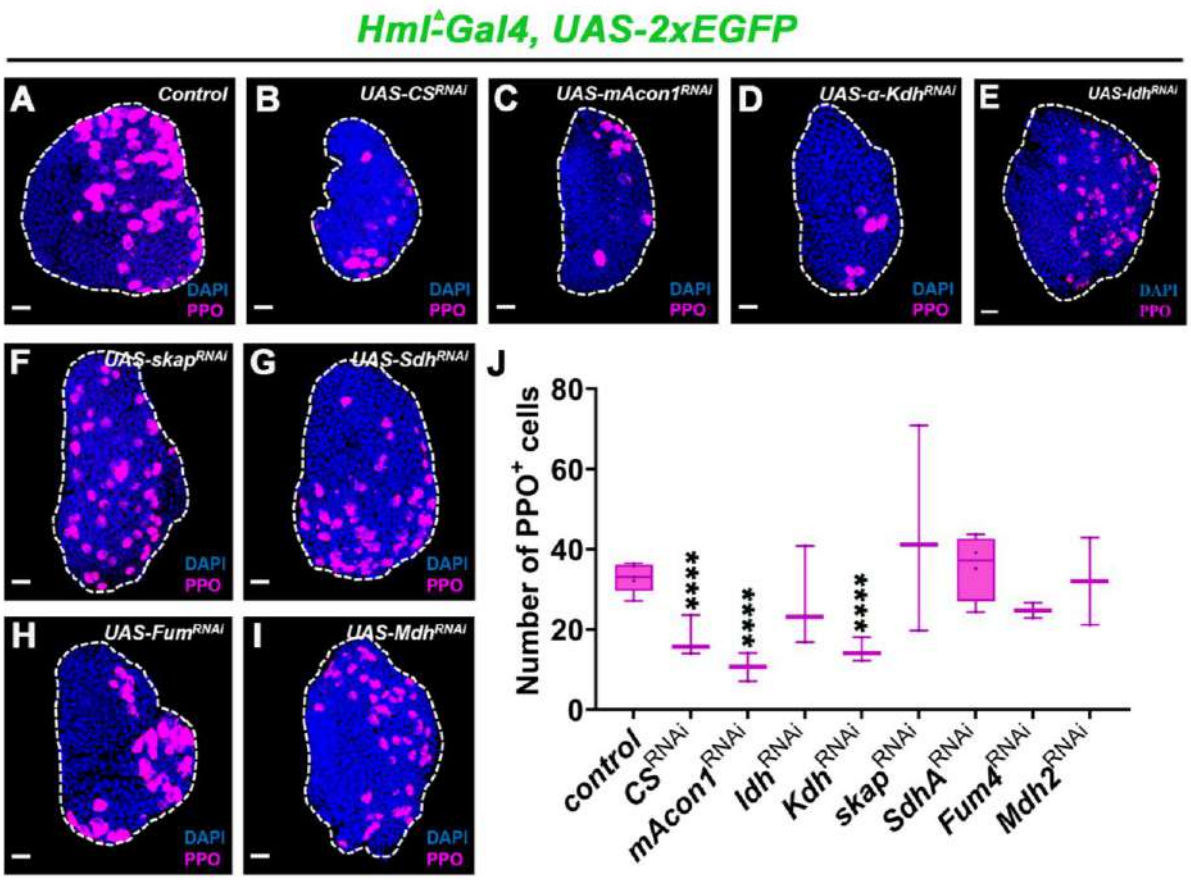

Figure 17: Loss of certain steps of TCA cycle in CZ leads to reduction in crystal cell population in LG.

(A) *Control* (*Hml$^{\Delta}$-GAL4,UAS-2X EGFP/+*) lymph gland showing general distribution of mature plasmatocytes (*Pxn^{+}*; red and *P1^{+}*; magenta) population at 3rd instar larval stage, **(B)** expressing *CS^{RNAi}* (*Hml$^{\Delta}$-GAL4,UAS-2X EGFP;UAS-CS^{RNAi}*), **(C)** *mAcon1^{RNAi}* (*Hml$^{\Delta}$-GAL4,UAS-2X EGFP;UAS-mAcon1^{RNAi}*), **(D)** *α-Kdh^{RNAi}* (*Hml$^{\Delta}$-GAL4,UAS-2X EGFP;UAS-α-Kdh^{RNAi}*), **(E)** *Idh^{RNAi}* (*Hml$^{\Delta}$-GAL4,UAS-2X EGFP;UAS-Idh^{RNAi}*), **(F)** *Skap^{RNAi}* (*Hml$^{\Delta}$-GAL4,UAS-2X EGFP;UAS-Skap^{RNAi}*), **(G)** *Sdh^{RNAi}* (*Hml$^{\Delta}$-GAL4,UAS-2X EGFP;UAS-Sdh^{RNAi}*), **(H)** *Fum^{RNAi}* (*Hml$^{\Delta}$-GAL4,UAS-2X EGFP;UAS-Fum^{RNAi}*),and **(I)** *Mdh^{RNAi}* (*Hml$^{\Delta}$-GAL4,UAS-2X EGFP;UAS-Mdh^{RNAi}*), **(C, E and H)** lymph glands shows decrease in early plasmatocytes marker (*Pxn^{+}*; red), this decrease is due to expansion of mature plasmatocytes (*P1+*; magenta), and no effect on progenitors (blue) was observed except for *α-Kdh^{RNAi}* compare to **(A)** *control*. **(J)** Quantification is relative % area with respect to total lymph gland area for *Pxn^{+}* (red) and *P1^{+}* (magenta) cells, *Hml$^{\Delta}$-GAL4,UAS-2X EGFP/+* (*control*, n=67), *Hml$^{\Delta}$-GAL4,UAS-2X EGFP/CS^{RNAi}* (n=30, p<0.0001), *Hml$^{\Delta}$-GAL4,UAS-2X EGFP /mAcon1^{RNAi}* (n=47, p<0.0001), *Hml$^{\Delta}$-GAL4,UAS-2X EGFP/α-Kdh^{RNAi}* (n=38, p<0.0001), *Hml$^{\Delta}$-GAL4,UAS-2X EGFP /Idh^{RNAi}* (n=31, p=0.2050), *Hml$^{\Delta}$-GAL4,UAS-2X EGFP /Skap^{RNAi}* (n=31, p=0.7689), *Hml$^{\Delta}$-GAL4,UAS-2X EGFP /Sdh^{RNAi}* (n=71, p=0.1610), *Hml$^{\Delta}$-GAL4,UAS-2X EGFP /Fum^{RNAi}* (n=52, p=0.4062), *Hml$^{\Delta}$-GAL4,UAS-2X EGFP /Mdh^{RNAi}* (n=33, p=0.9199). Data is presented as median plots (*p<0.05; **p<0.01; ***p<0.001; ****p<0.0001), ordinary one-way ANOVA. Scale bar: 20µm. 'n'=lymph gland lobes. DAPI marks DNA, Progenitors (blue), Differentiating population (*Pxn^{+}*; red and *P1^{+}*; magenta). Comparisons for significance are with control values.

Similar results were obtained in the CZ, where growth defect were observed upon knockdown of *CS, mAcon1, and α-Kdh.* This result mirrors that of the MZ, suggesting that these enzymatic steps are essential for proliferation of both progenitors (MZ) and differentiating population (CZ). Notably, lymph gland growth has been reported to be biphasic, i.e. initial phase driven by progenitor proliferation, which slows at the onset of differentiation, followed by second phase achieve through proliferation of Hml^{+} cells in the CZ.

3.3 TCA cycle regulation in IZ of lymph gland

Next, to determine whether the CZ phenotype is specific to the Hml+ population or instead arises from a small subset of $Dome^{+}$ Hml^{+} double positive population, we utilized ChIZ- GAL4, which marks the IZ, an overlapping population of MZ and CZ ($Dome^{+}$ Hml^{+}). Manipulation of the TCA cycle in this compartment does not lead to changes in the progenitor population (blue). However, an expansion of the $P1^{+}$ (magenta) population was observed within the differentiating population area (Pxn^{+}), indicating that there is no feedback from the IZ to progenitor maintenance via the TCA cycle. Instead, the IZ appear to influence regulation of fate specification (Figure 18: A-J).

The results in the IZ were somewhat distinct. Here, *CS* knockdown do not produce a size defect, but *Idh* knockdown become important. Notably, the timing of CHIZ population ($Dome^{+}$ Hml^{+}) coincide with the onset of differentiation, i.e. around mid to late 2nd instar larval stage, now here *Idh* connecting *mAcon1* and *α-Kdh*steps make sense as all these steps now join together to form a cycle, TCA cycle, for keeping a check on the differentiation and thereby maintaining progenitor pool.

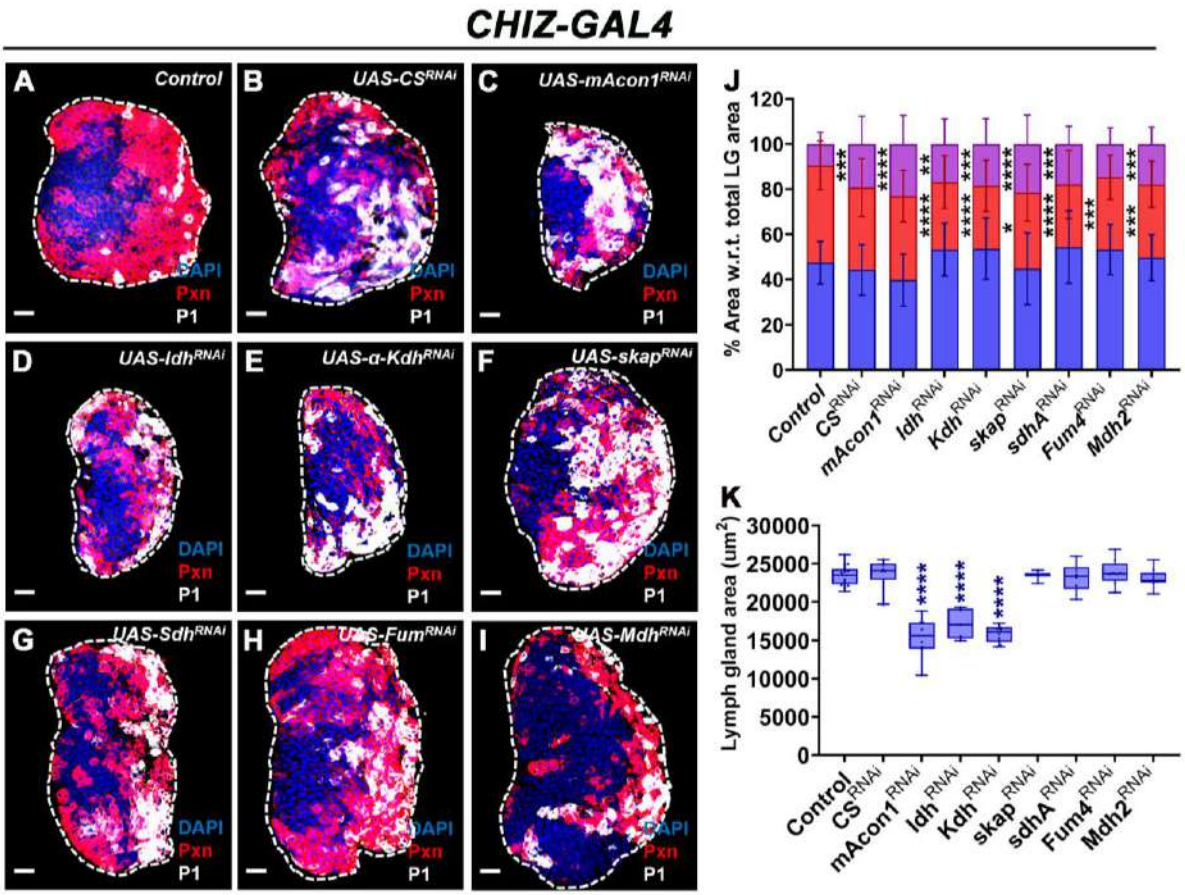

Figure 18: Loss of TCA cycle in IZ favours plasmatocyte fate in LG.

(A) *Control* (*ChIZ-GAL4/+*) lymph gland showing general distribution of immature (Pxn^{+}; red) and mature plasmatocytes ($P1^{+}$; magenta) population at 3rd instar larval stage, **(B)** expressing CS^{RNAi} (*ChIZ-GAL4;UAS-*CS^{RNAi}), **(C)** $mAcon1^{RNAi}$ (*ChIZ-GAL4;UAS-mAcon1*^{RNAi}), **(D)** α-Kdh^{RNAi} (*ChIZ-GAL4;UAS-α-*Kdh^{RNAi}), **(E)** Idh^{RNAi} (*ChIZ-GAL4;UAS-Idh*^{RNAi}), **(F)** $Skap^{RNAi}$ (*ChIZ-GAL4;UAS-Skap*^{RNAi}), **(G)** Sdh^{RNAi} (*ChIZ-GAL4;UAS-*Sdh^{RNAi}), **(H)** Fum^{RNAi} (*ChIZ-GAL4;UAS-Fum*^{RNAi}),and **(I)** Mdh^{RNAi} (*ChIZ-GAL4;UAS-Mdh*^{RNAi}), **(D-I)** lymph glands shows decrease in early plasmatocytes marker (Pxn^{+}; red), this decrease is due to expansion of mature plasmatocytes ($P1^{+}$; magenta) (B-I), and no significant effect on progenitors (blue) was observed compare to **(A)** *control*. Also **(C-E)** smaller LG were observed in $mAcon1^{RNAi}$, Idh^{RNAi} and α-Kdh^{RNAi}**. (J)** Quantification is relative % area with respect to total lymph gland area for maintenance and differentiation profile, *ChIZ-GAL4/+* (*control*, n=40), *ChIZ-GAL4/*CS^{RNAi} (n=23, blue: p=0.9114; red: p=0.1603; gray: p=0.0009), *ChIZ-GAL4/*$mAcon1^{RNAi}$ (n=26, blue: p=0.0807; red: p=0.2272; gray: p<0.0001), *ChIZ-GAL4/A-*Kdh^{RNAi} (n=31, blue: p=0.1790; red: p<0.0001; gray: p=0.0007), *ChIZ-GAL4/*Idh^{RNAi} (n=39, blue: p=0.1858; red: p<0.0001; gray: p=0.0047), *ChIZ-GAL4/*$Skap^{RNAi}$ (n=18, blue: p=0.9780; red: p=0.0286; gray: p<0.0001), *ChIZ-GAL4/*Sdh^{RNAi} (n=30, blue: p=0.1105; red: p<0.0001; gray: p=0.0023), *ChIZ-GAL4/*Fum^{RNAi} (n=40, blue: p=0.1858; red: p=0.0002; gray: p=0.0847), *ChIZ-GAL4/*Mdh^{RNAi} (n=40, blue: p=0.9627; red: p=0.0004; gray: p=0.0009), **(K)** Quantification is total lymph gland area, *ChIZ-GAL4/+* (*control*, n=168), *ChIZ-GAL4/*CS^{RNAi} (n=53, p>0.9999), *ChIZ-GAL4 /*$mAcon1^{RNAi}$ (n=75, p<0.0001), *ChIZ-GAL4/A-*Kdh^{RNAi} (n=94, p<0.0001), *ChIZ-GAL4/*Idh^{RNAi} (n=67, p<0.0001), *ChIZ-GAL4/*$Skap^{RNAi}$ (n=21, p>0.9999), *ChIZ-GAL4/*Sdh^{RNAi} (n=73, p>0.9999), *ChIZ-GAL4/*Fum^{RNAi} (n=95, p=0.9997), *ChIZ-GAL4/*Mdh^{RNAi} (n=93, p=0.9996). Data is presented as median plots (*p<0.05; **p<0.01; p<0.001; ****p<0.0001), ordinary one-way ANOVA. Scale bar: 20µm. 'n'=lymph gland lobes. DAPI marks, (blue), Differentiating population (Pxn^{+}; red and $P1^{+}$; gray). Comparisons for significance are with control values.

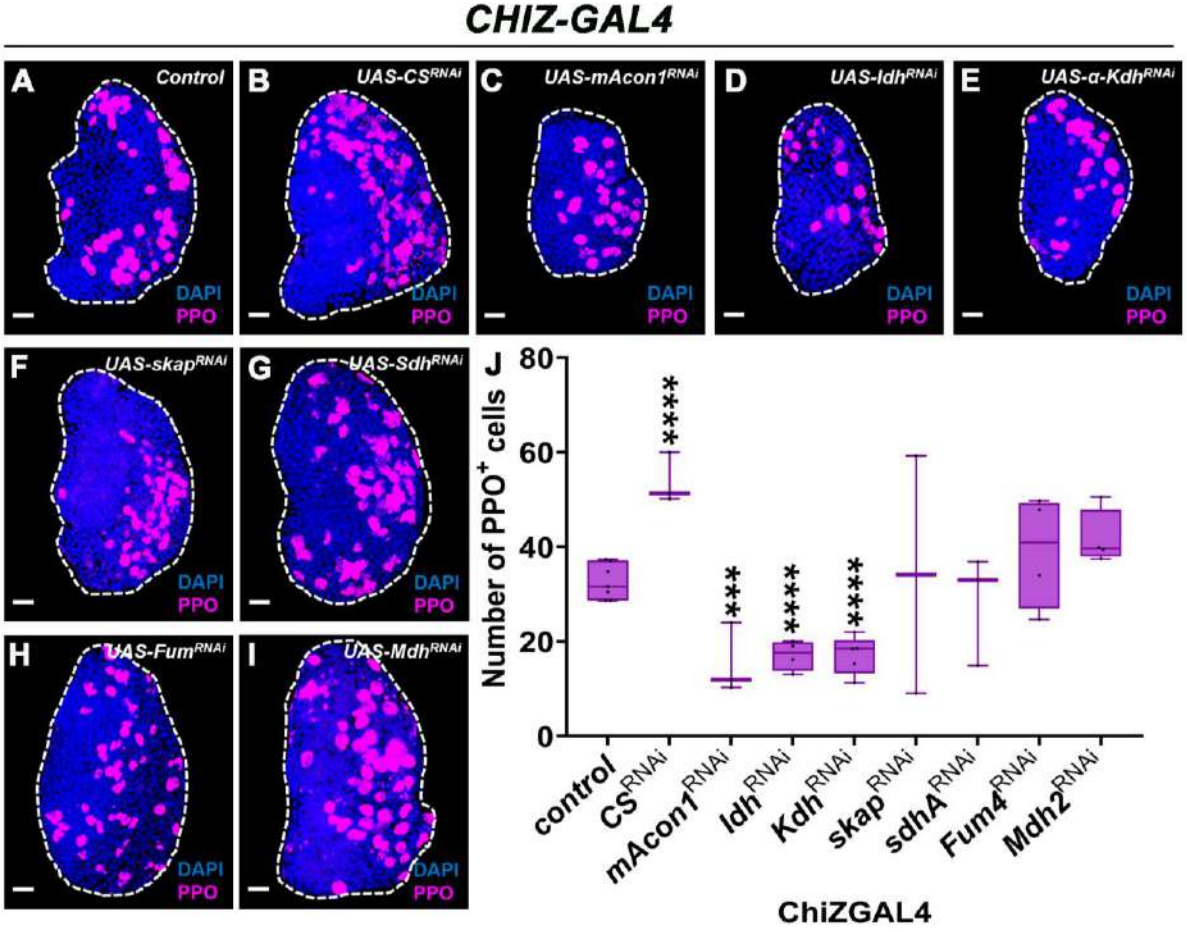

Figure 19: Loss of TCA cycle in IZ impacts crystal cell fate in LG.

(A) *Control* (*ChIZ-GAL4/+*) lymph gland showing general distribution of mature plasmatocytes (*Pxn*$^{+}$; red and *P1*$^{+}$; magenta) population at 3rd instar larval stage, **(B)** expressing *CS*^{RNAi} (*ChIZ-GAL4;UAS-CS*^{RNAi}), **(C)** *mAcon1*^{RNAi} (*ChIZ-GAL4;UAS-mAcon1*^{RNAi}), **(D)** *α-Kdh*^{RNAi} (*ChIZ-GAL4;UAS-α-Kdh*^{RNAi}), (**E**) *Idh*^{RNAi} (*ChIZ-GAL4;UAS-Idh*^{RNAi}), (**F**) *Skap*^{RNAi} (*ChIZ-GAL4;UAS-Skap*^{RNAi}), (**G**) *Sdh*^{RNAi} (*ChIZ-GAL4;UAS-Sdh*^{RNAi}), **(H)** *Fum*^{RNAi} (*ChIZ-GAL4;UAS-Fum*^{RNAi}),and **(I)** *Mdh*^{RNAi} (*ChIZ-GAL4;UAS-Mdh*^{RNAi}), **(C, E and H)** lymph glands shows decrease in early plasmatocytes marker (*Pxn*$^{+}$; red), this decrease is due to expansion of mature plasmatocytes (*P1*+; magenta), and no effect on progenitors (blue) was observed except for *α-Kdh*^{RNAi} compare to **(A)** *control*. **(J)** Quantification is relative % area with respect to total lymph gland area for *Pxn*$^{+}$ (red) and *P1*$^{+}$ (magenta) cells, *ChIZ-GAL4/+* (*control*, n=120), *ChIZ-GAL4/CS*^{RNAi} (n=36, p<0.0001), *ChIZ-GAL4 /mAcon1*^{RNAi} (n=59, p=0.0003), *ChIZ-GAL4/α-Kdh*^{RNAi} (n=54, p<0.0001), *ChIZ-GAL4/Idh*^{RNAi} (n=51, p<0.0001), *ChIZ-GAL4/Skap*^{RNAi} (n=14, p=0.8251), *ChIZ-GAL4/Sdh*^{RNAi} (n=43, p=0.2181), *ChIZ-GAL4/Fum*^{RNAi} (n=53, p=0.1091), *ChIZ-GAL4/Mdh*^{RNAi} (n=54, p=0.8251). Data is presented as median plots (*p<0.05; **p<0.01; ***p<0.001; ****p<0.0001), ordinary one-way ANOVA. Scale bar: 20µm. 'n'=lymph gland lobes. DAPI marks DNA, Progenitors (blue), Differentiating population (*Pxn*$^{+}$; red and *P1*$^{+}$; magenta). Comparisons for significance are with control values.

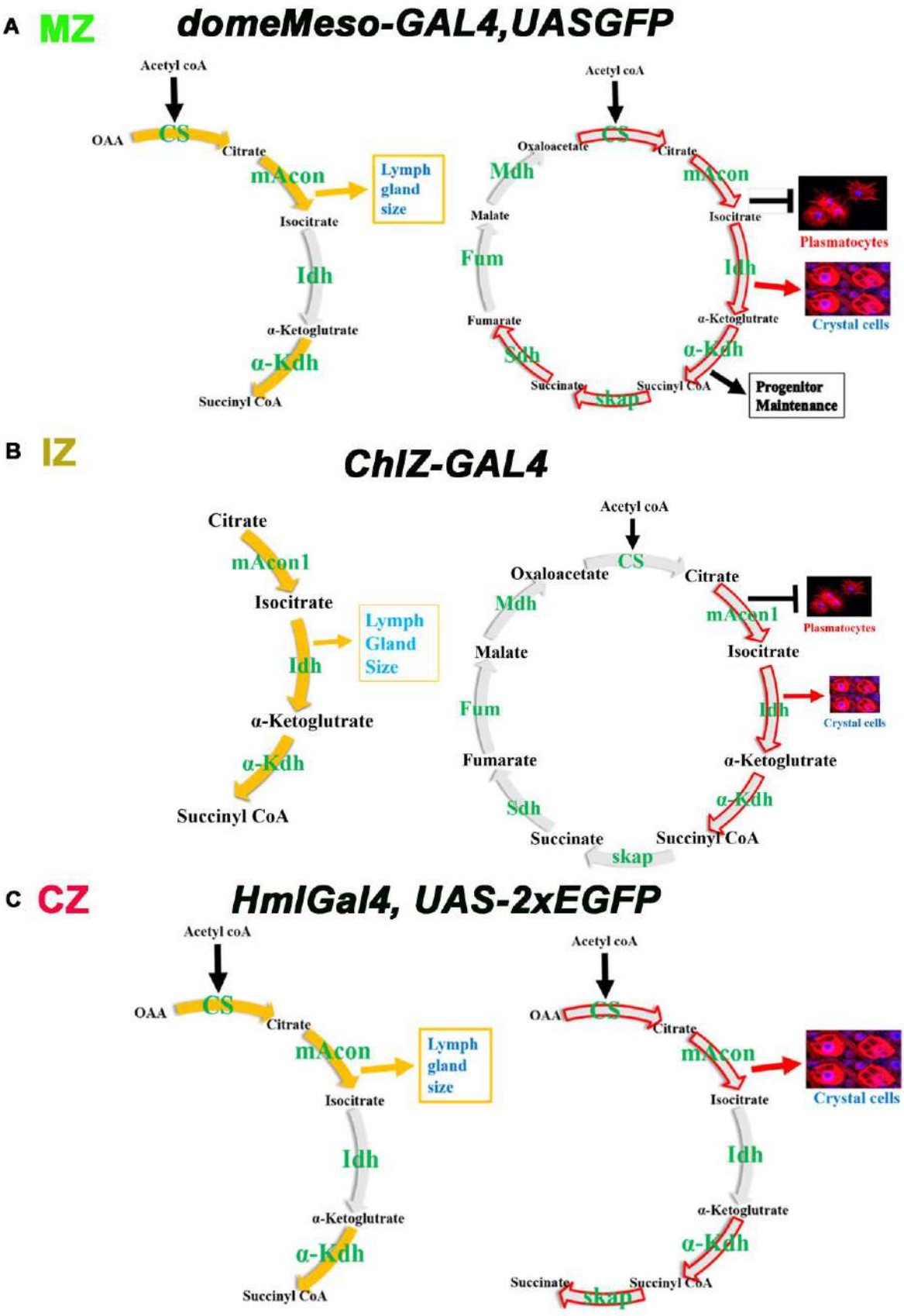
A MZ
domeMeso-GAL4,UASGFP
Acetyl coA
OAA
CS
Citrate
mAcon
Lymph gland size
Isocitrate
Idh
α-Ketoglutrate
α-Kdh
Succinyl CoA
Oxaloacetate
Mdh
Malate
Fum
Fumarate
Sdh
Succinate
skap
Plasmatocytes
Crystal cells
Progenitor Maintenance
B IZ
ChIZ-GAL4
Citrate
mAcon1
Isocitrate
Idh
Lymph Gland Size
α-Ketoglutrate
α-Kdh
Succinyl CoA
Acetyl coA
CS
Oxaloacetate
Citrate
Mdh
Malate
Fum
Fumarate
Sdh
Succinate
skap
Plasmatocytes
Crystal cells
C CZ
HmlGal4, UAS-2xEGFP
Acetyl coA
OAA
CS
Citrate
mAcon
Lymph gland size
Isocitrate
Idh
α-Ketoglutrate
α-Kdh
Succinyl CoA
Crystal cells

Figure 20: Summary of TCA cycle regulation in different zones.

(A) represent the involvement of TCA cycle in two very different aspects of development of lymph gland in medullary zone (MZ) marked by *domeMeso>GFP*; first growth, where only *CS*, *mAcon1* and *Kdh* are necessary steps and there also a disconnect between *mAcon1* and *Kdh* is evident, which highlights the individuality of steps of TCA cycle, on the hand it also brings about the cyclic nature of TCA cycle for the maintenance of progenitors in lymph gland by regulating their differentiation capcity **(B)** represent the TCA cycle regulation in the intermediary zone (IZ) with the help of *ChIZ-GAL4*, here also we observed dual phenotype, growth and fate specification. This population appears around the 60h AEL in development and is $Dome^{+}Hml^{+}$ double positive, which means these cells are going to loose their progenitor status and give rise to the cortical zone, which harbors functionally mature cells. Here intersestingly, the connection between *mAcon1* and Kdh is established in terms of growth (*Idh*) and also this is the probable time point where the steps of TCA cycle come together to operate in syn with each other for the futher maintenance of progenitors as well as acquire a pool of differentiated cell, **(C)** represent the TCA cycle's control in the cortical zone (CZ) marked by Hml^{Δ}*-GAL4,UAS-2X EGFP*. Even though we could not find any feedback regulation of progenitors through cortical zone manipulations but we did find the growth regulation, as we already know that cortical zone proliferation is also necessary for the growth of LG, infact it's the second phase of proliferation which triples the cells in lymph gland (62).

3.4 TCA enzymes transcript distribution in the LG

To understand the distribution and availability of TCA enzymes during lymph gland development, we performed Signal Amplification by Exchange reaction Fluorescence *in-Situ* Hybridization (SABER FISH) to track the transcript expression of the TCA enzymes across developmental stages. SABER FISH, as the name suggests, enhances the conventional FISH signal by amplifying fluorescent probes through the Primer Exchange Reaction (PER) technique (210). The PER technique utilizes catalytic hairpins and a strand displacement polymerase to generate long DNA concatemers that acts as multiple binding sites for fluorophores, enabling highly sensitive and multiplexed detection of nucleic acids (210) (Figure 21). Here we designed 35-60 probes per gene to enhance the signal such that we can visualize single transcript in a cell.

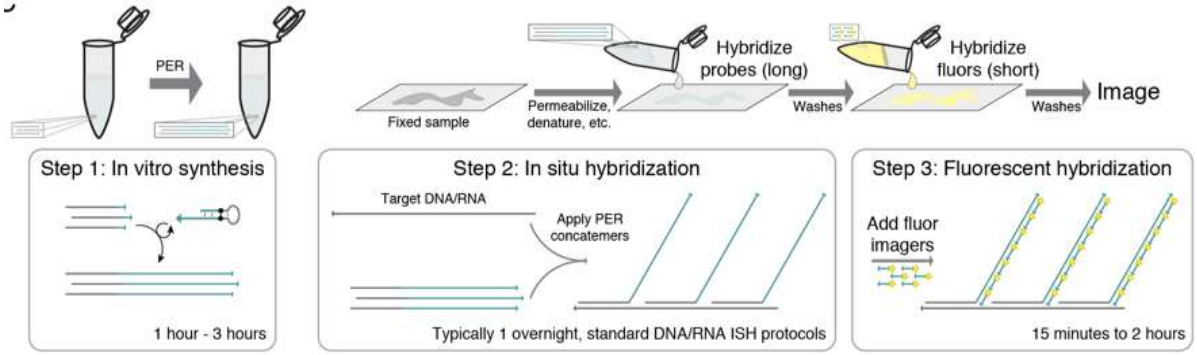

Figure 21: Schematic representation of SABER FISH technique (210, 211)

This technique has been standardized using known genes whose expression patterns is known in the LG. Here, we primarily used *Hml* labelled with two different fluorophores (green, 488nm and red, 546nm) to validate the binding efficiency, assess false positivity, and confirm the expression pattern (Figure 22). We found that the *Hml* transcripts labelled with two different fluorophores overlapped approximately 95-97%, validating the very low to negligible false positivity of the technique (Figure 22). The expression pattern was predominantly observed in the upper and lower z-stack during the imaging and was minimal at the centre, which further validate the efficiency of binding, as the *Hml* protein is a differentiation marker and the differentiation (or cortical) zone exists at the periphery of the LG (Figure 22). We also used *Dome* for validation, and its transcripts were found to be present throughout the LG, with slightly higher concentration in the MZ.

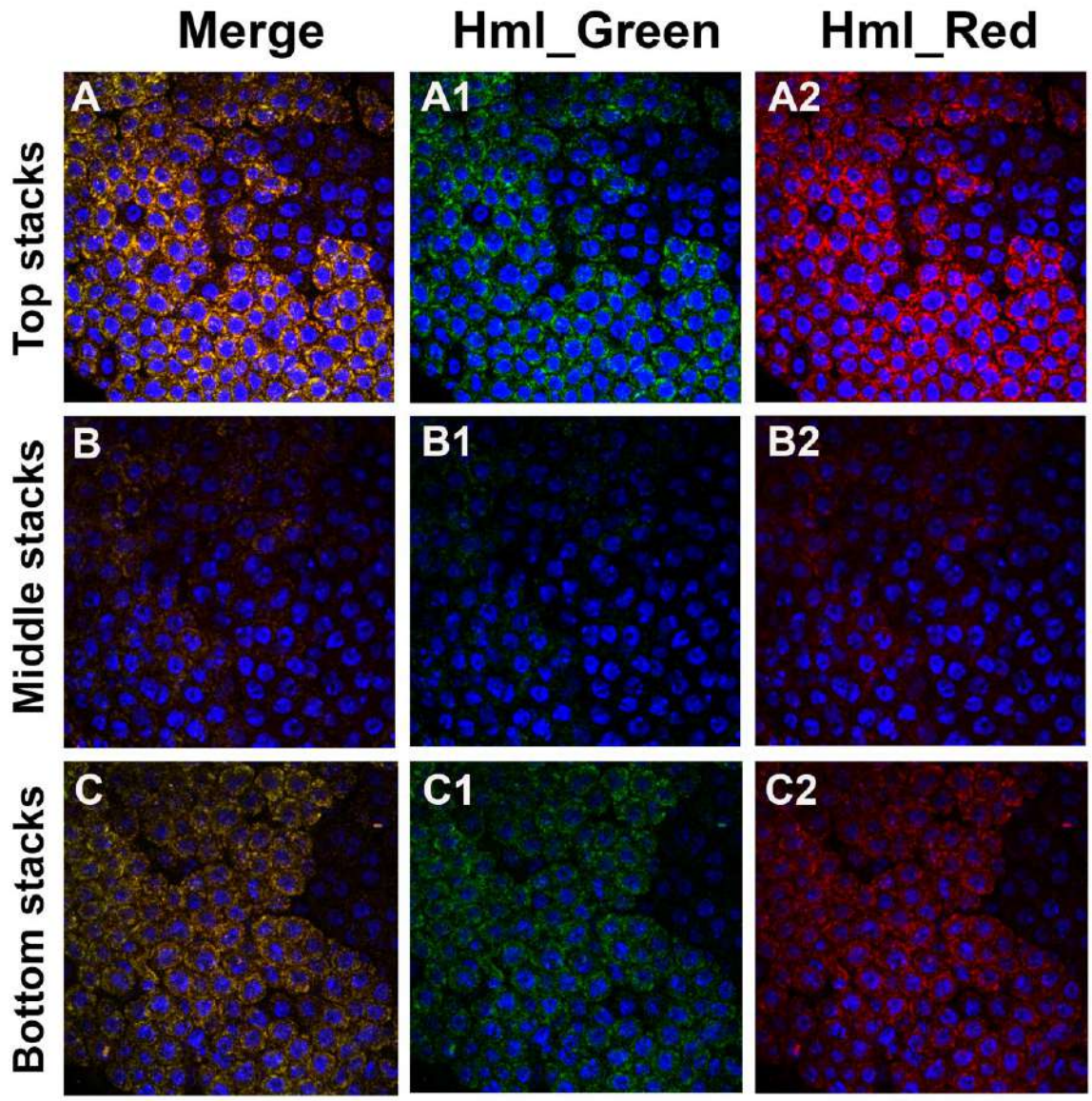

Figure 22: Positive control LG images of SABER FISH to verify the technique.

(A-A2) Top stack of LG showing merge and separate *Hml* transcript, **(B-B2)** Middle stack of LG showing merge and separate *Hml* transcript, **(C-C2)** Bottom stack of LG showing merge and separate *Hml* transcript. Here 4 stacks of 0.5um are merged into one stack to make representative stack for top, middle and bottom stacks. The proof of concept experiment was done by marking same gene transcript by two different fluorophores (green and red) to rule out non-specific binding of the probes and even the high concentration of the transcript in top and bottom stack, in comparison to middle stack, also highlight the spatial distribution of *Hml* transcripts. This spatial distribution is same as we see with the help of *Hml$^{\Delta}$-GAL4,UAS-2X EGFP* construct in previous results (Figure 15). Images were acquired at 60X oil immersion objective with 2X digital zoom, and stack size was 0.5um. Scale bar: 20µm. DAPI marks DNA, gene transcripts (red, green)

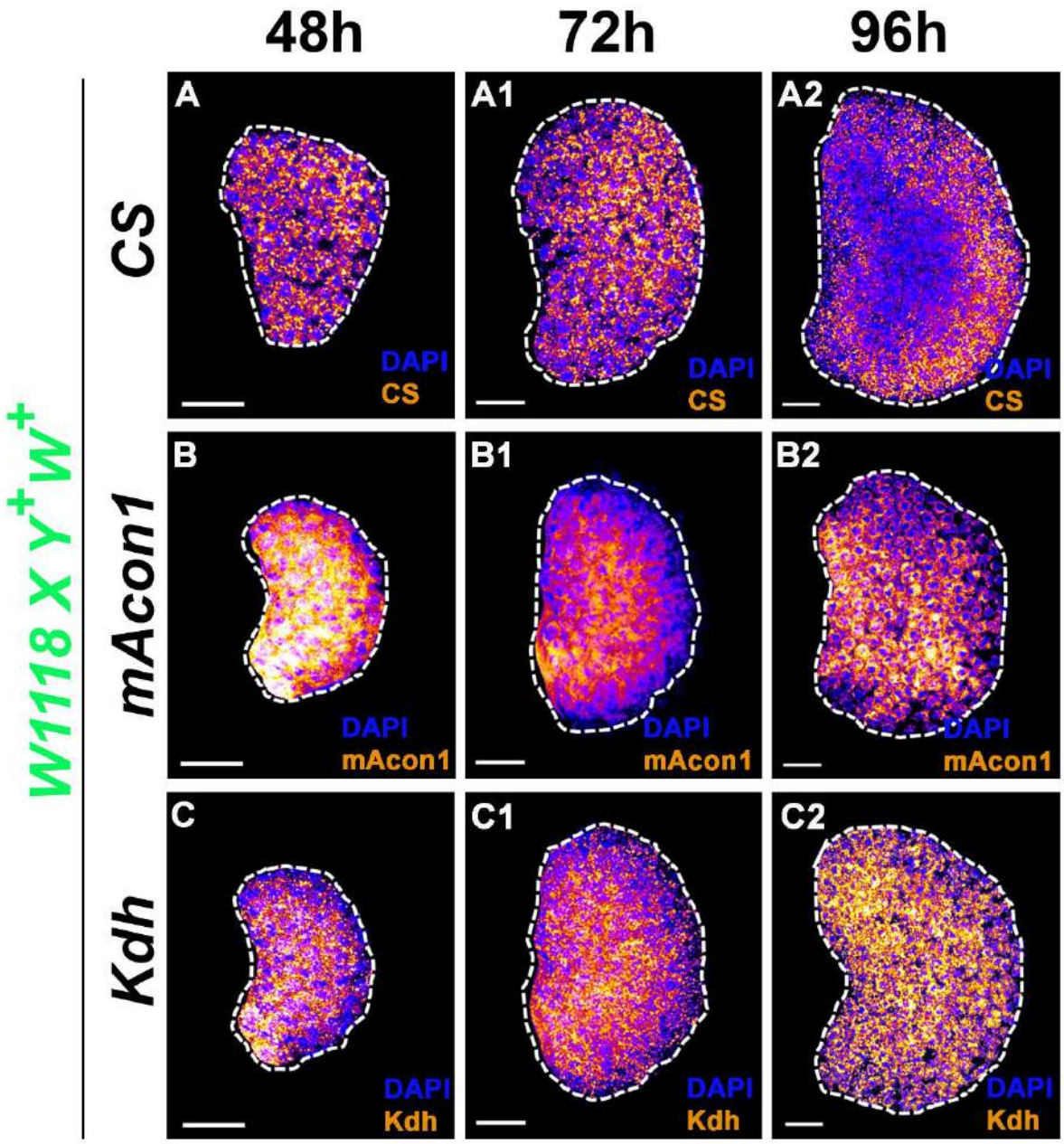

Figure 23a: Temporal distribution of TCA cycle enzymes transcripts, involved in LG growth, using SABER FISH.

(A-A2) citrate synthase (*CS*) transcript distribution in 48h, 72h and 96h LG, it was observed that transcript levels shift from MZ to CZ with development**. (B-B2)** *Aconitase* (*mAcon1*) levels remained high in the MZ across development. **(C-C2)** *α-Kdh*levels were also observed to be concentrated in MZ at 48h but with development transcripts were seen all over LG. Scale bar: 20µm. DAPI marks DNA, gene transcripts (Fire).

With the validation completed, we set out to use this technique to identify the distribution pattern of the TCA enzymes at 48h, 72h, and 96h after egg laying (AEL). We observed that at 48h the *CS* transcripts were highly enriched in the medullary zone but with time at around 96h we can see that the transcript levels starkly shift from MZ to CZ (Figure 23a: A-A2). For *mAcon1*, at 48h, the transcript levels were very high in the MZ and by 96h also even though the levels go down but they remain concentrated in the MZ only (Figure 23a: B-B2). *α-Kdh*transcript levels were found to be highly enriched in MZ and later at 96h in both MZ and CZ (Figure 23a: C-C2). *Gdh* levels were found to be concentrated in the MZ throughout the development (Figure 23a: D-D2). *Sdh* levels were found to be low initially at 48h but slowly build up and then concentrate at the CZ and *Mdh* levels were always found to be lower and equally distributed in MZ and CZ (Figure 23b: A-B2).

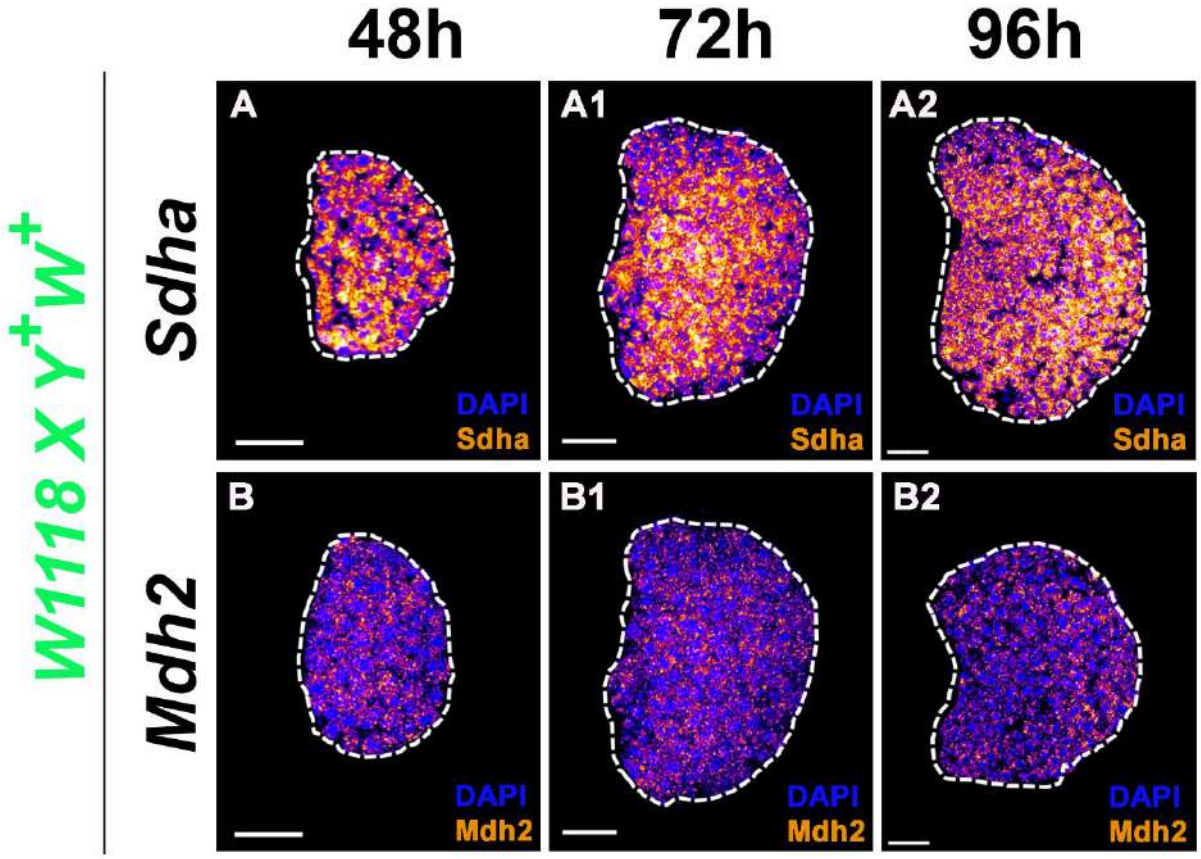

Figure 23b: Temporal distribution of TCA cycle enzymes transcript, using SABER FISH.

(A-A2) *Sdh* transcript distribution in 48h, 72h and 96h LG, it was observed that transcript levels shift from MZ to CZ with development. **(B-B2)** *Mdh* levels remained same across development in both MZ and CZ. Scale bar: 20µm. DAPI marks DNA, gene transcripts (Fire).

4. TCA cycle metabolites regulating progenitor proliferation and thereby controlling growth of lymph gland.

4.1 Source of citrate during LG development

Citrate, as mentioned earlier, is formed by condensation of OA and Acetyl CoA, with the help of citrate synthase enzyme. Here, Acetyl CoA and OA both have multiple source and entry point into the mitochondria. The conventionally accepted source of Acetyl CoA for the TCA cycle is Glycolysis derived pyruvate, which is catalysed by *Pdha* to produce Acetly CoA, and for OA, the full run of the TCA cycle should regenerate the OA utilized in Citrate production. In our LG growth defect phenotype (Figure 9: B, D-G), we identified that at least in the case of LG growth regulation, the TCA cycle does not function strictly as a cycle, rather as two separate groups of enzymes (*CS/mAcon1*, and *α-Kdh /Gdh*), working towards the same goal. Since, here TCA cycle does not operate as a complete cycle, OA regeneration and the source of Acetyl CoA becomes our next important quest.

First, we investigated the source of Acetyl CoA and examined *Pdha* function. To our surprise, although we found $Pdha^{RNAi}$ replicated the differentiation phenotype observed in most of the TCA cycle steps (Figure 24: A-C and D-F), it did not show the growth defect of LG at the 3rd instar larval stage (Figure 24: A, B and G). This result confirms that *Pdh* catalysed Acetyl CoA is not the primary substrate for the early development of the lymph gland; rather, it becomes relevant around 60-65h AEL, when the full cycle operates in MZ for the maintenance of the progenitors (Figure 24: A-G). SABER FISH based transcript analysis highlighted the low abundance of *Pdha* trancripts in early stage (48h AEL) of lymph gland development (Figure 24: H-J). To pinpoint the actual source of Acetyl CoA in early development of LG, other metabolic avenues such as β-oxidation of fats or amino acids catabolism need to be explored.

Next we examined the sources of oxaloacetate (OA) and from literature review, we explored the pyruvate to OA conversion with the help of pyruvate decarboxylase (*Pcb*). We found that Pcb^{RNAi} mutant not only recapitulated the differentiation/progenitor loss phenotype but also the size/growth defect phenotype. In this case, we did not observe significant expansion of the

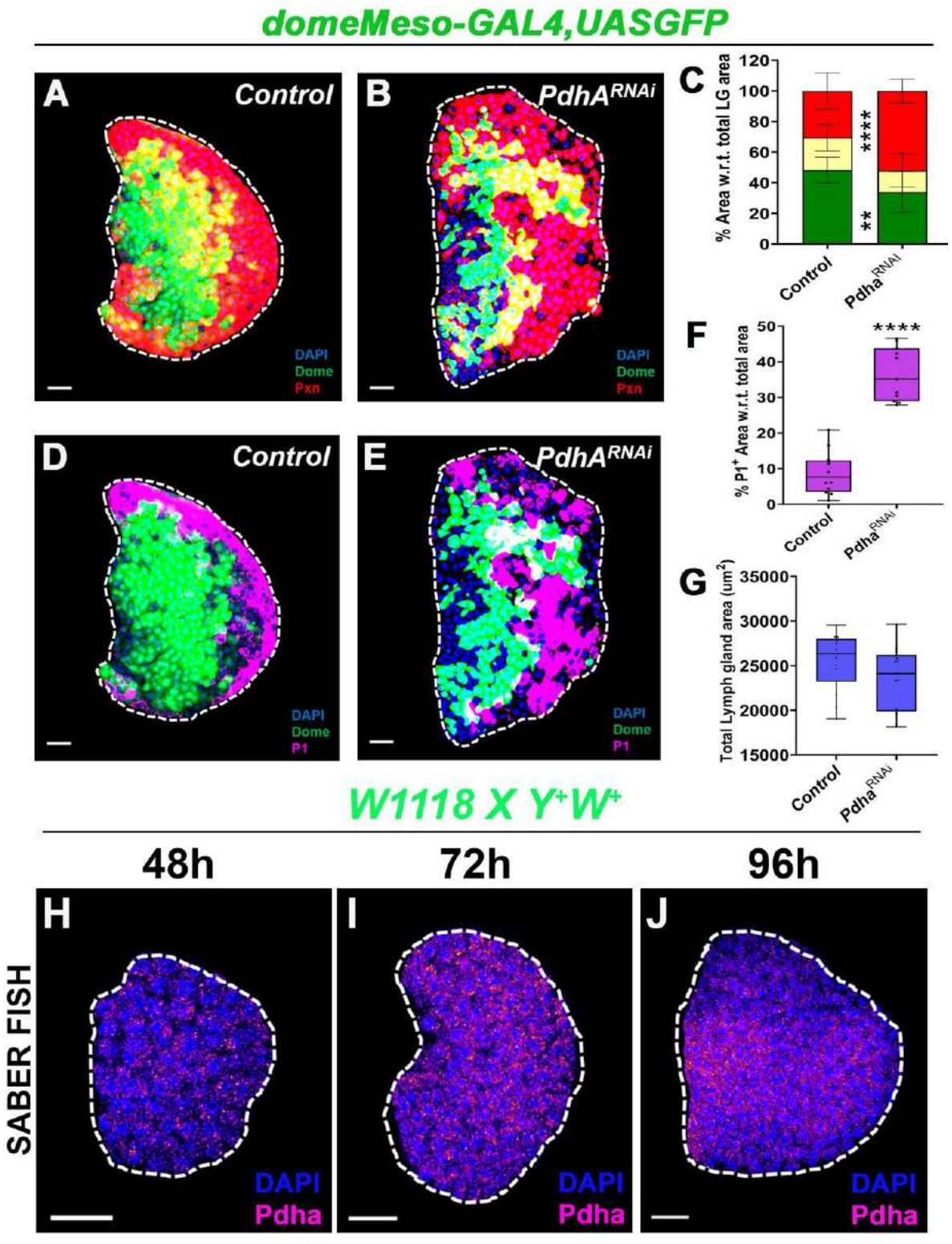

Figure 24: *Pdha* derived Acetyl CoA does not fuel the TCA cycle in the early growth of LG in *Drosophila* larva.

(**A**) *Control* (*domeMeso-Gal4,UAS-GFP/+*) lymph gland showing general distribution of progenitor (*Dome*$^{+}$; green), differentiating (*Dome*$^{+}$*Pxn*$^{+}$; yellow and only *Pxn*+ ; red) population at 3rd instar larval stage, **(B)** expressing *Pdha*^{RNAi} (*domeMeso-Gal4,UAS-GFP;UAS-Pdha*^{RNAi}), it shows reduction in progenitor population (*Dome*$^{+}$; green), which is encroached by expansion of plasmatocyte specific *Pxn*$^{+}$ population (red) in comparision to the (**A**) control **(C)** graph representing the quantification is relative % area with respect to total lymph gland area for (*Dome*+; green), differentiating (*Dome*$^{+}$*Pxn*$^{+}$; yellow and only *Pxn*$^{+}$; red), *domeMeso>GFP/+* (*control*,

n=13), *domeMeso>GFP/Pdha*^{RNAi} (n=13, green: p=0.0051; yellow: p=0.0908; red: p<0.0001), **(D)** *Control* (*domeMeso-Gal4,UAS-GFP/+*) lymph gland showing general distribution of plasmatocyte terminal differentiation marker (*P1*; magenta) at 3rd instar larval stage, **(E)** expressing *Pdha*^{RNAi} (*domeMeso-Gal4,UAS-GFP;UAS-Pdha*^{RNAi}), it shows increase in plasmatocyte specific *P1*$^{+}$ population (magenta) in comparision to the (**A)** control **(F)** graph representing the quantification is relative % area with respect to total lymph gland area for plasmatocytes (*P1*$^{+}$; magenta), *domeMeso>GFP/+* (*control*, n=12), *domeMeso>GFP/Pdha*^{RNAi} (n=11, magenta: p<0.0001), **(G)** graph representing the quantification, it is total lymph gland area, *domeMeso>GFP/+* (*control*, n=13), *domeMeso>GFP/Pdha*^{RNAi} (n=13, p=0.1254), **(H-J)** represent the *Pdha* transcript levels during the development of LG, with the help of SABER FISH, we found the *Pdha* transcript levels (Fire) were low across the development in both MZ and CZ. Data is presented as median plots (*p<0.05; **p<0.01; ***p<0.001; ****p<0.0001), student unpaired t-test (Mann-Whitney test). Scale bar: 20µm. 'n'=lymph gland lobes. DAPI marks DNA, Progenitors (*Dome*$^{+}$; Green), differentiating (*Dome*$^{+}$ *Pxn*$^{+}$; yellow and only *Pxn*$^{+}$; red) population, and differentiated population (*P1*$^{+}$ and *PPO*$^{+}$; magenta). Comparisons for significance are with control values.

differentiating (*Pxn+*) population into progenitors; rather, the differentiating (*Pxn*$^{+}$; red) population matured into terminally differentiated (*P1*$^{+}$; magenta) cells. The size defect was also consistent with that observed in *CS*^{RNAi} and *mAcon1*^{RNAi} mutants. SABER FISH based transcript analysis also shows high abundance of *Pcb* transcripts from the early stages of development. These results highlight the importance of *Pcb* as a source of OA for the synthesis of citrate, which is crucial for the early development of LG.

4.2 TCA cycle disconnect between iso-citrate and α-KG

Next we focused our work on the MZ to understand the growth defect arising from the knockdown of specific TCA cycle steps. The next question we asked was: if not *CS* and *mAcon1*, what fuels the *α-Kdh* enzyme? As mentioned previously, mt-glutamate can be converted into α-KG by *Gdh* enzyme, therefore, we decided to pursue this course. (18, 19, 146–149). We first tested *Gdh* for its effect on progenitor loss, differentiation profile and growth defect at 3rd install larval stage, as was done for all other steps. We found that *Gdh*^{RNAi} recapitulated all the phenotypes of *α-Kdh* knockdown, including reduction in the progenitor (*Dome*$^{+}$; green) population. Although the double positive (*Dome*$^{+}$*Pxn*$^{+}$; yellow) differentiating population was reduced in *Gdh* loss of function, there was an increase in *Pxn*$^{+}$ differentiating, plasmatocyte (*P1*$^{+}$; magenta) population, amd a decrease in crystal cells (*PPO*$^{+}$; magenta) along with significant growth defect. These results indicated that *α-Kdh* is fueled by *Gdh* during early development of LG. This was the missing link in the puzzle which highlights the fact that *CS* directly or indirectly to regulate LG growth.

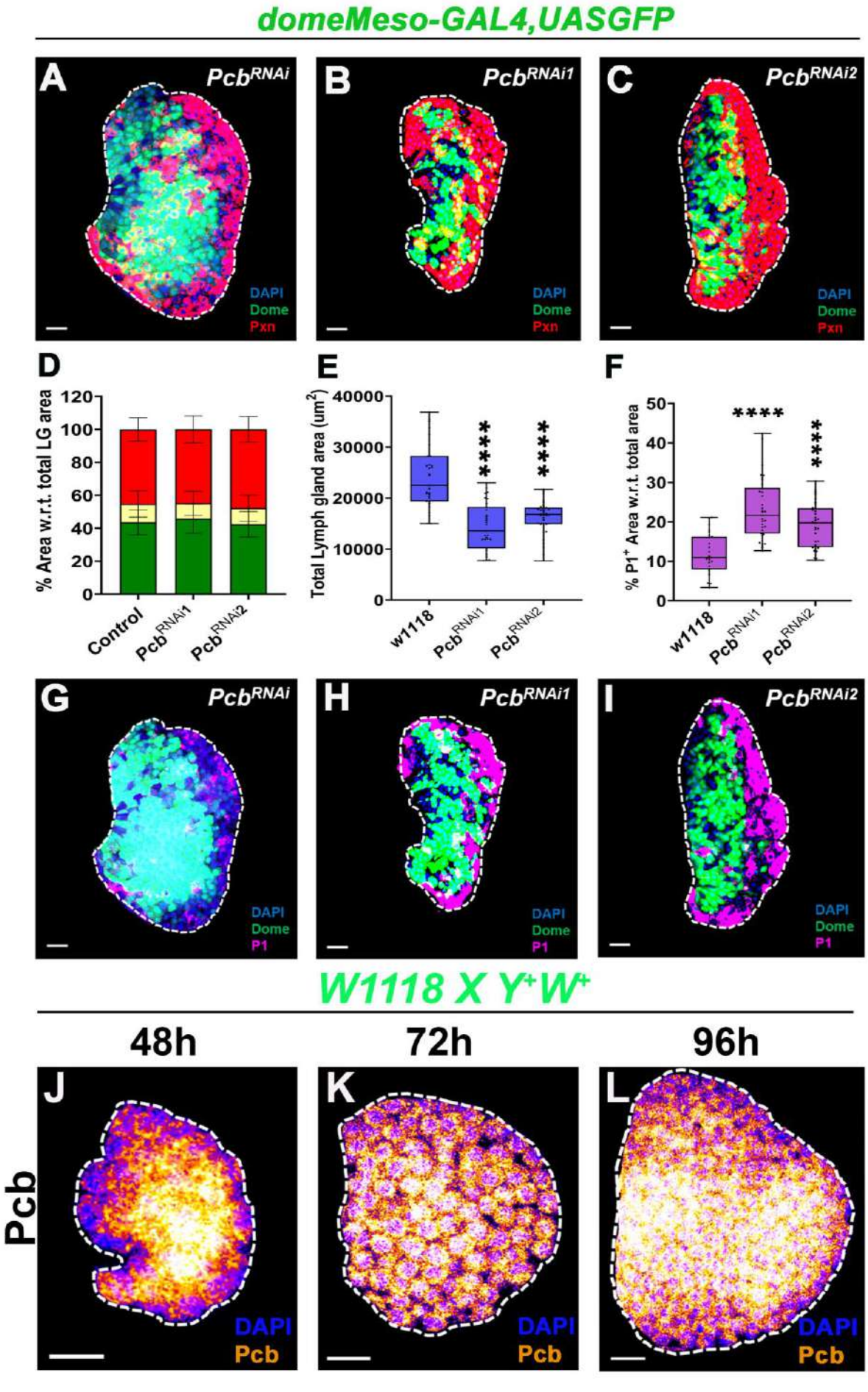
domeMeso-GAL4,UASGFP
A
Pcb^RNAi
DAPI
Dome
Pxn
B
Pcb^RNAi1
DAPI
Dome
Pxn
C
Pcb^RNAi2
DAPI
Dome
Pxn
D
% Area w.r.t. total LG area
120
100
80
60
40
20
0
Control
Pcb^RNAi1
Pcb^RNAi2
E
Total Lymph gland area (um^2)
40000
30000
20000
10000
0
****
****
w1118
Pcb^RNAi1
Pcb^RNAi2
F
% P1+ Area w.r.t. total area
50
40
30
20
10
0
****
****
w1118
Pcb^RNAi1
Pcb^RNAi2
G
Pcb^RNAi
DAPI
Dome
P1
H
Pcb^RNAi1
DAPI
Dome
P1
I
Pcb^RNAi2
DAPI
Dome
P1
W1118 X Y+W+
48h
72h
96h
Pcb
J
DAPI
Pcb
K
DAPI
Pcb
L
DAPI
Pcb

Figure 25: Pyruvate carboxylase *(Pcb)* catalysed Oxaloacetate (OA) fuels the TCA cycle in the early growth of LG in *Drosophila* larva.

(**A)** *Control* (*domeMeso-Gal4,UAS-GFP/+*) lymph gland showing general distribution of progenitor (*Dome*$^{+}$; green), differentiating (*Dome*$^{+}$*Pxn*$^{+}$; yellow and only *Pxn*$^{+}$; red) population at 3rd instar larval stage, **(B,C)** expressing *Pcb*^{RNAi} (*domeMeso-Gal4,UAS-GFP;UAS-Pcb*^{RNAi}), it does not shows any change in either of the three population (differentiation profile) in comparison to the (**A)** control **(D)** graph representing the quantification is relative % area with respect to total lymph gland area for (*Dome*$^{+}$; green), differentiating (*Dome*$^{+}$*Pxn*$^{+}$; yellow and only *Pxn*$^{+}$; red), *domeMeso>GFP/+* (*control*, n=25), *domeMeso>GFP/Pcb*^{RNAi1} (n=31, green: p=0.4798; yellow: p=0.5839; red: p=0.9682), *domeMeso>GFP/Pcb*^{RNAi2} (n=31, green: p=0.8210; yellow: p=0.7174; red: p=0.3731), **(E)** graph representing the quantification, it is total lymph gland area, *domeMeso>GFP/+* (*control*, n=31), *domeMeso>GFP/Pcb*^{RNAi1} (n=31, p<0.0001), *domeMeso>GFP/*^{PcbRNA2} (n=36, p<0.0001), **(G)** *Control* (*domeMeso-Gal4,UAS-GFP/+*) lymph gland showing general distribution of plasmatocyte terminal differentiation marker (*P1*; magenta) at 3rd instar larval stage, **(H, I)** expressing *Pcb*^{RNAi} (*domeMeso-Gal4,UAS-GFP;UAS-Pcb*^{RNAi}), it shows increase in plasmatocytes specific *P1*$^{+}$ population (magenta) in comparison to the (**G)** control **(F)** graph representing the quantification is relative % *P1* area with respect to total lymph gland area for plasmatocytes (*P1*$^{+}$; magenta), *domeMeso>GFP/+* (*control*, n=27), *domeMeso>GFP/Pcb1/2RNAi* (n=33, magenta: p<0.0001), **(J-L)** images represent the *Pcb* transcript levels in developing LG, we observed high levels of *Pcb* transcripts are high and remain high in CZ developmentally. Data is presented as median plots (*p<0.05; **p<0.01; ***p<0.001; ****p<0.0001), ordinary one-way ANOVA. Scale bar: 20µm. 'n'=lymph gland lobes. DAPI marks DNA, Progenitors (*Dome*$^{+}$; Green), differentiating (*Dome*$^{+}$ *Pxn*$^{+}$; yellow and only *Pxn*$^{+}$ red) population, and differentiated population (*P1*$^{+}$ and *PPO*$^{+}$; magenta). Comparisons for significance are with control values.

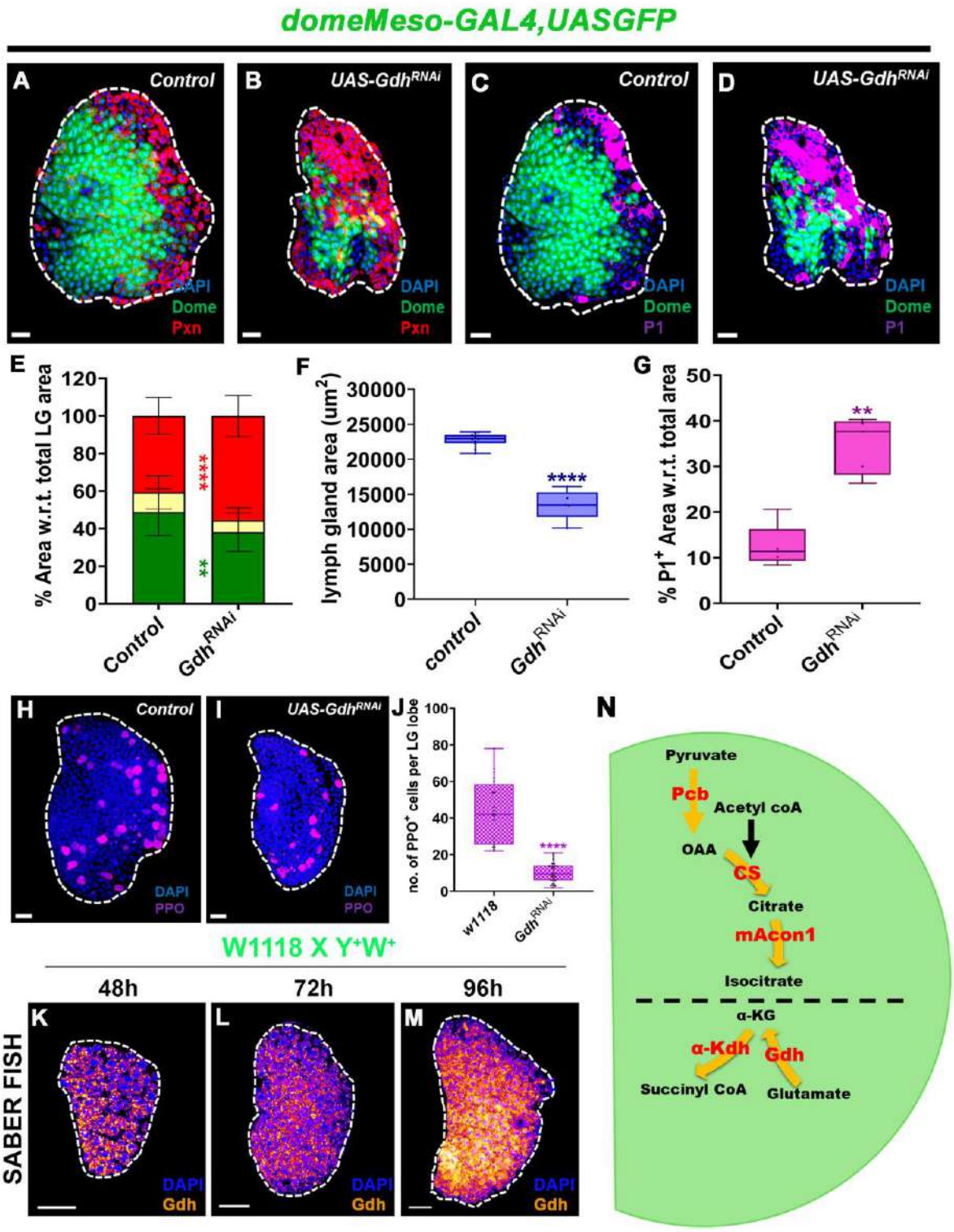

Figure 26: *Gdh* fuels the TCA cycle via *α-Kdh* to regulated progenitor homeostasis and growth of LG in early development of *Drosophila* larva.

(**A**) *Control* (*domeMeso-Gal4,UAS-GFP/+*) lymph gland showing general distribution of progenitor (*Dome*$^+$; green), differentiating (*Dome*$^+$*Pxn*$^+$; yellow and only *Pxn*$^+$; red) population at 3rd instar larval stage, **(B)** expressing *Gdh*^{RNAi} (*domeMeso-Gal4,UAS-GFP;UAS-Gdh*^{RNAi}), it shows reduction in progenitor population (*Dome*$^+$; green), as well as in double positive differentiating population (*Dome*$^+$ *Pxn*$^+$; yellow), which is encroached by expansion of plasmatocyte specific *Pxn*$^+$ population (red) in comparison to the (**A**) control, **(E)** graph representing the

quantification is relative % area with respect to total lymph gland area for (*Dome*$^{+}$; green), differentiating (*Dome*$^{+}$*Pxn*$^{+}$; yellow and only *Pxn*$^{+}$; red), *domeMeso>GFP/+* (*control*, n=24), *domeMeso>GFP/Gdh*^{RNAi} (n=35, green: p=0.0015; yellow: p=0.0746; red: p<0.0001), **(F)** graph representing the quantification, it is total lymph gland area, *domeMeso>GFP/+* (*control*, n=43), *domeMeso>GFP/Gdh*^{RNAi} (n=48, p<0.0001), **(C)** *Control* (*domeMeso-Gal4,UAS-GFP/+*) lymph gland showing general distribution of plasmatocytes (*P1+*; magenta) population at 3rd instar larval stage, **(D)** expressing *Gdh*^{RNAi} (*domeMeso-Gal4,UAS-GFP;UAS-Gdh*^{RNAi}), plasmatocyte population (*P1+*; magenta) was found to be expanded, in comparison to **(C)** control, **(G)** graph representing the quantification, it is relative % area with respect to total lymph gland area for plasmatocyte (*P1+*; magenta), *domeMeso>GFP/+* (*control*, n=24), *domeMeso>GFP/Gdh*^{RNAi} (n=28, p=0.0079), **(H)** *Control* (*domeMeso-Gal4,UAS-GFP/+*) lymph gland showing general distribution of crystal cells (*PPO+*; magenta) at 3rd instar larval stage, **(I)** expressing *Gdh*^{RNAi} (*domeMeso-Gal4,UAS-GFP;UAS-Gdh*^{RNAi}), the crystal cell population was found to be decreased in comparison to **(H)** control **(J)** graph representing the quantification, it is total number of crystal cells in lymph gland (*PPO+*; magenta), *domeMeso>GFP/+* (*control*, n=20), *domeMeso>GFP/Gdh*^{RNAi} (n=32, p<0.0001), **(K-M)** images represent the *Gdh* transcript levels in developing LG, we observed high levels of *Gdh* transcripts are high and remain high in CZ developmentally. **(N)** schematic representing the sources of Citrate and α-KG in the development of LG. Data is presented as median plots (*p<0.05; **p<0.01; ***p<0.001; ****p<0.0001), ordinary one-way ANOVA. Scale bar: 20µm. 'n'=lymph gland lobes. DAPI marks DNA, Progenitors (*Dome*$^{+}$; Green), differentiating (*Dome*$^{+}$ *Pxn*$^{+}$; yellow and only *Pxn*$^{+}$; red) population, and differentiated population (*P1*$^{+}$ and *PPO*$^{+}$; magenta). Comparisons for significance are with control values.

4.3 Temporal analysis of LG growth

The growth defect phenotype was common among all four *CS*^{RNAi}, *mAcon1*^{RNAi}, *α-Kdh*^{RNAi} and *Gdh*^{RNAi} mutants, at the wandering 3rd instar larval stage. This could be due to two different mechanisms: a) cell death (apoptosis) or b) lack of proliferation (cell cycle arrest). We first examined the possibility of apoptosis by staining the wandering 3rd instar larval lymph gland with Cleaved-Caspase 3 antibody to mark apoptotic nuclei in all the mutant backgrounds exhibiting the growth phenotype. *Hml*$^{\Delta}$*-Gal4, UAS-GFP; UAS-Hid* was used as a positive control for *Hid* being activator of apoptosis, Caspase 3 puncta were observed around the nuclei. In contrast, the mutants under study did not show any considerable change in comparison to the positive control, thereby ruling out apoptosis as a cause of the size defect.

We then performed a temporal analysis of *CS*^{RNAi}, *mAcon1*^{RNAi}, *α-Kdh*^{RNAi} and *Gdh*^{RNAi} to determine whether they function together or as separate groups in regulating growth of LG. The initial results were obtained from wandering 3rd instar larvae, where all mutants exhibited smaller LGs. For this study, we utilized the progenitor specific *domeMESO-GAL4,UAS-GFP*. We dissected the LG at 48h, 72h, 96h and 120h after egg laying (AEL). Initial analysis, based on total number of cells in the LG, revealed that *CS*^{RNAi} and *mAcon1*^{RNAi} mutants displayed a growth defect from the 96h (Figure 27 A-C3 & Figure 28 A), whereas *α-Kdh*^{RNAi} and *Gdh*^{RNAi} mutants showed size defect at early as 48h itself (Figure 27 A-A3, D-E3 & Figure 28 A). This finding was crucial, indicating that two separate groups of enzymes indeed regulate LG growth, *α-Kdh* and *Gdh* are required early in development, whereas *CS* and *mAcon1* function later (Figure 27).

We then deepened our analysis by dividing the total LG cell population into *Dome*$^{+}$ (green) and *Dome*$^{-}$ (blue) subsets. Incorporating this layer of analysis revealed a loss of progenitor (*Dome*$^{+}$; green) population as early as 72h itself, highlighting that *CS* and *mAcon1* enzymes are required by this stage rather than 96h, as suggested by total cell count in the LG. This discripency could not be identified initially as the non-progenitor (blue) population compensated for the loss of progenitor population in *CS* and *mAcon1* loss of function mutants (Figure 27 A-C3 & Figure 28 B-C). However, the proliferative capacity of *Dome*$^{-}$ cells was insufficient at later stages, culminating in a visible growth defect by 96hIn contrast, in *α-Kdh*^{RNAi} and *Gdh*^{RNAi}, both progenitor (*Dome*$^{+}$; green) and non-progenitor (*Dome*$^{-}$; blue) compartments were compromised, resulting in an overall reduction in size of LG (Figure 27 A-A3, D-E3 & Figure 28 B-C). These finding further support the concept that *CS*/*mAcon1* and *α-Kdh/Gdh* function as two distinct enzyme modules within the MZ. To determine whether the size defect is due to the proliferative incapacity, we next assessed the mitotic index temporally across all four genotypes using phosphohistone H3 (pH3) antibody staining at 48h, 72h and 96h AEL. Interestingly, in *CS*^{RNAi}, elevated proliferation was observed at 48h, specifically within the *Dome*- (blue) non- progenitor compartment (Figure 29 A-I'). This was not observed in *α-Kdh*^{RNAi} and *Gdh*^{RNAi} mutants; rather in the *α-Kdh*^{RNAi} mutant, high proliferation occurred within *Dome*$^{+}$ (green) progenitor compartment (Figure 29 A-C' & J-O').

This interesting observation in the *CS*^{RNAi} mutant led us to hypothesize that *Dome*$^{+}$ progenitors may undergo precocious differentiation, thereby losing their proliferative capacity early in development. To test this, we perform temporal staining for the plasmatocytes markers *Pxn* and *P1* at 48h, 72h and 96h AEL. Under homeostasis, *Pxn* expression appears around 60-65h AEL in the lymph gland. However, consistent with our hypothesis, we observed premature expression of *Pxn* and occasionally *P1* at 48h AEL in both *CS*^{RNAi} and *mAcon1*^{RNAi} mutants, whereas no staining was detected in control (Figure 30 A-A', D-D'& G-G'). Even at 72h AEL, staining for both *Pxn* and *P1* were stronger than in control for *CS*^{RNAi} and *mAcon1*^{RNAi} mutants (Figure 30 B-B', E-E'& H-H '). The early appearance of fate specific markers (plasmatocytes; *Pxn* and *P1*) likely renders the progenitors incapacitated of proliferation, ultimately leading to the observed LG size defect.

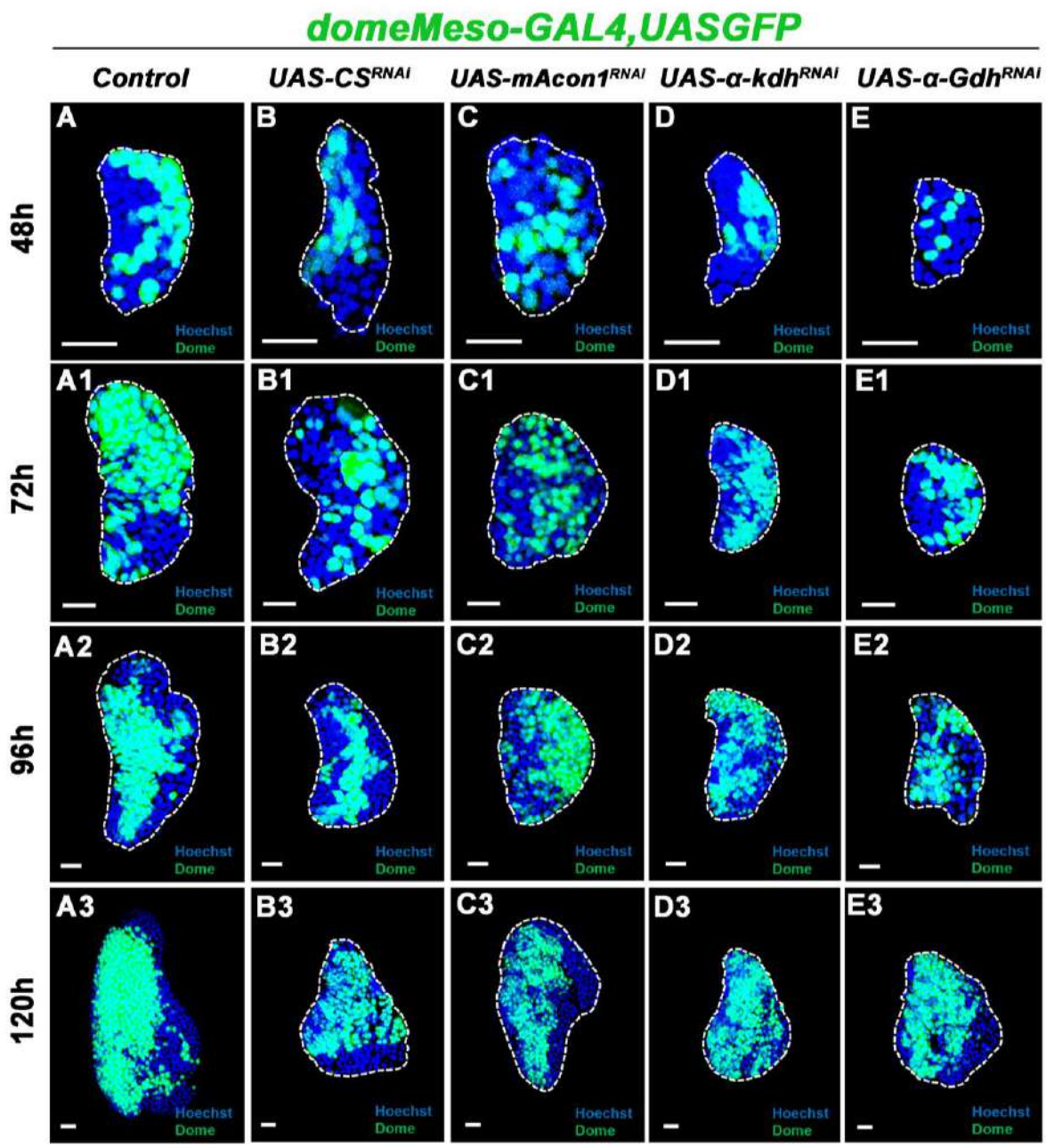

Figure 27: Temporal analysis of *CS^{RNAi}*, *mAcon1^{RNAi}*, *α-Kdh^{RNAi}* and *Gdh^{RNAi}*.

(**A-A3)** *Control* (*domeMeso-Gal4,UAS-GFP/+*) lymph gland showing general distribution of progenitor (*Dome*$^{+}$; green), and non-progenitor (*Dome*$^{-}$; blue) population at 48h, 72h, 96h and 120h AEL in *Drosophila* larval stage, **(B-B3)** expressing *CS^{RNAi}* (*domeMeso-Gal4,UAS-GFP;UAS-CS^{RNAi}*), **(C-C3)** expressing *mAcon1^{RNAi}* (*domeMeso-Gal4,UAS-GFP;UAS-mAcon1^{RNAi}*), **(D-D3)** expressing α-*Kdh^{RNAi}* (*domeMeso-Gal4,UAS-GFP;UAS-*α-*Kdh^{RNAi}*), (**E-E3)** expressing *Gdh^{RNAi}* (*domeMeso-Gal4,UAS-GFP;UAS-Gdh^{RNAi}*), for *CS^{RNAi} and mAcon1^{RNAi}* we do not see any size defect, based on total nuclei count (blue) at 48h and 72h **(B-B1 and C-C1),** but from 96h onwards we see small size of lymph gland in both mutants **(B2-B3 and C2-C3),** in comparison to control **(A-A3).** Also in terms of progenitor (*Dome*$^{+}$; Green) v/s non-progenitor (*Dome*$^{-}$; blue) population, the defect can be evident at the 72h itself, with mutants showing reduction in progenitor (*Dome*$^{+}$; Green) and a compensatory increase in non-progenitor (*Dome*$^{-}$; blue) population, which is the reason why we do not see overall size defect at 72h in both mutants **(B1 and C1),** in comparison to control **(A1)**. For α-*Kdh^{RNAi} and Gdh1^{RNAi}* the size defect is seen at 48h itself with both progenitor (*Dome*$^{+}$; Green) and non-progenitor (*Dome*-; blue) population being compromised from the start, ultimately leading to small LG at the 3rd instar larval stage **(D-D3 and E-E3),** in comparison to control **(A-A3).** Scale bar: 20µm. DAPI marks DNA, Progenitors (*Dome*$^{+}$; Green), and non-progenitor (*Dome*-; blue) population. All comparisons for significance are with control values.

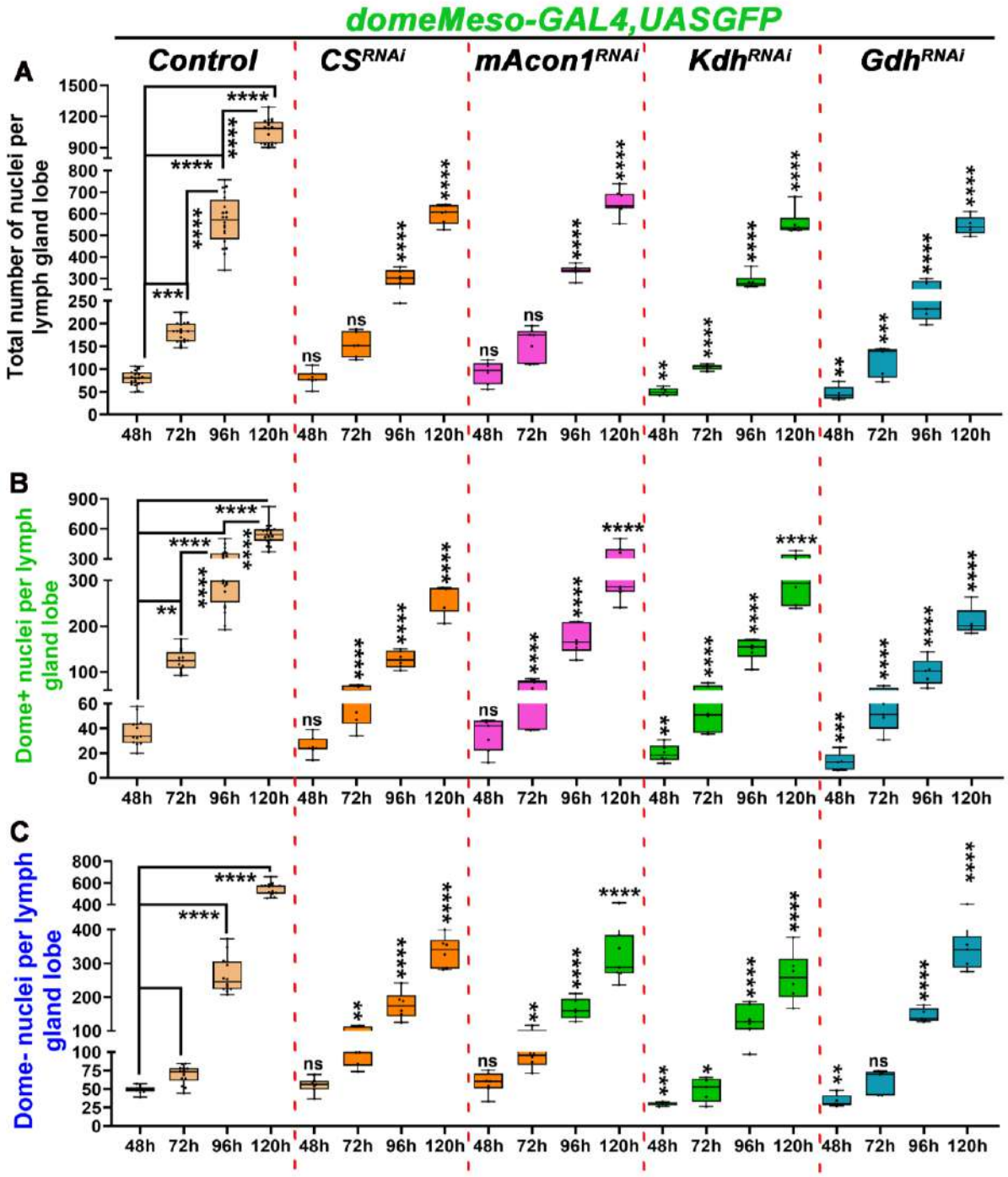

Figure 28: Quantification for temporal analysis for *CS^{RNAi}*, *mAcon1^{RNAi}*, *α-Kdh^{RNAi}* and *Gdh^{RNAi}*.

(**A)** graph representing total number of cells (based on nuclei count) per lymph gland **,** *domeMeso>GFP/+* (*control*, 48h, n=171; 72h, n=164, p=0.0010; 96h, n=171, p<0.0001; 12h, n=132, p<0.0001), *domeMeso>GFP/CS^{RNAi}* (48h, n=54, p>0.9999; 72h, n=50 , p=0.0998; 96h, n=55 , p<0.0001; 120h, n=41 , p<0.0001), *domeMeso>GFP/mAcon1^{RNAi}* (48h, n=69, p=0.3259; 72h, n=69 , p=0.1540; 96h, n=65 , p<0.0001; 120h, n=66 , p<0.0001), *domeMeso>GFP/α-Kdh^{RNAi}* (48h, n=37, p=0.0023; 72h, n=48 , p<0.0001; 96h, n=63 , p<0.0001; 120h, n=49 , p<0.0001), and *domeMeso>GFP/Gdh^{RNAi}* (48h, n=34, p=0.0016; 72h, n=45 , p<0.0001; 96h, n=39 , p<0.0001; 120h, n=50 , p<0.0001), **(B)** graph representing number of progenitor cells (*Dome*+; green) per lymph gland **,** *domeMeso>GFP/+* (*control*, 48h, n=127; 72h, n=116, p=0.0083; 96h, n=171, p<0.0001; 12h, n=132, p<0.0001), *domeMeso>GFP/CS^{RNAi}* (48h, n=51, p=0.0687; 72h, n=50 , p<0.0001; 96h, n=55 , p<0.0001; 120h, n=41 , p<0.0001), *domeMeso>GFP/mAcon1^{RNAi}* (48h, n=69, p=0.9681; 72h, n=69 , p<0.0001; 96h, n=65 , p<0.0001; 120h, n=66 , p<0.0001), *domeMeso>GFP/α-Kdh^{RNAi}* (48h, n=37, p=0.0050; 72h, n=48 , p<0.0001; 96h, n=63 , p<0.0001; 120h, n=49 , p<0.0001), and *domeMeso>GFP/Gdh^{RNAi}* (48h, n=34, p=0.0002; 72h, n=45 ,

p<0.0001; 96h, n=39 , p<0.0001; 120h, n=50 , p<0.0001), **(C)** graph representing number of non-progenitor cells (*Dome*-; blue) per lymph gland **,** *domeMeso>GFP/+* (*control*, 48h, n=124; 72h, n=128, p=0.4206; 96h, n=118, p<0.0001; 12h, n=109, p<0.0001), *domeMeso>GFP/CS*^{RNAi} (48h, n=54, p=0.4544; 72h, n=49 , p=0.0017; 96h, n=55 , p=0.0006; 120h, n=41 , p<0.0001), *domeMeso>GFP/mAcon1*^{RNAi} (48h, n=69, p=0.1282; 72h, n=63 , p=0.0062; 96h, n=65 , p=0.0001; 120h, n=66 , p<0.0001), *domeMeso>GFP/α-Kdh*^{RNAi} (48h, n=37, p=0.0002; 72h, n=48 , p=0.0447; 96h, n=63 , p<0.0001; 120h, n=49 , p<0.0001), and *domeMeso>GFP/Gdh*^{RNAi} (48h, n=34, p=0.0054; 72h, n=45 , p=0.5900; 96h, n=39 , p<0.0001; 120h, n=50 , p<0.0001). Data is presented as median plots (*p<0.05; **p<0.01; ***p<0.001; ****p<0.0001), ordinary one-way ANOVA. Scale bar: 20µm. 'n'=lymph gland lobes. DAPI marks DNA, Progenitors (*Dome*$^{+}$; Green), differentiating (*Dome*$^{+}$ *Pxn*$^{+}$; yellow and only *Pxn*$^{+}$; red) population, and differentiated population (*P1*$^{+}$ and *PPO*$^{+}$; magenta). Comparisons for significance are with control values.

These differentiation results, in combination with the temporal analysis and proliferative index, suggest that *CS*^{RNAi} and *mAcon1*^{RNAi} mutants inhibit precocious differentiation of progenitors and restrict premature proliferation of non-progenitors. This regulation non-autonomously supports the progenitors in maintaining their homeostatic function, i.e. proliferation. In contrast, *α-Kdh*^{RNAi} and *Gdh*^{RNAi} mutants autonomously regulate progenitor proliferation, as evidenced by the observation that loss of *α-Kdh* leads to size defect across all four compartments (Figure 30 A-A', J-J'& M-M'). These results further support our hypothesis that *CS* and *mAcon1* mutants function as an enzymatic unit to support the activity of *α-Kdh* and *Gdh*, which together form another unit. As a positive control for the temporal analysis, we also dissected the LGs from the mutants that did not show any size defects. For this, we chose *Sdh*^{RNAi} and *Mdh*^{RNAi} and no inconsistencies were observed in the control, neither in the *Dome*$^{+}$ v/s *Dome*$^{-}$ population nor in *Pxn*/*P1* marker staining at 48h, 72h, 96h and 120h AEL (Figure 31 A-C3).

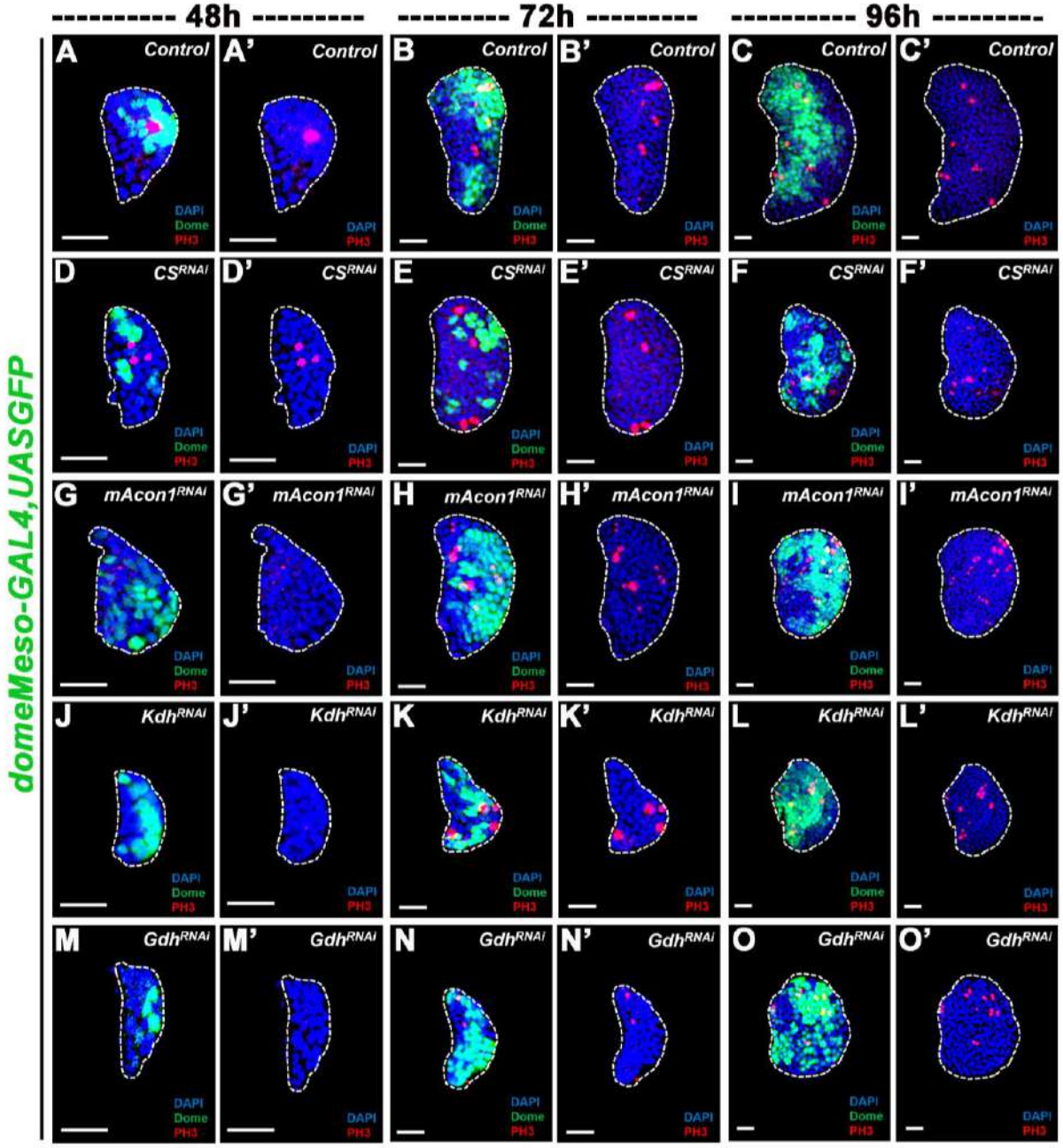

Figure 29: Temporal analysis to get the mitotic index for *CS^{RNAi}, mAcon1^{RNAi}, α-Kdh^{RNAi} and Gdh^{RNAi}.*

(**A-C'**) *Control* (*domeMeso-Gal4,UAS-GFP/+*) lymph gland showing general distribution of pH3^{+} cells in progenitor (*Dome*$^{+}$; green), and non-progenitor (*Dome*$^{-}$; blue) population at 48h, 72h, 96h and 120h AEL in *Drosophila* larval stage, **(D-F')** expressing *CS^{RNAi}* (*domeMeso-Gal4,UAS-GFP;UAS-CS^{RNAi}*), **(G-I')** expressing *mAcon1RNAi* (*domeMeso-Gal4,UAS-GFP;UAS-mAcon1^{RNAi}*), **(J-L')** expressing α-*Kdh^{RNA}i* (*domeMeso-Gal4,UAS-GFP;UAS-α-Kdh^{RNAi}*), (**M-O')** expressing *Gdh^{RNAi}* (*domeMeso-Gal4,UAS-GFP;UAS-Gdh^{RNAi}*), for *CS^{RNAi} and mAcon1^{RNAi}* we see more pH3^{+} cells in the *Dome*$^{-}$ (blue) population at the 48h itself and it persists in 72h, highlighting the higher proliferative capacity of the non-progenitors, which was also observed in the *Dome*$^{+}$ vs *Dome*$^{-}$ cell counts at 72h **(D-I')**, whereas in α-*Kdh^{RNAi} and Gdh^{RNAi}* we did not observe any mitotic activity at 48h in either of the *Dome*$^{+}$ (green) or *Dome*$^{-}$ (blue) compartment, which is consistent with the fact that size reduction in α-*Kdh^{RNAi} and Gdh1^{RNAi}* was noticed at the 48h in development itself **(J-O'),** in comparison to control **(A-C')**. Scale bar: 20μm. DAPI marks DNA, Progenitors (*Dome*$^{+}$; Green), and non-progenitor (*Dome*$^{-}$; blue) population. All comparisons for significance are with control values.

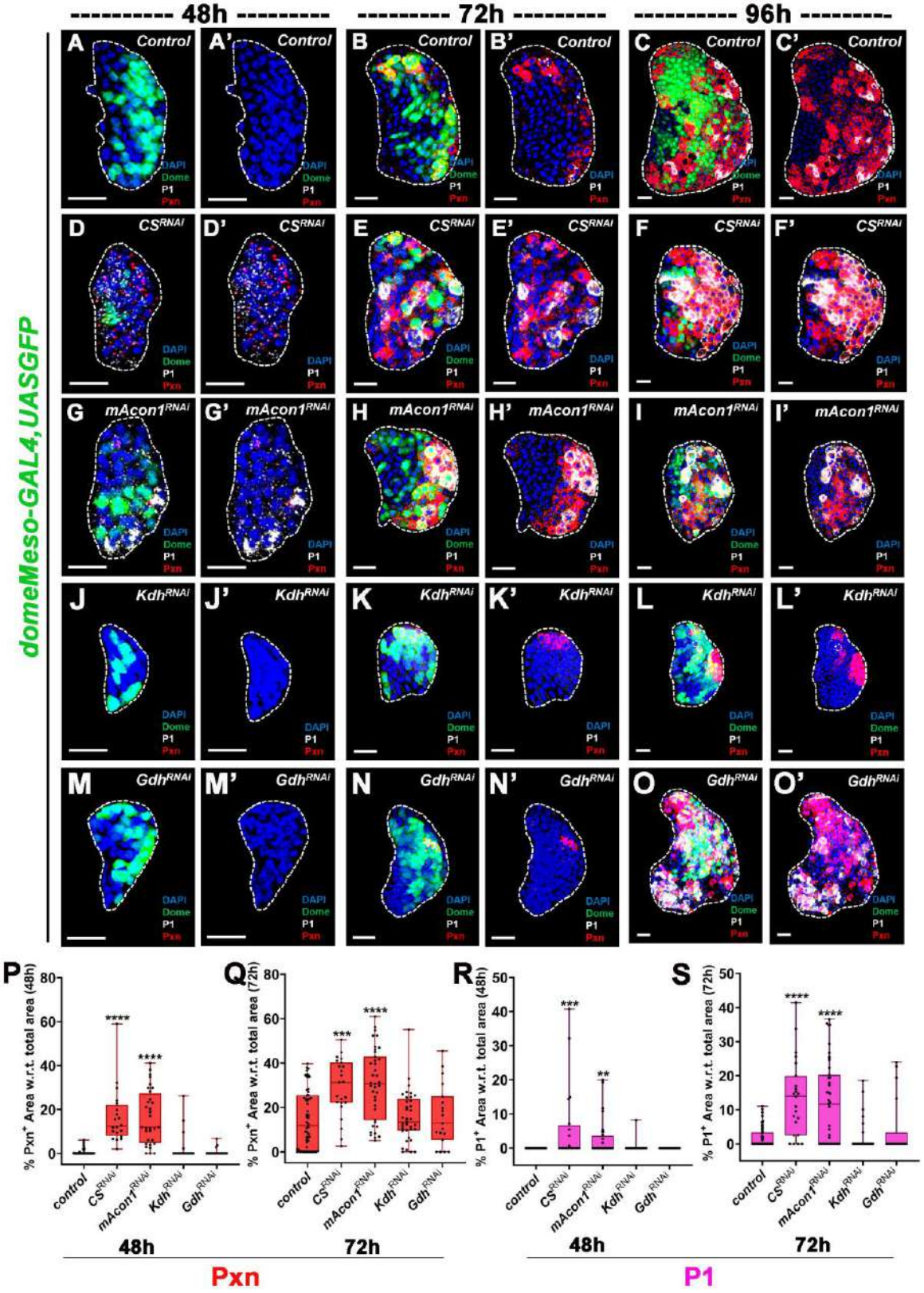
---------- 48h ---------
--------- 72h ---------
---------- 96h ---------
domeMeso-GAL4,UASGFP
A Control
A' Control
B Control
B' Control
C Control
C' Control
D CS^RNAi
D' CS^RNAi
E CS^RNAi
E' CS^RNAi
F CS^RNAi
F' CS^RNAi
G mAcon1^RNAi
G' mAcon1^RNAi
H mAcon1^RNAi
H' mAcon1^RNAi
I mAcon1^RNAi
I' mAcon1^RNAi
J Kdh^RNAi
J' Kdh^RNAi
K Kdh^RNAi
K' Kdh^RNAi
L Kdh^RNAi
L' Kdh^RNAi
M Gdh^RNAi
M' Gdh^RNAi
N Gdh^RNAi
N' Gdh^RNAi
O Gdh^RNAi
O' Gdh^RNAi
DAPI
Dome
P1
Pxn
P
% Pxn+ Area w.r.t. total area (48h)
Q
% Pxn+ Area w.r.t. total area (72h)
R
% P1+ Area w.r.t. total area (48h)
S
% P1+ Area w.r.t. total area (72h)
control
CS^RNAi
mAcon1^RNAi
Kdh^RNAi
Gdh^RNAi
48h
72h
Pxn
P1

Figure 30: Temporal analysis for differentiation profile in *CS^{RNAi}, mAcon1^{RNAi}, α-Kdh^{RNAi} and Gdh^{RNAi}*

(**A-C')** *Control* (*domeMeso-Gal4,UAS-GFP/+*) lymph gland showing general distribution of progenitor (*Dome+*; green), and non-progenitor (*Dome^{-}*; blue) population, along with the expression pattern of differentiation markers *Pxn* (red) and *P1*(gray) at 48h, 72h, 96h and 120h AEL in *Drosophila* larval stage, **(D-F')** expressing *CS^{RNAi}* (*domeMeso-Gal4,UAS-GFP;UAS-CS^{RNAi}*), **(G-I')** expressing *mAcon1^{RNAi}* (*domeMeso-Gal4,UAS-GFP;UAS-mAcon1^{RNAi}*), **(J-L')** expressing α-*Kdh^{RNAi}* (*domeMeso-Gal4,UAS-GFP;UAS-α-Kdh^{RNAi}*), (**M-O')** expressing *Gdh^{RNAi}* (*domeMeso-Gal4,UAS-GFP;UAS-Gdh^{RNAi}*), for *CS^{RNAi} and mAcon1^{RNAi}* we do see the presence of the differentiation markers *Pxn* (red) and *P1*(gray) at the 48h itself, which is uncommon as the differentiation kicks in around 60-65h AEL in the normal development. And even at 72h we see aggressive differentiation which is due to the absence of citrate from the system to check precocious differentiation **(D-I'),** in comparison to control **(A-C').** But in case of α-*Kdh^{RNAi} and Gdh^{RNAi}* differentiation markers were not observed early in development, just that the LG was small due to low to negligible mitotic activity at early stage of development (pH3)**(J-O'),** in comparison to control**(A-C'). (P)** Quantification is relative % area with respect to total lymph gland area for differentiation profile (*Pxn^{+}*) at 48h, *domeMeso-Gal4,UAS-GFP/+ (*control*, n=50), domeMeso-Gal4,UAS-GFP;UAS-CS^{RNAi} (n=20, p<0.0001), domeMeso-Gal4,UAS-GFP;UAS-mAcon1^{RNAi} (n=32, p<0.0001), domeMeso-Gal4,UAS-GFP;UAS-α-Kdh^{RNAi} (n=19, p>0.9999), domeMeso-Gal4,UAS-GFP;UAS-Gdh^{RNAi} (n=20, p>0.9999),* **(Q)** Quantification is relative % area with respect to total lymph gland area for differentiation profile (*Pxn^{+}*) at 72h, *domeMeso-Gal4,UAS-GFP/+ (*control*, n=58), domeMeso-Gal4,UAS-GFP;UAS-CS^{RNAi} (n=23, p=0.0001), domeMeso-Gal4,UAS-GFP;UAS-mAcon1^{RNAi} (n=39, p<0.0001), domeMeso-Gal4,UAS-GFP;UAS-α-Kdh^{RNAi} (n=37, p=0.9910), domeMeso-Gal4,UAS-GFP;UAS-Gdh^{RNAi} (n=19, p=0.9985),* **(R)** Quantification is relative % area with respect to total lymph gland area for differentiation profile (*P1^{+}*) at 48h, *domeMeso-Gal4,UAS-GFP/+ (*control*, n=35), domeMeso-Gal4,UAS-GFP;UAS-CS^{RNAi} (n=20, p=0.0002), domeMeso-Gal4,UAS-GFP;UAS-mAcon1^{RNAi} (n=32, p=0.0021), domeMeso-Gal4,UAS-GFP;UAS-α-Kdh^{RNAi} (n=18, p>0.9999), domeMeso-Gal4,UAS-GFP;UAS-Gdh^{RNAi} (n=20, p>0.9999),* **(S)** Quantification is relative % area with respect to total lymph gland area for differentiation profile (*P1^{+}*) at 72h, *domeMeso-Gal4,UAS-GFP/+ (*control*, n=57), domeMeso-Gal4,UAS-GFP;UAS-CS^{RNAi} (n=23, p<0.0001), domeMeso-Gal4,UAS-GFP;UAS-mAcon1^{RNAi} (n=39, p<0.0001), domeMeso-Gal4,UAS-GFP;UAS-α-Kdh^{RNAi} (n=37, p>0.9999), domeMeso-Gal4,UAS-GFP;UAS-Gdh^{RNAi} (n=18, p=0.6233). Data is presented as median plots (*p<0.05; **p<0.01; p<0.001; ****p<0.0001), ordinary one-way ANOVA. Scale bar: 20µm. 'n'=lymph gland lobes. DAPI marks, (blue), Differentiating population (Pxn+; red and P1+; gray). Comparisons for significance are with control values.*

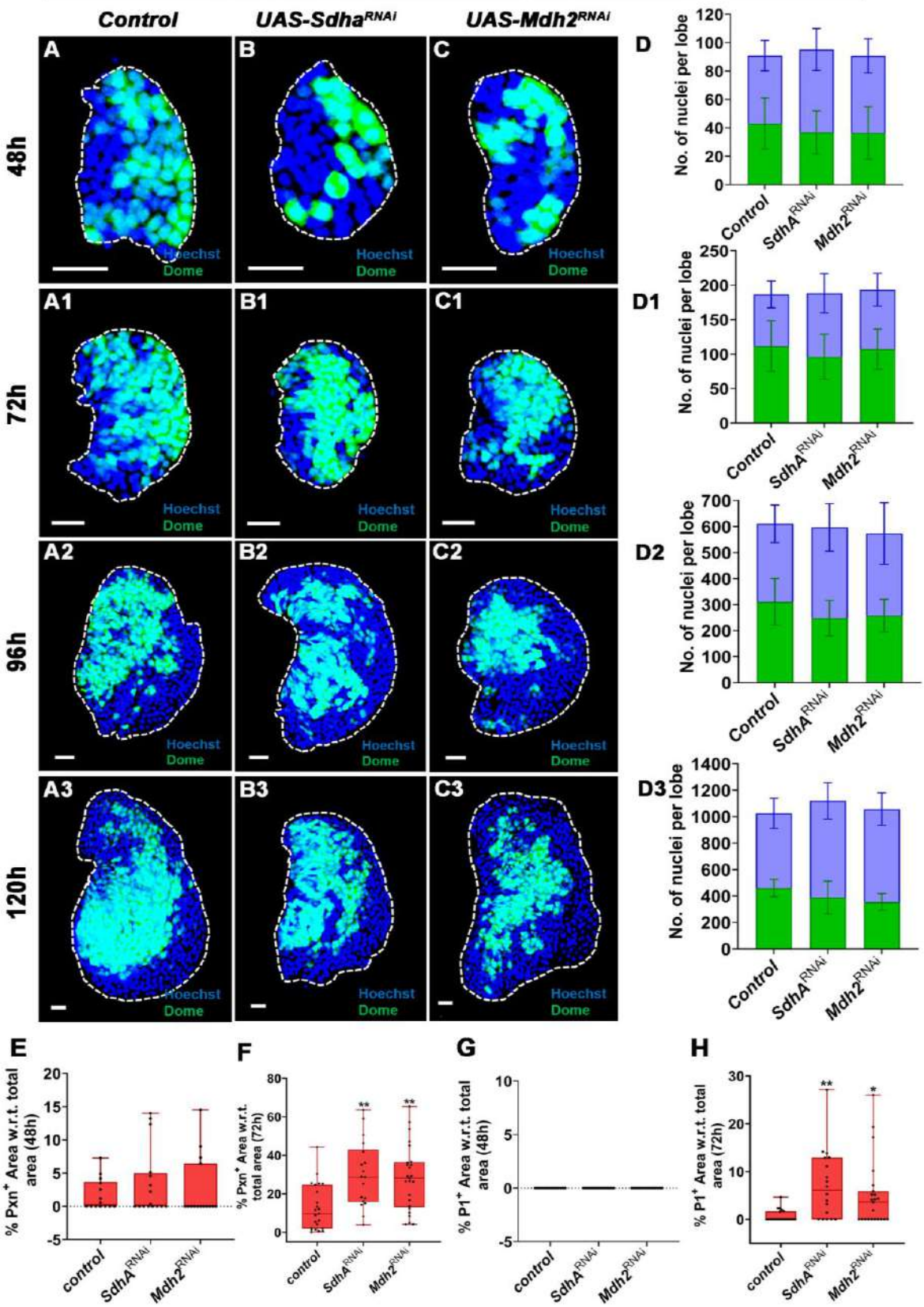
domeMeso-GAL4,UASGFP
Control
UAS-Sdha^RNAi
UAS-Mdh2^RNAi
48h
72h
96h
120h
A
B
C
A1
B1
C1
A2
B2
C2
A3
B3
C3
Hoechst
Dome
D
D1
D2
D3
No. of nuclei per lobe
Control
SdhA^RNAi
Mdh2^RNAi
E
F
G
H
% Pxn+ Area w.r.t. total area (48h)
% Pxn+ Area w.r.t. total area (72h)
% P1+ Area w.r.t. total area (48h)
% P1+ Area w.r.t. total area (72h)
control

Figure 31: Developmental profile of *Sdh^{RNAi} and Mdh^{RNAi}* in LG of *Drosophila* larva.

(***A-A3)*** Control (*domeMeso-Gal4,UAS-GFP/+*) lymph gland showing general distribution of *progenitor (Dome^{+};* green), differentiating *(Dome-;* blue*)* population at 3rd instar larval stage, **(B-B3)** expressing *Sdh^{RNAi}* (*domeMeso-Gal4,UAS-GFP;UAS-Sdh^{RNAi}*), **(C-C3)** expressing *Mdh^{RNAi}* (*domeMeso-Gal4,UAS-GFP;UAS-Mdh^{RNAi}*), **(D-D3)** graphs showing progenitors (*Dome^{+}*) vs Non-Progenitors (*Dome^{-}*) population ratio. This was done as a positive control for the temporal analysis we did for the genotypes showing size defect, it was observed that unlike the mutants with size defect, *Sdh^{RNAi}* and *Mdh^{RNAi}* did not show any issues with *Dome^{+}* vs *Dome^{-}* population. *domeMeso>GFP/+* (control, 48h, n=32; 72h, n=44; 96h, n=54; 120h, n=31), *domeMeso>GFP/Sdh^{RNAi}* (48h, n=36, total, p=0.5349; green, p=0.3078, blue, p=0.1229; 72h, n=49, total, p=0.1682; green, p=0.2342, blue, p=0.0505; 96h, n=43, total, p=0.8749; green, p=0.0675, blue, p=0.0311; 120h, n=39, total, p=0.2920; green, p=0.0066, blue, p=0.0010), *domeMeso>GFP/Mdh^{RNAi}* (48h, n=37, total, p=0.4209; green, p=0.6636, blue, p=0.2814; 72h, n=50, total, p=0.5932; green, p=0.9619, blue, p=0.2308; 96h, n=46, total, p=0.7150; green, p=0.0892, blue, p=0.3123; 120h, n=41, total, p=0.8168; green, p=0.0002, blue, p=0.0046), **(E)** Quantification is relative % area with respect to total lymph gland area for differentiation profile (*Pxn+*) at 48h, *domeMeso-Gal4,UAS-GFP/+* (control, n=14), *domeMeso-Gal4,UAS-GFP;UAS-Sdh^{RNAi}* (n=16, p=0.4418), *domeMeso-Gal4,UAS-GFP;UAS-Mdh^{RNAi}* (n=15, p=0.8450), **(F)** Quantification is relative % area with respect to total lymph gland area for differentiation profile (*Pxn+*) at 72h, *domeMeso-Gal4,UAS-GFP/+* (control, n=23), *domeMeso-Gal4,UAS-GFP;UAS-Sdh^{RNAi}* (n=18, p=0.0013), *domeMeso-Gal4,UAS-GFP;UAS-Mdh^{RNAi}* (n=25, p=0.0018), **(G)** Quantification is relative % area with respect to total lymph gland area for differentiation profile (*P1+*) at 48h, *domeMeso-Gal4,UAS-GFP/+* (control, n=14), *domeMeso-Gal4,UAS-GFP;UAS-Sdh^{RNAi}* (n=18, p=NA), *domeMeso-Gal4,UAS-GFP;UAS-Mdh^{RNAi}* (n=15, p=NA), **(H)** Quantification is relative % area with respect to total lymph gland area for differentiation profile (*P1+*) at 72h, *domeMeso-Gal4,UAS-GFP/+* (control, n=22), *domeMeso-Gal4,UAS-GFP;UAS-Sdh^{RNAi}* (n=18, p=0.0015), *domeMeso-Gal4,UAS-GFP;UAS-Mdh^{RNAi}* (n=23, p=0.0299). Data is presented as median plots (*p<0.05; **p<0.01; ***p<0.001; ****p<0.0001), ordinary one-way ANOVA. Scale bar: 20µm. 'n'=lymph gland lobes. DAPI marks DNA, Progenitors (*Dome^{+}*; Green), non-progenitors (*Dome^{-}*; blue only). Comparisons for significance are with control values.

4.4 Importance of citrate for the development of lymph gland

Since loss of *CS*, *mAcon1*, *α-Kdh* and *Gdh* led to the growth defects, we attempted to rescue the phenotype by supplementing the affected/depleted metabolite. We supplemented the food with Citrate (the product of *CS*) and Succinate (a downstream of *α-Kdh*). Based on available literature and preliminary screening, we standardized the concentration of citrate to be 1% weight/volume and succinate to be 3% weight/volume. We transferred the first instar larvae from the normal food (NF) to 1% citrate food (CF) and 3% succinate food (SF), allowed them to develop and dissected the LGs at 3rd instar larval stage (120h). Intrestingly, under 1%CF supplementation, both knockdowns as well as control LGs were further reduced in size compared to their respective replicates on NF (Normal food) (Figure 32a B-B4). Since the larvae were reared completely on the 1% citrate supplemented food, the size defect might be due to excess citrate, which can also act as a stress signal.

To understand this, we initially worked with *CS^{RNAi}* and 1% CF only, and divided the larval growth trajectory into two phases based on the onset of differentiation i.e., pre- differentiation and post-differentiation phase separated at 60h after egg laying (AEL) time point (Figure 32a A). We next transferred the 2nd instar larvae at 60h AEL onto the 1%CF, allowed them to develop, and

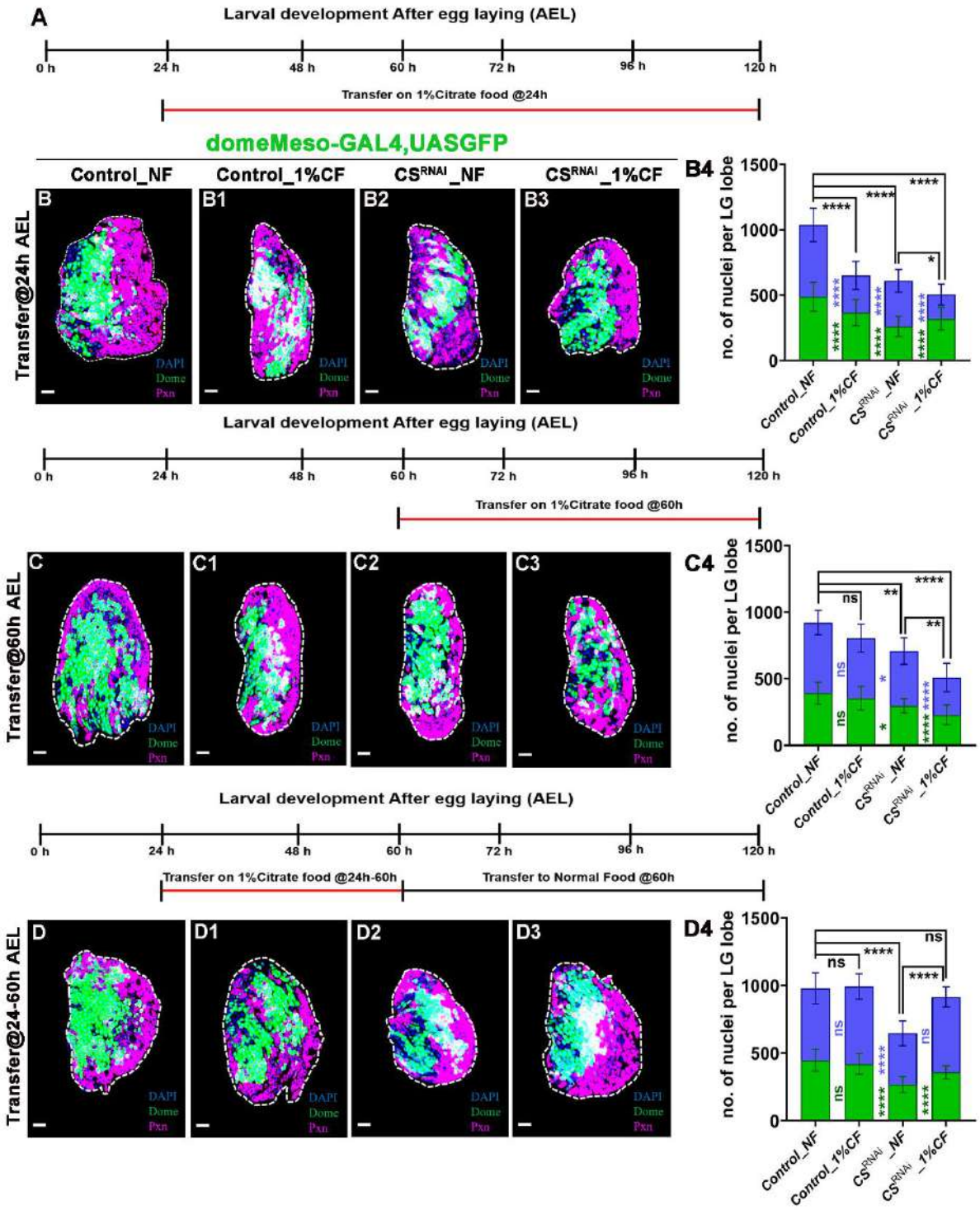

Figure 32a*:* Citrate is necessary for the early development of LG in *Drosophila* larva.

(***A*)** Timeline of larval development after egg laying (AEL). Based on the timeline three different time period were chosen to assess the importance of citrate in the development of lymph gland, first one being from 24h AEL to 3rd instar (120h), second 60h AEL to 3rd instar (120hAEL) and third from 24h AEL to 60h AEL. **(B-B1)** Control (*domeMeso-Gal4,UAS-GFP/+*) lymph gland showing growth of lymph gland on NF **(B)** and 1% CF **(B1), (B2-B3)** expressing CS^{RNAi} (*domeMeso-Gal4,UAS-GFP;UAS-*CS^{RNAi}) on NF (B2) and 1% CF **(B3)**, respectively from embryos (0h AEL) stage itself to 120h AEL. **(C-C1)** Control (*domeMeso-Gal4,UAS-GFP/+*) lymph gland showing growth of lymph gland on NF **(C)** and 1% CF **(C1), (C2-C3)** expressing CS^{RNAi} (*domeMeso-Gal4,UAS-GFP;UAS-CSRNAi*) on NF (C2) and 1% CF **(C3)**, respectively from 60h AEL stage to wandering 3rd instar larval

stage. **(D-D1)** Control (*domeMeso-Gal4,UAS-GFP/+*) lymph gland showing growth of lymph gland on NF **(D)** and 1% CF **(D1), (D2-D3)** expressing CS^{RNAi} (*domeMeso-Gal4,UAS-GFP;UAS-*CS^{RNAi}) on NF (D2) and 1% CF **(B3)**, respectively from embryos (0h AEL) stage to 60h AEL, showing the distribution pattern of progenitor (*Dome+*; green) vs non-progenitor (*Dome-*; blue*)* population at 3rd instar larval stage. As observed earlier (Figure X), the size of LG reduces, even in control if we supplement citrate throughout the larval development (B-B3, E). Even this situation could not be addressed if we feed the citrate supplemented food from 60h AEL till larval development (C-C3, F), but when we feed the citrate food from 0-60h AEL and then allow the larva to grow on NF, we not only rescue the size but also the progenitor homeostasis (D-D3, G). **(E)** graphs showing the size (total number of cells), and progenitor homeostasis upon citrate food supplementation from 24h AEL to 120h AEL, *domeMeso>GFP/+* (control, NF, n=45; 1%CF, n=33, total, p<0.0001; green, p<0.0001, blue, p<0.0001), *domeMeso>GFP/*CS^{RNAi} (NF, n=21, total, p<0.0001; green, p<0.0001, blue, p<0.0001; 1%CF, n=17, total, p<0.0001; green, p<0.0001, blue, p<0.0001) (NF to 1%CF total, p=0.0166); **(F)** graphs showing the size (total number of cells), and progenitor homeostasis upon citrate food supplementation from 60h AEL to 120h AEL, *domeMeso>GFP/+* (control, NF, n=9; 1%CF, n=11, total, p=0.0125; green, p=0.5236, blue, p=0.2062), *domeMeso>GFP/*CS^{RNAi} (NF, n=12, total, p=0.0017; green, p=0.0167, blue, p=0.0294; 1%CF, n=11, total, p<0.0001; green, p<0.0001, blue, p<0.0001) (NF to 1%CF total, p=0.0028); **(G)** graphs showing the size (total number of cells), and progenitor homeostasis upon citrate food supplementation from 24h AEL to 60h AEL, *domeMeso>GFP/+* (control, NF, n=29; 1%CF, n=32, total, p=0.9304; green, p=0.2479, blue, p=0.1982), *domeMeso>GFP/*CS^{RNAi} (NF, n=28, total, p<0.0001; green, p<0.0001, blue, p<0.0001; 1%CF, n=27, total, p=0.1036; green, p<0.0001, blue, p=0.6157) (NF to 1%CF total, p<0.0001). Data is presented as median plots (*p<0.05; **p<0.01; ***p<0.001; ****p<0.0001), ordinary one-way ANOVA. Scale bar: 20µm. 'n'=lymph gland lobes. DAPI marks DNA, Progenitors (*Dome*$^+$; Green), non-progenitors (*Dome-*; blue only). Comparisons for significance are with control values.

dissected the LG at the wandering 3rd instar (120h) for the analysis. Even under these conditions, we could not rescue growth defect (Figure 32a C-C4). In another set of experiments (pre-differentiation phase), we transferred 24h AEL larvae to 1% CF and at 60h AEL, transferred them back to NF for further development, followed by dissection at 120h AEL, and this time, we observed that the growth defects were rescued, along with restoration of progenitor homeostasis (Figure 32a D-D4). These results highlight the importance of citrate in the early development of the lymph gland. As established earlier through temporal experiments, CS^{RNAi} knockdown do not show any size defect at 48h AEL, but the progenitors are lost to differentiation (Figure 27 A-A3, D-E3 & Figure 28 B-C). This indicates that progenitors are dividing to differentiate, as evident from the appearance of differentiation markers *Pxn*$^+$ (red) and *P1*$^+$ (gray) (Figure 30 A-A', D-D'& G-G') at 48h AEL. This prompted us to ask whether citrate supplementation can rescue the early differentiation phenotype. For this, we chose two developmental time points 48h and 72h AEL. We transferred the 24h AEL (first instar) larvae to 1% CF and dissected the lymph gland at 48h AEL. For the 72h time point, we transferred the larvae back to NF at 60h AEL and dissected them 12h later and we observed that early citrate supplementation completely suppressed precoecious differentiation (Figure 32b A-D1 & I). At the 72h timepoint, the extensive differentiation was also reduced to normal and even below the respective control levels (Figure 32b E-H1 & J). These early rescues of differentiation, along with the 3rd instar rescue of growth and progenitor homeostasis, confirms the necessecity of citrate in early development of the lymph gland.

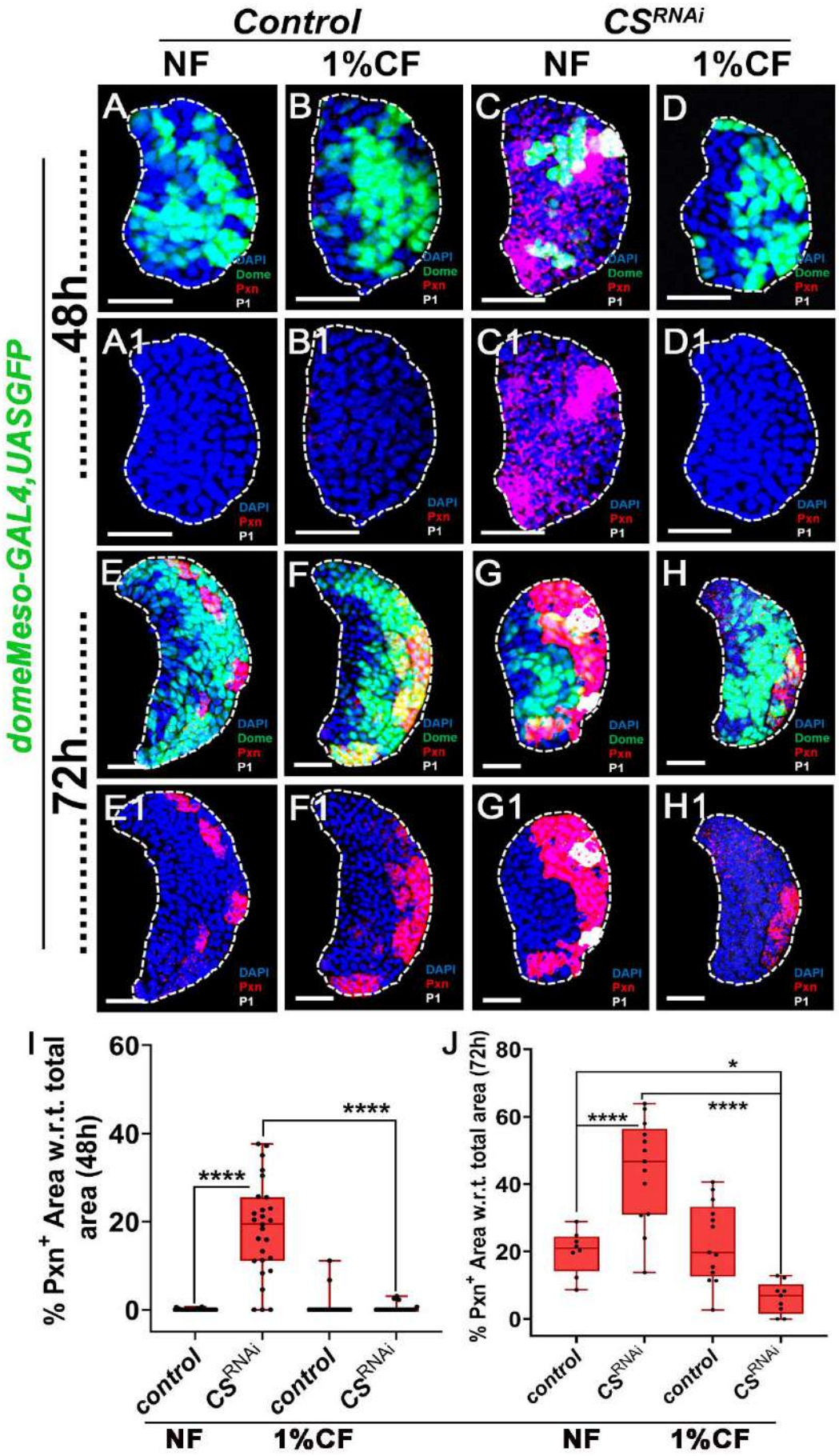
Control
CS^RNAi
NF
1%CF
NF
1%CF
domeMeso-GAL4,UASGFP
48h
72h
A
B
C
D
A1
B1
C1
D1
E
F
G
H
E1
F1
G1
H1
DAPI
Dome
Pxn
P1
I
% Pxn+ Area w.r.t. total area (48h)
J
% Pxn+ Area w.r.t. total area (72h)
****
*
control
CS^RNAi
NF
1%CF

Figure 32b: Citrate is necessary for the early development of LG in *Drosophila* larva.

(***A)*** In the previous result we have shown the rescue at the 3rd instar larval stage, as the requirement of citrate was found to be early in development and we saw in previous results that unavailability of citrate at early stage leads to precocious differentiation (Figure X). We than sort after the rescue of differentiation phenotype at 48h and 72h as there was no size defect observe at these timeline of larval development. **(A-A1; B-B1)** Control (*domeMeso-Gal4,UAS-GFP/+*) lymph gland showing growth of lymph gland on NF **(A-A1)** and 1% CF **(B-B1), (C-C1;D-D1)** expressing CS^{RNAi} (*domeMeso-Gal4,UAS-GFP;UAS-CSRNAi*) on NF **(C-C1)** and 1% CF **(D-D1)**, respectively at 48h AEL, we can see there is none differentiated cells (*Pxn+*; Red) in control (both NF and 1%CF) at 48h (A-B1), whereas in CS^{RNAi} mutant we can clearly see precocious differentiation (*Pxn+*; Red) in NF at 48h (C-C1), which is rescued by 1% citrate feeding (D-D1). Similarly **(E-E1; F-F1)** Control (*domeMeso-Gal4,UAS-GFP/+*) lymph gland showing growth of lymph gland on NF **(E-E1)** and 1% CF **(F-F1), (G-G1;H-H1)** expressing CS^{RNAi} (*domeMeso-Gal4,UAS-GFP;UAS-*CS^{RNAi}) on NF **(G-G1)** and 1% CF **(H-H1)**, respectively at 72h AEL, we can see a few differentiated cells (*Pxn+*; Red) in control (both NF and 1%CF) at 72h **(E-F1)**, whereas in CS^{RNAi} mutant we can clearly see aggressive (almost half of the LG) differentiation (*Pxn+*; Red) in NF at 72h **(G-G1)**, which is rescued by 1% citrate feeding **(H-H1)**. **(I)** Quantification is relative % area with respect to total lymph gland area for differentiation profile (*Pxn+*) at 48h, *domeMeso-Gal4,UAS-GFP/+* (control, NF, n=28; 1%CF, n=27, p>0.9999), *domeMeso-Gal4,UAS-GFP;UAS-*CS^{RNAi} (NF, n=27, p<0.0001; 1%CF, n=22, p>0.9999) (NF to 1%CF, p<0.0001), **(J)** Quantification is relative % area with respect to total lymph gland area for differentiation profile (*Pxn+*) at 72h, *domeMeso-Gal4,UAS-GFP/+* control, NF, n=8; 1%CF, n=13, p<0.0001), *domeMeso-Gal4,UAS-GFP;UAS-*CS^{RNAi} (NF, n=13, p=0.08865; 1%CF, n=9, p=0.0429) (NF to 1%CF, p<0.0001). Data is presented as median plots (*p<0.05; **p<0.01; ***p<0.001; ****p<0.0001), ordinary one-way ANOVA. Scale bar: 20µm. 'n'=lymph gland lobes. DAPI marks DNA, Progenitors ($Dome^{+}$; Green), non-progenitors ($Dome^{-}$; blue only). Comparisons for significance are with control values.

4.5 Importance of succinate for the development of lymph gland

As mentioned earlier, we also supplemented succinate besides the citrate supplementation, to all the size/growth knockdowns. Succinate supplimetation was done from the first instar larval stage itself and the larvae were allowed to grow till wandering 3rd instar stage (120h AEL), post that they were dissected to harvest lymph gland. We observe that under 3% SF conditions, CS^{RNAi} knockdown larvae were fully rescued, while all others showed partially rescue (Figure 33 A-E, A2-E2 & Figure 34 A). Upon detailed quantification, dividing the total lymph gland cells into progenitor (green) and non-progenitor (blue) population, we confirmed that the rescue stemmed from the contribution of both progenitors and non-progenitor proliferation (Figure 33 A-E, A2-E2 & Figure 34 A-C).

From the available data we concluded that initially there are groups of enzymes (CS/mAcon1 & Kdh/Gdh) contributing separately to achieve the same goal of achieving the appropriate size of LG through the maintenance of stemness and proliferative capacity of the progenitors. This is followed up by the complete TCA cycle for the regulated differentiation fate as well as establishment of CZ via proliferation of differentiating as well as progenitor population (Figure 35).

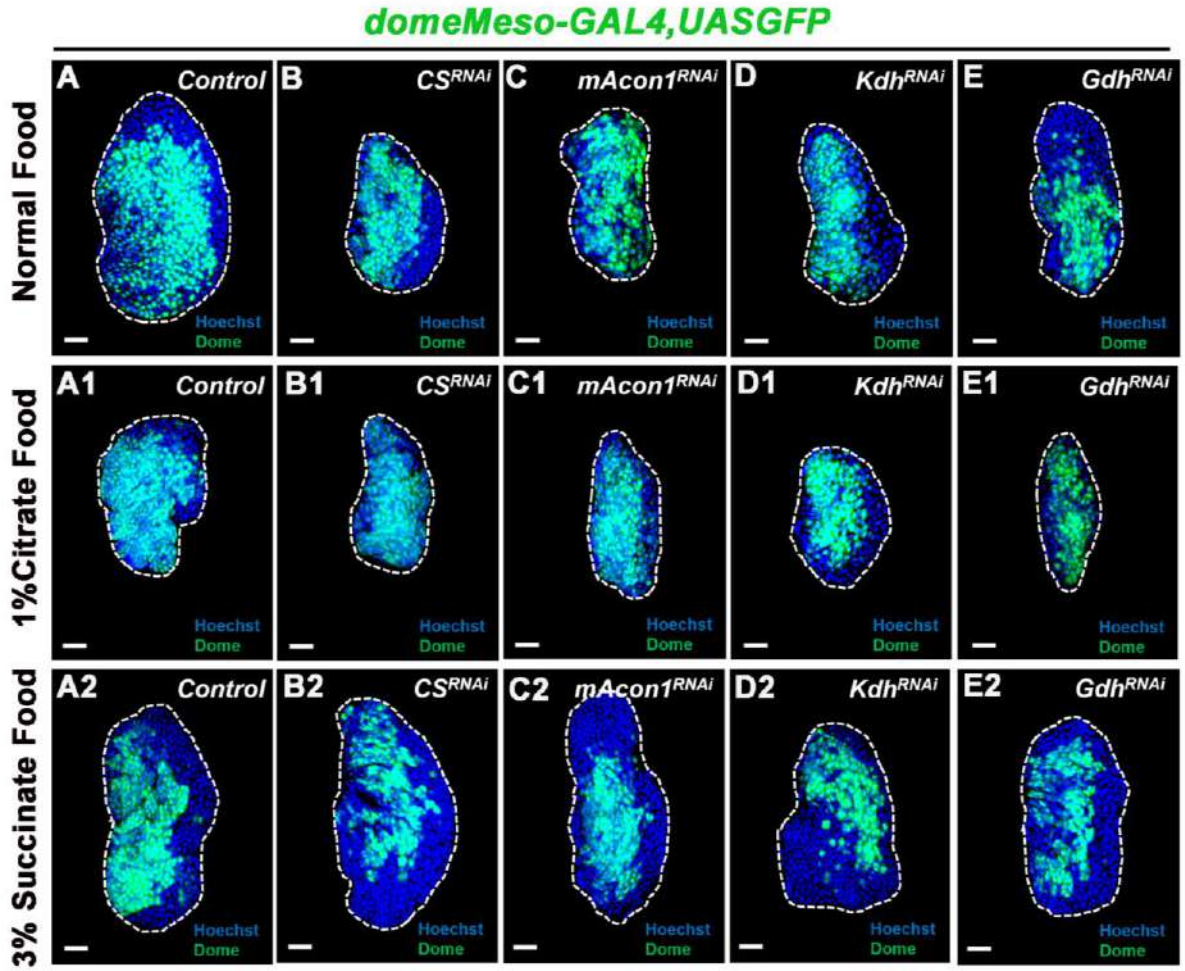

Figure 33: Citrate and succinate food supplementation from the hatching itself to rescue the LG growth.

(***A-A2)*** Control (*domeMeso-Gal4,UAS-GFP/+*) lymph gland showing growth of lymph gland on NF **(A)**, 1% CF **(A1)** and 3% SF **(A2)**, respectively, with the distribution pattern of progenitor (*Dome+*; green) vs non-progenitor (*Dome-*; blue*)* population at 3rd instar larval stage, **(B-B2)** expressing CS^{RNAi} *(domeMeso-Gal4,UAS-GFP;UAS-*CS^{RNAi}), **(C-C2)** expressing *mAcon1RNAi* (*domeMeso-Gal4,UAS-GFP;UAS-*$mAcon1^{RNAi}$), **(D-D2)** expressing *α-*Kdh^{RNAi} (*domeMeso-Gal4,UAS-GFP;UAS-α-*Kdh^{RNAi}), **(E-E2)** expressing Gdh^{RNAi} (*domeMeso-Gal4,UAS-GFP;UAS-*Gdh^{RNAi}), **(A1-E1)** in all the genotypes including control the size of the LG is further reduced in 1%CF supplementation from hatching, clearly citrate is acting as some king of stressor in the system and resulting in further compromised LG. **(A2-E2)** In the 3% succinate supplementation from the hatching of larva we observed full or partial recovery in the LG size but the progenitor homeostasis is compromised. DAPI marks DNA, Progenitors ($Dome^{+}$; Green), non-progenitors ($Dome^{-}$; blue only). Comparisons for significance are with control values.

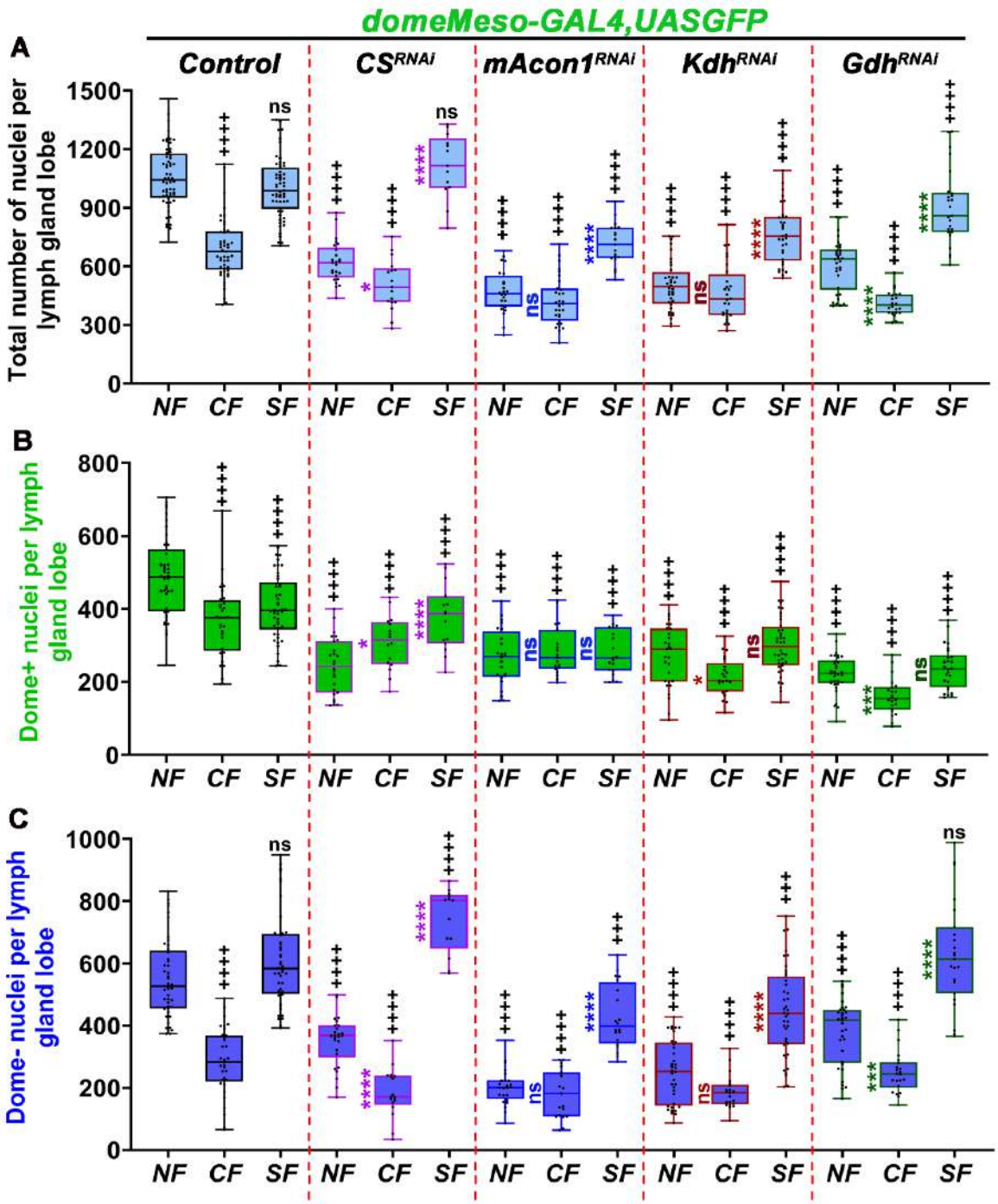

Figure 34: Quantification for temporal analysis for *CS*^{RNAi}, *mAcon1*^{RNAi}, *α-Kdh*^{RNAi} and *Gdh*^{RNAi}

(A) graph representing total number of cells (based on nuclei count) per lymph gland **,** *domeMeso>GFP/+* (*control*, NF, n=60; CF, n=49, p<0.0001; SF, n=56, p=0.2973), *domeMeso>GFP/CS*^{RNAi} (NF, n=25, p<0.0001; CF, n=17, p<0.0001, p=0.0114; SF, n=13, p=0.9083, p<0.0001), *domeMeso>GFP/mAcon1*^{RNAi} (NF, n=24, p<0.0001; CF, n=31, p<0.0001, p=0.2296; SF, n=19, p<0.0001, p<0.0001), *domeMeso>GFP/α-Kdh*^{RNAi} (NF, n=36, p<0.0001; CF, n=28, p<0.0001, p=0.4512; SF, n=33, p<0.0001, p<0.0001), and *domeMeso>GFP/Gdh*^{RNAi} (NF, n=34, p<0.0001; CF, n=22, p<0.0001, p<0.0001; SF, n=25, p<0.0001, p<0.0001), **(B)** graph representing number of progenitor cells (*Dome+*; green) per lymph gland **,** *domeMeso>GFP/+* (*control*, NF, n=45; CF, n=33, p<0.0001; SF, n=46, p<0.0001), *domeMeso>GFP/CS*^{RNAi} (NF, n=26, p<0.0001; CF, n=16, p<0.0001, p=0.0255; SF, n=15, p<0.0001, p<0.0001), *domeMeso>GFP/mAcon1*^{RNAi} (NF, n=24, p<0.0001; CF, n=19, p<0.0001, p=0.6584; SF, n=19, p<0.0001, p=0.7850), *domeMeso>GFP/α-Kdh*^{RNAi} (NF, n=29, p<0.0001; CF, n=21, p<0.0001, p=0.0169; SF, n=40, p<0.0001, p=0.2333), and *domeMeso>GFP/Gdh*^{RNAi} (NF, n=34, p<0.0001; CF, n=22, p<0.0001, p=0.0001; SF, n=26, p<0.0001, p=0.4301), **(C)** graph representing number of non-progenitor cells (*Dome-*; blue)

per lymph gland , *domeMeso>GFP/+* (*control*, NF, n=45; CF, n=33, p<0.0001; SF, n=44, p=0.1191), *domeMeso>GFP/CS*^{RNAi} (NF, n=26, p<0.0001; CF, n=17, p<0.0001, p<0.0001; SF, n=13, p<0.0001, p<0.0001), *domeMeso>GFP/mAcon1*^{RNAi} (NF, n=24, p<0.0001; CF, n=19, p<0.0001, p=0.5601; SF, n=20, p=0.0010, p<0.0001), *domeMeso>GFP/α-Kdh*^{RNAi} (NF, n=36, p<0.0001; CF, n=21, p<0.0001, p=0.0741; SF, n=40, p=0.0004, p<0.0001), and *domeMeso>GFP/Gdh*^{RNAi} (NF, n=33, p<0.0001; CF, n=22, p<0.0001, p=0.0005; SF, n=23, p=0.0861, p<0.0001). Data is presented as median plots ($^{*/+}$p<0.05; $^{**/++}$p<0.01; $^{***/+++}$p<0.001; $^{****/++++}$p<0.0001), ordinary one-way ANOVA. Scale bar: 20µm. 'n'=lymph gland lobes. DAPI marks DNA, Progenitors (*Dome*$^{+}$; Green), differentiating (*Dome*$^{+}$ *Pxn*$^{+}$; yellow and only *Pxn*$^{+}$; red) population, and differentiated population (*P1*$^{+}$ and *PPO*$^{+}$; magenta). Comparisons for significance are with control values.

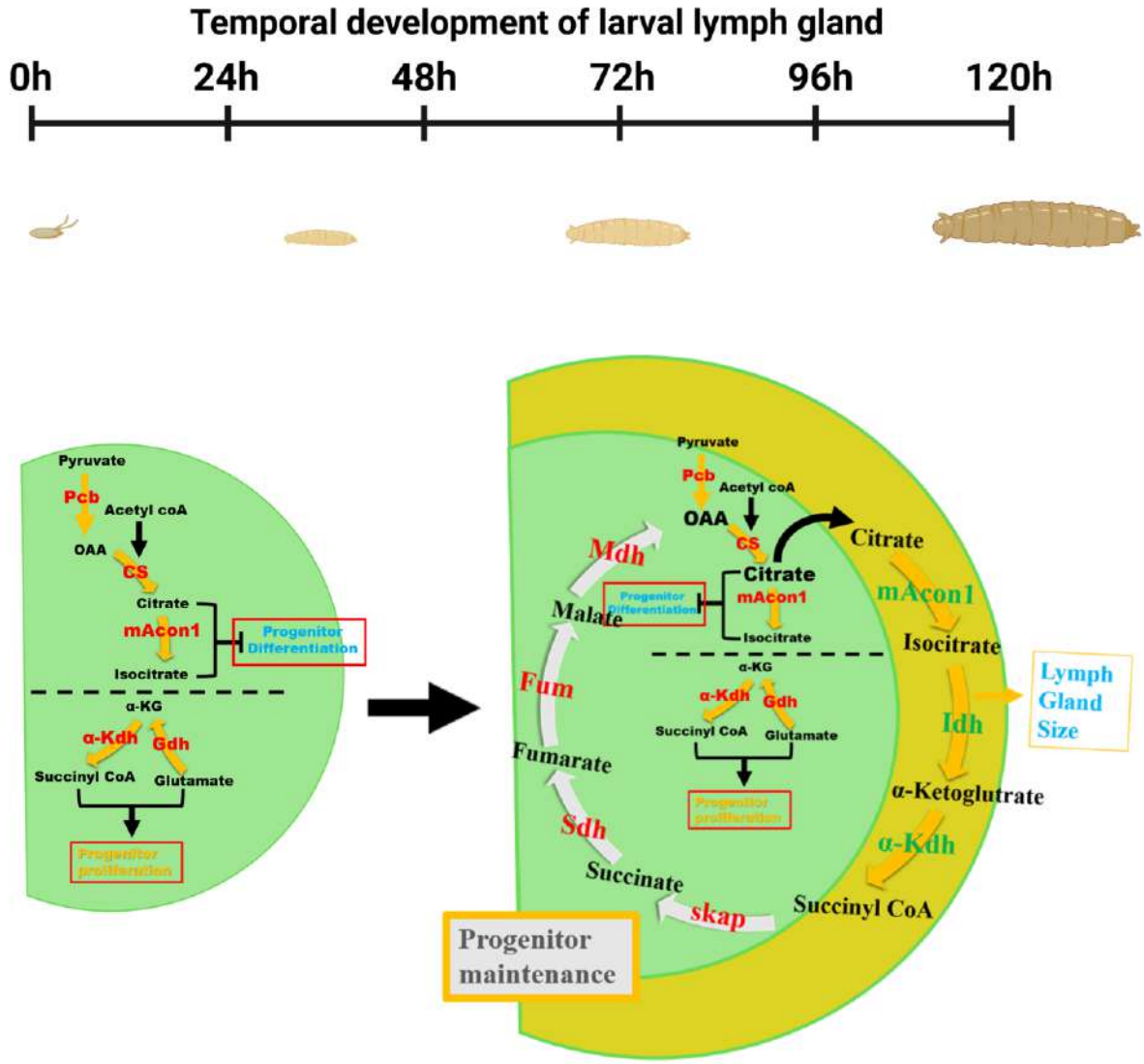

Figure 35: The making of TCA cycle from early growth of LG to the maintaninance of progenitors.

The illustration depicting the growth trajectory of the *Drosophila* larva and the Lymph gland development during the larval growth. Here we have deciphered how initially different groups of reactions work for the progenitor proliferation autonomously (*α-Kdh* and *Gdh*), as well as non-autonomously (*Pcb, CS* and *mAcon1*) supporting the proliferation by keeping a tight regulation on progenitor differentiation. Once a desired number of cells is achieved, around 60h AEL of development the progenitors takes on the differentiation trajectory and give rise to intermediary zone. Progenitors to IZ cells transition and their proliferation is very tightly regulated so that the progenitor pool do not exhaust and at the same time IZ and subsequently CZ can be established. It is this regulation of progenitor maintenance for which the whole TCA cycle work together.

5. Gene expression profile in TCA cycle mutants

To understand the impact of loss of TCA cycle enzyme and the cyclic nature of TCA cycle in the LG, we performed Bulk-RNA sequencing at wandering 3rd instar larval stage using *dome*MESO-Gal4,UAS-GFP. We have dissected LG from control (DW), and following knockdowns: $Pdha^{RNAi}$ (DP), $mAcon1^{RNAi}$ (DA), $\alpha\text{-}Kdh^{RNAi}$ (DK), Sdh^{RNAi} (DS) and Mdh^{RNAi} (DM) to understand their impact on blood cell development. We have taken the whole LG for this experiment without segregating its distinct zones, eventhough the *dome*MESO-Gal4,UAS-GFP marks only MZ and IZ but not CZ this is one of the caviats of this experiment which can have some unknown effect on the results. The experiments were performed in two batches, Batch 1 (control, $\alpha\text{-}Kdh^{RNAi}$ and Sdh^{RNAi}) and Batch 2 (control, $Pdha^{RNAi}$, $mAcon1^{RNAi}$ and Mdh^{RNAi}).

Sample	Total no of reads	Total no of reads after filtering {Adapter trimming + quality}	Mapped reads	Uniquely mapped reads
DW_I	18,769,264	18,669,681	17,520,532 (93.8%)	17,687,810 (94.74%)
DW_II	19,288,085	19,218,090	17,708,353 (92.1%)	17,882,469 (93.05%)
DS_I	41,748,501	41,464,056	40,471,939 (97.6%)	37,033,447 (89.31%)
DS_II	37,206,243	36,964,356	35,589,257 (96.2%)	33,021,786 (89.33%)
DK_I	43,523,464	43,070,210	40,994,231 (95.1%)	39,434,888 (91.56%)
DK_II	42,953,890	42,676,682	40,982,680 (96.0%)	39,783,774 (93.22%)

Table 1: RNA sequencing read statisti*CS* for the Batch-1 (DW, *Control*; DS, $Sdha^{RNAi}$; DK, $\alpha\text{-}Kdh^{RNAi}$)

In both batches, the percentage of uniquely mapped readout was satisfactory (Table 1 and 2) and each of the batches had its own internal control. We then performed principal component analysis (PCA) for the respective batches and also combined them (Figure 36). The controls from both batches clustered closely together, indicating minimal variance between them. We next generated normalized read counts for each knockdowns and proceeded with differential gene expression analysis of which top 50 are represented as heatmap from both the batches (Figure 37 & 38). Differentially expressed genes (DEGs) from each knockdown sample were further represented with the help of volcano plots (Figure 39-43). This analysis yielded Gene ontology (GO) terms for each knockdowns. The top enriched GO categories are shown in Figure 44-46. Since the variance between the two control groups was minimal, we also compared the overlap between differentially expressed genes from all the five knockdowns using venn diagram. Surprisingly, we did not identify any major signaling gene in the overlap between all five knockdowns. This observation further suggests that the TCA cycle operates in

a non-cyclic or branched manner in the LG (Figure 39). However, we found significant regulation of immune related and metabolism related genes in all conditions, suggesting that instead of conventional signalling pathways, metabolites themselves may act as signalling molecules regulating TCA cycle functioning.

Sample	Total no of reads	Total no of reads after filtering {Adapter trimming + quality}	Mapped reads	Uniquely mapped reads
DW_I	30,385,140	30,048,900	29,716,123 (98.89%)	28,688,050 (95.47%)
DW_II	30,605,948	30,333,851	27,774,443 (91.56%)	26,601,720 (87.70%)
DW_III	28,928,580	28,810,363	28,283,085 (97.76%)	27,149,795 (94.24%)
DA_I	31,926,942	31,729,205	30,872,303 (97.29%)	29,507,176 (93.00 %)
DA_II	31,132.936	31,011,948	30,661,967 (98.87%)	29,753,780 (95.94%)
DA_III	28,476,980	28,416,660	28,005,972 (98.55%)	21,769,332 (76.61%)
DM_I	35,280,155	35,199,015	34,736,675 (98.68%)	33,686,134 (95.70%)
DM_II	35,518,104	35,434,039	35,019,673 (98.83%)	34,330,471 (96.89%)
DM_III	32,077,263	31,992,894	31,484,999 (98.41%)	29,243,263 (91.41%)
DP_I	32,899,079	32,542,537	32,019,446 (98.39%)	30,986,896 (95.22%)
DP_II	34,118,623	34,037,314	33,625,296 (98.78%)	32,655,874 (95.94%)
DP_III	34,728,515	34,649,007	34,183,242 (98.65%)	32,922,153 (95.02%)

Table 2: RNA sequencing read statisti*CS* for the Batch-2 (DW, *Control*; DA, *mAcon1*^{RNAi}; DM, *Mdh*^{RNAi}; DP, *Pdha*^{RNAi})

Sample	Total no of reads	Total no of reads after filtering {Adapter trimming + quality}	Mapped reads	Uniquely mapped reads
DW_I	18,769,264	18,669,681	17,520,532 (93.8%)	17,687,810 (94.74%)
DW_II	19,288,085	19,218,090	17,708,353 (92.1%)	17,882,469 (93.05%)
DW_Ia	30,385,140	30,048,900	29,716,123 (98.89%)	28,688,050 (95.47%)
DW_IIa	30,605,948	30,333,851	27,774,443 (91.56%)	26,601,720 (87.70%)
DW_IIIa	28,928,580	28,810,363	28,283,085 (97.76%)	27,149,795 (94.24%)

Table 3: RNA sequencing read statisti*CS* between Batch-1 and Batch-2 controls (DW_I, *Control* Batch 1, DW_Ia, *control* Batch-2)

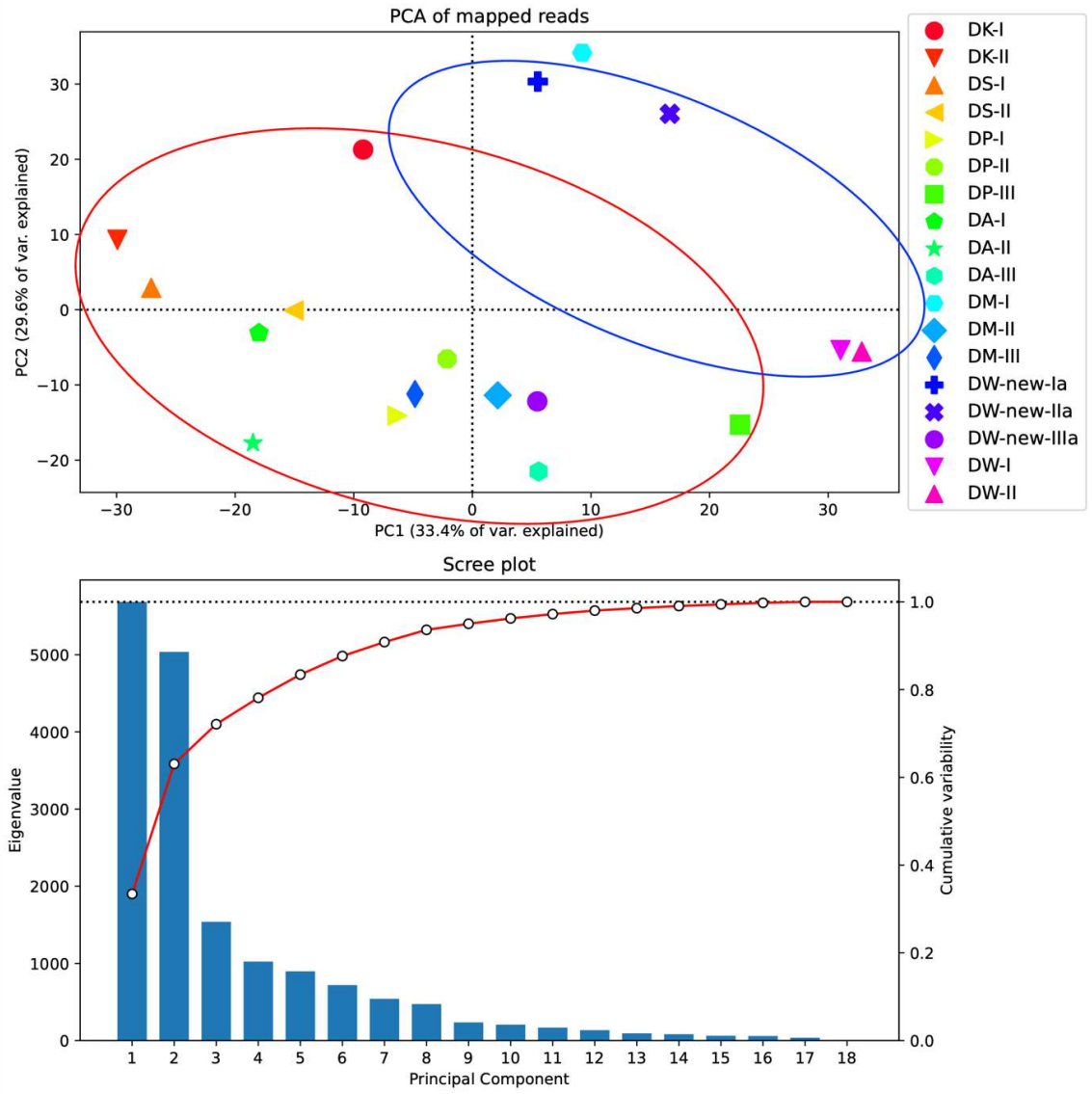

Figure 36: PCA of the mapped reads for both batches together (DW, Control; DS, *Sdha*^{RNAi}; DK, *α-Kdh*^{RNAi}; DA, *mAcon1*^{RNAi}; DM, *Mdh*^{RNAi}; DP, *Pdha*^{RNAi})

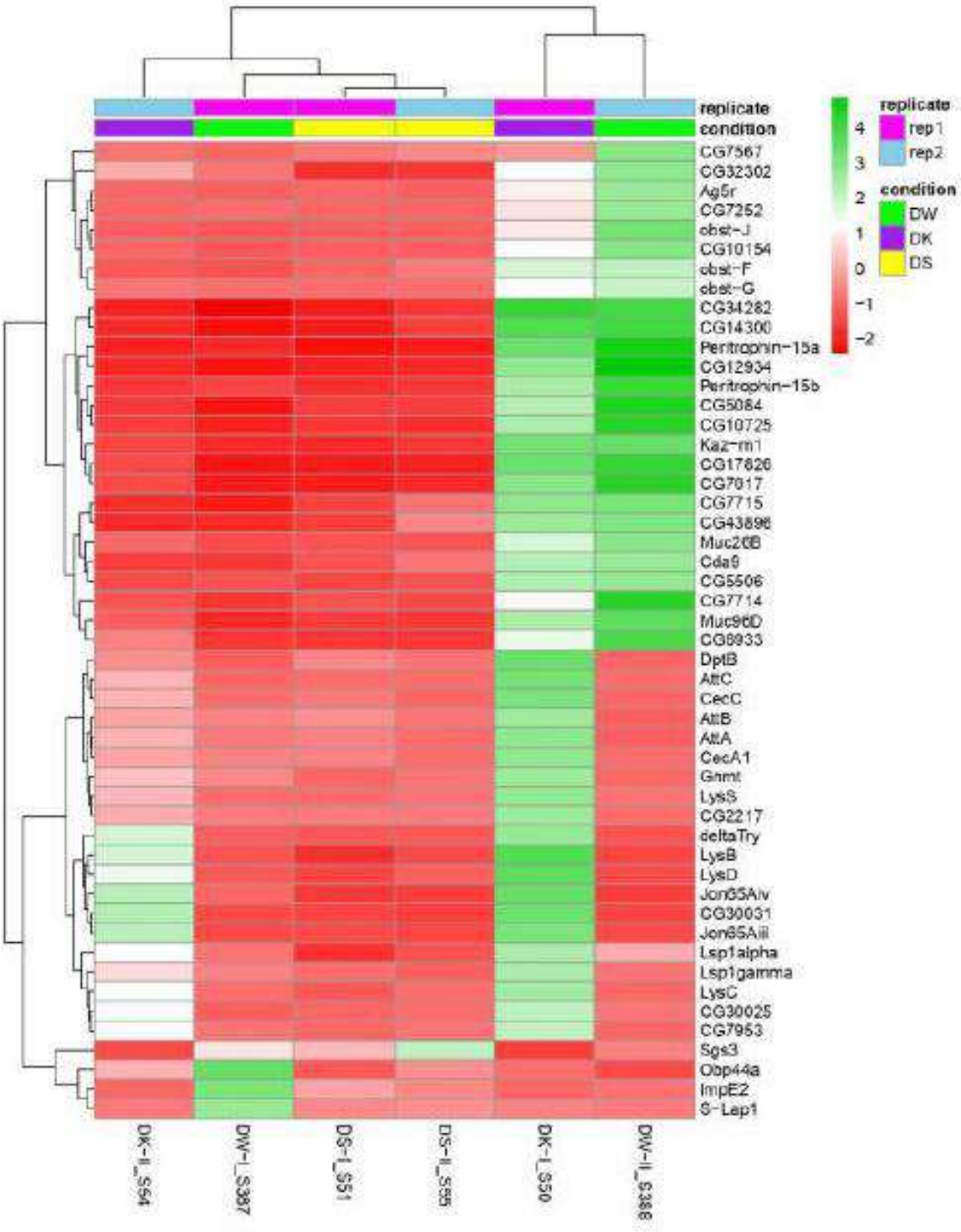

Figure 37: Heatmap of 6 samples, showing top 50 genes with most variance (DW, Control; DS, *Sdha*^{RNAi}; DK, *α-Kdh*^{RNAi}; I and II are replicates)

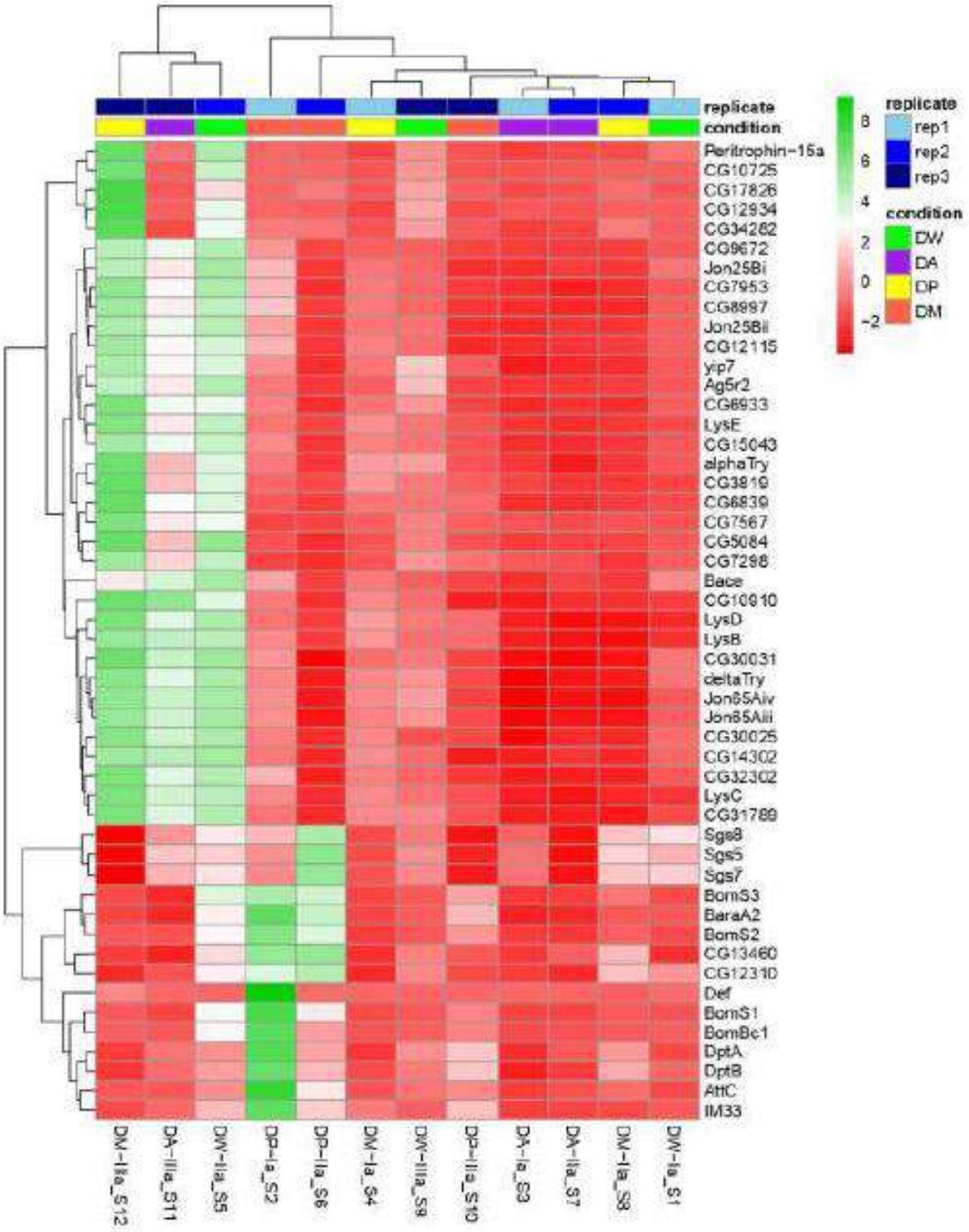

Figure 38: Heatmap of 12 samples, showing top 50 genes with most variance (DW, Control; DA, *mAcon1*^{RNAi}; DM, *Mdh*^{RNAi}; DP, *Pdha*^{RNAi} ; Ia, IIa and IIIa are replicates)

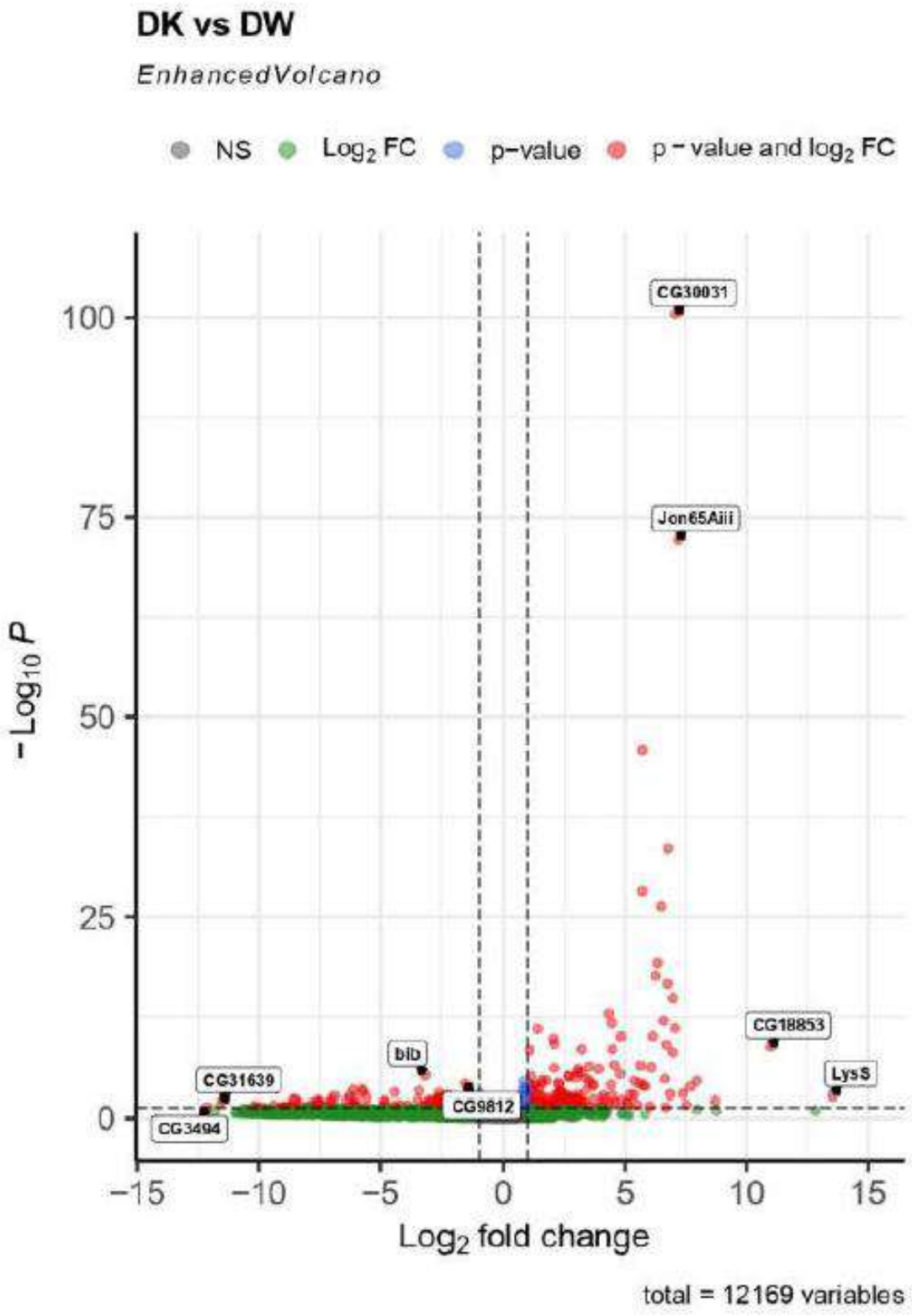

Figure 39: Volcano plot showing top DEGs for DK vs DW.

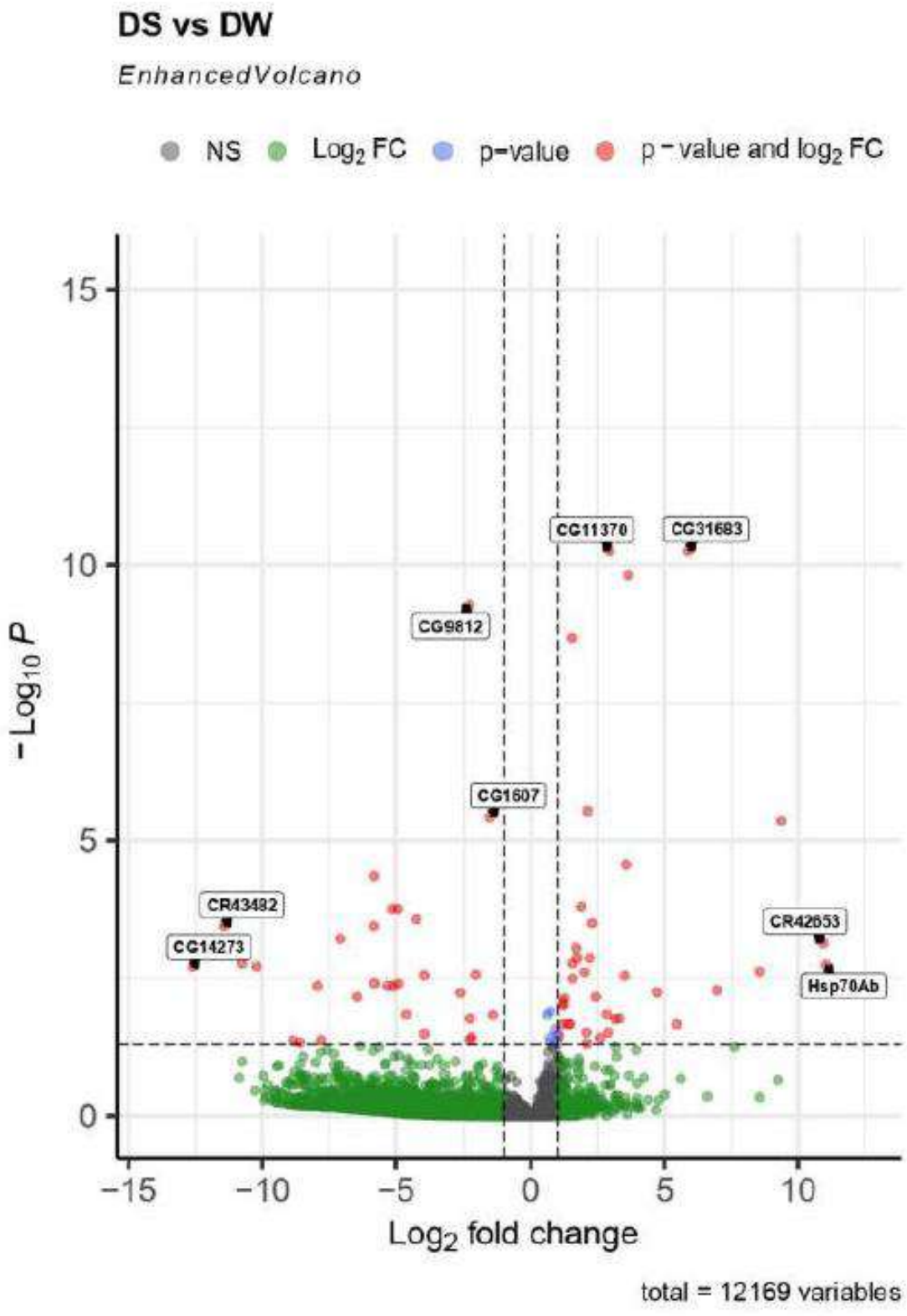

Figure 40: Volcano plot showing top DEGs for DS vs DW.

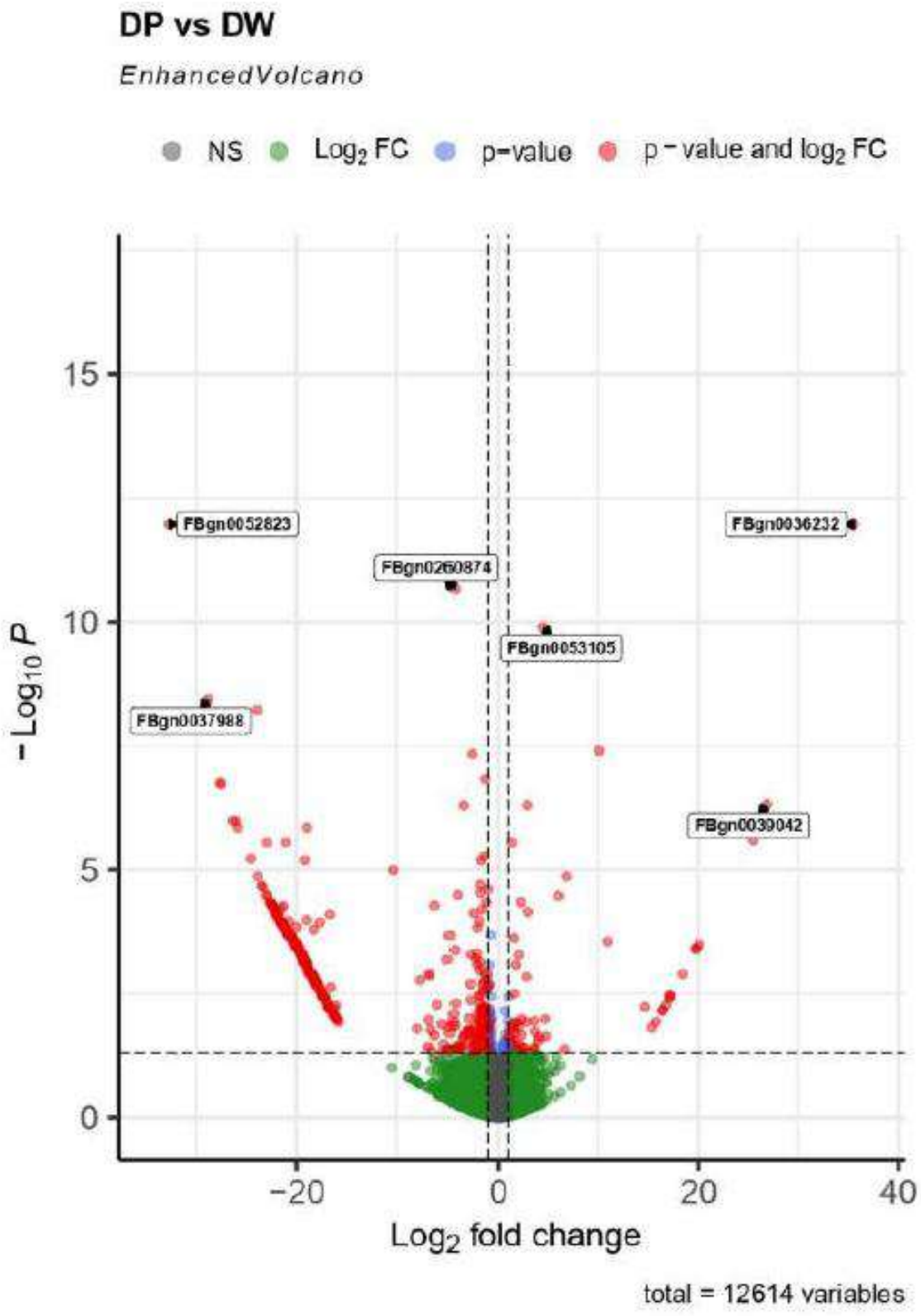

Figure 41: Volcano plot showing top DEGs for DP vs DW.

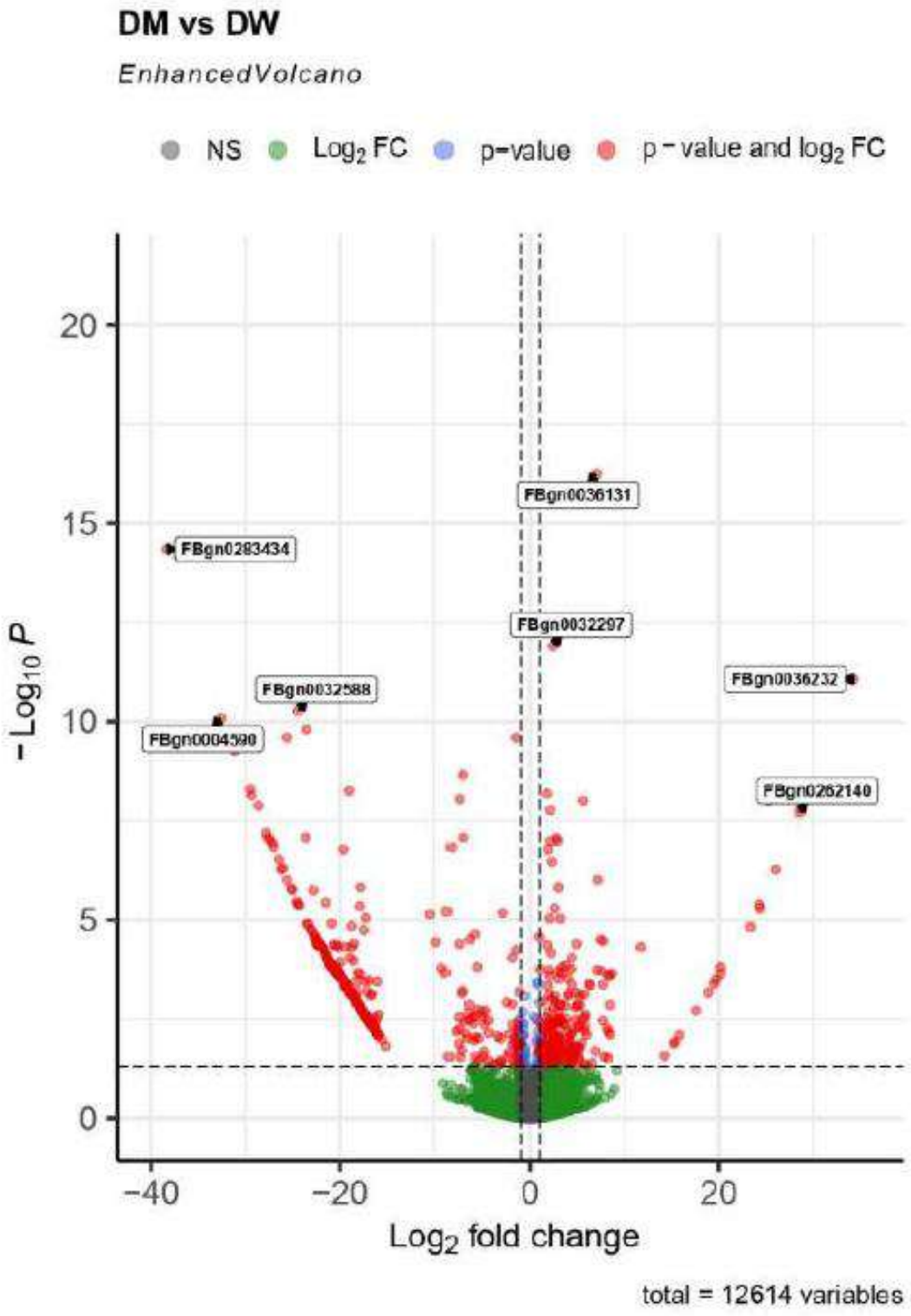

Figure 42: Volcano plot showing top DEGs for DM vs DW.

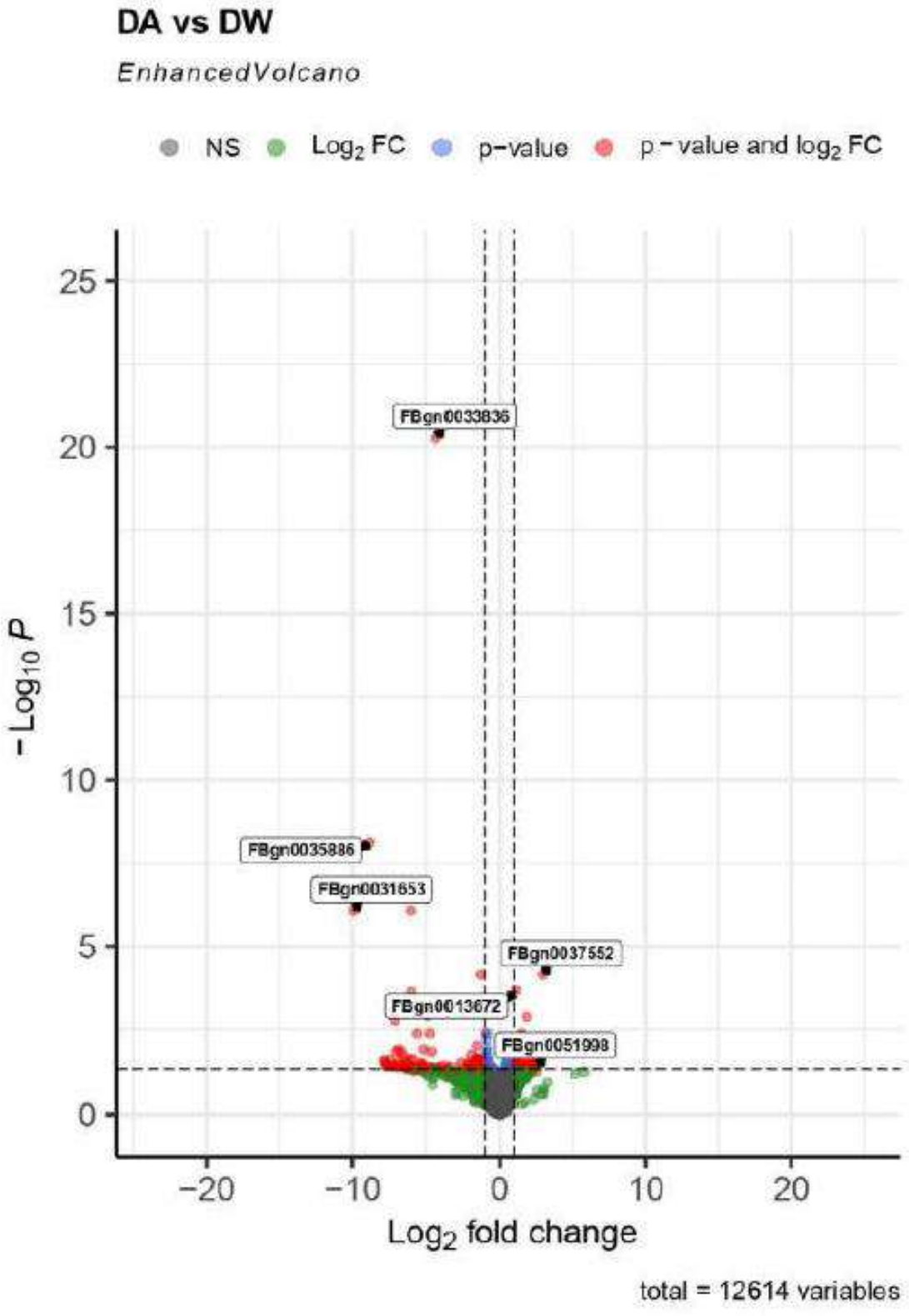

Figure 43: Volcano plot showing top DEGs for DA vs DW.

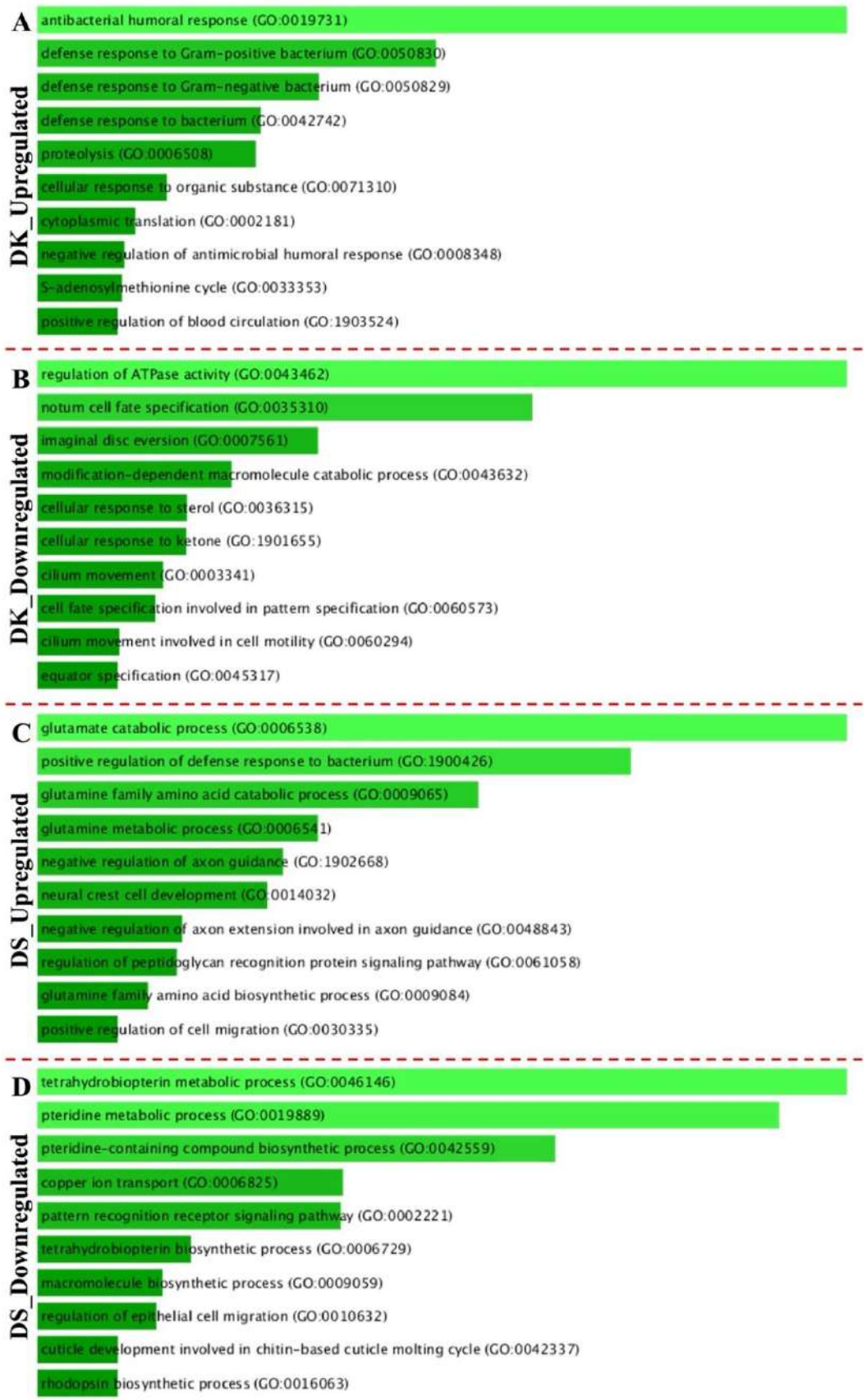

Figure 44: GO terms analysis of (A-B) *α-Kdh*^{RNAi} and (C-D) *Sdha*^{RNAi} (both upregulated and downregulated) (DS, *Sdha*^{RNAi}; DK, *A-Kdh*^{RNAi}).

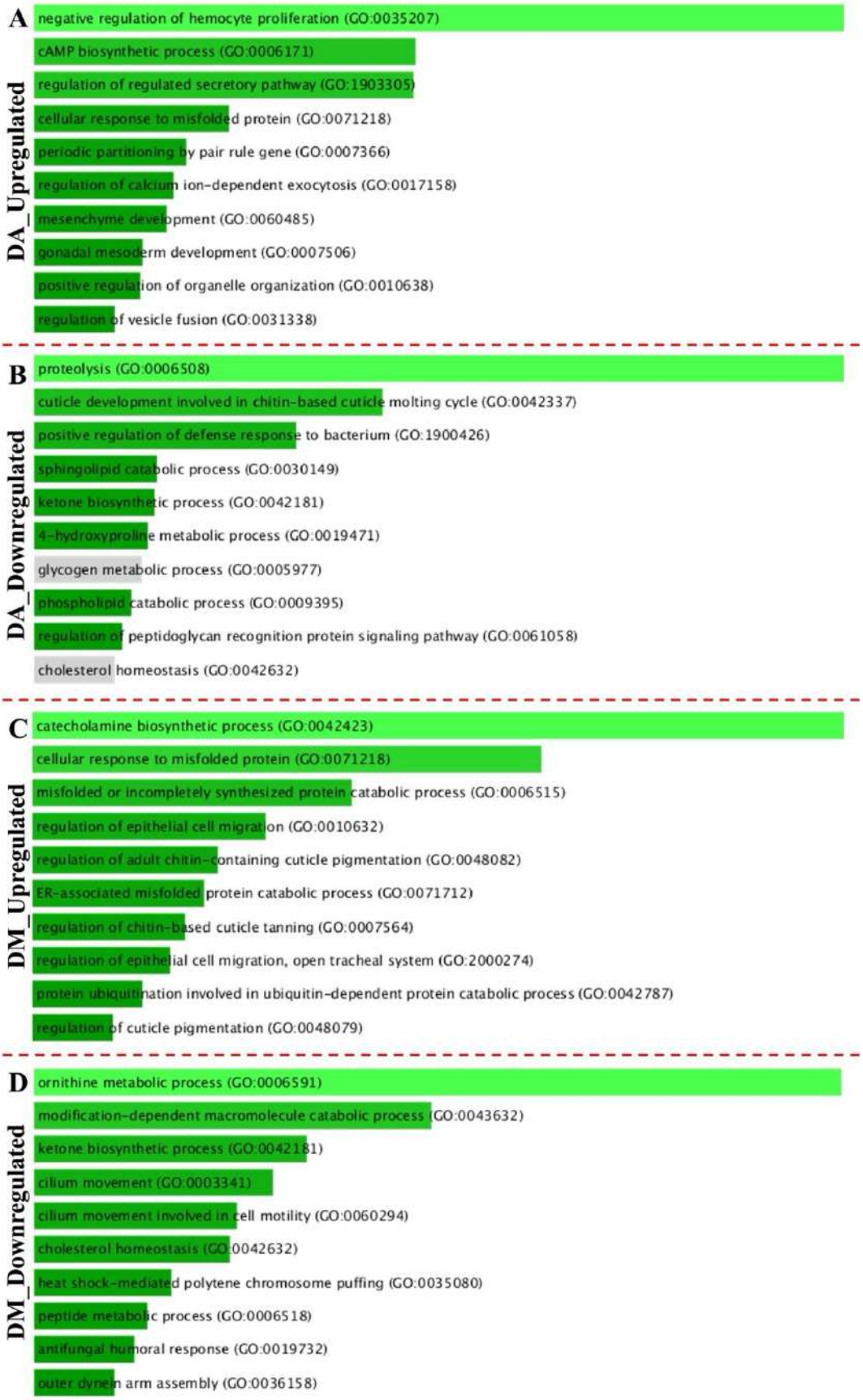

Figure 45: GO terms analysis of (A-B) *mAcon1*^{RNAi} and (C-D) *Mdh*^{RNAi} (both upregulated and downregulated) (DA, *mAcon1*^{RNAi}; DM, *Mdh*^{RNAi})

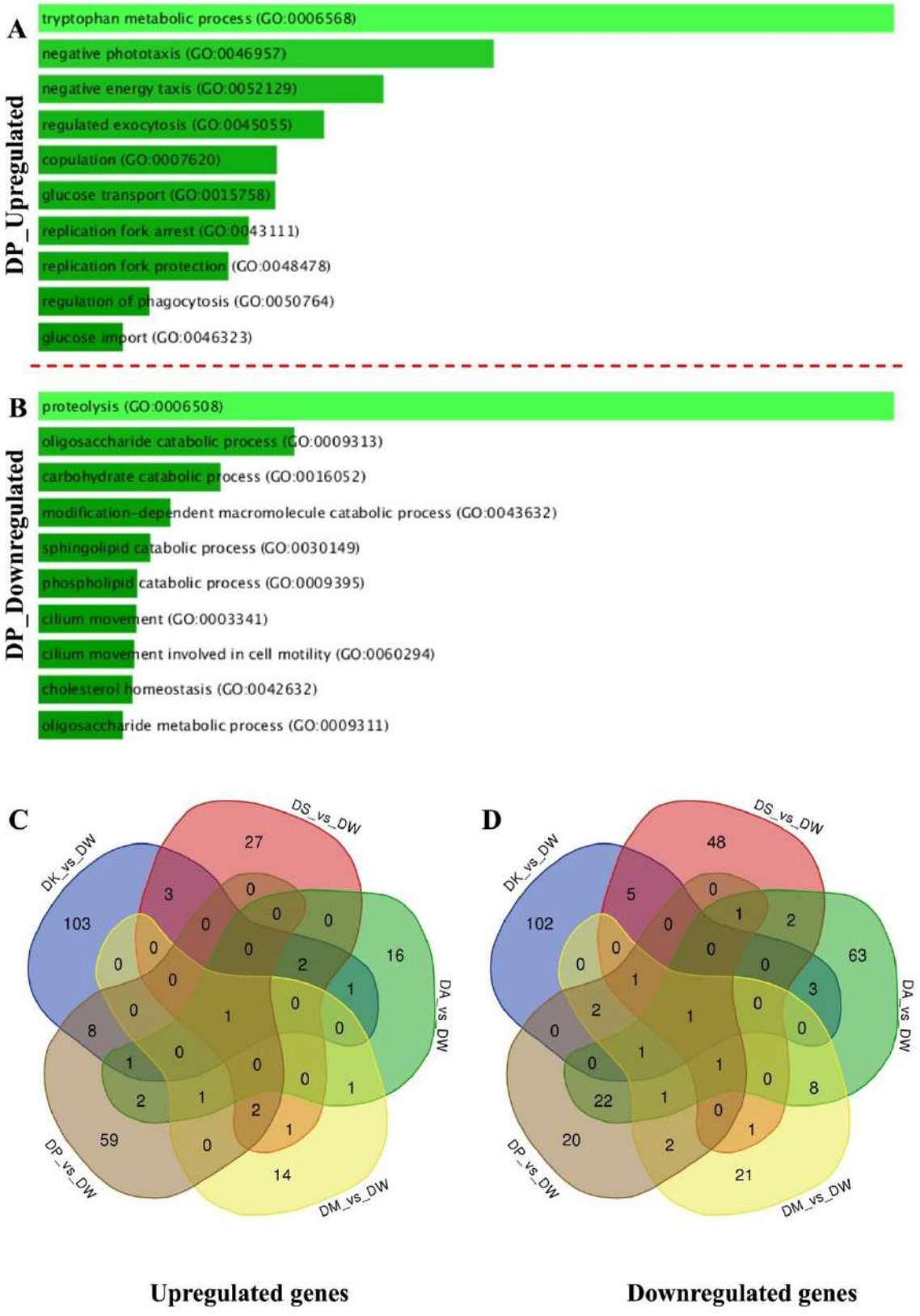

Figure 46: GO terms analysis of (A-B) *Pdha*^{RNAi} (both upregulated and downregulated) (DP, *Pdha*^{RNAi}), (C-D) Venn diagram representing overlap between all the mutants (Upregulated and downregulated).

6. Material and methods

6.1 *Drosophila* husbandry, stocks and genetiCS

All fly stocks were reared on corn meal agar medium with yeast supplementation at 25°C incubator unless specified. The crosses involving RNAi lines were maintained at 29ºC to maximize the efficacy of the *GAL4/UAS RNAi* system. Controls refers to either w1118 (wild type) or Gal4 drivers crossed with w1118. The following *Drosophila* stocks were received as gifts from Banerjee lab, UCLA, USA: w1118 (control), *dome*MESO-Gal4,UAS-GFP, *ChIZ-GAL4,* and *Tep4-GAL4,UASmcherry,* while *Hml⊿-Gal4, UAS-2xEGFP* (S. Sinenko lab). The RNAi stocks used in this study were obtained from Vienna *Drosophila* Resource Centre (VDRC) and Bloomington *Drosophila* Stock centre (BDSC), these stocks are:

Id numbers	Genes associated	Source
60900	CS^{RNAi}	BDSC
34028	$mAcon1^{RNAi}$	BDSC
41708, 56203	Idh^{RNAi}	BDSC
34101, 33686	α-Kdh^{RNAi}	BDSC
53255	Gdh^{RNAi}	BDSC
55168, 50939	$Skap^{RNAi}$	BDSC
v330053	$Sdha^{RNAi}$	VDRC
65195	Fum^{RNAi}	BDSC
62230, 62228, v101551	$Mdh2^{RNAi}$	BDSC, VDRC
55345	$Pdha^{RNAi}$	BDSC
v41576, v101551	Pcb^{RNAi}	VDRC

Table 4: Fly lines used in the study and their source.

6.2 Immunostaining and immunohistochemistry

For staining blood cell progenitors, 3rd instar larval lymph glands were dissected out in 1X PBS and fixed in 4% formaldehyde solution, for 15 min. Post-fixation the tissues were permeabilized by 3 washes of 15 min each in 0.3% PBST (0.3% Triton-X in 1X PBS). Tissues were then blocked in 5% NGS (Normal Goat Serum), followed by overnight primary antibody treatment. Next day tissues were washed (as earlier) and incubated in secondary antibody for 2-3 hours, followed by washing (as earlier) and mounting in mounting media.

Immunohistochemistry on lymph gland was performed with the following primary antibodies:

Antibody	Dilution	Source
mouse α-*P1*	1:30	I. Ando lab
rabbit α-*Pxn*	1:1000	J. Shim lab
mouse α-Myo	1:100	DSHB (CF.6G11)
rabbit α-*PPO*	1:200	H. M. Müller
rabbit α-pH3	1:100	*CS*T 3642S
rabbit α-Caspase 3	1:200	*CS*T 9661S
Hoechst-33342	1:4000	Thermo Fisher Scientific

Table 5: Antibodies used in the study and their source.

All the secondary antibodies were used at 1:500 dilutions, those are FITC, Cy3 and Cy5 (Jackson Immuno Research Laboratories) and Alexa Fluor 488, 546, 647 (Invitrogen). Samples were mounted in mounting media (Vectashield, Vector Laboratories).

6.3 Imaging and quantification of lymph gland phenotypes

Immuno-stained images of lymph glands were acquired using Olympus FV3000 confocal microscopy on 40X and 60X oil-immersion objective. Image was scanned with frame size of 800 X 800 with 0.5/1/2um thickness for Z-stack, depending upon the experiment.
All images were quantified using ImageJ software (NIH, USA). The details of the quantifications carried out are as under:

6.3.1 Lymph gland and Zone area analysis

Roughly, middle two confocal Z-stacks were merged and area was selected according to the respective stainings and measured with the help of freehand selection tool of ImageJ software, followed by using the "measure tool" under "analysis tool" to get the area values. This was done for respective zones, where *Tep4* or *Dome* area represents the progenitor zone, *Dome*/*Pxn* area represent differentiating or intermediary zone, *Pxn*/*P1* and Hml/*P1* area represent differentiated zone. The areas were represented in percent values with respect to the total area of the respective lobe. Controls were analysed in parallel to the tests every time. A minimum of 10-15 animals were analysed each time and the experiment was repeated at least three times. The quantifications represent the mean (% area) of the independent experimental sets.

6.3.2 Crystals cells, and Caspase 3^+ cells analysis

Crystal cell population, as well as Caspase 3^+ cells were analysed by counting total number of cell across the Z-stacks by merging all the stacks of lymph gland. These cell counts are represented as total number of cells per lymph gland lobe.

6.3.3 Total, *Dome*$^+$, and *Dome*$^-$ nuclei analysis

To count the total nuclei, we used the ImageJ software (NIH, USA). All the stacks of the lymph gland were merged with the help of "Z stack tool" and the primary lobe was outlined by the freehand selection tool, followed by "clear outside tool" under "edit option" to remove the other tissues (e.g. ring gland, secondary, tertiary lobes, dorsal vessel etc.). The nuclei of the remaining primary lobe were then thresholded using "threshold tool" under "Image-adjust option" to obtain 8-bit image in single channel. The image obtained is then subjected to "watershed tool" under "Process-Binary option" followed by "particle analysis" with particle size 3-infinity and circularity of 0.04-1.00. This gave the total number of particles (nuclei) which were marked by Hoechst dye, in blue channel. Similarly, for *Dome*+ nuclei only green channel was subjected to this mentioned processing and for the *Dome*- nuclei *Dome*+ nuclei were subtracted from total nuclei for the respective lobes.

6.3.4 Mitotic index for *Dome*$^+$ and *Dome*$^-$ population

Total pH3+ cells were counted by merging all the Z-stack together to get total number of pH3+ cells in the entire lobe. For assessing $pH3^+$ population in *Dome*$^+$ zone, *domeGFP* channel was overlaid onto pH3 channel and for the *Dome*$^-$ $pH3^+$ cells *Dome*$^+$ $pH3^+$ cells were subtracted from total $pH3^+$ cells. For calculating mitotic index $pH3^+$ cells were divided by total number of cells per LG lobe and same is done for *Dome*$^+$ and *Dome*$^-$ mitotic index.

6.4 SABER FISH

Reagents: Quick-load 100bp DNA ladder (N0467S; NEB), SYBR Gold Nucleic Acid Gel Stain (S11494; Invitrogen), Bst DNA Polymerase, Large fragment (M0275L; NEB), Deoxynucleotide (dNTP) Solution set (N0446S; NEB), Formamide (AM9342; Invitrogen), Triton X-100 (T8787-50ML; Sigma Aldrich), Dextran sulfate sodium (D8906-10G; Sigma Aldrich), TWEEN® 20 (P9416-50ML; Sigma Aldrich), Propyl gallate (P3130-100G; Sigma Aldrich), Magnesium Sulfate (MgSO4) Solution (B1003S; NEB), UltraPure DNase/RNase-Free Distilled Water, PBS - Phosphate-Buffered Saline (10X) pH 7.4, RNase-free (AM9624; Invitrogen), UltraPure SSC, 20X (15557044; Invitrogen).

The protocol was adapted from Kishi and coworkers, with slight modification wherever needed according to the *Drosophila* tissue (211). The protocol is as under:

DAY1

Setting up of PER reaction

Add all the reagents to the tube, EXCEPT for probes/primers and keep the tube at 37°C for enzyme activation for 15min

Add specific probes to the tubes and incubate for 2h/3h depending upon the hairpin in use

Terminate the reaction at 80°C for 20min and then the extended probes can be stored at 4°C for years

Confirm the extension by 1% agarose gel

DAY2

Dissected the LG of 48h, 72h and 96h in PBS in NUNC 4 well dish

Fixed the tissues with 4% PFA (Formaldehyde does not work very well in this protocol) for 15 min at room temperature (RT)

Tissue permeabilization: 0.3% PBST (Triton X) was for 15 min at RT

Washing: 0.1% PBSTw (Tween-20) (3 X 5min at RT)

Primary Hybridisation: previous day prepared/extended probes along with hybridisation solution, in a humid chamber for overnight (16h) at 45°C

DAY3

Wash with Tissue wash buffer-A (40% Formamide) (2 X 30min at 37°C)

Wash with Tissue wash buffer-B (25% Formamide) (2 X 45min at 37°C)

Wash with 2X SSCT buffer (2 X 15min at 37°C)

Developing: Add Hybridisation solution-2 (fluorophores) and incubate for 2-3h at 37°C

Wash with PBSTw (3 X 15 min at 37°C)

Mount the samples in vectasheild and image.

NOTE:

1) activation of enzyme without probes is crucial, otherwise there will be problems with extension

2) Imagers/fluorophores works at the 0.2um concentration for tissues too

3) Imaging can be done at confocal microscope also it does not bleach the sample that quick

Following are the reagents (primers, hairpins and imagers) used in the SABER FISH study:

Table 6: Primers for Hml

S.no.	start	stop	sequence+p40 (Hml)
1	13858049	13858078	CATATGCCGTGCTGGTTACACTCCTTGGCA-TTT-A-**atcctacaa-A-atcctacaa**
2	13858079	13858109	GGGACACAGTTGCGGTCTTCTCCAATTGGTG-**TTT-A-atcctacaa-A-atcctacaa**
3	13858357	13858392	TGCACTTATCCTTCTTCCATTTCTCGTCAGGCAAGT-**TTT-A-atcctacaa-A-atcctacaa**
4	13858398	13858434	CCACACACGTGGTCTTTCCTTTAGAATCACACTGACA-**TTT-A-atcctacaa-A-atcctacaa**
5	13858143	13858173	TGATGGTATCGCAATTCTTAGCACAGCCGCA-**TTT-A-atcctacaa-A-atcctacaa**
6	13858435	13858468	GCGCAGATATTTTCCTCCACCTGGCACTTCTTTT-**TTT-A-atcctacaa-A-atcctacaa**
7	13858228	13858264	CGCTCCGAACTCAAACACATTTCATCAGTCTTAACGG-**TTT-A-atcctacaa-A-atcctacaa**
8	13858469	13858502	CACGCTGACTATGGTCTCAGGTCTATAGCCTTCG-**TTT-A-atcctacaa-A-atcctacaa**
9	13858265	13858294	TTTCCAGGAGGACAGAAGCAGCCCTCGAAT-**TTT-A-atcctacaa-A-atcctacaa**
10	13858539	13858568	AGCAAGGCACAGTTTGGATGGGTCCTTCGT-**TTT-A-atcctacaa-A-atcctacaa**
11	13859000	13859036	TGAACTTTGTGGCTTCGTCGAGCTCATACTGAACAAT-**TTT-A-atcctacaa-A-atcctacaa**
12	13858569	13858598	TTGTCCAGGACCGCAAATGGGCACTAGAGG-**TTT-A-atcctacaa-A-atcctacaa**
13	13858729	13858760	CCTGGAAGCAGCTCCCGCAGCTCAATTATTTC-**TTT-A-atcctacaa-A-atcctacaa**
14	13859068	13859099	AGGAACATGTCTCCTGCTTGCAAACCTCCTTG-**TTT-A-atcctacaa-A-atcctacaa**
15	13859100	13859129	TGACAACCTGGGCATTGCCATCCGGACCAT-**TTT-A-atcctacaa-A-atcctacaa**
16	13859130	13859160	GCGCAGTCAGTGAGACACTGTTCCAAAGTGC-**TTT-A-atcctacaa-A-atcctacaa**
17	13859494	13859523	CGACTCGGCCAAGGAAACGGGTAAACAAGA-**TTT-A-atcctacaa-A-atcctacaa**
18	13859195	13859225	ACGAAGTCTGGACACACTTGCCACAGCATTT-**TTT-A-atcctacaa-A-atcctacaa**
19	13859239	13859274	GCCGACTTCCAAAGTGCGTTGACTTCGTATAGTTTT-**TTT-A-atcctacaa-A-atcctacaa**
20	13859275	13859310	TCCTTCTTCAGGCAACTGTAGGTAGTGCAATTGTCC-**TTT-A-atcctacaa-A-atcctacaa**
21	13859595	13859624	GAGGAGCAGGCACCCTCGCAGTCGGTGAAG-**TTT-A-atcctacaa-A-atcctacaa**
22	13859319	13859354	CATCCGGACATACTTCTCTCGAGGTGGTAACCAAAA-**TTT-A-atcctacaa-A-atcctacaa**
23	13859355	13859385	TGGTACAACAGGTGGGATAGGCAACTACCCA-**TTT-A-atcctacaa-A-atcctacaa**
24	13859673	13859709	CACGGAAATCGGATGATAGGATTTTATGCTGCAGCAA-**TTT-A-atcctacaa-A-atcctacaa**
25	13859854	13859884	CCTGCTGCATTCGCACATCGATTGCAGAGTC-**TTT-A-atcctacaa-A-atcctacaa**
26	13855419	13855448	TTATGGCCACCAAGCACACAGACGCAATCC-**TTT-A-atcctacaa-A-atcctacaa**
27	13859885	13859916	GCCGAGTAATTGGAGTAGTGGAGACTGCGCAT-**TTT-A-atcctacaa-A-atcctacaa**
28	13855479	13855509	GGTAATCACTGGACGCAATTTACCGCCCAGA-**TTT-A-atcctacaa-A-atcctacaa**
29	13846081	13846117	CACTGCCAAGCTGTTAGTCCTGTTTAAAATCCAGCTT-**TTT-A-atcctacaa-A-atcctacaa**
30	13855510	13855541	GGACAAGGTTCGCACTTACAGAAACAGTCGCT-**TTT-A-atcctacaa-A-atcctacaa**
31	13855576	13855612	CCTGAACACCATTGCACCACAGAATTTCGGGTATACA-**TTT-A-atcctacaa-A-atcctacaa**
32	13855645	13855675	GGCTGACGTCCGGCTCAACAGTGAATGAATC-**TTT-A-atcctacaa-A-atcctacaa**
33	13855825	13855861	ACACCTGCTTCGAGAAGGTGAACATCTTTGACATCTT-**TTT-A-atcctacaa-A-atcctacaa**
34	13847308	13847337	GACTGAACATTGGACGGCAGTTGGAGGGCT-**TTT-A-atcctacaa-A-atcctacaa**
35	13855898	13855934	GGCATAGCCAGAATTTGTTCCTTGGACGAGATGAACT-**TTT-A-atcctacaa-A-atcctacaa**
36	13847372	13847405	CTGAAACGTCCTGTGCGAAACTATAGCCAGTTGG-**TTT-A-atcctacaa-A-atcctacaa**
37	13855968	13855998	GGGAATGGGCACACAAGTGAACTCATCGCAC-**TTT-A-atcctacaa-A-atcctacaa**
38	13856049	13856085	CGCACTCATGTCCAATTCCACATCGTATTTCTCAGGA-**TTT-A-atcctacaa-A-atcctacaa**
39	13847469	13847499	CATGGAGGTGTACATTGTGCCTGACAGGGTG-**TTT-A-atcctacaa-A-atcctacaa**
40	13856153	13856189	ACAGTTCCATCAAAGGTGGTAAAACTCTTGCCACTGA-**TTT-A-atcctacaa-A-atcctacaa**
41	13856190	13856221	CCAGGATGTGGCTGCAAGGTCCGTATTTGAAA-**TTT-A-atcctacaa-A-atcctacaa**

42	13856378	13856408	GGATCAACTCATTGCCAGCCTCGGTGTCTTG-**TTT-A-atcctacaa-A-atcctacaa**
43	13847905	13847941	ACTGACAGACATTGAAACTAATGCACTGACCTCCGTT-**TTT-A-atcctacaa-A-atcctacaa**
44	13856423	13856459	GCTGCACTGTGAACTCATAGCCATTAAACTTGAGCTT-**TTT-A-atcctacaa-A-atcctacaa**
45	13856463	13856499	ACAACGAATGAAGCCTTGCAAATGGGCGAATTTATCA-**TTT-A-atcctacaa-A-atcctacaa**
46	13856507	13856541	TATTTGGTGGACACGGCCAGAAGAGTCTTGCCCGG-**TTT-A-atcctacaa-A-atcctacaa**
47	13848221	13848257	GGGCAGGCAGATATTGTCCTTGCAGATAGTTACACTT-**TTT-A-atcctacaa-A-atcctacaa**
48	13856575	13856611	TGTGCGAATAAACTTGGATGATATGCCCACTTTGACG-**TTT-A-atcctacaa-A-atcctacaa**
49	13856638	13856674	ACCATCTGGTGATCTCTTGTCATCCTTTTGGTTTCCA-**TTT-A-atcctacaa-A-atcctacaa**
50	13848507	13848543	CCAGATCCCGATATTTTGCGAGCAGAGCAAGTAGTTT-**TTT-A-atcctacaa-A-atcctacaa**
51	13856681	13856714	ACCAACTGTCGCCGAACTTTTCGGTATTTGGAAT-**TTT-A-atcctacaa-A-atcctacaa**
52	13848667	13848703	TGGGGTTTTGTCGATGACGATATCCAAATTGTTGCTC-**TTT-A-atcctacaa-A-atcctacaa**
53	13848704	13848733	ACCACCCCAAGTGGTGCAAAGTGCTGGTCG-**TTT-A-atcctacaa-A-atcctacaa**
54	13856908	13856944	GCAGCTTCGAGGCAGTAATTGTTAAGGAATTGCTTGT-**TTT-A-atcctacaa-A-atcctacaa**
55	13848879	13848915	AGCCATAAGGACAAGCCTTCAGGATAATGTCGAATGT-**TTT-A-atcctacaa-A-atcctacaa**
56	13857034	13857070	GCCACAGCTCTCCATGTAGTCAATTGAACTAGTGGAT-**TTT-A-atcctacaa-A-atcctacaa**
57	13849202	13849231	TTTTCCCCACATTTGGGGTCCCGCCTGCAC-**TTT-A-atcctacaa-A-atcctacaa**
58	13857170	13857199	CATCCCGGGAAGCAGGCATCCGGAAGTACT-**TTT-A-atcctacaa-A-atcctacaa**
59	13849296	13849325	CTGCGAAGGCCTTGACCGTGGCCAACTTTT-**TTT-A-atcctacaa-A-atcctacaa**
60	13857357	13857387	GGAATGTGTGGACACCAGGGAGGACGACATC-**TTT-A-atcctacaa-A-atcctacaa**

Table 7: Primers for *Dome*

S.no.	start	stop	sequence+p38 (*Dome*)
1	19676446	19676482	CGGCTGAAGATGAGTTGATGAATTATCGATGCGAACG-**TTT-A-aacatacta-A-aacatacta**
2	19676516	19676550	TAAATGATGAGCGCTCCGGTATCTTAGAGGACGTG-**TTT-A-aacatacta-A-aacatacta**
3	19676670	19676699	CCACGGTGGCGGCCAGAGGTGGCTTTATCA-**TTT-A-aacatacta-A-aacatacta**
4	19676970	19676999	CGGAAGGTACTGCTGGCGACCCAAACGGTT-**TTT-A-aacatacta-A-aacatacta**
5	19677000	19677030	GAACTGGAGCCGGATTGAACCGAGATTGTGG-**TTT-A-aacatacta-A-aacatacta**
6	19677098	19677134	GCAGTCGAAGGAACTGAGAACGTGTGATCATTATCCG-**TTT-A-aacatacta-A-aacatacta**
7	19677137	19677166	GGACCGTTGCCGCCCCAGCTCTTCATCTGT-**TTT-A-aacatacta-A-aacatacta**
8	19677351	19677382	TTGGCCCTGTCTCGTGATTGTCATCGTATCCA-**TTT-A-aacatacta-A-aacatacta**
9	19677439	19677468	CGAGCTCTCACTGCCGCAGCTACTGAAGTC-**TTT-A-aacatacta-A-aacatacta**
10	19677563	19677592	CCCAGGCCACCCATGTCTATGGGCTTCTTC-**TTT-A-aacatacta-A-aacatacta**
11	19677593	19677622	ATGGTCTCCATGATTCCCTGCGGCAGCACT-**TTT-A-aacatacta-A-aacatacta**
12	19677625	19677661	ACCGATATCGGACATCTTGCGGTATTTCTTGTACACG-**TTT-A-aacatacta-A-aacatacta**
13	19677724	19677753	CTTCACGCTGTGCGTGTCCGGTGTACAGAT-**TTT-A-aacatacta-A-aacatacta**
14	19677858	19677889	GTGCCTCGCATCCCTTGCCGTTGGTCGACATA-**TTT-A-aacatacta-A-aacatacta**
15	19677892	19677921	CAAAACGGCACCTTCCGCTGCATCCGCTCC-**TTT-A-aacatacta-A-aacatacta**
16	19678109	19678138	CTTGGCGGTTCCCAGTCGAGACGTGAGCTC-**TTT-A-aacatacta-A-aacatacta**
17	19678139	19678172	TGATCCGGATTGTTGATCACGTACAGTTGTGGCG-**TTT-A-aacatacta-A-aacatacta**
18	19678340	19678370	GTACTTGGTGAATGCGGTGAGATTGCCCAGC-**TTT-A-aacatacta-A-aacatacta**
19	19678585	19678614	CGGTGCGGTTGACCAGCTCGTCGCTGTACT-**TTT-A-aacatacta-A-aacatacta**
20	19678615	19678644	TGCTGACCCGCGAGTCCGAATACATCAGCA-**TTT-A-aacatacta-A-aacatacta**
21	19678645	19678674	TCTTGACACTGTAGTCCGTGTAGGGCACCA-**TTT-A-aacatacta-A-aacatacta**

22	19678826	19678855	GCTGGTGGCCACATCGATCGACGGCTCCAT-**TTT-A-aacatacta-A-aacatacta**
23	19678856	19678887	CTTGGCCAAATCGTCCTTCTTGTCGCTACTGC-**TTT-A-aacatacta-A-aacatacta**
24	19678888	19678917	AGATCGCCCAGTGTAGGCCCGTATTATGCG-**TTT-A-aacatacta-A-aacatacta**
25	19678948	19678977	GCGTGAGCAGTTGGTCCGGTGACGTGGTGA-**TTT-A-aacatacta-A-aacatacta**
26	19679124	19679157	TTGTTGGTCGGATGATAGACGCTGCGTATGTTCC-**TTT-A-aacatacta-A-aacatacta**
27	19678371	19678400	CGGTAGGTGATGGGCTTCTCGTTGTTCACC-**TTT-A-aacatacta-A-aacatacta**
28	19678675	19678710	GATTCTGGATGACGTGCTTGTTCGTATAGCGATCGA-**TTT-A-aacatacta-A-aacatacta**
29	19678310	19678339	ATAGACGGTCCGCGCACGCACGCTAATCTC-**TTT-A-aacatacta-A-aacatacta**
30	19679042	19679071	CGGCTTGGGCACGCACCAGAAAACGGTGTA-**TTT-A-aacatacta-A-aacatacta**
31	19677754	19677787	GAATCCGTAGATGCCCCAATCGGATCTGTAGAGC-**TTT-A-aacatacta-A-aacatacta**
32	19676802	19676831	GTGGCGAAGTTGCTGGCGAAGATCCCGCAA-**TTT-A-aacatacta-A-aacatacta**
33	19678791	19678820	CAGACGCGCTCCGACCAACTGACCGTCAGT-**TTT-A-aacatacta-A-aacatacta**
34	19679220	19679249	ACAGACAGACCCTGGCTATTGCTGCTGCGG-**TTT-A-aacatacta-A-aacatacta**
35	19676206	19676242	TATTGCGTTACAAATACTTTCTGCCTCACACGCATCG-**TTT-A-aacatacta-A-aacatacta**
36	19683457	19683486	CCCCGCTCGCGATGCTGACGATATATGTTG-**TTT-A-aacatacta-A-aacatacta**
37	19677922	19677951	GTTCAACTGCGGATGCTGCTCCACGTTGAT-**TTT-A-aacatacta-A-aacatacta**
38	19682144	19682173	CAGCTGGGCCGCGTGATGGGCTCAAAGTTT-**TTT-A-aacatacta-A-aacatacta**
39	19678079	19678108	TCGTAGAAATCAATGCGTCCGGCCGGCGTC-**TTT-A-aacatacta-A-aacatacta**
40	19677500	19677529	GAGTCGTCCACCCGTGTGCACACGATGCCT-**TTT-A-aacatacta-A-aacatacta**
41	19682725	19682754	GATGTGCTTGGAATCGCGGTAGACGCGGCC-**TTT-A-aacatacta-A-aacatacta**
42	19682062	19682091	CACCCGGAGCGTGTAGTTGTAGCCGGCGAA-**TTT-A-aacatacta-A-aacatacta**
43	19676892	19676921	CCGAGGCCTGCACGTAGTTGTCCATGTTGA-**TTT-A-aacatacta-A-aacatacta**
44	19679250	19679280	ATGAGGAAGTGATGGACGGCACTCATGCTCC-**TTT-A-aacatacta-A-aacatacta**
45	19676551	19676580	CCGATTGTGGGCCATGGCGTTCAGATCCTG-**TTT-A-aacatacta-A-aacatacta**
46	19677409	19677438	AGAGGAGGACGCTGTGCGCAGCAGCAGTTT-**TTT-A-aacatacta-A-aacatacta**
47	19682335	19682364	CTGCGTCTCGTGGCCCAGGGCATTGGAGAT-**TTT-A-aacatacta-A-aacatacta**
48	19677068	19677097	GACAGCGGCTGGGACATCGGAGCGGTCATT-**TTT-A-aacatacta-A-aacatacta**
49	19682926	19682955	GGCAAGCAGCATGAGCAGCAGGACGAGCTG-**TTT-A-aacatacta-A-aacatacta**
50	19677693	19677723	CCACGGTCACCTCAATGGTCTGGTACATGGC-**TTT-A-aacatacta-A-aacatacta**
51	19678740	19678769	CCGGCCGAGCGCTGGCAGTAGGTCAGATTA-**TTT-A-aacatacta-A-aacatacta**
52	19676700	19676729	GCCCAGTGAGCTGCAACTGCTCCATGGTGG-**TTT-A-aacatacta-A-aacatacta**
53	19683487	19683516	TCGACGAGTTGCTTGTCCGCAGTGTGACCG-**TTT-A-aacatacta-A-aacatacta**

Table 8: Primers for Kdh

S.no.	start	stop	sequence+p28 (Kdh)
1	16964040	16964069	AAGTGGCCTTGTCGACCAGCTGGTGGTGCA-**TTT-A-caacttaac-A-caacttaac**
2	16962834	16962865	GCGAACTGGGTGAAGATCTGGTTCAAGGGCTT-**TTT-A-caacttaac-A-caacttaac**
3	16962996	16963027	CGACAGCCAGGCGGATGTTCTTGTTTGTAACG-**TTT-A-caacttaac-A-caacttaac**
4	16963541	16963570	CGGTGACAGTGCCCTCGGCGATCAGTTTGT-**TTT-A-caacttaac-A-caacttaac**
5	16963444	16963473	GGGCTCGTCGATCTCGTTGTGTCCATTGCG-**TTT-A-caacttaac-A-caacttaac**
6	16962358	16962387	TCCGATGAAGGTAGTGCTGGGCAGCTTGAA-**TTT-A-caacttaac-A-caacttaac**
7	16963509	16963540	CGGCATACAGGTCGAGACAGTTCTTGTGCTTG-**TTT-A-caacttaac-A-caacttaac**
8	16964132	16964161	GTGCTCGAAACCAAGCACTGCGTACTCCGA-**TTT-A-caacttaac-A-caacttaac**

9	16963158	16963189	GCATAGTTTCATAGACGACGCCCTGTCCGCAG-**TTT-A-caacttaac-A-caacttaac**
10	16964193	16964222	TGAAGTCTCCGAACTGAGCCTCCCACAGCA-**TTT-A-caacttaac-A-caacttaac**
11	16964602	16964631	TTGTCGGGGATGATGCGCTGGAACTCGCTG-**TTT-A-caacttaac-A-caacttaac**
12	16964253	16964282	GCACCCACTTTGACTGACCGCTGGAGATGA-**TTT-A-caacttaac-A-caacttaac**
13	16964223	16964252	ACTGATCGATGATCGACTGGGCCGTGTTGC-**TTT-A-caacttaac-A-caacttaac**
14	16962513	16962549	CCAGAGAGTTGATGAACATGAACTCCACGCCAATCTT-**TTT-A-caacttaac-A-caacttaac**
15	16962585	16962614	CTCCTCGGGCGAGAAGTTAAGGACGCCGGG-**TTT-A-caacttaac-A-caacttaac**
16	16963604	16963633	CCAGAGCGAATGCCTCCTCGCAAATGTTCT-**TTT-A-caacttaac-A-caacttaac**
17	16962645	16962674	CTTGGCCAGGAAAGCCTCAAAGCCGGTGGC-**TTT-A-caacttaac-A-caacttaac**
18	16963691	16963722	CGCTACCTTCAATGGGTCTTTGCCCTCGAAAA-**TTT-A-caacttaac-A-caacttaac**
19	16962550	16962579	CAAAACGCTTGCGGATCCAGTTGCATTGCT-**TTT-A-caacttaac-A-caacttaac**
20	16959105	16959141	GGCTGTGTGGGCTCTATGCATTTTGTAGCTTTACAAA-**TTT-A-caacttaac-A-caacttaac**
21	16962615	16962644	ACGGGTCAAACGGGCCAGGATCAGACGCTT-**TTT-A-caacttaac-A-caacttaac**
22	16964635	16964664	TTCACATTGCTGGGATTCTGGCCGGCGGGA-**TTT-A-caacttaac-A-caacttaac**
23	16962675	16962709	CCCTCCAGACCGAAACGTTTCTCAGAAGAGTACTT-**TTT-A-caacttaac-A-caacttaac**
24	16967946	16967982	GGGTGTCAAAACTTCGCGTGGCTTGAGATAGTTTAGT-**TTT-A-caacttaac-A-caacttaac**
25	16964940	16964969	CGGCTGTGGTTCAAGGCGGTGAGGAAACGA-**TTT-A-caacttaac-A-caacttaac**
26	16963890	16963919	CCTTTTCGTCCACCATTGCCTTGCGAGCGG-**TTT-A-caacttaac-A-caacttaac**
27	16968077	16968113	GGTGATGAACTTAAGCACAGCTCTGTTTGGTTTGTCA-**TTT-A-caacttaac-A-caacttaac**
28	16964665	16964694	TAGACGCGGCCCGAGCAGAAGACGACCTTC-**TTT-A-caacttaac-A-caacttaac**
29	16968156	16968192	TCGTAATCAAAGCTTCCAGTCCAATTTACTGGGGAGT-**TTT-A-caacttaac-A-caacttaac**
30	16968242	16968278	GCTGCATTTTGATGCGCTCCATAAAGGGTATCCAAAA-**TTT-A-caacttaac-A-caacttaac**
31	16959848	16959877	CTCCTGATGATGGCCTGGACGGCCAGATGG-**TTT-A-caacttaac-A-caacttaac**
32	16963310	16963344	GTTGACGTGGAAAATAGGAGCATTGACGACACGAG-**TTT-A-caacttaac-A-caacttaac**
33	16964437	16964468	TCGAGCAGTTTGCCACGATCCAGTTAATGTCG-**TTT-A-caacttaac-A-caacttaac**
34	16964880	16964909	TTGTGCTCCTCTTGGGCCCACACGAGTTCG-**TTT-A-caacttaac-A-caacttaac**
35	16962740	16962772	TCCACTCCCAACTCCGTTGATACGTCGATGATC-**TTT-A-caacttaac-A-caacttaac**
36	16959725	16959754	AAGTTGGGCGGGCTAACGTAGCTGTTGCTG-**TTT-A-caacttaac-A-caacttaac**
37	16963375	16963404	AGTAGCACGCCACTCAGCAGCCACCTTGCA-**TTT-A-caacttaac-A-caacttaac**
38	16962803	16962833	GCGGCATACATTGGCCAAGGTGTTAAGACGT-**TTT-A-caacttaac-A-caacttaac**
39	16967810	16967846	TGCGAGTTCTCATCACTTCAAATGTATGCGCATAGGT-**TTT-A-caacttaac-A-caacttaac**
40	16963407	16963443	GCGGTATCCGACCAAATCAATAACACAATCCTTGTGGc-**TTT-A-caacttaac-A-caacttaac**
41	16963767	16963796	TCAGCAGCGTTCGGTGGTGGCGACGAGAAG-**TTT-A-caacttaac-A-caacttaac**
42	16968296	16968327	GGTCCTGATTGGACTCCGTCCGTGGATCAAAA-**TTT-A-caacttaac-A-caacttaac**
43	16964501	16964530	CAGGGGCTTGCGGAAAGGCAATGCGATCTG-**TTT-A-caacttaac-A-caacttaac**
44	16964471	16964500	TCGGCGCAGGATGTGGTAGTAGTTGGCGGG-**TTT-A-caacttaac-A-caacttaac**
45	16963950	16963979	GGATTCCCTCCTTCAGCAGAGAGCCGAAGG-**TTT-A-caacttaac-A-caacttaac**
46	16964732	16964761	CTCCACGCGCACAATGGCGATTTCGCCCTC-**TTT-A-caacttaac-A-caacttaac**
47	16963030	16963059	ATCCACAGCCTCCAGATGGGACGGGTTGGC-**TTT-A-caacttaac-A-caacttaac**
48	16959768	16959797	GTTGAAGGCGGTCAGCGGCAGAGTGTTGGC-**TTT-A-caacttaac-A-caacttaac**
49	16963571	16963603	CGTATTTAGCGGCAACCGACTTAACCTCCTCGG-**TTT-A-caacttaac-A-caacttaac**
50	16963920	16963949	CCATGGCCTCTCCCAAAGCCCAATCAGCGA-**TTT-A-caacttaac-A-caacttaac**
51	16964070	16964099	GATCTGGGTACATGTGCTGCAGCGAGTTGT-**TTT-A-caacttaac-A-caacttaac**
52	16963474	16963508	CGGATCTTCTGGTACATCAAGGGTTGCGTGAACAT-**TTT-A-caacttaac-A-caacttaac**
53	16964283	16964312	GGGGCAGGAGCATTACCAGACCCGATTGGC-**TTT-A-caacttaac-A-caacttaac**

54	16968610	16968644	TCAGGGCTGTTGACAACTCATTTTGCCTTGTGTAA-**TTT-A-caacttaac-A-caacttaac**
55	16959354	16959383	CATCTCCTCCACGTAGGAGGCGGTGCTGCC-**TTT-A-caacttaac-A-caacttaac**
56	16964010	16964039	GCACATGGTGGCGATGCGAGAAGGTACCAC-**TTT-A-caacttaac-A-caacttaac**
57	16959178	16959207	GCTGCTGCTCTTGAGCAGCCATGTGGCGAA-**TTT-A-caacttaac-A-caacttaac**
58	16963190	16963219	GGGTGGTGTAGTCGGGCAGGTCCGAAAGAT-**TTT-A-caacttaac-A-caacttaac**
59	16967415	16967444	TCACGGATGTGCTGGGCCTTGGATCCGGTG-**TTT-A-caacttaac-A-caacttaac**
60	16963068	16963097	TAGAACTGCTCGGCACGGGTCTTGCCCTGC-**TTT-A-caacttaac-A-caacttaac**

Table 9: Primers for *Sdha*

S.no.	start	stop	sequence+p29 (*Sdha*)
1	19395734	19395763	TTCCGGACATGTTTGGCTGGGCTGTGAGGT-**TTT-A-tctaaaatc-A-tctaaaatc**
2	19394384	19394413	CTGCTGGCGGCCGTGTGTGATGTGGTAACT-**TTT-A-tctaaaatc-A-tctaaaatc**
3	19394294	19394323	GGCTCCTCCTGCTCCCACGACGATCGCATC-**TTT-A-tctaaaatc-A-tctaaaatc**
4	19393107	19393136	CATGCACGTCCGAAGACCACCAGATCCAGC-**TTT-A-tctaaaatc-A-tctaaaatc**
5	19394045	19394074	GTTCTCCAGCTCAATGACAGCCTTGGGCGC-**TTT-A-tctaaaatc-A-tctaaaatc**
6	19393331	19393360	AACACCGGCGAAGATCATGGCGGTCTCGGA-**TTT-A-tctaaaatc-A-tctaaaatc**
7	19393382	19393411	GAGCTGCTTGGGCGGCAAGTGGTGCAGTTG-**TTT-A-tctaaaatc-A-tctaaaatc**
8	19392436	19392467	TCGTTGTCCAGCGTGGTATCGATCACGTTTCT-**TTT-A-tctaaaatc-A-tctaaaatc**
9	19395802	19395834	AGGTTTTACGCGCTTGTAAGATGGGGTGTTTGG-**TTT-A-tctaaaatc-A-tctaaaatc**
10	19395904	19395940	TACAAACTTTCAAATGTTGTGTGTGAACTGCCGCTCG-**TTT-A-tctaaaatc-A-tctaaaatc**
11	19393611	19393641	ATGCCAGTAGGATGGAACTGCACGAACTCCA-**TTT-A-tctaaaatc-A-tctaaaatc**
12	19392537	19392566	CATGGGCTTCTTCTGCTGACCATCCAGGGG-**TTT-A-tctaaaatc-A-tctaaaatc**
13	19393202	19393231	CAGTCCCGGCACAATCACATCCTTGCCATC-**TTT-A-tctaaaatc-A-tctaaaatc**
14	19392687	19392716	CGATTCCTTGCGCGCCTCAGCGCTCACAAT-**TTT-A-tctaaaatc-A-tctaaaatc**
15	19393672	19393703	CCATAGCAGTACCGTCACCGGTACATGTGTGC-**TTT-A-tctaaaatc-A-tctaaaatc**
16	19393232	19393267	CTTGTCAATGGTGATTACCTGGCCGCGATAGTTAGT-**TTT-A-tctaaaatc-A-tctaaaatc**
17	19392004	19392040	CATTTGCTTCTAAACAGGCTGCGTAGTCAATATCGCC-**TTT-A-tctaaaatc-A-tctaaaatc**
18	19392748	19392777	AGCTCCAGCGTCTCCACCAGATCGGAGTTC-**TTT-A-tctaaaatc-A-tctaaaatc**
19	19393734	19393765	TATCCACCGGTGGCAATGACCGTGTTCTTAGC-**TTT-A-tctaaaatc-A-tctaaaatc**
20	19392094	19392130	AAATAACCGACAACCAAACAGTAACCAAATGGAGGGC-**TTT-A-tctaaaatc-A-tctaaaatc**
21	19392877	19392911	TGTAGATCTCCTTCATCTTGTTCACACCGTCCTGCt-**TTT-A-tctaaaatc-A-tctaaaatc**
22	19392203	19392239	ATCTGGATTTACGTTTCATCACAAAATGCCCGGAACC-**TTT-A-tctaaaatc-A-tctaaaatc**
23	19392240	19392270	GCTGCCGAGTTCCCAGTTACCAATTGGTAGC-**TTT-A-tctaaaatc-A-tctaaaatc**
24	19392944	19392974	ATGCTGCATGGTCTTCTGCATCTTCAGACGC-**TTT-A-tctaaaatc-A-tctaaaatc**
25	19393838	19393873	CAGATCCAGGGCAAAGTACTCCACAAAGTAGTTGCA-**TTT-A-tctaaaatc-A-tctaaaatc**
26	19392285	19392321	TTGGCGATTTGACAAAATTTATTTACTGGCGCCCACA-**TTT-A-tctaaaatc-A-tctaaaatc**
27	19392987	19393016	GTGATCTGGCCGTTGGCATGGCGCAGCTTA-**TTT-A-tctaaaatc-A-tctaaaatc**
28	19393906	19393935	GCAGCAGCGAGTGACCAGTACGATCAGCCA-**TTT-A-tctaaaatc-A-tctaaaatc**
29	19392368	19392397	ATGCGGGTGTTCTGCAACTCCAAGTCTTGA-**TTT-A-tctaaaatc-A-tctaaaatc**
30	19392399	19392435	TTAATAGGAGCGAATCGCTGGTGGAACAGTAGAGACT-**TTT-A-tctaaaatc-A-tctaaaatc**
31	19393077	19393106	GGCTTATTCAGCTCGGCGATGGTCTTGGCG-**TTT-A-tctaaaatc-A-tctaaaatc**
32	19393982	19394011	CTGTCCACCGAAGGCGCGCTGGTAGATCTT-**TTT-A-tctaaaatc-A-tctaaaatc**
33	19395941	19395970	TCGGCACTGCAGTTCGGTTCACTGACTCGC-**TTT-A-tctaaaatc-A-tctaaaatc**

34	19394140	19394169	ACATGTGCCACTTCCAGTCGTCCTCCTCCA-**TTT-A-tctaaaatc-A-tctaaaatc**
35	19393137	19393166	AGAGAGTTGGCACCCAGACGGTTGGCACCA-**TTT-A-tctaaaatc-A-tctaaaatc**
36	19393442	19393471	GCCACGACCCTCCATGATCTCGATGGTCAT-**TTT-A-tctaaaatc-A-tctaaaatc**
37	19394207	19394236	GATCGTGTGCGAGCGGGTGGGGAAAAGCTT-**TTT-A-tctaaaatc-A-tctaaaatc**
38	19393412	19393441	CAGGTACACGTGATCCTTCTCGGGTCCAGC-**TTT-A-tctaaaatc-A-tctaaaatc**
39	19394075	19394104	CTCGCGGGTCATGTAGTGGATGGCATCCTG-**TTT-A-tctaaaatc-A-tctaaaatc**
40	19394324	19394353	GTAGGCGTGATCCACCACCGGGTACTGCTT-**TTT-A-tctaaaatc-A-tctaaaatc**
41	19393952	19393981	GGCCTGTCCGCCCTTGCCGAACTTCAGACT-**TTT-A-tctaaaatc-A-tctaaaatc**
42	19393508	19393537	GGCCACAGGAGCATAGCGCTCCATGAAGCG-**TTT-A-tctaaaatc-A-tctaaaatc**
43	19393047	19393076	TTTTCCTTGAGGGTGGGAGCCGGTGCACCA-**TTT-A-tctaaaatc-A-tctaaaatc**
44	19392914	19392943	GATGGGGCCATCGCGGAACACAGCAGCATG-**TTT-A-tctaaaatc-A-tctaaaatc**
45	19393704	19393733	GCCGAGGTGCAGGAGAAGAATGCTCGTCCA-**TTT-A-tctaaaatc-A-tctaaaatc**
46	19392717	19392747	AGTCATCTGGGCATTGGCCAACAGATTCTGC-**TTT-A-tctaaaatc-A-tctaaaatc**
47	19393172	19393201	CGAGCTGGAAGCAGCCTCACCAGCGGCATA-**TTT-A-tctaaaatc-A-tctaaaatc**
48	19393538	19393571	CTCACCATTACCGTTGATCAGGTAACCACCCTCA-**TTT-A-tctaaaatc-A-tctaaaatc**
49	19393268	19393297	CGGCACACCGCCCATGTTGTAATGCACGGT-**TTT-A-tctaaaatc-A-tctaaaatc**
50	19393766	19393795	GCGGAATCGGTGCAGTGTGCCATCCTCCAG-**TTT-A-tctaaaatc-A-tctaaaatc**
51	19392329	19392365	TTAAGTAGACATCCGTACGAGTGATGGTATGGGGTGT-**TTT-A-tctaaaatc-A-tctaaaatc**
52	19393017	19393046	TCGAGGTTAGCAACAGAGGCCTCGCCAGCG-**TTT-A-tctaaaatc-A-tctaaaatc**
53	19393301	19393330	CAACACGGGGATGGGCTCACGGGTCACATC-**TTT-A-tctaaaatc-A-tctaaaatc**
54	19395704	19395733	TTTTGGCCAAAATCGATGGCACACGCATGA-**TTT-A-tctaaaatc-A-tctaaaatc**
55	19394237	19394266	GGTGATCACCGCCGTGCGAAATCCCTCAGC-**TTT-A-tctaaaatc-A-tctaaaatc**
56	19393581	19393610	CCCTCGGTGATGAGACATCCGGCGCCGTAG-**TTT-A-tctaaaatc-A-tctaaaatc**
57	19393874	19393905	GTCGTAGCTCAGCGATTGACCGTATAGCGTGT-**TTT-A-tctaaaatc-A-tctaaaatc**
58	19392468	19392501	GTAGTCCAGCGTAATGTCTCCGTTGTCATTGCAC-**TTT-A-tctaaaatc-A-tctaaaatc**
59	19393642	19393671	GATCCTGAGAGGGCAGTCCCTGGCGTGCAA-**TTT-A-tctaaaatc-A-tctaaaatc**
60	19392507	19392536	CGAGAGCGTGTGCTTGCGCCAGTGCTGATC-**TTT-A-tctaaaatc-A-tctaaaatc**

Table 10: Primers for *Pdha*

S.no.	start	stop	sequence+p30 (*Pdha*)
1	4703602	4703633	TGTAGTACTTGAGGGCCTGATCCTTGGTCAGC-**TTT-A-aatactctc-A-aatactctc**
2	4703634	4703663	TCTCCAACCGACGGATCGTCTGCATCTGTG-**TTT-A-aatactctc-A-aatactctc**
3	4704753	4704782	TGGCCCGATGACTTAGTGATTGACGCCCTT-**TTT-A-aatactctc-A-aatactctc**
4	4703999	4704028	ACCATCACCGTAGAGGGCCAGGCACATGCC-**TTT-A-aatactctc-A-aatactctc**
5	4704825	4704861	TGTCTGTCAGTGATTTGTGTTTGCTGTTCGGTTTTCT-**TTT-A-aatactctc-A-aatactctc**
6	4704029	4704058	AGCCTCGAACACCTGTCCTTGATTGGCGGC-**TTT-A-aatactctc-A-aatactctc**
7	4703936	4703965	GCCGGCACCCAAAGGAACTTGAGCACCCAC-**TTT-A-aatactctc-A-aatactctc**
8	4704059	4704090	ACAGGCAGTTTCCACAGGTAGGCCATGTTGTA-**TTT-A-aatactctc-A-aatactctc**
9	4703966	4703995	ATTGCCCTTGTACTTGCAGGCCAAGCCAAC-**TTT-A-aatactctc-A-aatactctc**
10	4703876	4703905	GTACATGTGCATGGAGCCACCCTTGCCGCG-**TTT-A-aatactctc-A-aatactctc**
11	4703906	4703935	GATGCCATTGCCTCCGTAGAAGTTCGGTGC-**TTT-A-aatactctc-A-aatactctc**
12	4704976	4705010	TGTGTGGTTGGAGTGCTCCGATTAGCTAAGCTTTT-**TTT-A-aatactctc-A-aatactctc**
13	4705011	4705040	AGTACCCCAGAGTTATGTGGTGCGCTACGA-**TTT-A-aatactctc-A-aatactctc**

14	4702807	4702840	CCTGCTTGGGCTGCATTCTGGAATAAACCGAAAA-**TTT-A-aatactctc-A-aatactctc**
15	4704460	4704489	AGCTCGATGCACAGCTCCTTGAAGGAGGTG-**TTT-A-aatactctc-A-aatactctc**
16	4704657	4704686	GTACACGTCCGTCCAGAGGTGGCTCACGCC-**TTT-A-aatactctc-A-aatactctc**
17	4703694	4703725	GCCGGAATACAGATGACAGAAGCCGCGAATGA-TTT-A-aatactctc-A-aatactctc
18	4703834	4703863	CTGGACACCGGTGAGCTCAGCCAGTACGCC-TTT-A-aatactctc-A-aatactctc
19	4704689	4704718	GTGCCGCGCAGCTTGGGCTCCAGATTGTTG-**TTT-A-aatactctc-A-aatactctc**
20	4702449	4702484	GGGGCTTTCTATATGCGGATTGTCCGGATCTAGAAT-**TTT-A-aatactctc-A-aatactctc**
21	4704217	4704249	CCGCGGGTATAGTAATCAGTGTTGCAGGAAGCA-**TTT-A-aatactctc-A-aatactctc**
22	4703741	4703770	CACATCCCGCATCGCCGCCTTCATGCCAAC-**TTT-A-aatactctc-A-aatactctc**
23	4702530	4702560	TCGCTAACGCGTGACAGAGTACGCAACATTT-**TTT-A-aatactctc-A-aatactctc**
24	4703801	4703830	GGGTGAGACGCCCATCAGGTAGGTCCATCC-**TTT-A-aatactctc-A-aatactctc**
25	4702382	4702415	GCCGCGCGTCGTTGTAAGTTAAACAATCGGAAAA-**TTT-A-aatactctc-A-aatactctc**
26	4704909	4704945	CGGGGTTCTCATCGTTCAACTTTCGGCTTATGATCTA-TTT-A-aatactctc-A-aatactctc
27	4704362	4704394	GGACATGGAGTGTCCAGAGTATCGGTACGTGTT-**TTT-A-aatactctc-A-aatactctc**
28	4704430	4704459	ATGGGATCACGCTTCTGGCGCACCTCCTGG-**TTT-A-aatactctc-A-aatactctc**
29	4702841	4702874	GGCCTCCGTGGCATAATTGTTGGTTTTCGAAACA-TTT-A-aatactctc-A-aatactctc
30	4704329	4704361	CGTCTCCATCACCAAAGGTCCGTGAGTGTTCAC-**TTT-A-aatactctc-A-aatactctc**
31	4704400	4704429	ATCTCCTCGCGTGTGCGGTACGATGTGCCC-**TTT-A-aatactctc-A-aatactctc**
32	4702493	4702529	TCGCTGTGTTATTCTCGTTCGACTGACAGAAATTGGA-**TTT-A-aatactctc-A-aatactctc**
33	4703664	4703693	TCTTCTCCTTGTACAGATTACCGGCGGCCG-**TTT-A-aatactctc-A-aatactctc**
34	4703771	4703800	GTGGACACGGTACGCCGAGATGATGTTGTC-**TTT-A-aatactctc-A-aatactctc**
35	4704719	4704752	GCGCTCCTGGATGTGATCAATATCGTAGGCGATG-TTT-A-aatactctc-A-aatactctc
36	4702416	4702448	CGCACGCTATATATCTGGTGTCTCAGTCGCACC-**TTT-A-aatactctc-A-aatactctc**
37	4704257	4704286	ATCCATGCCGTCCACCCAGATTCCGGGCAG-**TTT-A-aatactctc-A-aatactctc**
38	4704299	4704328	ATAGTTGATGGCGAACTCGGTGGCGCTGCG-TTT-A-aatactctc-A-aatactctc
39	4703572	4703601	TTCACTTCCGTGGCGGGTCCTTCGTCCAGG-TTT-A-aatactctc-A-aatactctc
40	4704946	4704975	TGTGGGTCTCTTCGGATCCGTTCCGTTCTA-**TTT-A-aatactctc-A-aatactctc**

Table 11: Primers for *Gdh*

S.no.	start	stop	sequence+p31 (*Gdh*)
1	23937856	23937885	ACAATGGTGCCGTGCTCGTTCTTGTAGTCC-**TTT-A-ttattcact-A-ttattcact**
2	23937916	23937946	TTGTACAGAGTGCCGTCGTGCTCAATGACAC-**TTT-A-ttattcact-A-ttattcact**
3	23937826	23937855	CCCTCGTAGGGCTTGGCGTTCTGGTAGCCC-**TTT-A-ttattcact-A-ttattcact**
4	23943050	23943086	TTTTATTCTGTTCTACACAACCGCTCGCTACTCGACG-**TTT-A-ttattcact-A-ttattcact**
5	23942917	23942946	GACTGCATCACAGCGGTGGGCAGTGCCTTG-**TTT-A-ttattcact-A-ttattcact**
6	23938393	23938422	CGGGTGATCTTCTCCAGCTCGTGCTCGGAG-**TTT-A-ttattcact-A-ttattcact**
7	23943009	23943041	CATGCTGCTAATCGCTTGGATTCTTCGGGTTCC-**TTT-A-ttattcact-A-ttattcact**
8	23937480	23937511	CGTGGTTCAGGTTCTTCAGCCACTCGAAGAAG-**TTT-A-ttattcact-A-ttattcact**
9	23938130	23938164	TCATGTAGTTGGCCTCGTTGATGAAGTTCTCCAGG-**TTT-A-ttattcact-A-ttattcact**
10	23938492	23938521	AAGGTCATCAGGGCGGACAGGGCTTTGACC-**TTT-A-ttattcact-A-ttattcact**
11	23936244	23936280	TGCATTTCGGTTTTGTGACTTTTCATCTAAGACGGCG-**TTT-A-ttattcact-A-ttattcact**
12	23938287	23938316	ATCGGCAATCCAGGACATCTCGCGCTCACC-**TTT-A-ttattcact-A-ttattcact**
13	23938522	23938551	TCATCGCGTGACACATCCAACGAGAAACGG-**TTT-A-ttattcact-A-ttattcact**

14	23936348	23936377	GGGGCTAATCAGCACACTCAGCGGGCTTAG-**TTT-A-ttattcact-A-ttattcact**
15	23938363	23938392	CCCTTCTTGGCCAACTCAAGGGTGAAGCGA-**TTT-A-ttattcact-A-ttattcact**
16	23936412	23936442	TCTTCTCAATGGAGTTGACGTAGGCAGCGGT-**TTT-A-ttattcact-A-ttattcact**
17	23942979	23943008	GCCCTGGCGGGCCAGACTCTTCAGGTGATA-**TTT-A-ttattcact-A-ttattcact**
18	23942736	23942765	CTTCTGCTTCTTCTCGTCGCGGGTCAGCTT-**TTT-A-ttattcact-A-ttattcact**
19	23935988	23936024	TTAATGTTACGGCAACGGAGCGATCGTACGATAAACG-**TTT-A-ttattcact-A-ttattcact**
20	23942766	23942795	GCCCTTCATGTCGTCCACCAGCGATTCCTC-**TTT-A-ttattcact-A-ttattcact**
21	23936123	23936159	AAGCTCGCAACTTGTTCAACTTAATACGAAACACGGG-**TTT-A-ttattcact-A-ttattcact**
22	23942826	23942855	CTCGACCATGTCGAAGAAGCGCGGATCCTT-**TTT-A-ttattcact-A-ttattcact**
23	23936443	23936472	TCTGAGGTCCAGGCCCAGGTTGTACTTCAT-**TTT-A-ttattcact-A-ttattcact**
24	23942676	23942705	GGGGAAGGCGATCTCGATGATGTGGTCGCA-**TTT-A-ttattcact-A-ttattcact**
25	23937542	23937572	AGATCGGGAATGACCAGGATGTTGCGATCGA-**TTT-A-ttattcact-A-ttattcact**
26	23942625	23942654	CTGGGCGCGGTAGCCGGTGATCATCTCGTA-**TTT-A-ttattcact-A-ttattcact**
27	23937448	23937479	CTCATACTTGAAGGTCAGGCGACCGTACGAGA-**TTT-A-ttattcact-A-ttattcact**
28	23937886	23937915	TCCAGCAGCTTAGGGTCAATGCCCTCCGGG-**TTT-A-ttattcact-A-ttattcact**
29	23938192	23938221	GAGACGCGTCCGTGGATACCGCCCTGGTTG-**TTT-A-ttattcact-A-ttattcact**
30	23936610	23936639	GGCCGAAGCGACGCTCCAGGGACTCTTGAA-**TTT-A-ttattcact-A-ttattcact**
31	23938462	23938491	CCGAATGGCACATCCACGCAGGCGCACTTG-**TTT-A-ttattcact-A-ttattcact**
32	23938333	23938362	GCGGGCACATCGACACCGGGTCCAATGAAG-**TTT-A-ttattcact-A-ttattcact**
33	23942796	23942825	GGCGATTTGGCAGCCGCGATGGAAGAAATA-**TTT-A-ttattcact-A-ttattcact**
34	23938254	23938286	GATGTCCAGGTGACCGATGGTCTTGGCATAAGT-**TTT-A-ttattcact-A-ttattcact**
35	23936498	23936527	GAGCGCTCCATGGTGTAGTCCAGGCCGGAG-**TTT-A-ttattcact-A-ttattcact**
36	23937997	23938026	ACGTTACCGAAGCCCTGGACGATGAAGGTC-**TTT-A-ttattcact-A-ttattcact**
37	23937790	23937825	ATGAAGATGTCGCACTTCTCGAACATGAGGTTCTCG-**TTT-A-ttattcact-A-ttattcact**
38	23936528	23936557	TGCACGATATCCTTCTCGGAGGCGCCGGAG-**TTT-A-ttattcact-A-ttattcact**
39	23942859	23942888	GGTGGGCACATCCTTGAGGCGGTCGGGAAT-**TTT-A-ttattcact-A-ttattcact**
40	23937512	23937541	GAGACGGTGACACCACCGGCGTTGATGTAC-**TTT-A-ttattcact-A-ttattcact**
41	23937967	23937996	CGGGTCAGATAGCGAGTGGTGTGCAGGCCC-**TTT-A-ttattcact-A-ttattcact**
42	23942706	23942735	GGGCTGCATCAGCATGAGGATGCCCTTCAC-**TTT-A-ttattcact-A-ttattcact**
43	23938224	23938253	GGGCTTGCCGGTGACACAGGCATGAGCATT-**TTT-A-ttattcact-A-ttattcact**
44	23938423	23938455	TACTCCTTAGGGTTGATCTTCAGACCGGCCTTG-**TTT-A-ttattcact-A-ttattcact**
45	23936382	23936411	CCAGGCCGGCATCGCGGTATGTGGTGAAGA-**TTT-A-ttattcact-A-ttattcact**
46	23937760	23937789	CTGGTGATGACCTTCTCGACGGCAGCGGGA-**TTT-A-ttattcact-A-ttattcact**

Table 12: Primers for *Skap*

S.no.	start	stop	sequence+p33 (*Skap*)
1	8939686	8939715	TTGAGGTTCCTCAGCTGCTGGACGGCGATG-**TTT-A-ccttctatt-A-ccttctatt**
2	8939716	8939747	TGAGCAGACTGTAGGAAACGTGTTCCTGGACA-**TTT-A-ccttctatt-A-ccttctatt**
3	8940534	8940564	CCTGAGCCTTCAGCACCAGGTTATCGGTCTT-**TTT-A-ccttctatt-A-ccttctatt**
4	8941103	8941139	TCCTTCTTGACGAACAGGTCATACAGATTCAACAGCA-**TTT-A-ccttctatt-A-ccttctatt**
5	8940757	8940786	TTTGCAGATGCGACCGGCTGCTCCGGTTTG-**TTT-A-ccttctatt-A-ccttctatt**
6	8940565	8940594	AGGTTCCTTTGCCTCGTCCTCCGGCCAAAA-**TTT-A-ccttctatt-A-ccttctatt**
7	8941140	8941170	GGCATAGGGGTTGATCTCAACCAAGAGGGCA-**TTT-A-ccttctatt-A-ccttctatt**

8	8940717	8940753	GGTGACCAGAAGCTGATCGATCATTTTGCTTGAAAGT-**TTT-A-ccttctatt-A-ccttctatt**
9	8941467	8941496	CTCCTGGGTCCAATCGCGCAGCGCAAACAG-**TTT-A-ccttctatt-A-ccttctatt**
10	8941968	8941997	GCACGGCGAGATCGGCAGCCTTATCTAGAT-**TTT-A-ccttctatt-A-ccttctatt**
11	8940595	8940625	ACTCGCACACCTCCCTTCAGGCCATTCTTAA-**TTT-A-ccttctatt-A-ccttctatt**
12	8941799	8941828	AGACGCACAACCACGGGCATGTTCAGATTC-**TTT-A-ccttctatt-A-ccttctatt**
13	8941696	8941727	CAGAATGCAAAGCACCTTCGGATCGGAAGTGA-**TTT-A-ccttctatt-A-ccttctatt**
14	8941769	8941798	AGATCCTTGGTGGCGGAGATGATACCCTCG-**TTT-A-ccttctatt-A-ccttctatt**
15	8942073	8942109	TGAGTGTTGACTTAGCCGGTAACTGATGGAGCTATCT-**TTT-A-ccttctatt-A-ccttctatt**
16	8941908	8941937	TACGAATCAGTTCGCGGGCCTCCTTGACTT-**TTT-A-ccttctatt-A-ccttctatt**
17	8941732	8941768	GCAATGACATCACAACGCATAATACCACCGAAGATGT-**TTT-A-ccttctatt-A-ccttctatt**
18	8940932	8940961	TATCAACACCACCCTCCTTGGAGGCGATCA-**TTT-A-ccttctatt-A-ccttctatt**
19	8940504	8940533	CAGCTTGGTGGCGATATCGTTGGCCTCCTT-**TTT-A-ccttctatt-A-ccttctatt**
20	8940787	8940816	GGGGAACTTCCTTTCGGCAACCATCACCTT-**TTT-A-ccttctatt-A-ccttctatt**
21	8941998	8942027	CGCGGGCCAGTTTGACGATTTGCGCCAAGT-**TTT-A-ccttctatt-A-ccttctatt**
22	8941531	8941562	GCCGATAGTGCCATCCAGGGCAATGTAGTTCA-**TTT-A-ccttctatt-A-ccttctatt**
23	8940992	8941027	AGCCAGTGCCTATATCGATGGGTTCGTACAAAATGG-**TTT-A-ccttctatt-A-ccttctatt**
24	8940817	8940846	CATCATCACGGCGAAGTAGAACTCACGGCG-**TTT-A-ccttctatt-A-ccttctatt**
25	8938804	8938840	TCGTGCCAAGAATGAAGCCATTTTGTTCTGAAATCGA-**TTT-A-ccttctatt-A-ccttctatt**
26	8941432	8941466	CTCCTTCTGACGAAACTCGGCGTTGTCATCAAATC-**TTT-A-ccttctatt-A-ccttctatt**
27	8941073	8941102	TCTGGACATGTGTGTCCTCGCCATCGCCGC-**TTT-A-ccttctatt-A-ccttctatt**
28	8941666	8941695	TGATCTTGAAGGCGGCCTTGACCGCCTCGG-**TTT-A-ccttctatt-A-ccttctatt**
29	8941938	8941967	CATCGCGGGCCAGAATCTTCAGTCCAGATG-**TTT-A-ccttctatt-A-ccttctatt**
30	8940962	8940991	CATCTGGACTGCTGGCAGCCACCTCCTCAA-**TTT-A-ccttctatt-A-ccttctatt**
31	8942028	8942064	GCATCGGGAATCTCGAAGTTCACGTCCATCTTCATTT-**TTT-A-ccttctatt-A-ccttctatt**
32	8941608	8941641	GGAAATTGGCCGGTTCACCGCCATACAACTTAAT-**TTT-A-ccttctatt-A-ccttctatt**
33	8938851	8938880	TGGCCGCTGGCCTAACGGTTTCGATCAGGG-**TTT-A-ccttctatt-A-ccttctatt**
34	8941028	8941060	TCTTGACGATCTTTTCGGCCTGTTCACTGGTCA-**TTT-A-ccttctatt-A-ccttctatt**
35	8941497	8941530	GATTGTATTTGGCAGCCTCGACTTCCTTGGGATC-**TTT-A-ccttctatt-A-ccttctatt**
36	8941578	8941607	GATATCCATGGTGGCCATGGCCAGACCGGC-**TTT-A-ccttctatt-A-ccttctatt**

Table 13: Primers for *CS*

S.no.	start	stop	sequence+p34 (*CS*)
1	6350866	6350901	GCTGCTCCTTGAGATTGCCAGTCACGTTATCCTTTT-**TTT-A-ctctactac-A-ctctactac**
2	6350757	6350790	GTTGAAAGGCAAAATGATGGCCCAAAGAGCCATT-**TTT-A-ctctactac-A-ctctactac**
3	6359078	6359107	GAGGTCTCGGTGACCAGGGCCTTGATGCCG-**TTT-A-ctctactac-A-ctctactac**
4	6359007	6359036	CTTGGTGGCGCCATGCTGCTTGCGGAAGTT-**TTT-A-ctctactac-A-ctctactac**
5	6359358	6359387	ATTCAGCGCAGTGACGGCGGCAGCAAACTG-**TTT-A-ctctactac-A-ctctactac**
6	6359606	6359635	AGATAGAGACGCATCAGCTCGGTGAAGGGG-**TTT-A-ctctactac-A-ctctactac**
7	6359419	6359451	CGTACTCCCAGTACTTGCTCTTGTGCACACCAT-**TTT-A-ctctactac-A-ctctactac**
8	6359192	6359221	CAGAAGAGACCCTCGGGCAGGGGCTCAGTG-**TTT-A-ctctactac-A-ctctactac**
9	6359483	6359512	CAGTAGATGGTGGCCGCCACCACTGGGAGC-**TTT-A-ctctactac-A-ctctactac**
10	6359297	6359326	TTCAACATGGTGACCACGTGCTGGGGCAGG-**TTT-A-ctctactac-A-ctctactac**
11	6359558	6359589	GCATCTTCACAAAGTTCGCCGACCAATCCAGG-**TTT-A-ctctactac-A-ctctactac**

12	6360569	6360605	GCTCTTCTCCTCAACTACACATCTCCAACTCCCTCAA-**TTT-A-ctctactac-A-ctctactac**
13	6361239	6361268	ACACTTGCACGGCGATGAACGAACGCGTTT-**TTT-A-ctctactac-A-ctctactac**
14	6350806	6350842	GGAGTCCCAATGGACTTCGAGTCCCACATAGAATTTT-**TTT-A-ctctactac-A-ctctactac**
15	6359666	6359695	CCCACCAAGTGAACGGTGTGGGCAGACACG-**TTT-A-ctctactac-A-ctctactac**
16	6360828	6360864	GGCGCAAACATTTTACTCTCTCTGCCTGTCCCTATAT-**TTT-A-ctctactac-A-ctctactac**
17	6359696	6359725	AAGGAGAGGTAGGGATCGCTGAGGGCGGAG-**TTT-A-ctctactac-A-ctctactac**
18	6359781	6359810	CTTCTGCAGCTTGCGCAGCCACACGAGCAC-**TTT-A-ctctactac-A-ctctactac**
19	6360942	6360978	TCGTGGTTAGTCCATCGATCGGCTAAGATGAACAAAA-**TTT-A-ctctactac-A-ctctactac**
20	6361202	6361238	GCAGCTTCCACTGGTGGAGTTGACAATAACTACTCTC-**TTT-A-ctctactac-A-ctctactac**
21	6360330	6360365	GCTTACTTCTGGACCATTTTGACCAGCAGATCGGTG-**TTT-A-ctctactac-A-ctctactac**
22	6360093	6360124	GCACCACCTTGTAGATCTTCGACACCAGCTGG-**TTT-A-ctctactac-A-ctctactac**
23	6360401	6360430	ACGTCCATCGTCCTCCGGCTACAAAAGGTT-**TTT-A-ctctactac-A-ctctactac**
24	6350720	6350756	TCCGAAACGGCGTACGAACATTACTACTTTTAGCTGT-**TTT-A-ctctactac-A-ctctactac**
25	6360125	6360154	TCACCTTGCCGGTCTCGGTCAGAATTGGTG-**TTT-A-ctctactac-A-ctctactac**
26	6360632	6360668	AGTTGCAGTGTGTTGCAGTTTTCTTCTGGTTTTCGTT-**TTT-A-ctctactac-A-ctctactac**
27	6358977	6359006	CTTTACGCGCTCCTGCTCCTGGGGCACCTT-**TTT-A-ctctactac-A-ctctactac**
28	6360015	6360044	GTGTAGCGGGGATCGGTCTTGCGGAGCACG-**TTT-A-ctctactac-A-ctctactac**
29	6359139	6359168	CTTTTGGCACTCGGGAATGGAGAGGCCGCG-**TTT-A-ctctactac-A-ctctactac**
30	6359452	6359481	TGGCGATCAGGTCCATGCTGTCCTCGTAGA-**TTT-A-ctctactac-A-ctctactac**
31	6360715	6360751	AGTGGTTGCTTGTCGGTTGCCCTTCGTTAATTATTTT-**TTT-A-ctctactac-A-ctctactac**
32	6360300	6360329	GAGAATGACTTGGGGCGCTCGATGGGCAGG-**TTT-A-ctctactac-A-ctctactac**
33	6359528	6359557	CTGGAGTCAATCGAACGGGAGCCCTTGCCG-**TTT-A-ctctactac-A-ctctactac**
34	6359327	6359356	GACATCGGGTGCAGGGTGGTGGGCATGTTG-**TTT-A-ctctactac-A-ctctactac**
35	6359108	6359137	AAGCGGATACCCTCGTCAGCATCCAGCACC-**TTT-A-ctctactac-A-ctctactac**
36	6359388	6359418	CCGAGTATGCCTTGGCGAATTTGCTGTCGTG-**TTT-A-ctctactac-A-ctctactac**
37	6360888	6360917	GAGTGGGTATCGTGGGCGGTTTCGGGTGGG-**TTT-A-ctctactac-A-ctctactac**
38	6359817	6359846	CTTGAGCTGCTCCTCCGACGGGTTGTTGCC-**TTT-A-ctctactac-A-ctctactac**
39	6360063	6360092	AACGTCTCGTCCTCGGGCAGGTGCTTCAGC-**TTT-A-ctctactac-A-ctctactac**
40	6360371	6360400	GAACTCCAGCTCCTCCCGCTCCTCCTGCTC-**TTT-A-ctctactac-A-ctctactac**
41	6359847	6359879	CTGTCCGGACTTGAGGGTCTTCCAGATGTACTC-**TTT-A-ctctactac-A-ctctactac**
42	6360185	6360214	TCATGCCGTAGTACTGCAGCAGCACACCGG-**TTT-A-ctctactac-A-ctctactac**
43	6359636	6359665	TTGCCACCCTCGTGGTCACTGTGGATGGTC-**TTT-A-ctctactac-A-ctctactac**
44	6360215	6360247	CGCCGAACAACACGGTGTAGTAGTTCATCTCCT-**TTT-A-ctctactac-A-ctctactac**
45	6359037	6359067	CGTACATCATGTCGATGGTCGTCTCGCCCAT-**TTT-A-ctctactac-A-ctctactac**
46	6358920	6358949	GCCATCGGCGGCGATCATGCGAACATAGGC-**TTT-A-ctctactac-A-ctctactac**
47	6360155	6360184	AATGGGCATCTACATTGGGCCAGGGGTTCT-**TTT-A-ctctactac-A-ctctactac**
48	6350902	6350931	TGTTCAAGGTTTCCGGAGTCGCCGATTGTT-**TTT-A-ctctactac-A-ctctactac**

Table 14: Primers for *mAcon1*

S.no.	start	stop	sequence+p35 (*mAcon1*)
1	21171055	21171084	GCGCTGGTTGAAGGGGAACAGAGAGGTGGT-**TTT-A-taaaaactc-A-taaaaactc**
2	21168733	21168768	CGCGTCCTGATTAAGCGATACTCGAAATAAACCCGA-**TTT-A-taaaaactc-A-taaaaactc**
3	21168652	21168688	CAGCCCTCTCAGCCGGAAGATTTTAAGACAGACTAAA-**TTT-A-taaaaactc-A-taaaaactc**

4	21171085	21171115	CACGGCCTGTCGATTTCAGGTAATCAGCCAT-**TTT-A-taaaaactc-A-taaaaactc**
5	21168696	21168732	CGAAATTGATATTGCAGCAAATGCTTCGAAGCCGTCA-**TTT-A-taaaaactc-A-taaaaactc**
6	21172133	21172165	AGCTACCGTTGCGTTGGTTCTTGATGTTGTTCA-**TTT-A-taaaaactc-A-taaaaactc**
7	21170259	21170288	AACTTGGACAGAGCCACTTTGGAGGCGGTG-**TTT-A-taaaaactc-A-taaaaactc**
8	21168622	21168651	TTCTTTACCACGGCGACCAGTGTTAGCTGG-**TTT-A-taaaaactc-A-taaaaactc**
9	21171432	21171461	ATGGTGGCACGGATCTGCTCTGATCCGGGA-**TTT-A-taaaaactc-A-taaaaactc**
10	21171248	21171277	CGCCTAGCTTGCTGATGGGATGGCCCAAAT-**TTT-A-taaaaactc-A-taaaaactc**
11	21171492	21171521	GCGTTGGCCAGAACGGTACCGCCGAACTTG-**TTT-A-taaaaactc-A-taaaaactc**
12	21170620	21170651	CAGGTGCTGGCCAAGAAATCGTACACTTCCTT-**TTT-A-taaaaactc-A-taaaaactc**
13	21171314	21171349	ACGAAGAGTTGGTGCAAGAGCCAATAAGACCTACAC-**TTT-A-taaaaactc-A-taaaaactc**
14	21171552	21171587	ACAATGGTGTTCTTGTCGCCCTTCTTAACGTCCTTA-**TTT-A-taaaaactc-A-taaaaactc**
15	21172572	21172601	ACCAGCCGATCTGTAGGTCGTTCAGGGTGT-**TTT-A-taaaaactc-A-taaaaactc**
16	21171623	21171652	TGACAAAGCAATGGGTGGCCGGGTTAGCGT-**TTT-A-taaaaactc-A-taaaaactc**
17	21170405	21170434	TACCGCGCACGATGTCCTGGTTTGCGGGAT-**TTT-A-taaaaactc-A-taaaaactc**
18	21170778	21170807	CCACCAACGCCAATGCACAGGCCACCCAAG-**TTT-A-taaaaactc-A-taaaaactc**
19	21172675	21172708	ACAGGAAGAAGGTTGGGATCAGGCTTCTTGACTG-**TTT-A-taaaaactc-A-taaaaactc**
20	21171903	21171932	GACTTGGGGTCGACAGCCACCTTGACATTT-**TTT-A-taaaaactc-A-taaaaactc**
21	21171716	21171747	GAACTTCTTGCCATCAGCACCAGTAAGCTCGT-**TTT-A-taaaaactc-A-taaaaactc**
22	21171933	21171962	TCAAAAGGCTCCAGCAGCTGCAGACGCGTC-**TTT-A-taaaaactc-A-taaaaactc**
23	21171963	21171992	AGATCGGTCAGATCCTGGCCGTTCCACTTG-**TTT-A-taaaaactc-A-taaaaactc**
24	21172366	21172395	ATCGTAATCAGCGGGATTGGCGAAGGTGAG-**TTT-A-taaaaactc-A-taaaaactc**
25	21172473	21172506	GCAAGGGATTTCAGGTTGAGCAGGGAGATTTTGC-**TTT-A-taaaaactc-A-taaaaactc**
26	21170868	21170898	GCCGCTGATCTTGCCAGTCAAATTGACACCA-**TTT-A-taaaaactc-A-taaaaactc**
27	21172065	21172096	TGTTGTTGGAGATGTTGTCCAAATGGCCACGG-**TTT-A-taaaaactc-A-taaaaactc**
28	21170990	21171024	GGTGGCCATGCCTGTACAAGAGATAGAGTCAACAC-**TTT-A-taaaaactc-A-taaaaactc**
29	21170899	21170929	CCTTCAGGATAACATCCTTGGGCGAGGTCCA-**TTT-A-taaaaactc-A-taaaaactc**
30	21172271	21172300	CACGACCACCAAGGTGACGGGGCTCCAAAG-**TTT-A-taaaaactc-A-taaaaactc**
31	21171993	21172026	GGTGCACTTTCCCTTAACCTTGATCAGCACAGTC-**TTT-A-taaaaactc-A-taaaaactc**
32	21171748	21171777	CAGCTCGTCGCCGAAGGGAGCCTTGAGCTT-**TTT-A-taaaaactc-A-taaaaactc**
33	21170525	21170554	AGTGAACAGTGGAGGGCACAGCCACCTTTT-**TTT-A-taaaaactc-A-taaaaactc**
34	21170930	21170959	TGCCTCCCTTGACGGTCAGGATATCGGCAA-**TTT-A-taaaaactc-A-taaaaactc**
35	21170960	21170989	CCTTGCCGTGATACTCAATGATGGCACCGG-**TTT-A-taaaaactc-A-taaaaactc**
36	21171181	21171217	CCAGGGTGTCTAGGTTGATTTCAATCAGCTCATCGTA-**TTT-A-taaaaactc-A-taaaaactc**
37	21173057	21173090	CGGGATGAATTGACGGCACTTATTGTCCGCTTTT-**TTT-A-taaaaactc-A-taaaaactc**
38	21172507	21172536	TTGATTTCGGCATCTACGGGCTTTCCAGGC-**TTT-A-taaaaactc-A-taaaaactc**
39	21171146	21171176	CAGTTCTTGTCAGCGGACAGAATCTTGGCCT-**TTT-A-taaaaactc-A-taaaaactc**
40	21170715	21170744	ATCATCAGCAGGCCGGGGAAAGCGTAGTTC-**TTT-A-taaaaactc-A-taaaaactc**
41	21171462	21171491	TCGAACACCTCAGAGATGCCGTCGCGCTCG-**TTT-A-taaaaactc-A-taaaaactc**
42	21170838	21170867	ATCACCTTGGGGCACTTCAGCTCCCAGGGG-**TTT-A-taaaaactc-A-taaaaactc**
43	21172537	21172571	GGTTAAGCTTGATCCTCTCGACCTTGTCGCCATTC-**TTT-A-taaaaactc-A-taaaaactc**
44	21172709	21172744	CGATTGCTTCCGTTGTGAATTTGAGTGTGTTCACCT-**TTT-A-taaaaactc-A-taaaaactc**
45	21170199	21170228	GTGGCTTCGGACGCAACATGCTTGCCCAGT-**TTT-A-taaaaactc-A-taaaaactc**
46	21170555	21170589	GGGTCCACCAATCTGGGCCTCGATTAAATGATCAC-**TTT-A-taaaaactc-A-taaaaactc**
47	21170652	21170681	GGCTTCCAGAAGCCCAATCCGTACTTTGCA-**TTT-A-taaaaactc-A-taaaaactc**
48	21171686	21171715	CGGTCAGCGGGTTGAAGTCCAGACGACCGG-**TTT-A-taaaaactc-A-taaaaactc**

49	21171396	21171431	GTCACATTGAAAGGAATCTTCGACTTGAGGCCATGG-**TTT-A-taaaaactc-A-taaaaactc**
50	21172610	21172639	CAGCTCCTTCATGCGGTTGAGAGCGCTGCC-**TTT-A-taaaaactc-A-taaaaactc**
51	21171116	21171145	GGTACTTCTGGGCTTCGGAGGCAATGCCAG-**TTT-A-taaaaactc-A-taaaaactc**
52	21171782	21171811	AGGTGTCCTGGCCGGGATCGAAACCCTTGG-**TTT-A-taaaaactc-A-taaaaactc**
53	21172334	21172365	AGGCAGAAGACCCTGTTTCTTCAGGTTGGTCT-**TTT-A-taaaaactc-A-taaaaactc**
54	21171653	21171682	TGGACAGAGCGGTGACCAACTCGGGACTAG-**TTT-A-taaaaactc-A-taaaaactc**
55	21170435	21170464	CACGATCGGGGCGAAGACGCAGGTACGAAG-**TTT-A-taaaaactc-A-taaaaactc**
56	21170345	21170374	AGAGAGTCAGTGGGCGGTTCAAGCGACCGC-**TTT-A-taaaaactc-A-taaaaactc**
57	21168769	21168798	CTGGGCGTTCATCAATCTCGCAGCCATGGT-**TTT-A-taaaaactc-A-taaaaactc**
58	21172097	21172132	TCTCGTTGTTTTCGTAGTTGGTGGCTCCGATAAACA-**TTT-A-taaaaactc-A-taaaaactc**
59	21171218	21171247	CGGGAGTGAATGGTCCGTTAACATGGGGCT-**TTT-A-taaaaactc-A-taaaaactc**

Table 15: Primers for *Idh*

S.no.	start	stop	sequence+p36 (*Idh*)
1	8358836	8358872	AGACGCGCTCTAACCGTAACTGATAACTGTAAAGTGC-**TTT-A-aactaatct-A-aactaatct**
2	8357509	8357538	GGCGACCGATCACAATAGGCTTCTGCCAGC-**TTT-A-aactaatct-A-aactaatct**
3	8357539	8357568	CAGTCACCAGACGGGGCACGTTCTTGCAGA-**TTT-A-aactaatct-A-aactaatct**
4	8357380	8357411	TACCGGGGCCCTTGAAGTCATTAATGACCTCA-**TTT-A-aactaatct-A-aactaatct**
5	8357350	8357379	AATCGTCCGTGTTGAACATTCCCAGGGCAA-**TTT-A-aactaatct-A-aactaatct**
6	8357087	8357116	ATCACCGTCGTAGTTCTTGCAGGCCCACAC-**TTT-A-aactaatct-A-aactaatct**
7	8357569	8357598	TGATTGCCTCACGGAAGACGGTTCCTCCCA-**TTT-A-aactaatct-A-aactaatct**
8	8357026	8357055	GCAGCACGGAGGTCATCAGACCCAGAGATC-**TTT-A-aactaatct-A-aactaatct**
9	8358873	8358905	CGTTAAGCGCTACAGTTTCCGACTCTCTTGGGT-**TTT-A-aactaatct-A-aactaatct**
10	8356921	8356950	CAATGGGGTTGGTGGAGGTCTCCTTGCCCT-**TTT-A-aactaatct-A-aactaatct**
11	8356736	8356766	GTAGTCCCTGCGAGTAACGGCGTTGATGTTG-**TTT-A-aactaatct-A-aactaatct**
12	8356861	8356890	GCTCATTGTTGTCCAGCTTGGCACGATGCA-**TTT-A-aactaatct-A-aactaatct**
13	8357184	8357213	CCCGCCGCCTCGTACTCCTTCTTGTACTGC-**TTT-A-aactaatct-A-aactaatct**
14	8357724	8357753	GCACAGTCAATGGTGACCTGGTCCTCGGTT-**TTT-A-aactaatct-A-aactaatct**
15	8356566	8356602	AATATTGTGAATATGGTGACGAGGACAAGGCATCGCT-**TTT-A-aactaatct-A-aactaatct**
16	8357317	8357349	ATTTGAAAGAGGCGTGGGCAAAGTCCACAATGG-**TTT-A-aactaatct-A-aactaatct**
17	8358906	8358937	GGCGTACAATCGTCAAATTGTTGCGCAATCGG-**TTT-A-aactaatct-A-aactaatct**
18	8357287	8357316	TGTACAGCGGCAGCTTGCGGTCCAGAGCAT-**TTT-A-aactaatct-A-aactaatct**
19	8357756	8357790	ATCGCGGTTCTCAATACCAAGATCGTAGGTATGCA-**TTT-A-aactaatct-A-aactaatct**
20	8356603	8356635	GAGTAGTTTTCTAGAGATGCGAGGCCTGCTGCT-**TTT-A-aactaatct-A-aactaatct**
21	8356801	8356830	CGCCGCTCTCAATTGTGTCGATGCACACCT-**TTT-A-aactaatct-A-aactaatct**
22	8357663	8357692	CTTCTCGTCGGGAGTGATTGTGGCGCACTT-**TTT-A-aactaatct-A-aactaatct**
23	8358641	8358670	CGGCGCAGGGCGAACATTTTACAACCGGAT-**TTT-A-aactaatct-A-aactaatct**
24	8356671	8356700	GCATTCTTGGCCAGGGCACCCTCCAGGTTC-**TTT-A-aactaatct-A-aactaatct**
25	8357250	8357286	CCATCGTACTTCTTCAGAATGGTGTTCTTGGTGCTCA-**TTT-A-aactaatct-A-aactaatct**
26	8357791	8357822	GCTCAATGTCCAGGAAGGGCAGAATCAGTTGG-**TTT-A-aactaatct-A-aactaatct**
27	8357693	8357723	GATGCCCACGTTGTACTTCTTGATGGCCTCA-**TTT-A-aactaatct-A-aactaatct**
28	8358799	8358835	ATTTTCGGACAAAGCAAAATTAAATGCTGTGGGCGTC-**TTT-A-aactaatct-A-aactaatct**
29	8357823	8357858	CTCTTAATGGAGTCCCAAATGATGCGGGTCATCTCG-**TTT-A-aactaatct-A-aactaatct**

30	8357890	8357919	TGATCTTCTGGGCCATCTGTTCGGGAGAGC-**TTT-A-aactaatct-A-aactaatct**
31	8357214	8357249	TTGTTGTACAGGTCCTCGAATATGTCCTTGAAGCGT-**TTT-A-aactaatct-A-aactaatct**
32	8357057	8357086	GTAGCCCTGGGCAACGGAGTCCGACTGCAC-**TTT-A-aactaatct-A-aactaatct**
33	8356996	8357025	CAGCCTCCACGGTCTTGCCATCGGGGCATA-**TTT-A-aactaatct-A-aactaatct**
34	8356831	8356860	GCTCAAGGGTGTCGGCGAACTGCTTCAGTG-**TTT-A-aactaatct-A-aactaatct**
35	8357629	8357662	TCCACATCTTCTTCAGGTTGAACTCCTCTACGCG-**TTT-A-aactaatct-A-aactaatct**
36	8356701	8356735	TTGGCCAGCGTGTTAATGAACTCAAAAGTCTCCTG-**TTT-A-aactaatct-A-aactaatct**
37	8356951	8356980	GCTGGTAGAAGCGGAAGTGACGCGTCACCG-**TTT-A-aactaatct-A-aactaatct**
38	8357117	8357146	GAAGCCACCCTCCGACTTCATGGCATAAGC-**TTT-A-aactaatct-A-aactaatct**
39	8356891	8356920	GCAGGCCACGGGTCCAGGCGAATATCGAGG-**TTT-A-aactaatct-A-aactaatct**
40	8357479	8357508	CGACGGCCTTGTACTGATCGGCGTGGGCAT-**TTT-A-aactaatct-A-aactaatct**
41	8357448	8357477	GTCAGCTTGCCGGGTCCGGGAACCACGTAG-**TTT-A-aactaatct-A-aactaatct**
42	8356767	8356800	CCTTTAATGCAGATGGCCAGATCCTTGGTCATGG-**TTT-A-aactaatct-A-aactaatct**
43	8357860	8357889	CACCGAGGACATCCACAACGGGACCGGCTT-**TTT-A-aactaatct-A-aactaatct**
44	8356636	8356665	CGGACTGAGTGCCGGATAGTCATTTGGCAG-**TTT-A-aactaatct-A-aactaatct**
45	8358611	8358640	CGGTGGACCGACGTCATCATTGCGGCTGTG-**TTT-A-aactaatct-A-aactaatct**
46	8356471	8356503	TTTTGCGTCTCGCAGAGACAATGAAACAGTGGG-**TTT-A-aactaatct-A-aactaatct**
47	8357412	8357441	TCGATCACCTGACCGTCGGTTCCCTTCCAG-**TTT-A-aactaatct-A-aactaatct**
48	8357599	8357628	AGATGTTACGGATGGTACCGTTGGGCGACT-**TTT-A-aactaatct-A-aactaatct**
49	8357147	8357183	AACCATATCGTCGATGAGACGGTGTTCATACCAGATG-**TTT-A-aactaatct-A-aactaatct**
50	8358692	8358728	TATTATGAATGAACCGACCGACGACTGGAAACGAGAG-**TTT-A-aactaatct-A-aactaatct**
51	8358751	8358787	TGAAACAATACGAGACAATATGACACTGGAGTCCCGG-**TTT-A-aactaatct-A-aactaatct**

Table 16: Primers for *Mdh2*

S.no.	start	stop	sequence+p27 (*Mdh2*)
1	18228628	18228664	TGGTTTCATTTTACACCACACACTAGGCGCAGATCTA-**TTT-A-catcatcat-A-catcatcat**
2	18228476	18228505	GATCGCTTAGGCGTTGGCAAAGTCAATGCC-**TTT-A-catcatcat-A-catcatcat**
3	18228539	18228575	GGGTAGTTTGCCAATTCACAATAGGCGCTAATGAAGT-**TTT-A-catcatcat-A-catcatcat**
4	18228576	18228611	GCCGACTTGAGACGAAAGATTTGCTAGGGGTAGTAT-**TTT-A-catcatcat-A-catcatcat**
5	18228319	18228348	AAGGTAGCCTCCGTGACGGTGGACTGCACG-**TTT-A-catcatcat-A-catcatcat**
6	18228349	18228378	TTCTTGCCCAGCACCAGGGGTGTGGAGAAG-**TTT-A-catcatcat-A-catcatcat**
7	18228383	18228412	GAGCTTGGGCAGGCCGAGGTTCTCCTGGAC-**TTT-A-catcatcat-A-catcatcat**
8	18228413	18228442	GGCCTCCAGCAGCTTCTTCTCGTAGTCGTT-**TTT-A-catcatcat-A-catcatcat**
9	18226478	18226514	ACTTGCTTCAGCATATTTGCACGGGTTTTGGTTACAA-**TTT-A-catcatcat-A-catcatcat**
10	18226774	18226804	ATTCTGCTTGAGGAGCAGCGACAGCGGCTGG-**TTT-A-catcatcat-A-catcatcat**
11	18226879	18226908	CCGATGAATCCGGCGGTCTTGCTCTTGGTG-**TTT-A-catcatcat-A-catcatcat**
12	18227772	18227801	ATGTCCTTGATGATGCCGGCGTTCACGTTG-**TTT-A-catcatcat-A-catcatcat**
13	18227802	18227831	TTGGGGCAGTTCTTGGCAATGGAGTTGGAG-**TTT-A-catcatcat-A-catcatcat**
14	18227984	18228014	GCACCACATCCAAGGTGGAGACTCCGAACAG-**TTT-A-catcatcat-A-catcatcat**
15	18228020	18228049	CACACCAAGGGCATGGCCGATGAAGGCACG-**TTT-A-catcatcat-A-catcatcat**
16	18228088	18228117	GAGAGCACAGGCAGGATGGTCACGCCGGAG-**TTT-A-catcatcat-A-catcatcat**
17	18228149	18228178	GATGCGCACGGTAAGCTTCTCGATGGTGTC-**TTT-A-catcatcat-A-catcatcat**
18	18228218	18228247	GTAGGCCATCGACAGAGTGGCGGAACCGGC-**TTT-A-catcatca-A-catcatcat**

19	18227834	18227863	TCACCGGGTTGGTGATGATGGCCACCAGGG-**TTT-A-catcatcat-A-catcatcat**
20	18228119	18228148	CTGGTTGCCCTTGAACAGGGGCTGGCTCTG-**TTT-A-catcatcat-A-catcatcat**
21	18226805	18226834	ATCGTAGAGCGCCAAGTCGGTGACCAGGGG-**TTT-A-catcatcat-A-catcatcat**
22	18228288	18228317	AGGAGCACTCGATAACGTTCTTCTCGCCGT-**TTT-A-catcatcat-A-catcatcat**
23	18228050	18228079	GATCACGGGGATCTGCACGGTCTGGGGATC-**TTT-A-catcatcat-A-atcatcat**
24	18227868	18227897	TTGAGGATCTCGGCAGCGATGGGCACGCAG-**TTT-A-catcatcat-A-catcatcat**
25	18226515	18226544	CGCACTCCCTGCAGGGCCAATTGCTTCGTC-**TTT-A-catcatcat-A-catcatcat**
26	18226402	18226431	ATCCCACGGGCCAATGAAACAGATTTGCGA-**TTT-A-catcatcat-A-catcatcat**
27	18228443	18228475	CTTCTGGATGTTCTTCTTCAGCTCGGGAATGGC-**TTT-A-catcatcat-A-catcatcat**
28	18228258	18228287	TCAGTCCCTTCAGCAGGGAGCCGGCGAAAC-**TTT-A-catcatcat-A-catcatcat**
29	18227742	18227771	AACAGATCATCGCGGGTCATGCCCGGCTTG-**TTT-A-catcatcat-A-catcatcat**
30	18228179	18228208	GGCCTTAACGACCTCAGTACCGGCCTCCTG-**TTT-A-catcatcat-A-catcatcat**
31	18226849	18226878	TCGATATGCGACAGATCGGCGGCCACACCG-**TTT-A-catcatcat-A-catcatcat**

Table 17: Primers for *Pcb*

S.no.	start	stop	sequence+p42 (*Pcb*)
1	9852336	9852365	GCTCATGGAGTCGACGGCCACGTCCACCAC-**TTT-A-cttacaaac-A-cttacaaac**
2	9854934	9854963	AGCGACCGGTGTTGGGCTGAAAATCGTTGG-**TTT-A-cttacaaac-A-cttacaaac**
3	9854964	9854993	CCGGATCTTCGGTGGTCACACGGCACTGAA-**TTT-A-cttacaaac-A-cttacaaac**
4	9851272	9851301	ACCCTTCTCCACTTTGTCGCCAACCTTCAC-**TTT-A-cttacaaac-A-cttacaaac**
5	9852749	9852778	AGGTTGGGCAGGTAGTTGAGCGAGTCGAAC-**TTT-A-cttacaaac-A-cttacaaac**
6	9855334	9855363	CAGATGCACTACATTCCCGGCCTTGTCTCC-**TTT-A-cttacaaac-A-cttacaaac**
7	9852559	9852590	GGGCTTGAGCAGACCAGCCATATCCTTTATGC-**TTT-A-cttacaaac-A-cttacaaac**
8	9852719	9852748	GCCTTTCCAGCGGCTTCCATGCCGAGGATC-**TTT-A-cttacaaac-A-cttacaaac**
9	9851941	9851970	CGCTCCAGCACTTGATCGGCGGTCAGGTCA-**TTT-A-cttacaaac-A-cttacaaac**
10	9852638	9852674	TAGTATTTCAGATCATACTTGGTGCGCTTGGGATCGC-**TTT-A-cttacaaac-A-cttacaaac**
11	9852779	9852808	ACCCTGAAGATGTCCATGCCGGTCTGCACA-**TTT-A-cttacaaac-A-cttacaaac**
12	9851890	9851919	GAGCCCTGCAAGTACTCCACCACCGACTTG-**TTT-A-cttacaaac-A-cttacaaac**
13	9851481	9851510	GACCGCGCGCAGCTGGCCATTCAACTCAAA-**TTT-A-cttacaaac-A-cttacaaac**
14	9854594	9854625	ACCTCACCCATATAGTTGAGCAGCTTCTGGGC-**TTT-A-cttacaaac-A-cttacaaac**
15	9855870	9855899	CGTCGGCCTTTTGTCGGTGCATGTGCATCT-**TTT-A-cttacaaac-A-cttacaaac**
16	9855469	9855498	CTCCTCCACATCCTCCATTTTGCGGACGAC-**TTT-A-cttacaaac-A-cttacaaac**
17	9854687	9854716	AGAACGCCGTGGAGGAACTTCTGGTTCTCC-**TTT-A-cttacaaac-A-cttacaaac**
18	9851971	9852003	TTCTGCACCATGAACTGGGCAAGATCACCTACC-**TTT-A-cttacaaac-A-cttacaaac**
19	9852809	9852839	GCCAGCTCACAGAACTTGTAGACCACGTTGT-**TTT-A-cttacaaac-A-cttacaaac**
20	9851511	9851540	GAATACCTCGCGGATACCGTTGGGCTTGAG-**TTT-A-cttacaaac-A-cttacaaac**
21	9855509	9855538	CGACCTCCGCCTCCGTAAGCGGCCTTGAAG-**TTT-A-cttacaaac-A-cttacaaac**
22	9854717	9854751	AGCACGTTTAGGAGGAAGGGGATATTGGTCTTGAC-**TTT-A-cttacaaac-A-cttacaaac**
23	9852004	9852034	ACCTTCGACGAGGGCGTCACCTTGATAATGT-**TTT-A-cttacaaac-A-cttacaaac**
24	9851063	9851099	GTTTTCACTTAATTTTACATTGGGTGTGTGCGGTGGC-**TTT-A-cttacaaac-A-cttacaaac**
25	9851541	9851570	ATCGGCGGACACAGCCAGAGCTTTCACGCT-**TTT-A-cttacaaac-A-cttacaaac**
26	9854657	9854686	TGCGGGTGCTCGTCGATGAAGTAGGTGTCG-**TTT-A-cttacaaac-A-cttacaaac**
27	9854782	9854811	GTTCATCTTGGAGGCGGAGCTCTGCAGATC-**TTT-A-cttacaaac-A-cttacaaac**

28	9850875	9850911	TGGGCACGAACTTATGCAATCCGATATATTTTGGCAG-**TTT-A-cttacaaac-A-cttacaaac**
29	9855087	9855116	CGATGCCTGTTATCTCCTCGGTGACCGTGT-**TTT-A-cttacaaac-A-cttacaaac**
30	9851100	9851133	AGCTTAGACAATGGACATTTTGATCCGGTGGCAC-**TTT-A-cttacaaac-A-cttacaaac**
31	9855990	9856019	CCAGCACTGACCGGATGGGCTTGTACTCCA-**TTT-A-cttacaaac-A-cttacaaac**
32	9851571	9851600	CAGCGTCTTACCGCGCTCCAGAGGTACGTC-**TTT-A-cttacaaac-A-cttacaaac**
33	9850927	9850963	TTGACCAGTTACTCATGGTCGATTGATCCTGGAAACA-**TTT-A-cttacaaac-A-cttacaaac**
34	9851174	9851206	TTCGTTCCGTTGGCAATTTCCAGCTTCTTGACA-**TTT-A-cttacaaac-A-cttacaaac**
35	9852065	9852096	CCTTCTTAACGTCCTCGAAGAAGTCGCCCAGA-**TTT-A-cttacaaac-A-cttacaaac**
36	9855117	9855146	GCTCCACTTGTAGACGGGCGTTCACTTCGA-**TTT-A-cttacaaac-A-cttacaaac**
37	9856101	9856130	TTTTGAAGATGGCGTTGAGCCGGACGCGTG-**TTT-A-cttacaaac-A-cttacaaac**
38	9852870	9852899	CTCCGCGCAACAGCATCTGGAAGGGAATGT-**TTT-A-cttacaaac-A-cttacaaac**
39	9854842	9854873	GGAGTCGTAGTATGGCGAAATGATGGCTCCGG-**TTT-A-cttacaaac-A-cttacaaac**
40	9855179	9855208	AACTCCACGGTTCCGGCGTTTTCATAGCCC-**TTT-A-cttacaaac-A-cttacaaac**
41	9855147	9855178	TGAAGTAGAAGTTGCCGGACTCGTCGCAAAGG-**TTT-A-cttacaaac-A-cttacaaac**
42	9855218	9855247	GCCAAGCGCACTGCTGCCTCCGTCATCTTG-**TTT-A-cttacaaac-A-cttacaaac**
43	9853031	9853060	GGGGAGATCTTCAGCAGATCGTGGGAACGC-**TTT-A-cttacaaac-A-cttacaaac**
44	9851667	9851703	CTTTTCGCGGAAGTTTAGGAAATCATTCGTCACCTGC-**TTT-A-cttacaaac-A-cttacaaac**
45	9854904	9854933	CCATACCCTCGCCAGATCGGAAGACCTCCA-**TTT-A-cttacaaac-A-cttacaaac**
46	9855274	9855303	CGCTGGGGCGATCTCCACCACCTTCTGGTG-**TTT-A-cttacaaac-A-cttacaaac**
47	9860410	9860439	TTGTCGTTGTCCTGGCGCAAAGTGGGTAAT-**TTT-A-cttacaaac-A-cttacaaac**
48	9852157	9852186	TAGACATCGGCGTTGCCCGACCGCATTGTT-**TTT-A-cttacaaac-A-cttacaaac**
49	9860440	9860473	CGCTGCTCCAGCACTACAAAACAATTTCAAACGG-**TTT-A-cttacaaac-A-cttacaaac**
50	9860475	9860511	TCGTGAGTCAACGTGGTTTCTTTAGCTTATGTACCGC-**TTT-A-cttacaaac-A-cttacaaac**
51	9860522	9860558	TACAAATTCACGGTTCCTATGTATCCTATGTGCGCGA-**TTT-A-cttacaaac-A-cttacaaac**
52	9855701	9855730	AAGCGCAGTCCAGCATCAATCACCGCTTGG-**TTT-A-cttacaaac-A-cttacaaac**
53	9851810	9851839	GACGTCCCTCGATGCGGGGCATGTCCTTGA-**TTT-A-cttacaaac-A-cttacaaac**
54	9853113	9853142	GTAGCAGTTCCTTACGGTTGCGCACCTCCT-**TTT-A-cttacaaac-A-cttacaaac**
55	9855761	9855790	TAGCCGGGATGCACGGCATCCACATCGTTC-**TTT-A-cttacaaac-A-cttacaaac**

Table 18: List of Hairpins used

S.no.	Hairpin ID	Hairpin Sequence
1	h40.40	AATCCTACAAGGGCCTTTTGGCCCTTGTAGGATTTTGTAGGATTTTTTTT
2	h26.26	AATAAACCTAGGGCCTTTTGGCCCTAGGTTTATTTAGGTTTAT**TTTTTTT**
3	h38.38	AAACATACTAGGGCCTTTTGGCCCTAGTATGTTTTAGTATGTT**TTTTTTT**
4	h39.39	ATTCATTTACGGGCCTTTTGGCCCGTAAATGAATGTAAATGAA**TTTTTTT**
5	h28.28	ACAACTTAACGGGCCTTTTGGCCCGTTAAGTTGTGTTAAGTTG**TTTTTTT**
6	h35.35	ATAAAAACTCGGGCCTTTTGGCCCGAGTTTTTATGAGTTTTTA**TTTTTTT**
7	h29.29	ATCTAAAATCGGGCCTTTTGGCCCGATTTTAGATGATTTTAGA-**TTTTTTT**
8	h31.31	ATTATTCACTGGGCCTTTTGGCCCAGTGAATAATAGTGAATAA-TTTTTTT
9	h34.34	ACTCTACTACGGGCCTTTTGGCCCGTAGTAGAGTGTAGTAGAG-**TTTTTTT**
10	h27.27	ACATCATCATGGGCCTTTTGGCCCATGATGATGTATGATGATG-**TTTTTTT**
11	h42.42	ACTTACAAACGGGCCTTTTGGCCCGTTTGTAAGTGTTTGTAAG-**TTTTTTT**
12	h30.30	AAATACTCTCGGGCCTTTTGGCCCGAGAGTATTTGAGAGTATT-**TTTTTTT**

Table 19: List of Imagers used

S.no.	Imager ID	Imager sequence
1	HmlA_i40*	/5ATTO488N/ttTTGTAGGATtTTGTAGGATt
2	HmlB_i26*	/5ATTO565N/ttTAGGTTTATtTAGGTTTATt
3	*Dome*A_i38*	/5ATTO488N/ttTAGTATGTTtTAGTATGTTt
4	*Dome*B_i39*	/5ATTO565N/ttGTAAATGAAtGTAAATGAAt
5	Kdh_i28*	/5ATTO565N/ttGTTAAGTTGtGTTAAGTTGt
6	*mAcon1*_i35*	/5ATTO647N/ttGAGTTTTTAtGAGTTTTTAt
7	*Sdha*_i29*	/5ATTO647N/tt-GATTTTAGA-tGATTTTAGA-t
8	*Gdh*_i31*	/5ATTO647N/tt-AGTGAATAA-t-AGTGAATAA-t
9	*CS*_i34*	/5ATTO565N/tt-GTAGTAGAG-t-GTAGTAGAG-t
10	*Mdh*2_i27*	/5ATTO488N/tt-ATGATGATG-t-ATGATGATG-t
11	*Pcb*_i42*	/5ATTO647N/tt-GTTTGTAAG-t-GTTTGTAAG-t
12	*Pdha*_i30*	/5ATTO488N/tt-GAGAGTATT-t-GAGAGTATT-t

6.5 Metabolite supplementation

Supplemented food was prepared by adding metabolites (1% citrate (Sodium citrate tribasic dihydrate, Sigma, C7254) and 3% succinate (Sodium succinate dibasic hexahydrate, Sigma, S9637; weight/volume) to the regular fly food. Eggs or larvae of respective stages were transferred to the supplemented food according to the experimental requirements for lymph gland analysis. In early feeding (upto 60h) or late (60-120h) feeding the larvae were transferred back to the regular food after rearing on supplemented food for further development. Controls for the respective experiments were always treated similarly, un-supplemented controls were always kept alongside.

6.6 RNA sequencing

Sample preparation was done following the below mentioned protocol;

- Lymph gland(Tissue) were dissected in PBS and stored in the Trizol.
- to it chloroform was added (1/5 volume of Trizol).
- incubation on ice for 15 min
- Centrifuge@12000g/30min/4 degree
- aqueous phase transferred to different tubeand isopropanol was added (1/2 vol of Trizol)
- Overnight incubation at -80 degrees
- centrifuge@12000g/30min/4 degree

- supernatant discarded and pellet was washed 2 times with 70% ethanol@7500g/5min/4 degree
- sample was dried at heat block 60 degree/15 min
- 20ul Nuclease free water was added and pellet was dissolved.

Post this sample was processed with the help of Hiseq2500 platform using 1x100bp sequencing read length for data acquisition.

6.7 Software and Statistical analyses

All the images were processed in Imagej (Fiji) software and the figure panels were prepared in Microsoft power point 2010 and Adobe Photoshop. Data post-calculation was stored in Microsoft excel 2010. All statistical analyses were performed using GraphPad Prism 10 software. The means were analysed using ordinary one-way ANNOVA or unpaired Student t-test (Mann-Whitney test). For all the experiments batch effect were plotted.

7. Discussion

7.1 Temporal and spatial regulation of TCA cycle

TCA cycle is one of the evolutionary conserved pathways in all eukaryotes and it being used as a site for exchange and interconversion of many metabolites makes perfect sense, but recent studies have highlighted few of TCA cycle's core metabolites being the regulators of various fundamental cellular processes. Our study pans from the tempoaral to spatial understanding of the TCA cycle involvement in the development of lymph gland. Here with the help of four different blood cell specific GAL4's we have established the spatial discreteness of the TCA cycle. Our study has identified dual involvement or functionality of TCA cycle i.e., growth and maintenance or differentiation. In MZ (progenitors), marked by *Tep4GAL4;UASmCherry* and *domeMESOGAL4;UASGFP* the whole cycle was found to be involved in the maintenance of progenitors, as removing either of the steps leads to increase in differentiation whereas only a few steps (*CS, mAcon1,* and *α-Kdh*) were found to be involved in the early growth of the LG.

Adgf-A based adenosine regulation is one of the important signalling cue for progenitor proliferation as well as maintenance, this signal originates from the differentiating cells in CZ (42). Therefore, we also looked into the other zones i.e., IZ and CZ, of LG with the help of *CHIZ-GAL4* and *Hml$^{\Delta}$GAL4;UAS-2X EGFP*, respectively, to understand their contribution to LG development under the control of TCA cycle. Although from the CZ, we did not find any feedback relay for progenitor maintenance, but interestingly we found the same steps (*CS, mAcon1,* and *α-Kdh*) regulating the CZ proliferation, as in the case of progenitor proliferation. In case of IZ, the initiation of this zone is the result of differentiation of the progenitors, once they have achieved a desired number or growth of LG. The transition of progenitors into intermediary population and their proliferation is very tightly regulated, as the genetic experiments comfirms that IZ proliferative capacity is independent of *CS*, which means these cells need to internalize citrate from outside and to our understanding it is progenitors which supplies the citrate to IZ population. By regulating citrate levels, progenitors (MZ) can keep a check on the IZ population and thereby the CZ. We also found that this is the developmental time point (60h AEL), where the TCA cycle actually comes together as a cycle, by contribution from two zones (MZ and IZ) for keeping the progenitor pool maintained.

7.2 TCA cycle metabolites as regulators or signalling molecules

TCA cycle intermediates and byproducts are well known for their ability to act as signalling molecules. α-KG/Succinate ratio is well known parameter for the stem cell regulation, where

α-KG supports stemness, by promoting demethylation of histones and DNA with the help of KDM family of demethylases and TET family DNA demethylases, respectively (212, 213), on the other hand, high succinate levels promote differentiation. Another contrasting study highlight α-KG as a differentiation promoting cue, by regulating same family of enzymes TET and KDMs, in case of primed PS*CS* (214). Another scenario where α-KG/Succinate ratio as well as ROS and Fumarate accumulation plays a crucial role is HIF stabilization under hypoxia and pseudohypoxia conditions (140–143, 168, 215). Physiological ROS levels are importantant signal for progenitors to transition into differentiating cells, where the ROS levels comes down (53). Similar to these TCA metabolites acting as signalling molecules or regulators, we also uncovered the role of citrate as a regulator of progenitor proliferation and maintenance. Our finding of Citrate Synthase (*CS*) as one of the key candidate in MZ proliferation, made us identify the early importance of citrate in the LG growth. Citrate supports the progenitor proliferation by keeping a check on precocious differentiation of progenitors, which is citrate does not allow progenitors to take a path of divide to differentiate and thereby maintain the stable progenitor pool. On the other hand, amino acid derived (glutamate), α-KG autonomously regulates the progenitor proliferation in MZ as well as CZ proliferation, the mechanism behind it is yet to be explored. We also found that Succinate supplementation to the growth mutants could fully or partially rescue the LG size, though the progenitor homeostasis could not be restored. This result is an important finding where α-KG/Succinate ratio is found to be regulating an important developmental process i.e., growth of LG.

7.3 Building up of TCA cycle

Classically TCA cycle is regarded as a cyclic process, in recent past there are many examples where we found the variations/versions of TCA cycle e.g. glutamine dependent reductive carboxylation for citrate production (18, 19), ES*CS*, cancer cells and immune cells shuttling mt-citrate to cytosol, with the help of malate-citrate shuttle, to break it down into OA and acetyl CoA, using ATP citrate lyase for cell fate transition, functional maturity, or diverting excess resources towards lipid biosynthesis, etc. (205–209). All these and many more examples only talks about the variations or versions of TCA cycle in different physiological conditions. But, we here for the first time identified the making or building of TCA cycle from a few steps playing crucial part in the growth (progenitor proliferation) to a whole cycle involved in the maintenance of progenitor pool. Through the temporal and spatial analysis of LG we have pinpointed citrate and glutamate derived α-KG as two important molecules regulating the growth of LG. We have also identified that the oxalo acetate for the citrate production is coming

from the *Pcb* dependent pyruvate conversion to OA and, whereas we could only confirm that Acetyl CoA is not derived from the *Pdha* dependent pyruvate conversion. Also we found out that in early development α-KG is produced from glutamate as there is a disconnect between *mAcon1* and *α-Kdh* due to the absence of growth phrnotype in Idh^{RNAi} mutants. We have highlighted that the citrate is required from the get go for the development to the time of onset of differentiation. We have experimentally proven that in the absence of citrate (CS^{RNAi}), we see precocious differentiation, which can be restored by 1% w/v citrate supplementation. But if we allow CS^{RNAi} mutant larvae to grow on 1%CF throughout the larval stage, we end up blocking the onset of differentiation and therby stops the transition of progenitors into creation of IZ and subsequently CZ, which led to even smaller LG (Figure). Citrate also supports the progenitors transitioning in intermediary population, as in the IZ proliferation *CS* is not a party, which maybe another checkpoint by the progenitors to keep IZ transition and proliferation in control by synthesising and exporting citrate out for the IZ population to takeup and metabolise to proliferate. The onset of differentiation is also the timepoint where the remaining steps od TCA cycle coordinate between two zones (MZ and IZ) to makeup the complete cycle for the maintenance of the progenitor pool, with citrate still being supplied by MZ. We have also performed the SABER FISH to understand the distribution of the TCA cycle transcripts developmentally. Here we observed that some enzymes transcripts are abundantly concentrated in the MZ only throughout development (*mAcon1*, *Gdh* and *Pcb*), whereas others are same across the LG (*Kdh, Sdh*, *Mdh2* and *Pdha*), some are highly enriched and others are low in numbers (*Mdh2* and *Pdha*). Only *CS* has a curious case where it was found to be highly enriched in MZ initially (48h and 72h) but with development (96h) the transcripts levels are found to be high in CZ, which is consistent with the genetic reults. The difference in the distribution pattern of the transcripts along with the genetic data further strengthen the observation that TCA builds up with developmentally into a full cycle.

8. References

1. T. Lebestky, T. Chang, V. Hartenstein, U. Banerjee, Specification of *Drosophila* hematopoietic lineage by conserved transcription factors. *Science* **288**, 146–149 (2000).

2. K. P. Rehorn, H. Thelen, A. M. Michelson, R. Reuter, A molecular aspect of hematopoiesis and endoderm development common to vertebrates and *Drosophila*. *Dev. Camb. Engl.* **122**, 4023–4031 (1996).

3. U. Tepass, L. I. Fessler, A. Aziz, V. Hartenstein, Embryonic origin of hemocytes and their relationship to cell death in *Drosophila*. *Dev. Camb. Engl.* **120**, 1829–1837 (1994).

4. A. Holz, B. Bossinger, T. Strasser, W. Janning, R. Klapper, The two origins of hemocytes in *Drosophila*. *Dev. Camb. Engl.* **130**, 4955–4962 (2003).

5. A. Rugendorff, A. Younossi-Hartenstein, V. Hartenstein, Embryonic origin and differentiation of the *Drosophila* heart. *Rouxs Arch. Dev. Biol.* **203**, 266–280 (1994).

6. S. Akira, K. Takeda, T. Kaisho, Toll-like receptors: critical proteins linking innate and acquired immunity. *Nat. Immunol.* **2**, 675–680 (2001).

7. S. Cherry, N. Silverman, Host-pathogen interactions in *drosophila*: new tricks from an old friend. *Nat. Immunol.* **7**, 911–917 (2006).

8. D. Hultmark, Insect immunology. Ancient relationships. *Nature* **367**, 116–117 (1994).

9. A. Kleino, N. Silverman, The *Drosophila* IMD pathway in the activation of the humoral immune response. *Dev. Comp. Immunol.* **42**, 25–35 (2014).

10. C. J. Evans, U. Banerjee, Transcriptional regulation of hematopoiesis in *Drosophila*. *Blood Cells. Mol. Dis.* **30**, 223–228 (2003).

11. V. Hartenstein, Blood cells and blood cell development in the animal kingdom. *Annu. Rev. Cell Dev. Biol.* **22**, 677–712 (2006).

12. R. Lanot, D. Zachary, F. Holder, M. Meister, Postembryonic hematopoiesis in *Drosophila*. *Dev. Biol.* **230**, 243–257 (2001).

13. B. Lemaitre, E. Nicolas, L. Michaut, J. M. Reichhart, J. A. Hoffmann, The dorsoventral regulatory gene cassette spätzle/Toll/cactus controls the potent antifungal response in *Drosophila* adults. *Cell* **86**, 973–983 (1996).

14. N. S. Chandel, Evolution of Mitochondria as Signaling Organelles. *Cell Metab.* **22**, 204–206 (2015).

15. H. A. Krebs, L. V. Eggleston, The oxidation of pyruvate in pigeon breast muscle. *Biochem. J.* **34**, 442–459 (1940).

16. D. G. Ryan, L. A. J. O'Neill, Krebs Cycle Reborn in Macrophage Immunometabolism. *Annu. Rev. Immunol.* **38**, 289–313 (2020).

17. C. Lussey-Lepoutre, *et al.*, Loss of succinate dehydrogenase activity results in dependency on pyruvate carboxylation for cellular anabolism. *Nat. Commun.* **6**, 8784 (2015).

18. C. M. Metallo, *et al.*, Reductive glutamine metabolism by *IDH*1 mediates lipogenesis under hypoxia. *Nature* **481**, 380–384 (2011).

19. A. R. Mullen, *et al.*, Reductive carboxylation supports growth in tumour cells with defective mitochondria. *Nature* **481**, 385–388 (2011).

20. C. M. Bisbach, *et al.*, Succinate Can Shuttle Reducing Power from the Hypoxic Retina to the O2-Rich Pigment Epithelium. *Cell Rep.* **31**, 107606 (2020).

21. E. T. Chouchani, *et al.*, Ischaemic accumulation of succinate controls reperfusion injury through mitochondrial ROS. *Nature* **515**, 431–435 (2014).

22. J. B. Spinelli, *et al.*, Fumarate is a terminal electron acceptor in the mammalian electron transport chain. *Science* **374**, 1227–1237 (2021).

23. H. Agaisse, U.-M. Petersen, M. Boutros, B. Mathey-Prevot, N. Perrimon, Signaling Role of Hemocytes in *Drosophila* JAK/STAT-Dependent Response to Septic Injury. *Dev. Cell* **5**, 441–450 (2003).

24. L. I. Fessler, R. E. Nelson, J. H. Fessler, *Drosophila* extracellular matrix. *Methods Enzymol.* **245**, 271–294 (1994).

25. N. C. Franc, J.-L. Dimarcq, M. Lagueux, J. Hoffmann, R. A. B. Ezekowitz, Croquemort, A Novel *Drosophila* Hemocyte/Macrophage Receptor that Recognizes Apoptotic Cells. *Immunity* **4**, 431–443 (1996).

26. C. Hetru, L. Troxler, J. A. Hoffmann, *Drosophila* melanogaster Antimicrobial Defense. *J. Infect. Dis.* **187**, S327–S334 (2003).

27. M. A. Murray, L. I. Fessler, J. Palka, Changing distributions of extracellular matrix components during early wing morphogenesis in *Drosophila*. *Dev. Biol.* **168**, 150–165 (1995).

28. P. Tzou, E. De Gregorio, B. Lemaitre, How *Drosophila* combats microbial infection: a model to study innate immunity and host–pathogen interactions. *Curr. Opin. Microbiol.* **5**, 102–110 (2002).

29. L. Mandal, U. Banerjee, V. Hartenstein, Evidence for a fruit fly hemangioblast and similarities between lymph-gland hematopoiesis in fruit fly and mammal aorta-gonadal-mesonephros mesoderm. *Nat. Genet.* **36**, 1019–1023 (2004).

30. A. Medvinsky, E. Dzierzak, Definitive hematopoiesis is autonomously initiated by the AGM region. *Cell* **86**, 897–906 (1996).

31. H. H. El Shatoury, The structure of the lymph glands of*Drosophila* larvae. *Wilhelm Roux Arch. Entwicklungsmechanik Org.* **147**, 489–495 (1955).

32. U. Banerjee, J. R. Girard, L. M. Goins, C. M. Spratford, *Drosophila* as a Genetic Model for Hematopoiesis. *GenetiCS* **211**, 367–417 (2019).

33. B. Lemaitre, J. Hoffmann, The Host Defense of *Drosophila melanogaster*. *Annu. Rev. Immunol.* **25**, 697–743 (2007).

34. B. Parsons, E. Foley, Cellular immune defenses of *Drosophila* melanogaster. *Dev. Comp. Immunol.* **58**, 95–101 (2016).

35. B. Benmimoun, C. Polesello, L. Waltzer, M. Haenlin, Dual role for Insulin/TOR signaling in the control of hematopoietic progenitor maintenance in *Drosophila*. *Development* **139**, 1713–1717 (2012).

36. M. Crozatier, J.-M. Ubeda, A. Vincent, M. Meister, Cellular Immune Response to Parasitization in *Drosophila* Requires the EBF Orthologue Collier. *PLoS Biol.* **2**, e196 (2004).

37. N. S. Dey, P. Ramesh, M. Chugh, S. Mandal, L. Mandal, Dpp dependent Hematopoietic stem cells give rise to Hh dependent blood progenitors in larval lymph gland of *Drosophila*. *eLife* **5**, e18295 (2016).

38. S.-H. Jung, C. J. Evans, C. Uemura, U. Banerjee, The *Drosophila* lymph gland as a developmental model of hematopoiesis. *Development* **132**, 2521–2533 (2005).

39. R. J. Khadilkar, *et al.*, ARF1–GTP regulates Asrij to provide endocytic control of *Drosophila* blood cell homeostasis. *Proc. Natl. Acad. Sci.* **111**, 4898–4903 (2014).

40. J. Krzemień, *et al.*, Control of blood cell homeostasis in *Drosophila* larvae by the posterior signalling centre. *Nature* **446**, 325–328 (2007).

41. L. Mandal, J. A. Martinez-Agosto, C. J. Evans, V. Hartenstein, U. Banerjee, A Hedgehog- and Antennapedia-dependent niche maintains *Drosophila* haematopoietic precursors. *Nature* **446**, 320–324 (2007).

42. B. C. Mondal, *et al.*, Interaction between Differentiating Cell- and Niche-Derived Signals in Hematopoietic Progenitor Maintenance. *Cell* **147**, 1589–1600 (2011).

43. D. Pennetier, *et al.*, Size control of the *Drosophila* hematopoietic niche by bone morphogenetic protein signaling reveals parallels with mammals. *Proc. Natl. Acad. Sci.* **109**, 3389–3394 (2012).

44. Y. Tokusumi, T. Tokusumi, D. A. Shoue, R. A. Schulz, Gene Regulatory Networks Controlling Hematopoietic Progenitor Niche Cell Production and Differentiation in the *Drosophila* Lymph Gland. *PLoS ONE* **7**, e41604 (2012).

45. T. Lebestky, S.-H. Jung, U. Banerjee, A Serrate-expressing signaling center controls *Drosophila* hematopoiesis. *Genes Dev.* **17**, 348–353 (2003).

46. S. A. Sinenko, L. Mandal, J. A. Martinez-Agosto, U. Banerjee, Dual Role of Wingless Signaling in Stem-like Hematopoietic Precursor Maintenance in *Drosophila*. *Dev. Cell* **16**, 756–763 (2009).

47. M. Dragojlovic-Munther, J. A. Martinez-Agosto, Multifaceted roles of PTEN and TSC orchestrate growth and differentiation of *Drosophila* blood progenitors. *Development* **139**, 3752–3763 (2012).

48. D. R. Nässel, Y. Liu, J. Luo, Insulin/IGF signaling and its regulation in *Drosophila*. *Gen. Comp. Endocrinol.* **221**, 255–266 (2015).

49. A. Defaye, *et al.*, Genetic Ablation of *Drosophila* Phagocytes Reveals Their Contribution to Both Development and Resistance to Bacterial Infection. *J. Innate Immun.* **1**, 322–334 (2009).

50. J. Krzemien, J. Oyallon, M. Crozatier, A. Vincent, Hematopoietic progenitors and hemocyte lineages in the *Drosophila* lymph gland. *Dev. Biol.* **346**, 310–319 (2010).

51. S. Minakhina, R. Steward, Hematopoietic stem cells in *Drosophila*. *Development* **137**, 27–31 (2010).

52. P. Irving, *et al.*, New insights into *Drosophila* larval haemocyte functions through genome-wide analysis. *Cell. Microbiol.* **7**, 335–350 (2005).

53. E. Owusu-Ansah, U. Banerjee, Reactive oxygen species prime *Drosophila* haematopoietic progenitors for differentiation. *Nature* **461**, 537–541 (2009).

54. H. Gao, X. Wu, N. Fossett, Upregulation of the *Drosophila* Friend of GATA Gene *u-shaped* by JAK/STAT Signaling Maintains Lymph Gland Prohemocyte Potency. *Mol. Cell. Biol.* **29**, 6086–6096 (2009).

55. H. Gao, X. Wu, N. Fossett, *Drosophila* E-Cadherin Functions in Hematopoietic Progenitors to Maintain Multipotency and Block Differentiation. *PLoS ONE* **8**, e74684 (2013).

56. R. Baldeosingh, H. Gao, X. Wu, N. Fossett, Hedgehog signaling from the Posterior Signaling Center maintains U-shaped expression and a prohemocyte population in *Drosophila*. *Dev. Biol.* **441**, 132–145 (2018).

57. J. Shim, *et al.*, Olfactory Control of Blood Progenitor Maintenance. *Cell* **155**, 1141–1153 (2013).

58. G. B. Ferguson, J. A. Martinez-Agosto, The TEAD family transcription factor Scalloped regulates blood progenitor maintenance and proliferation in *Drosophila* through PDGF/VEGFR receptor (Pvr) signaling. *Dev. Biol.* **425**, 21–32 (2017).

59. R. Makki, *et al.*, A Short Receptor Downregulates JAK/STAT Signalling to Control the *Drosophila* Cellular Immune Response. *PLoS Biol.* **8**, e1000441 (2010).

60. V. Kulkarni, R. J. Khadilkar, S. M. S., M. S. Inamdar, Asrij Maintains the Stem Cell Niche and Controls Differentiation during *Drosophila* Lymph Gland Hematopoiesis. *PLoS ONE* **6**, e27667 (2011).

61. A. Sinha, R. J. Khadilkar, V. K. S., A. RoyChowdhury Sinha, M. S. Inamdar, Conserved Regulation of the JAK/STAT Pathway by the Endosomal Protein Asrij Maintains Stem Cell Potency. *Cell Rep.* **4**, 649–658 (2013).

62. A. Kapoor, A. Padmavathi, S. Madhwal, T. Mukherjee, Dual control of dopamine in *Drosophila* myeloid-like progenitor cell proliferation and regulation of lymph gland growth. *EMBO Rep.* **23**, e52951 (2022).

63. C. M. Spratford, *et al.*, Intermediate progenitor cells provide a transition between hematopoietic progenitors and their differentiated descendants. *Development* **148**, dev200216 (2021).

64. I. Anderl, *et al.*, Transdifferentiation and Proliferation in Two Distinct Hemocyte Lineages in *Drosophila melanogaster* Larvae after Wasp Infection. *PLoS Pathog.* **12**, e1005746 (2016).

65. H. Asha, *et al.*, Analysis of Ras-Induced Overproliferation in *Drosophila* Hemocytes. *GenetiCS* **163**, 203–215 (2003).

66. C. J. Evans, T. Liu, U. Banerjee, *Drosophila* hematopoiesis: Markers and methods for molecular genetic analysis. *Methods* **68**, 242–251 (2014).

67. A. Goto, *et al.*, A *Drosophila* haemocyte-specific protein, hemolectin, similar to human von Willebrand factor. *Biochem. J.* **359**, 99–108 (2001).

68. A. Goto, T. Kadowaki, Y. Kitagawa, *Drosophila* hemolectin gene is expressed in embryonic and larval hemocytes and its knock down causes bleeding defects. *Dev. Biol.* **264**, 582–591 (2003).

69. R. E. Nelson, *et al.*, Peroxidasin: a novel enzyme-matrix protein of *Drosophila* development. *EMBO J.* **13**, 3438–3447 (1994).

70. S. Yasothornsrikul, W. J. Davis, G. Cramer, D. A. Kimbrell, C. R. Dearolf, viking: identification and characterization of a second type IV collagen in *Drosophila*. *Gene* **198**, 17–25 (1997).

71. N. Martinek, J. Shahab, M. Saathoff, M. Ringuette, Haemocyte-derived SPARC is required for collagen-IV-dependent stability of basal laminae in *Drosophila* embryos. *J. Cell Sci.* **121**, 1671–1680 (2008).

72. M. Grigorian, T. Liu, U. Banerjee, V. Hartenstein, The proteoglycan Trol controls the architecture of the extracellular matrix and balances proliferation and differentiation of blood progenitors in the *Drosophila* lymph gland. *Dev. Biol.* **384**, 301–312 (2013).

73. R. P. Sorrentino, T. Tokusumi, R. A. Schulz, The Friend of GATA protein U-shaped functions as a hematopoietic tumor suppressor in *Drosophila*. *Dev. Biol.* **311**, 311–323 (2007).

74. G. *CS*ordás, E. Gábor, V. Honti, There and back again: The mechanisms of differentiation and transdifferentiation in *Drosophila* blood cells. *Dev. Biol.* **469**, 135–143 (2021).

75. V. Honti, G. *CS*ordás, É. Kurucz, R. Márkus, I. Andó, The cell-mediated immunity of *Drosophila melanogaster*: Hemocyte lineages, immune compartments, microanatomy and regulation. *Dev. Comp. Immunol.* **42**, 47–56 (2014).

76. P. Irving, *et al.*, New insights into *Drosophila* larval haemocyte functions through genome-wide analysis - Irving - 2005 - Cellular Microbiology - Wiley Online Library. (2004). Available at: https://onlinelibrary.wiley.com/doi/full/10.1111/j.1462-5822.2004.00462.x [Accessed 7 February 2025].

77. E. Kurucz, *et al.*, Nimrod, a putative phagocytosis receptor with EGF repeats in *Drosophila* plasmatocytes. *Curr. Biol. CB* **17**, 649–654 (2007).

78. M. Letourneau, *et al.*, *Drosophila* hematopoiesis under normal conditions and in response to immune stress. *FEBS Lett.* **590**, 4034–4051 (2016).

79. T. M. Rizki, R. M. Rizki, Larval adipose tissue of homoeotic bithorax mutants of *Drosophila*. *Developmental Biology* **65**, 476–482 (1978).

80. A. J. Nappi, E. Vass, F. Frey, Y. Carton, Superoxide anion generation in *Drosophila* during melanotic encapsulation of parasites. *Eur. J. Cell Biol.* **68**, 450–456 (1995).

81. R. Shrestha, E. Gateff, Ultrastructure and Cytochemistry of the Cell Types in the Larval Hematopoietic Organs and Hemolymph of *Drosophila* Melanogaster. *Dev. Growth Differ.* **24**, 65–82 (1982).

82. V. Honti, *et al.*, *In vivo* detection of lamellocytes in *Drosophila melanogaster*. *Immunol. Lett.* **126**, 83–84 (2009).

83. V. Honti, *et al.*, Cell lineage tracing reveals the plasticity of the hemocyte lineages and of the hematopoietic compartments in *Drosophila* melanogaster. *Mol. Immunol.* **47**, 1997–2004 (2010).

84. T. M. Rizki, R. M. Rizki, Lamellocyte differentiation in *Drosophila* larvae parasitized by Leptopilina. *Dev. Comp. Immunol.* **16**, 103–110 (1992).

85. R. B. Vivancos Valérie, A. Giangrande, *glide/gcm*Is Expressed and Required in the Scavenger Cell Lineage. *Dev. Biol.* **191**, 118–130 (1997).

86. P. Bangs, K. White, Regulation and execution of apoptosis during *Drosophila* development. *Dev. Dyn.* **218**, 68–79 (2000).

87. J. Manaka, *et al.*, Draper-mediated and phosphatidylserine-independent phagocytosis of apoptotic cells by *Drosophila* hemocytes/macrophages. *J. Biol. Chem.* **279**, 48466–48476 (2004).

88. S. Nonaka, K. Nagaosa, T. Mori, A. Shiratsuchi, Y. Nakanishi, Integrin αPS3/βv-mediated Phagocytosis of Apoptotic Cells and Bacteria in *Drosophila*. *J. Biol. Chem.* **288**, 10374–10380 (2013).

89. F. L. Watson, *et al.*, Extensive diversity of Ig-superfamily proteins in the immune system of insects. *Science* **309**, 1874–1878 (2005).

90. J.-L. Dimarcq, *et al.*, Treatment of l(2)mbn *Drosophila* tumorous blood cells with the steroid hormone ecdysone amplifies the inducibility of antimicrobial peptide gene expression. *Insect Biochem. Mol. Biol.* **27**, 877–886 (1997).

91. E. Roos, G. Björklund, Y. Engström, In vivo regulation of tissue-specific and LPS-inducible expression of the *Drosophila* Cecropin genes. *Insect Mol. Biol.* **7**, 51–62 (1998).

92. C. Samakovlis, D. A. Kimbrell, P. Kylsten, A. Engström, D. Hultmark, The immune response in *Drosophila*: pattern of cecropin expression and biological activity. *EMBO J.* **9**, 2969–2976 (1990).

93. J. C. Regan, *et al.*, Steroid hormone signaling is essential to regulate innate immune cells and fight bacterial infection in *Drosophila*. *PLoS Pathog.* **9**, e1003720 (2013).

94. M. T. M. Rizki, Alterations in the haemocyte population of *Drosophila* melanogaster. *J. Morphol.* **100**, 437–458 (1957).

95. H. Nam, I. Jang, H. You, K. Lee, W. Lee, Genetic evidence of a redox-dependent systemic wound response via Hayan Protease-Phenoloxidase system in *Drosophila* | The EMBO Journal. (2012). Available at: https://www.embopress.org/doi/full/10.1038/emboj.2011.476 [Accessed 1 May 2025].

96. H. Tang, Z. Kambris, B. Lemaitre, C. Hashimoto, Two Proteases Defining a Melanization Cascade in the Immune System of *Drosophila**. *J. Biol. Chem.* **281**, 28097–28104 (2006).

97. O. Binggeli, C. Neyen, M. Poidevin, B. Lemaitre, Prophenoloxidase Activation Is Required for Survival to Microbial Infections in *Drosophila*. *PLOS Pathog.* **10**, e1004067 (2014).

98. J. P. Dudzic, S. Kondo, R. Ueda, C. M. Bergman, B. Lemaitre, *Drosophila* innate immunity: regional and functional specialization of prophenoloxidases. *BMC Biol.* **13**, 81 (2015).

99. H.-J. Nam, I.-H. Jang, T. Asano, W.-J. Lee, Involvement of pro-phenoloxidase 3 in lamellocyte-mediated spontaneous melanization in *Drosophila*. *Mol. Cells* **26**, 606–610 (2008).

100. T. Tokusumi, *et al.*, Characterization of a Lamellocyte Transcriptional Enhancer Located within the misshapen Gene of *Drosophila* melanogaster. *PLOS ONE* **4**, e6429 (2009).

101. M. Stofanko, S. Y. Kwon, P. Badenhorst, A Misexpression Screen to Identify Regulators of *Drosophila* Larval Hemocyte Development. *GenetiCS* **180**, 253–267 (2008).

102. M. J. Williams, M.-L. Wiklund, S. Wikman, D. Hultmark, Rac1 signalling in the *Drosophila* larval cellular immune response. *J. Cell Sci.* **119**, 2015–2024 (2006).

103. M. J. Xavier, M. J. Williams, The Rho-family GTPase Rac1 regulates integrin localization in *Drosophila* immunosurveillance cells. *PloS One* **6**, e19504 (2011).

104. N. S. Chandel, Evolution of Mitochondria as Signaling Organelles. *Cell Metab.* **22**, 204–206 (2015).

105. N. S. Chandel, *et al.*, Mitochondrial reactive oxygen species trigger hypoxia-induced transcription. *Proc. Natl. Acad. Sci. U. S. A.* **95**, 11715–11720 (1998).

106. S. Herzig, R. J. Shaw, AMPK: guardian of metabolism and mitochondrial homeostasis. *Nat. Rev. Mol. Cell Biol.* **19**, 121–135 (2018).

107. X. Liu, C. N. Kim, J. Yang, R. Jemmerson, X. Wang, Induction of apoptotic program in cell-free extracts: requirement for dATP and cytochrome c. *Cell* **86**, 147–157 (1996).

108. A. P. West, G. S. Shadel, Mitochondrial DNA in innate immune responses and inflammatory pathology. *Nat. Rev. Immunol.* **17**, 363–375 (2017).

109. L. Shi, B. P. Tu, Acetyl-CoA and the regulation of metabolism: Mechanisms and consequences. *Curr. Opin. Cell Biol.* **33**, 125–131 (2015).

110. S. Sivanand, I. Viney, K. E. Wellen, Spatiotemporal Control of Acetyl-CoA Metabolism in Chromatin Regulation. *Trends Biochem. Sci.* **43**, 61–74 (2018).

111. J. V. Lee, *et al.*, Akt-dependent metabolic reprogramming regulates tumor cell histone acetylation. *Cell Metab.* **20**, 306–319 (2014).

112. M. Peng, *et al.*, Aerobic glycolysis promotes T helper 1 cell differentiation through an epigenetic mechanism. *Science* **354**, 481–484 (2016).

113. I. Martínez-Reyes, N. S. Chandel, Mitochondrial TCA cycle metabolites control physiology and disease. *Nat. Commun.* **11**, 102 (2020).

114. V. Infantino, V. Iacobazzi, F. Palmieri, A. Menga, ATP-citrate lyase is essential for macrophage inflammatory response. *Biochem. Biophys. Res. Commun.* **440**, 105–111 (2013).

115. W. M. Taylor, M. L. Halperin, Regulation of pyruvate dehydrogenase in muscle. Inhibition by citrate. *J. Biol. Chem.* **248**, 6080–6083 (1973).

116. N. C. Williams, L. A. J. O'Neill, A Role for the Krebs Cycle Intermediate Citrate in Metabolic Reprogramming in Innate Immunity and Inflammation. *Front. Immunol.* **9**, 141 (2018).

117. V. Infantino, *et al.*, The mitochondrial citrate carrier: a new player in inflammation. *Biochem. J.* **438**, 433–436 (2011).

118. V. Infantino, V. Iacobazzi, A. Menga, M. L. Avantaggiati, F. Palmieri, A key role of the mitochondrial citrate carrier (SLC25A1) in TNFα- and IFNγ-triggered inflammation. *Biochim. Biophys. Acta* **1839**, 1217–1225 (2014).

119. E. Mills, L. A. J. O'Neill, Succinate: a metabolic signal in inflammation. *Trends Cell Biol.* **24**, 313–320 (2014).

120. J.-Y. Wu, *et al.*, Cancer-Derived Succinate Promotes Macrophage Polarization and Cancer Metastasis via Succinate Receptor. *Mol. Cell* **77**, 213-227.e5 (2020).

121. I. Choi, H. Son, J.-H. Baek, Tricarboxylic Acid (TCA) Cycle Intermediates: Regulators of Immune Responses. *Life* **11**, 69 (2021).

122. F. Khodagholi, F. Shaerzadeh, F. Montazeri, Mitochondrial Aconitase in Neurodegenerative Disorders: Role of a Metabolism-related Molecule in Neurodegeneration. *Curr. Drug Targets* **19**, 973–985 (2018).

123. F. Mangialasche, *et al.*, Lymphocytic mitochondrial aconitase activity is reduced in Alzheimer's disease and mild cognitive impairment. *J. Alzheimers Dis. JAD* **44**, 649–660 (2015).

124. T. Cordes, *et al.*, Immunoresponsive Gene 1 and Itaconate Inhibit Succinate Dehydrogenase to Modulate Intracellular Succinate Levels. *J. Biol. Chem.* **291**, 14274–14284 (2016).

125. B. P. Daniels, *et al.*, The Nucleotide Sensor ZB*P1* and Kinase RIPK3 Induce the Enzyme IRG1 to Promote an Antiviral Metabolic State in Neurons. *Immunity* **50**, 64-76.e4 (2019).

126. V. Lampropoulou, *et al.*, Itaconate Links Inhibition of Succinate Dehydrogenase with Macrophage Metabolic Remodeling and Regulation of Inflammation. *Cell Metab.* **24**, 158–166 (2016).

127. K. Minton, Neuronal itaconate restricts viral infection. *Nat. Rev. Immunol.* **19**, 67 (2019).

128. M. Bambouskova, *et al.*, Electrophilic properties of itaconate and derivatives regulate the IκBζ-ATF3 inflammatory axis. *Nature* **556**, 501–504 (2018).

129. E. L. Mills, *et al.*, Itaconate is an anti-inflammatory metabolite that activates Nrf2 via alkylation of KEA*P1*. *Nature* **556**, 113–117 (2018).

130. C. Tang, *et al.*, 4-Octyl Itaconate Activates Nrf2 Signaling to Inhibit Pro-Inflammatory Cytokine Production in Peripheral Blood Mononuclear Cells of Systemic Lupus Erythematosus Patients. *Cell. Physiol. Biochem.* **51**, 979–990 (2018).

131. B. Everts, *et al.*, TLR-driven early glycolytic reprogramming via the kinases TBK1-IKKε supports the anabolic demands of dendritic cell activation. *Nat. Immunol.* **15**, 323–332 (2014).

132. A. K. Jha, *et al.*, Network integration of parallel metabolic and transcriptional data reveals metabolic modules that regulate macrophage polarization. *Immunity* **42**, 419–430 (2015).

133. A. Haseeb, M. S. Makki, T. M. Haqqi, Modulation of ten-eleven translocation 1 (TET1), Isocitrate Dehydrogenase (*IDH*) expression, α-Ketoglutarate (α-KG), and DNA hydroxymethylation levels by interleukin-1β in primary human chondrocytes. *J. Biol. Chem.* **289**, 6877–6885 (2014).

134. E. M. Palmieri, *et al.*, Acetylation of human mitochondrial citrate carrier modulates mitochondrial citrate/malate exchange activity to sustain NADPH production during macrophage activation. *Biochim. Biophys. Acta* **1847**, 729–738 (2015).

135. H. Abla, M. Sollazzo, G. Gasparre, L. Iommarini, A. M. Porcelli, The multifaceted contribution of α-ketoglutarate to tumor progression: An o*PPO*rtunity to exploit? *Semin. Cell Dev. Biol.* **98**, 26–33 (2020).

136. L. Chen, *et al.*, Regulation of glucose and lipid metabolism in health and disease. *Sci. China Life Sci.* **62**, 1420–1458 (2019).

137. W. Song, D. Li, L. Tao, Q. Luo, L. Chen, Solute carrier transporters: the metabolic gatekeepers of immune cells. *Acta Pharm. Sin. B* **10**, 61–78 (2020).

138. K. J. Harber, *et al.*, Succinate Is an Inflammation-Induced Immunoregulatory Metabolite in Macrophages. *Metabolites* **10**, 372 (2020).

139. P.-S. Liu, *et al.*, α-ketoglutarate orchestrates macrophage activation through metabolic and epigenetic reprogramming. *Nat. Immunol.* **18**, 985–994 (2017).

140. N. S. Chandel, *et al.*, Reactive oxygen species generated at mitochondrial complex III stabilize hypoxia-inducible factor-1alpha during hypoxia: a mechanism of O2 sensing. *J. Biol. Chem.* **275**, 25130–25138 (2000).

141. W. G. Kaelin, P. J. Ratcliffe, Oxygen sensing by metazoans: the central role of the HIF hydroxylase pathway. *Mol. Cell* **30**, 393–402 (2008).

142. D. A. Patten, *et al.*, Hypoxia-inducible factor-1 activation in nonhypoxic conditions: the essential role of mitochondrial-derived reactive oxygen species. *Mol. Biol. Cell* **21**, 3247–3257 (2010).

143. G. L. Semenza, Hypoxia-inducible factors in physiology and medicine. *Cell* **148**, 399–408 (2012).

144. M. Monné, D. V. Miniero, V. Iacobazzi, F. Bisaccia, G. Fiermonte, The mitochondrial oxoglutarate carrier: from identification to mechanism. *J. Bioenerg. Biomembr.* **45**, 1–13 (2013).

145. M. Scalise, L. Pochini, M. Galluccio, L. Console, C. Indiveri, Glutamine Transport and Mitochondrial Metabolism in Cancer Cell Growth. *Front. Oncol.* **7**, 306 (2017).

146. B. Li, *et al.*, Targeting glutaminase 1 attenuates stemness properties in hepatocellular carcinoma by increasing reactive oxygen species and suppressing Wnt/beta-catenin pathway. *EBioMedicine* **39**, 239–254 (2019).

147. M. J. Lukey, *et al.*, Liver-Type Glutaminase GLS2 Is a Druggable Metabolic Node in Luminal-Subtype Breast Cancer. *Cell Rep.* **29**, 76-88.e7 (2019).

148. J.-B. Wang, *et al.*, Targeting mitochondrial glutaminase activity inhibits oncogenic transformation. *Cancer Cell* **18**, 207–219 (2010).

149. H. C. Yoo, *et al.*, A Variant of SLC1A5 Is a Mitochondrial Glutamine Transporter for Metabolic Reprogramming in Cancer Cells. *Cell Metab.* **31**, 267-283.e12 (2020).

150. H. Yoo, M. R. Antoniewicz, G. Stephanopoulos, J. K. Kelleher, Quantifying Reductive Carboxylation Flux of Glutamine to Lipid in a Brown Adipocyte Cell Line. *J. Biol. Chem.* **283**, 20621–20627 (2008).

151. Z. E. Stine, C. V. Dang, Glutamine Skipping the Q into Mitochondria. *Trends Mol. Med.* **26**, 6–7 (2020).

152. C.-W. J. Lio, S. C.-C. Huang, Circles of Life: linking metabolic and epigenetic cycles to immunity. *Immunology* **161**, 165–174 (2020).

153. I. Yokota, Y. Kuroda, [Alpha-ketoglutarate dehydrogenase complex]. *Nihon Rinsho Jpn. J. Clin. Med.* **60 Suppl 4**, 130–132 (2002).

154. E. J. Griffiths, G. A. Rutter, Mitochondrial calcium as a key regulator of mitochondrial ATP production in mammalian cells. *Biochim. Biophys. Acta* **1787**, 1324–1333 (2009).

155. A. L. McLain, P. A. Szweda, L. I. Szweda, α-Ketoglutarate dehydrogenase: a mitochondrial redox sensor. *Free Radic. Res.* **45**, 29–36 (2011).

156. L. Tretter, V. Adam-Vizi, Alpha-ketoglutarate dehydrogenase: a target and generator of oxidative stress. *Philos. Trans. R. Soc. Lond. B. Biol. Sci.* **360**, 2335–2345 (2005).

157. E.-H. Cho, Succinate as a Regulator of Hepatic Stellate Cells in Liver Fibrosis. *Front. Endocrinol.* **9**, 455 (2018).

158. E. M. Palsson-McDermott, *et al.*, Pyruvate kinase M2 regulates Hif-1α activity and IL-1β induction and is a critical determinant of the warburg effect in LPS-activated macrophages. *Cell Metab.* **21**, 65–80 (2015).

159. J. Park, *et al.*, SIRT5-mediated lysine desuccinylation impacts diverse metabolic pathways. *Mol. Cell* **50**, 919–930 (2013).

160. G. M. Tannahill, *et al.*, Succinate is an inflammatory signal that induces IL-1β through HIF-1α. *Nature* **496**, 238–242 (2013).

161. F. Wang, *et al.*, SIRT5 Desuccinylates and Activates Pyruvate Kinase M2 to Block Macrophage IL-1β Production and to Prevent DSS-Induced Colitis in Mice. *Cell Rep.* **19**, 2331–2344 (2017).

162. Y. Zhang, *et al.*, Lysine desuccinylase SIRT5 binds to cardiolipin and regulates the electron transport chain. *J. Biol. Chem.* **292**, 10239–10249 (2017).

163. A. Viola, F. Munari, R. Sánchez-Rodríguez, T. Scolaro, A. Castegna, The Metabolic Signature of Macrophage Responses. *Front. Immunol.* **10** (2019).

164. E. L. Mills, *et al.*, Succinate Dehydrogenase Supports Metabolic Repurposing of Mitochondria to Drive Inflammatory Macrophages. *Cell* **167**, 457-470.e13 (2016).

165. F. Scialò, *et al.*, Mitochondrial ROS Produced via Reverse Electron Transport Extend Animal Lifespan. *Cell Metab.* **23**, 725–734 (2016).

166. J. Garaude, *et al.*, Mitochondrial respiratory-chain adaptations in macrophages contribute to antibacterial host defense. *Nat. Immunol.* **17**, 1037–1045 (2016).

167. A. Littlewood-Evans, *et al.*, GPR91 senses extracellular succinate released from inflammatory macrophages and exacerbates rheumatoid arthritis. *J. Exp. Med.* **213**, 1655–1662 (2016).

168. M. A. Selak, *et al.*, Succinate links TCA cycle dysfunction to oncogenesis by inhibiting HIF-alpha prolyl hydroxylase. *Cancer Cell* **7**, 77–85 (2005).

169. F. Humphries, *et al.*, Succination inactivates gasdermin D and blocks pyroptosis. *Science* **369**, 1633–1637 (2020).

170. B. Kelly, L. A. O'Neill, Metabolic reprogramming in macrophages and dendritic cells in innate immunity. *Cell Res.* **25**, 771–784 (2015).

171. M. P. Murphy, L. A. J. O'Neill, Krebs Cycle Reimagined: The Emerging Roles of Succinate and Itaconate as Signal Transducers. *Cell* **174**, 780–784 (2018).

172. N. K. Patil, J. K. Bohannon, A. Hernandez, T. K. Patil, E. R. Sherwood, Regulation of leukocyte function by citric acid cycle intermediates. *J. Leukoc. Biol.* **106**, 105–117 (2019).

173. R. J. W. Arts, *et al.*, Glutaminolysis and Fumarate Accumulation Integrate Immunometabolic and Epigenetic Programs in Trained Immunity. *Cell Metab.* **24**, 807–819 (2016).

174. M. M. Blewett, *et al.*, Chemical proteomic map of dimethyl Fumarate-sensitive cysteines in primary human T cells. *Sci. Signal.* **9**, rs10 (2016).

175. E. L. Mills, B. Kelly, L. A. J. O'Neill, Mitochondria are the powerhouses of immunity. *Nat. Immunol.* **18**, 488–498 (2017).

176. N. P. Riksen, M. G. Netea, Immunometabolic control of trained immunity. *Mol. Aspects Med.* **77**, 100897 (2021).

177. D. G. Ryan, L. A. J. O'Neill, Krebs cycle rewired for macrophage and dendritic cell effector functions. *FEBS Lett.* **591**, 2992–3006 (2017).

178. C. D. C. C. van der Heijden, *et al.*, Epigeneti*CS* and Trained Immunity. *Antioxid. Redox Signal.* **29**, 1023–1040 (2018).

179. S. Beeckmans, L. Kanarek, Demonstration of Physical Interactions between Consecutive Enzymes of the Citric Acid Cycle and of the Aspartate-Malate Shuttle. *Eur. J. Biochem.* **117**, 527–535 (1981).

180. P. minarik, N. Tomaskova, M. Kollarova, M. Antalik, Malate Dehydrogenases – Structure and Function. *Gen. Physiol. Biophys.* 257–265 (2002).

181. J. B. Robinson, L. Inman, B. Sumegi, P. A. Srere, Further characterization of the Krebs tricarboxylic acid cycle metabolon. *J. Biol. Chem.* **262**, 1786–1790 (1987).

182. M. G. Herrera, D. Kamm, N. Ruderman, G. F. Cahill, Non-hormonal factors in the control of gluconeogenesis. *Adv. Enzyme Regul.* **4**, 225–235 (1966).

183. K. F. Petersen, S. Dufour, D. Befroy, R. Garcia, G. I. Shulman, Impaired mitochondrial activity in the insulin-resistant offspring of patients with type 2 diabetes. *N. Engl. J. Med.* **350**, 664–671 (2004).

184. E. Struck, J. Ashmore, O. Wieland, Effects of glucagon and long chain fatty acids on glucose production by isolated perfused rat liver. *Adv. Enzyme Regul.* **4**, 219–224 (1966).

185. J. R. Williamson, R. A. Kreisberg, P. W. Felts, Mechanism for the stimulation of gluconeogenesis by fatty acids in perfused rat liver. *Proc. Natl. Acad. Sci.* **56**, 247–254 (1966).

186. E. O. Balasse, F. Féry, Ketone body production and disposal: effects of fasting, diabetes, and exercise. *Diabetes. Metab. Rev.* **5**, 247–270 (1989).

187. P. F. Finn, J. F. Dice, Proteolytic and lipolytic responses to starvation. *Nutrition* **22**, 830–844 (2006).

188. J. D. McGarry, D. W. Foster, Hormonal control of ketogenesis. Biochemical considerations. *Arch. Intern. Med.* **137**, 495–501 (1977).

189. M. M. Meguid, M. D. Collier, L. J. Howard, Uncomplicated and stressed starvation. *Surg. Clin. North Am.* **61**, 529–543 (1981).

190. P. J. Randle, D. A. Priestman, S. C. Mistry, A. Halsall, Glucose fatty acid interactions and the regulation of glucose disposal. *J. Cell. Biochem.* **55 Suppl**, 1–11 (1994).

191. G. Fiermonte, *et al.*, Identification of the human mitochondrial oxodicarboxylate carrier. Bacterial expression, reconstitution, functional characterization, tissue distribution, and chromosomal location. *J. Biol. Chem.* **276**, 8225–8230 (2001).

192. M. Huizing, *et al.*, Human mitochondrial transmembrane metabolite carriers: tissue distribution and its implication for mitochondrial disorders. *J. Bioenerg. Biomembr.* **30**, 277–284 (1998).

193. M. Monné, F. Palmieri, Antiporters of the mitochondrial carrier family. *Curr. Top. Membr.* **73**, 289–320 (2014).

194. S. Galván-Peña, L. A. J. O'Neill, Metabolic Reprograming in Macrophage Polarization. *Front. Immunol.* **5**, 420 (2014).

195. C. J. Zuurbier, *et al.*, Cardiac metabolism as a driver and therapeutic target of myocardial infarction. *J. Cell. Mol. Med.* **24**, 5937–5954 (2020).

196. Y. Liu, L. Hu, T. Ma, J. Yang, J. Ding, Insights into the inhibitory mechanisms of NADH on the αγ heterodimer of human NAD-dependent isocitrate dehydrogenase. *Sci. Rep.* **8**, 3146 (2018).

197. J. L. Gabriel, P. R. Zervos, G. W. Plaut, Activity of purified NAD-specific isocitrate dehydrogenase at modulator and substrate concentrations approximating conditions in mitochondria. *Metabolism.* **35**, 661–667 (1986).

198. K. F. LaNoue, J. Bryla, J. R. Williamson, Feedback Interactions in the Control of Citric Acid Cycle Activity in Rat Heart Mitochondria. *J. Biol. Chem.* **247**, 667–679 (1972).

199. L. G. Korotchkina, M. S. Patel, Site specificity of four pyruvate dehydrogenase kinase isoenzymes toward the three phosphorylation sites of human pyruvate dehydrogenase. *J. Biol. Chem.* **276**, 37223–37229 (2001).

200. M. C. Sugden, M. J. Holness, Recent advances in mechanisms regulating glucose oxidation at the level of the pyruvate dehydrogenase complex by PDKs. *Am. J. Physiol. Endocrinol. Metab.* **284**, E855-862 (2003).

201. M. Patron, *et al.*, The Mitochondrial Calcium Uniporter (MCU): Molecular Identity and Physiological Roles. *J. Biol. Chem.* **288**, 10750–10758 (2013).

202. G. Gherardi, H. Monticelli, R. Rizzuto, C. Mammucari, The Mitochondrial Ca2+ Uptake and the Fine-Tuning of Aerobic Metabolism. *Front. Physiol.* **11**, 554904 (2020).

203. R. M. Denton, P. J. Randle, B. R. Martin, Stimulation by calcium ions of pyruvate dehydrogenase phosphate phosphatase. *Biochem. J.* **128**, 161–163 (1972).

204. L. Castro, V. Tórtora, S. Mansilla, R. Radi, Aconitases: Non-redox Iron–Sulfur Proteins Sensitive to Reactive Species. *Acc. Chem. Res.* **52**, 2609–2619 (2019).

205. P. K. Arnold, *et al.*, A non-canonical tricarboxylic acid cycle underlies cellular identity. *Nature* **603**, 477–481 (2022).

206. N. Assmann, *et al.*, Srebp-controlled glucose metabolism is essential for NK cell functional responses. *Nat. Immunol.* **18**, 1197–1206 (2017).

207. P. Borst, “Hydrogen transport and transport metabolites” in *Funktionelle und Morphologische Organisation der Zelle*, (Springer Berlin Heidelberg, 1963), pp. 137–162.

208. G. Hatzivassiliou, *et al.*, ATP citrate lyase inhibition can suppress tumor cell growth. *Cancer Cell* **8**, 311–321 (2005).

209. R. A. Parlo, P. S. Coleman, Enhanced rate of citrate export from cholesterol-rich hepatoma mitochondria. The truncated Krebs cycle and other metabolic ramifications of mitochondrial membrane cholesterol. *J. Biol. Chem.* **259**, 9997–10003 (1984).

210. J. Y. Kishi, T. E. Schaus, N. Gopalkrishnan, F. Xuan, P. Yin, Programmable autonomous synthesis of single-stranded DNA. *Nat. Chem.* **10**, 155–164 (2018).

211. J. Y. Kishi, *et al.*, SABER amplifies FISH: enhanced multiplexed imaging of RNA and DNA in cells and tissues. *Nat. Methods* **16**, 533–544 (2019).

212. B. W. Carey, L. W. S. Finley, J. R. Cross, C. D. Allis, C. B. Thompson, Intracellular α-ketoglutarate maintains the pluripotency of embryonic stem cells. *Nature* **518**, 413–416 (2015).

213. Q.-L. Ying, *et al.*, The ground state of embryonic stem cell self-renewal. *Nature* **453**, 519–523 (2008).

214. T. TeSlaa, *et al.*, α-Ketoglutarate Accelerates the Initial Differentiation of Primed Human Pluripotent Stem Cells. *Cell Metab.* **24**, 485–493 (2016).

215. J. S. Isaa*CS*, *et al.*, HIF overexpression correlates with biallelic loss of Fumarate hydratase in renal cancer: novel role of Fumarate in regulation of HIF stability. *Cancer Cell* **8**, 143–153 (2005).